The intracellular trafficking of HIV-1 Gag protein and the role of its NCp7 domain

Salah Edin El Meshri

UNIVERSITE DE STRASBOURG

Ecole Doctorale des Sciences de la Vie et de la Santé

THESE

présentée pour obtenir le grade de

Docteur de l'Université de Strasbourg

Discipline : Sciences du Vivant

Domaine : Virologie, aspects moléculaires et médicaux

par

Salah Edin EL MESHRI

Etude du trafic intracellulaire de la protéine Gag du VIH et rôle de son domaine NCp7

Soutenue le 24 juin 2015 devant la commission d'examen :

Dr. Gilles MIRAMBEAU	**Rapporteur externe**
Dr. Serge BOUAZIZ	**Rapporteur externe**
Dr. Marc RUFF	**Rapporteur interne**
Dr. Hugues DE ROCQUIGNY	**Directeur de thèse**

UMR CNRS 7213, Faculté de Pharmacie, ILLKIRCH

Strasbourg University

Life and Health Doctoral School

PhD Thesis

Submitted to obtain the degree of

Doctor of Strasbourg University

Discipline: Life Sciences

Speciality: Virology, molecular and medical aspects

By

Salah Edin EL MESHRI

The intracellular trafficking of HIV-1 Gag protein and the role of its NCp7 domain

Defended on June, 24th, 2015 in front of the examining committee:

Dr. Gilles MIRAMBEAU	**External Reporter**
Dr. Serge BOUAZIZ	**External Reporter**
Dr. Marc RUFF	**Internal Reporter**
Dr. Hugues DE ROCQUIGNY	**Thesis Director**

UMR CNRS 7213, Faculty of Pharmacy, ILLKIRCH

Acknowledgments

First, I would like to thank Prof. Yves MELY, director of laboratory Biophotonics and Pharmacology UMR CNRS 7213 of the Faculty of Pharmacy of Strasbourg for giving me the opportunity to do my thesis in his laboratory.

I would like to thank all members of the Jury Dr. Gilles MIRAMBEAU, Dr.Serge BOUAZIZ and Dr. Marc RUFF for having kindly agreed to evaluate my work.

My sincere gratitude goes to my supervisor Dr. Hugues DE ROCQUIGNY for his continuous support during the PhD program. He taught me all basic things to perform my research e.g. from designing an experiment till its analysis to the outcome. His profound practical skills, immense knowledge and critical but valuable remarks led me to do a good research. Several times, I had extensive discussions with him which resulted in innovative ideas. Apart from research, he was always there to help me in my problems.

I also want to thank Dr. Emmanuel BOUTANT for his help in this project, his availability and responses to all my questions.

A special thanks to Dr. Denis DUJARDIN and Dr. Jean-Luc DARLIX for helping me in the project, for his availability, for discussions and scientific advice.

I express my gratitude to Dr. Ludovic RICHERT, Dr. Pascal DIDIER and Romain VAUCHELLES for their assistance on the imaging platform PIQ. Thanks to Dr. Eleonore REAL for her comments and rigorous scientific advice.

I am grateful to Marlyse WERNERT and Ingrid BARTHEL for their availability and administrative assistance.

A big thank to Dr. Kamal Kant SHARMA who encouraged me for the writing of my thesis, for his help, support and good humor. Warm thank for Dr. Marc MOUSLI for his kind moral support.

Acknowledgements

I would also like to thank the Cultural Affairs in Libyan embassy, ministry of high education, National Agency for Scientific Research and Biotechnology Research Center for the financial support of my thesis.

I wish to warmly thank the whole team of "biophotonics and pharmacology" and more specifically: Dr. Hala EL MEKDAD, Sarwat ZGHEIB, Nedal TAHA, Emilie CHRIST, Hassan KARNIB, Manuel PIRES, Waseem ASHRAF, Redouane BOUCHAALA, Liliyana ZAAYTER , Dr. Avisek GOSH, Rajhans SHARMA, Noémie, Marianna, Ievgen, Lesia and Vasyl.

To my parents who have always supported me to go through with my ambitions, who trusted me and gave me confidence. A special thanks to my wife who was next to me in all difficult stages of my thesis, for her encouragement and support every day. To my lovely children Elmutasmbellah, Kinan and Miral. A warm thanks to my brothers and my sisters for their love and support.

Table of Contents

TABLE OF CONTENTS

ABBREVIATIONS

aa	Amino Acid
ABCE1	ATP-Binding Cassette E1
AP	Adaptor Protein
APD	Avalanche Photodiode
APOBEC3G	APOlipoprotein B mRNA-Editing enzyme-Catalytic polypeptide-like 3G
ARV	Anti-RetroViral
CA	Capsid
CCR5	Chemokine CC motif Receptor 5
CDC	Centers for Disease Control
Cdk9	Cyclin-Dependent Protein Kinase 9
cDNA	Complementary DNA
co-IP	co-immunoprecipitation
Cryo-EM	Cryo-Electron Microscopy
CTD	C- Terminal Domain
CXCR4	Chemokine CXC motif receptor 4
CypA	Cyclophilin A
DIS	Dimerization Initiation Site
DLS	Dimer Linkage Structure
dNTPs	Deoxynucleotide triphosphates
DNA	DeoxyriboNucleic Acid
E. coli	Escherichia coli

eGFP	Enhanced Green Fluorescent Protein
EM	Electron Microscopy
Env	Envelope protein
ESCRT	Endosomal Sorting Complex Required for Transport
FLIM	Fluorescence Lifetime Imaging Microscopy
FRET	Förster Resonnance Energy Transfert
Gag	Group specific antigen
GAPDH	Glyceraldehyde 3-Phosphate Dehydrogenase
gRNA	Genomic RNA
GST	Glutathione-S-Transferase
HAART	Highly Active Anti-Retroviral Therapy
HBR	Highly Basic Region
HIV	Human Immunodeficiency Virus
HLA	Human leukocyte antigen
HMG	High Mobility Group Protein Isoform
hStau	Human Staufen protein
HTLV	Human T Lymphotropic Virus
ICTV	International Committee on Taxonomy of Viruses
IN	Integrase
IRES	Internal Ribosomal Entry Site
Kd	Dissociation Constant
Kb	Kilobase

KS	Kaposi Sarcoma
LAV	Lymphadenopathy-Associated Virus
LEDGF/p75	Lens Epithelium Derived Growth Factor
LTR	Long Terminal Repeat
LysRS	Lysyl-tRNA Synthetase
MA	Matrix
MHC	Major Histocompatibility Complex
MHR	Major Homology Region
MIP	Macrophage Inflammatory Proteins
MPMV	Mason Pfizer Monkey Virus
mRNA	Messenger RiboNucleic Acid
MVB	MultiViscular Body
NC	Nucleocapsid
NC^{Gag}	NC domain of Gag
NarL	Nitrate/nitrite response regulator
Nef	Negative Regulatory factor
NES	Nuclear Export Signals
NLS	Nuclear Localization Signal
NMR	Nuclear Magnetic Resonance
NPC	Nuclear Pore Complex
NRTIs	Nucleoside Analogue Reverse Transcriptase Inhibitors
nt	nucleotide

NTD	N- Terminal Domain
ODN	OligoDeoxyriboNucleotide
ORF	Open Reading Frame
$p6^{Gag}$	p6 domain at C-terminus of Gag
PBS	Primer Binding Site
PCR	Polymerase Chain Reaction
PCP	*peumocytis carinii* pneumonia
PEP	Post Exposure Prophylaxis
PIC	Pre-Integration Complex
PI (4,5) P_2	Phosphatidyl inositol (4.5) bisphosphate
PM	Plasma Membrane
Pol	Polymerase
Poly-A	PolyAdenine
PPT	PolyPurine Tract
PPTc	Central PolyPurine Tract
PR	Protease
PRR	Proline-Rich Region
Psi	(Ψ) Packaging signal
PTAP	Proline-Threonine-Alanine-Proline
Rev	Viral Regulatory Protein
RNA	RiboNucleic Acid
RNAP II	RNA polymerase II

RNase	Ribonuclease
RNP	RiboNucleoProtein
RPL7	Ribosomal Protein L7
RRE	Rev Responsive Element
RSV	Rous Sarcoma Virus
RT	Reverse Transcriptase
SDS	Sodium Dodecyl Sulfate
SIV	Simian Immunodeficiency Virus
SP	Spacer Peptide
SP1	Spacer 1
SP2	Spacer 2
SU	Surface Subunit
TAR	Tat Responsive element
Tat	Trans Activator of the Transcription
TBE	Tris Borate EDTA
TIRF	Total Internal Reflection Fluorescence Microscopy
TM	Trans-Membranous
TMG	TriMethylGuanosine
TMgp41	Transmembrane glycoprotein
TNF-α/β	Tumor Necrosis Factor α/β
Tris	Tris(hydroxymethyl)aminomethane
tRNA	Transfer Ribonucleic Acid

Tsg101	Tumor susceptibility gene 101
U3	Single 3 'sequence of the genomic RNA
U5	Single 5 'sequence of the genomic RNA
UNAIDS	United Nations Joint Programme on HIV/AIDS
UTR	Untranslated Region
UNG2	Nuclear Uracil-DNA Glycosylase 2
Vif	Viral infectivity factor
VLPs	Virus Like Particles
VHL	Von Hippel–Lindau tumor suppressor protein
Vpr	Viral protein R
VPS	Vacuolar Protein Sorting system
Vpu	Unique Viral Protein
vRNA	Viral RNA
WF	Wide-Field
WHO	World Health Organization
ZF	Zinc Finger

Bibliographic Review

INTRODUCTION

1. Human Immunodeficiency Virus

The human immunodeficiency virus (HIV) is a single-stranded, enveloped RNA lentivirus of the retrovirus family (*retroviridae*) and is the etiological agent of acquired Immunodeficiency Syndrome (AIDS). The family name retroviridae comes from the concept that they replicate by the reverse transcription of their genomic RNA (gRNA) into a linear double-stranded DNA copy and the subsequent covalent integration of this DNA into the host cell genome (Flint S.J. 2004). Furthermore, the AIDS is characterized by state of low immunity that leads to several illnesses due to a wide range of opportunistic infections and neoplasms (Strauss. 2002; Flint S.J. 2004).

1.1 Epidemiology and history of HIV infection

The unique pattern related to outbreak of *peumocytis carinii* pneumonia (PCP) (Gottlieb, Schroff et al. 1981) and Kaposi sarcoma (KS) (Friedman-Kien 1981) in 1981, leads to the first clinical AIDS. The Centers for Disease Control and Prevention (CDC) named these patterns of conditions the AIDS as these conditions of a rare opportunistic infection and neoplasm were known to be associated with severely suppressed immune status.

However, the first clue to AIDS etiology came in 1983 after the isolation of the virus from lymph nodes of a patient suffering with cervical lymphadenopathy. Françoise Barré-Sinoussi, Luc Montagnier, and co-workers found core proteins p25 of this virus immunologically unique, being only immune-precipitated with patient serum, hence they gave the isolate a different name: lymphadenopathy-associated virus (LAV) (Barre-Sinoussi, Chermann et al. 1983). Followed by this, another similar discovery by research group led by Robert Gallo (Gallo, Sarin et al. 1983), ICTV recommended the name HIV in 1986 (Flint S.J. 2004).

1.2 Genetic variability, grouping and distribution

High mutation and recombination of Reverse transcriptase enzyme is main case of HIV-1 evolution and genetic variability which leads to diverse populations of viral quasi-species in each infected individual, differing by up to 10% (Thomson, Perez-Alvarez et al. 2002). On the basis of variability in the envelope (*env*) gene, HIV-1 can be classified into four groups (Buonaguro, Tornesello et al. 2007): the "Major" group M, which accounts for more than 90% of HIV-1

infections; the "Outlier" group O that appears to be restricted to west-central Africa; the "New" group N, a group discovered in 1998 in Cameroon; and group P that has been identified in 2009 by J.C. Plantier, who isolated a new strain closely related to gorilla simian immunodeficiency virus from a Cameroonian woman (Plantier, Leoz et al. 2009). Within group M, there are nine genetically distinct subtypes or clades designated A, B, C, D, F, G, H, J and K, with no E or I groups, which have never been found in a pure form but combined with other subtypes in a recombinant form as A/E or A/I, …etc. HIV-1 subtypes are typically associated with certain geographical regions with the most widespread being subtypes C and A (Figure 1) and the Isolates may differ by 30–40% in the amino acid sequence of the gp120 SU protein (Lynch, Shen et al. 2009).

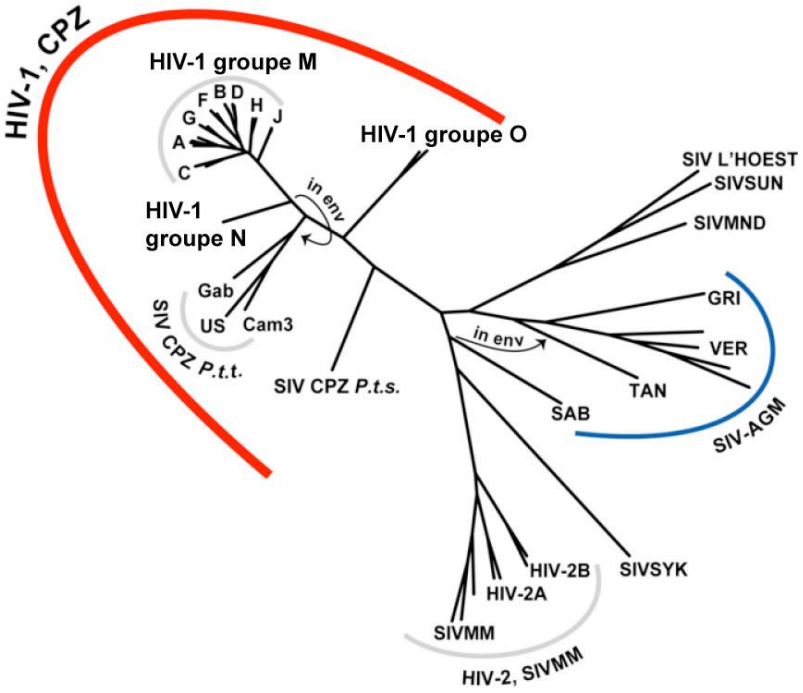

Figure 1: Phylogeny of primate lentiviruses. Five discrete groups of primate lentiviruses have so far been identified based on sequence analysis in *pol* gene. Members within each group share the same genomic organization and are more closely related to one another than to members of different groups. The human isolates are shown in color. For SIVmnd, SIVsyk, and SIVcpz, only one or a few isolates have been characterized and the prevalence in wild populations has not been determined. For HIV-1, HIV-2, SIVagm, and SIVmac, isolates appear to cluster within distinct clades (Nitahara-Kasahara, Kamata et al. 2007).

1.3 Global trend of HIV infection: an epidemic update

At the end of 2012, the WHO/UNAIDS reported a prevalence of 35.3 million [32.2 million–38.8 million] people estimated to be living with HIV, of which about 430,000 are children below the age of 15. The overall growth of the global AIDS epidemic appears to have been stabilized. Together with the significant reduction in mortality, the number of people living with HIV worldwide has increased (Figure 2)(WHO 2014). A comprehensive strategy implemented by the World Health organization (WHO) consisting in sustained and effective AIDS health education and health promotion programs, provides further evidence of decreasing incidence and safer sexual behavior among young adults. Accordingly, seven countries showed a statistically significant decline of 25% or more in HIV prevalence. Moreover, the number of people that are now receiving HIV antiretroviral therapy has been increased by 30% by the end of 2012 to reach 5 million worldwide (WHO 2014).

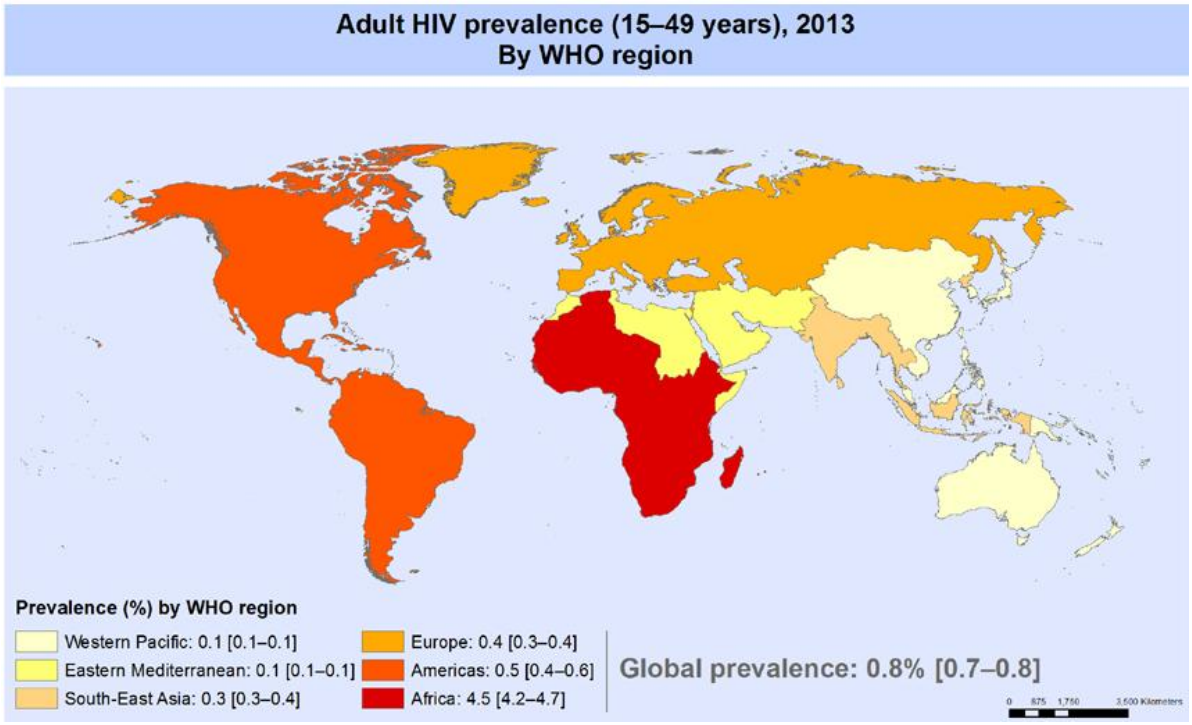

Figure 2: Global prevalence of HIV-1 infection in 2013. Estimated prevalence among young and adults per country, at the end of 2013(WHO 2014).

1.4 Modes of transmission

The virus can be present in most biological fluids and secretions of the infected patient that contain CD4+ T-lymphocytes, monocytes and macrophages (Flint S.J. 2004). The majority of HIV-1 infections, accounting for about 80%, are acquired through unprotected sexual contacts, either heterosexual (70%) or homosexual (10% of the total percentage). Additionally, the susceptibility of HIV infection increases considerably with the presence of ulcerative genital lesions due to other sexually transmitted diseases (Boily, Baggaley et al. 2009). Second mode of infection is associated with transfusion of contaminated blood and blood products that account for 5% of all transmissions (David L. Heymann. l.. Washington DC 18th (edn) 2004). Lastly, maternal transmission of HIV is also responsible for more than 90% of all HIV infections in infants and children (Cavarelli and Scarlatti 2011).

1.5 AIDS, the final stage of HIV infection

Lowering of CD4+ T lymphocyte count to <500 per µl (normal value 600–1200 cells/µl) referred as AIDS related complex (ARC) formation and the loss of cell-mediated immunity. Further decrease in CD4+ T-cell counts (<200 cell/µl) leads the onset of frank AIDS. At this point, the infected individual becomes susceptible to a variety of opportunistic infections and neoplasms and death usually proceeds within an average time interval of 9 months (Figure 3)(Pantaleo, Graziosi et al. 1993; Fauci A.S. 1997).

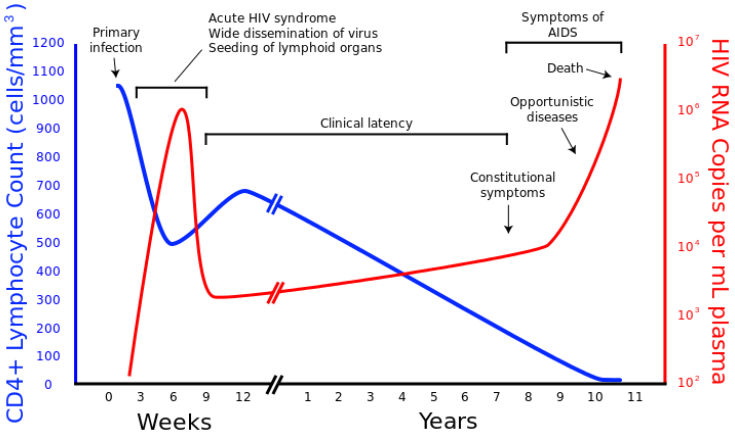

Figure 3: Typical course of HIV infection. Patterns of CD4+ T-cell decline (blue curve) and virus load increase (red curve) over the average course of untreated HIV infection; any particular individual's disease course may vary considerably. During the period following primary infection, HIV disseminates widely in the blood and lymphoid tissue; an abrupt decrease in CD4+ T cells in the peripheral circulation is often seen. An immune response to HIV ensures, with a decrease in detectable viremia. A period of clinical latency follows, during which CD4+ T cells counts continue to decrease, until they fall to a critical level below which there is a substantial risk of opportunistic infections (Pantaleo, Graziosi et al. 1993).

1.6 Prevention and control of HIV-1 infection

The CDC suggests post exposure prophylaxis (PEP) for HIV negative person who has recently been exposed to HIV for any reason. The risk of sero-conversion can be reduced by the use of Anti-RetroViral (ARV) drugs for at least four weeks (Smith, Grohskopf et al. 2005). Apart from this, the highly active antiretroviral therapy regimen (HAART) reduce considerably HIV morbidity and mortality (Adamson and Freed 2008). HAART regimens combine three drugs belonging to at least two classes of the 35 commercially available ARV agents: typically two nucleoside analogues reverse transcriptase inhibitors (NRTIs), plus either a protease inhibitor or non-nucleoside reverse transcriptase inhibitor (NNRTI) (Dybul, Fauci et al. 2002; Services 2011). However, HIV is known for its drug resistance due to high error rate of reverse transcriptase enzyme that represents a major barrier to the development of effective antiviral therapy (Adamson and Freed 2008). On the other hand, most ARV drugs are metabolically toxic, with low therapeutic indexes, and cause many adverse effects leading to poor patient compliance and adherence to treatment (Carr 2003; Calmy, Hirschel et al. 2009).

Next, considerable efforts are being performed in developing a potent vaccine against HIV. In this regard, Virus-Like Particles (VLPs) produced by Gag polyproteins of HIV and SIV have been shown to be potent stimulators of both cellular and humoral immune responses in animal models and therefore can be potentially excellent vaccine candidates (Gallo, Sarin et al. 1983; Jaffray, Shephard et al. 2004). However, a novel indicator for the design of a powerful antibody-based HIV vaccine should correlates with the isolation of multiple HIV broadly neutralizing monoclonal antibodies (MCAb) (Walker, Huber et al. 2011) which can be up to 10-100 fold more potent than the recently described PG9, PG16 and VRC01 (Binley, Wrin et al. 2004; Walker, Phogat et al. 2009; Wu, Yang et al. 2010; Walker, Huber et al. 2011).

2. Viral Life Cycle

The virus targets CD4+ bearing cells, which include dendritic cells, and macrophages and monocytes of the immune system (Roitt 1989). The life cycle of HIV-1 starts with the interaction of gp120 viral proteins with the CD4+ receptor on host cell. Next, membrane fusion is promoted by an additional interaction with a chemokine receptor, including CXCR4 and CCR5 (Clapham and Weiss 1997).

Membrane fusion is followed by the entry of the viral core into the cytoplasm. The two strands of viral RNA are then reverse transcribed into DNA by the viral RT. Once synthesized, the viral DNA is transported to the nucleus as part of a pre-integration complex composed of integrase, matrix, RT and Vpr, as well as the cellular host protein HMG-I. Then viral RNA is covalently integrated into the host cell genome by the catalytic activities of integrase (Turner and Summers 1999).

(A) **(B)**

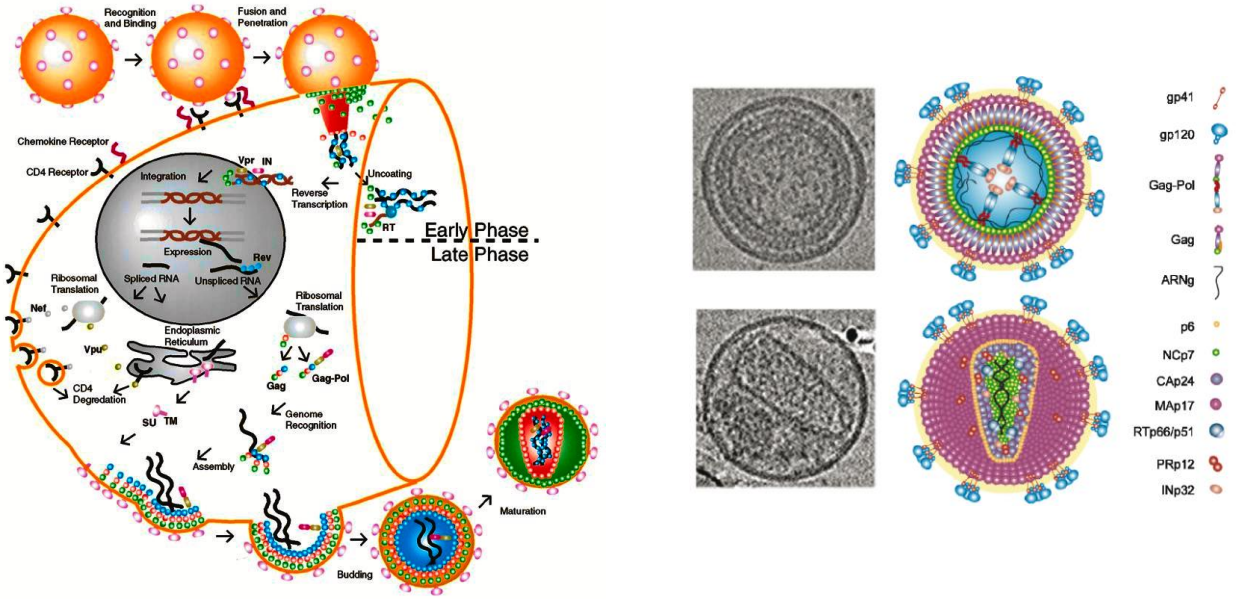

Figure 4: (A) General Features of the HIV-1 Replication Cycle and (B) Models for HIV-1 particle structure. During the early phase of replication (upper portion of the diagram), envelope glycoproteins on the surface of the virus bind to CD4 (black) and chemokine (red) receptors on the cell surface, triggering fusion of the viral and cellular membranes. During or after uncoating of the core (orange), the viral RNA genome is reverse-transcribed to proviral cDNA, which is transported to the nucleus and integrated into the cellular DNA by the viral integrase enzyme. Transcription during the late phase (lower portion of the diagram) produces the full-length viral RNA, which is capped at the 5′-end and polyadenylated at the 3′end by the cellular machinery and transported to the ribosomes. Translation of the unspliced RNA produces the viral Gag and, through an occasional read-through, Gag-Pol proteins, which assemble and bud to form immature particles. Proteolytic cleavage of Gag by the viral protease releases the matrix (MA, green), capsid (CA, pink) and nucleocapsid (NC, blue) proteins, which rearrange to form the mature particle (Lu, Heng et al. 2011).

After integration, the viral genome is transcribed into messenger RNAs (mRNAs) by the host machinery including RNA polymerase II. This RNA polymerase has to be activated by two molecular switches located in two regions at each end of the proviral DNA called long terminal repeats, LTRs. These LTRs are prepared for transcription by binding of NF-κβ/rel protein, which function to increase the transcriptional activity of the gene (Greene 1993).

Initially, short spliced RNA transcripts of about 2000 bases in length are produced which code for the regulatory proteins of the virus, e.g. Tat, Rev, and Nef. The Tat protein binds to the *trans* activation region (TAR) within the viral RNA leading to a phosphorylation of the RNA polymerase by a human kinase (Herrmann and Rice 1995). This phosphorylation augments transcription of the proviral DNA by at least 1000-fold. The Nef protein is believed to function in modifying the host cell to make it more suitable for manufacturing the HIV virion (Greene 1993). The third regulatory protein, Rev, is important for switching early phase infection into late stage infection by promoting transport of unspliced RNA transcripts to the cytoplasm (Turner and Summers 1999).

In the late stage, two new classes of RNA transcripts appear: long (unspliced) transcripts of 9,200 bases and medium length (singly spliced) of some 4,500 bases. Once the long and medium length transcripts reach the cytoplasm, the cellular machinery begins constructing the components of the new virus. *Gag* encodes the core proteins, *pol* encodes reverse transcriptase (RT), protease, integrase, and *env* encodes the two envelope proteins. In addition three other proteins are encoded for by the vpr, vif, and vpu genes essential for virus replication (see Figure 5). The viral particles then migrate to the outer surface of the cell and obtain their lipid bilayer when budding from the host cell. Subsequent to budding, the Gag polyproteins (hereinafter in this thesis, Gag polyprotein will be referred as Gag) are cleaved by the viral protease to produce the independent enzymes as well as the matrix, capsid, and nucleocapsid protein leading to the formation of the mature virus.

On the basis of literature and observed by cyro-EM, with the maturation of virion, MA remains associated with the viral membrane, GagNC interact with the dimeric gRNA, and CA forms a conical core shell enclosing the NC-RNA complex. This structural reorganization leads to mature infectious virion which disassembles upon entry into a new cell (Figure 4B) (Adamson and Freed 2007; Briggs and Krausslich 2011).

2.1 Structure of the viral particle

Mature HIV is roughly spherical particles measuring about 80-120 nm in diameter, surrounded by a lipoprotein envelope (Brugger, Glass et al. 2006) and studded with ~10 spikes separated from each other by about 22 nm (Zhu, Chertova et al. 2003). These spikes are composed of a trimer of envelope proteins gp120 [SU] and gp41 [TM] (Checkley, Luttge et al. 2011). HIV

envelope also contain a number of cellular proteins including proteins of MHC I, MHC II, and the intercellular adhesion molecules ICAM1, LFA1, CD28 and CD86 (Ott 2008). Its outer shell is formed of approximately 2000 copies of MA (p17), whereas ~1500-2000 copies of the capsid protein (CA, p24) that form a conical capsid core situated in the center of the viral particle (Fig. 5). This capsid core encloses two copies of the unspliced viral genome which is coated with approximately 2000 copies of the nucleocapsid protein (NCp7), ~10-12 copies of $tRNA_3^{Lys}$ (Isel, Ehresmann et al. 2010), the viral encoded enzymes: protease (PR), reverse transcriptase (RT) and integrase (IN) and a number of viral and cellular proteins (Ott 2008).

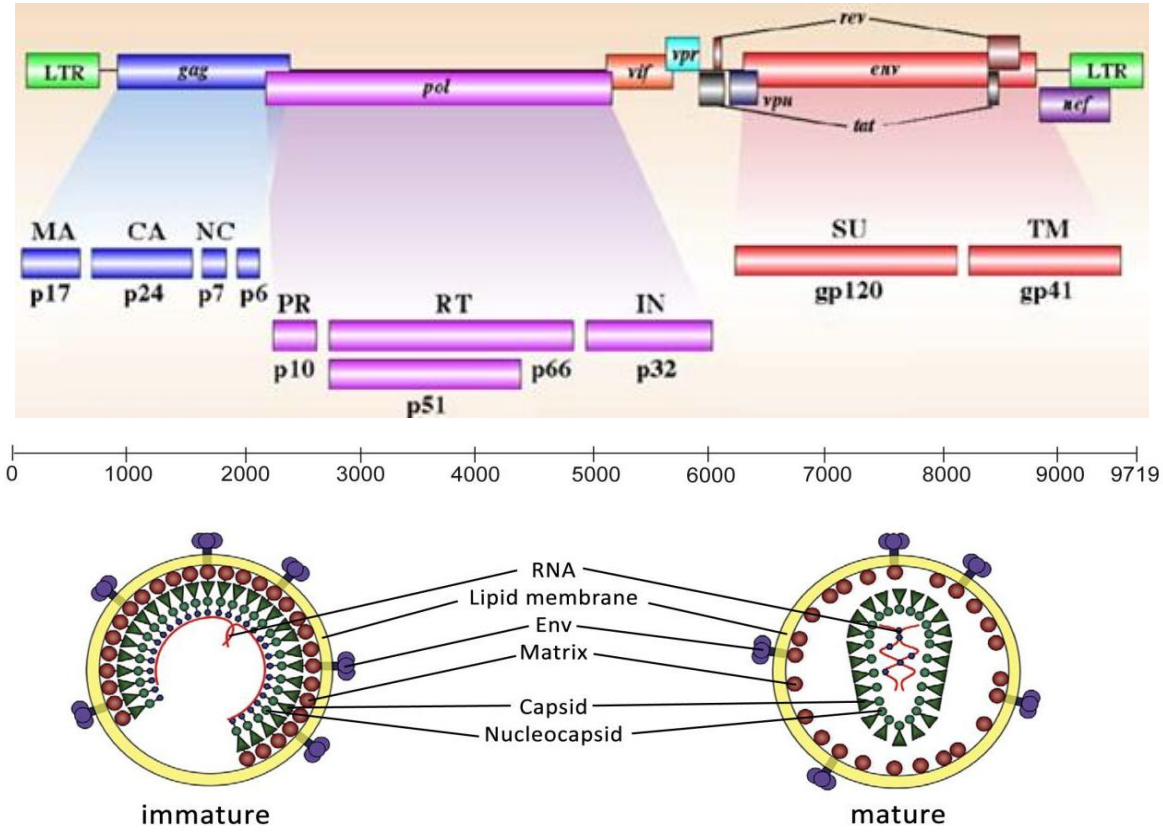

Figure 5: HIV-1 genome organization and virion structural features.
Above, the HIV-1 genome encodes 3 main genes: *gag*, *pol*, and *env*, as well as the accessory proteins *vif, vpu, vpr, tat, rev*, and *nef*. The RNA transcripts that give rise to these proteins are generated as unspliced (*gag* and *pol)*, singly spliced (*env, vif, vpr, vpu)* or multiply spliced (*tat, rev, nef)*. For *tat* and *rev*, the 5‘ and 3‘ exon splice junction sites are marked by a bold line. Sequences found at both the 5‘ and 3‘ ends of the genome contain the long-terminal repeats (LTRs), regions that dictate viral RNA synthesis and integration, while genome packaging into new progeny virions is directed by the packaging signal *psi* at the 5’ terminus of the transcript. The HIV-1 genome in this illustration is based on the HXB2 isolate. Below, a schematic of the structural features of the two virus forms: immature (left) and mature (right). The immature virus is characterized by a thick layer of uncleaved gag polyproteins underlying the virion membrane, whereas proteolytic processing of the gag polyproteins during maturation gives rise to a cone-shaped core that encloses the viral RNA and additional viral proteins. This processing step renders the virus infectious. Adapted from (Ganser-Pornillos, Yeager et al. 2008).

2.2 Structural and genetic organization of HIV-1 genome

2.2.1 The proviral DNA

The proviral cDNA is flanked by two LTRs and are divided into 3 domains (Figure 7): U3 (-454 to 1), the repeat sequence R (+1 to +94) and U5 (+95 to +179). The U3 region is further subdivided into: (i) the core promoter (-78 to 1), which harbors the TATA box (-25 to -50), (ii) the activator domain (-104 to -79) and (iii) the modulator domain (-454 to -105), which contains the direct repeat sequence (a stretch of 70-100 nt) that engaged in stimulating the transcription (Gaynor 1992; Jones and Peterlin 1994; Reicin, Paik et al. 1995; Coffin JM 1997). Three different classes of mRNA are being transcribed by active gene expression of this proviral cDNA, including the full-length species that forms the viral genome.

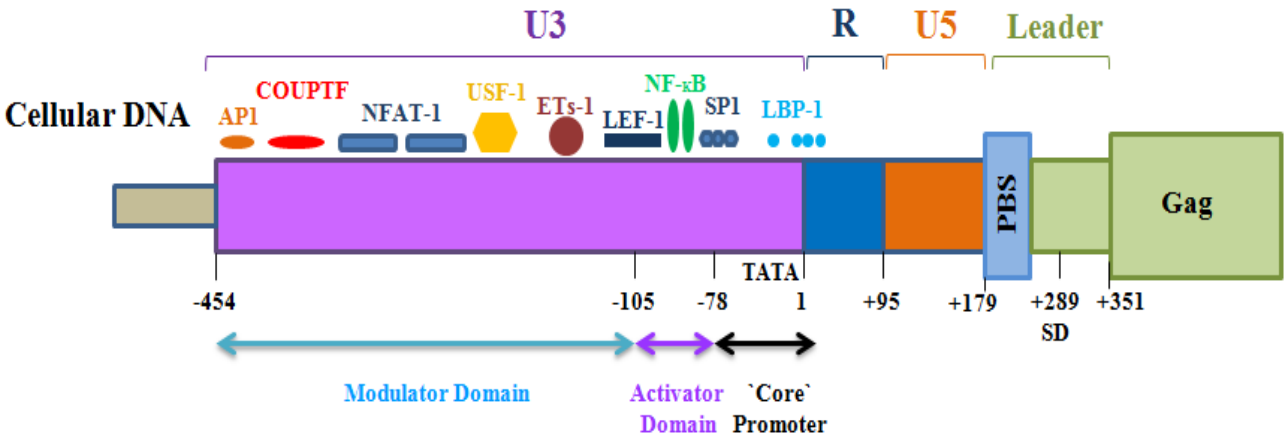

Figure 6: Illustration of the 5' LTR of proviral DNA integrated into the host genome. The LTR is divided into three regions U3, R and U5. The transcription starts at the beginning of the region R and the binding sites recognized by different transcription factors of RNAP II. These sites are represented upstream and are characterized into three regions: the "core" of the promoter (TATA box), the activator domain and the modulator domain(Ekram W. Abd El-Wahab, Redmond P. Smyth et al. 2014).

2.2.2 The viral genomic RNA

The HIV-1 genome is packaged as two 9,200 nucleotides long single stranded RNAs of positive polarity. Genome is modified post-transcriptionally in a similar way to eukaryotic mRNAs by the addition of a 3'-end tail of 100 to 200 A residues and a 5'-end cap, albeit with a trimethylguanosine (TMG)-capping (Yedavalli and Jeang 2010) (Figure 7). Furthermore, these

RNA molecules are associated non-covalently as a dimeric complex in a region near the 5'-end through the DLS (Dimer Linkage Structure) (Bender, Chien et al. 1978). Both copies of genomic RNA are full-length RNA, identical in term of cis acting sequences and are packaged as dimer giving rise to pseudo-homozygotes viruses (Temin 1995).This packaging also provides the opportunity for frequent template switching during reverse transcription, resulting in the generation of recombinant viruses genetically distinct from the two parental viruses and directly responsible for the spreading of resistant viruses (Coffin 1979; Hu and Temin 1990; Temin 1991; Rhodes, Wargo et al. 2003).

A. The Non-coding regions

The 5'-untranslated region (UTR) adopts complex secondary and tertiary structures that are involved in key steps of viral replication cycle (Figure 7). Based on extensive *in-vitro* and *ex-vivo* chemical and enzymatic studies, mutational analysis and phylogenetic comparison (Harrison and Lever 1992; Baudin, Marquet et al. 1993; Hayashi, Ueno et al. 1993; Clever and Parslow 1997; Damgaard, Dyhr-Mikkelsen et al. 1998; Clever, Miranda et al. 2002; Paillart, Dettenhofer et al. 2004; Wilkinson, Gorelick et al. 2008; Watts, Dang et al. 2009), its secondary structure was predicted (Figure 7).

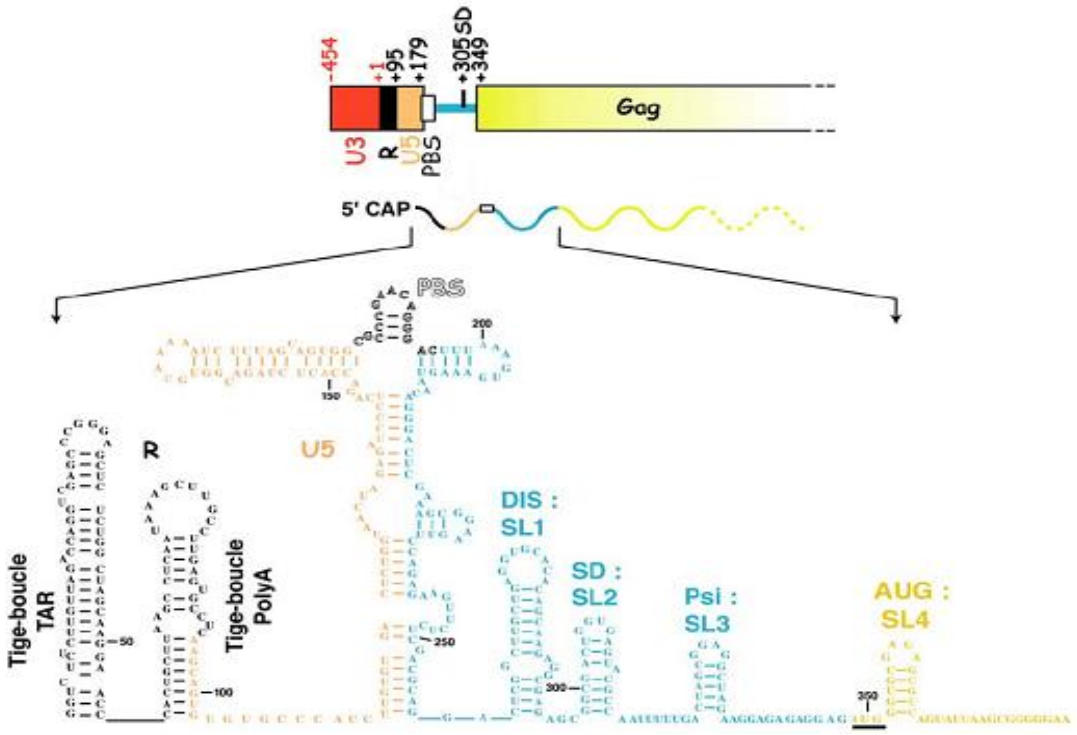

Figure 7: Secondary structure of the translated region 5 'of the MAL isolate of HIV-1 (adapted from (Berkhout 1996)).

A.1. The R region

The R region (Repeat) (98 nucleotides in HIV-1) is present as two copies of same polarity on both ends of the genome. At 5 ' end, it corresponds to the start site of transcription +1 and the cap site. This highly structured region can further be divided into two sub-domains with different functions:

(i) A stem loop called TAR (Trans-Activating Response element) comprises of 55 to 59 nucleotides (Figure 7). This sequence is important during the first strand transfer of the reverse transcription. It is also involved in the regulation of transcription of viral DNA *via* the Tat protein and it has been shown to bind with the protein cyclin T1 (Rana and Jeang 1999). Mutations affecting the sequence or the structure of TAR at its 5’ or 3' end, decreases viral replication (Klaver and Berkhout 1994; Klaver and Berkhout 1994; Das, Klaver et al. 1998).

(ii) A stem-loop containing the polyadenylation signal (AAUAAA), which is responsible for the addition in 3' poly (A) tail. This tail is necessary for the maturation of mRNA. It has been shown

that stabilization or destabilization of this stem-loop causes a defect in viral replication (Lopez-Lastra, Gabus et al. 1997).

A.2. The U5 region

The U5 region is composed of 83 nucleotides and is the first part of the genomic RNA to be retro-transcribed. A region of 18 nucleotides called PBS is present immediately at the 3' end of the U5 region that specifically binds to $tRNA^{Lys3}$.

A.3. The dimerization / packaging domain

This domain is important for dimerization of the genomic RNA and its selection in the packaging. It also contains the SD (splice donor site) for the splicing of mRNA. In HIV-1, this domain includes four stem-loops SL1 to SL4 (Harrison and Lever 1992; Clever and Parslow 1997).

The stem-loop SL1 displays a GC-rich 6-nt palindromic sequence at the top of its loop called the dimer initiation signal or DIS (Laughrea and Jette 1994; Paillart, Marquet et al. 1994; Skripkin, Paillart et al. 1994; Muriaux, Girard et al. 1995)and is essential for RNA dimerization (Skripkin, Paillart et al. 1994; Paillart, Marquet et al. 1996) as well as for RNA partner selection *in vivo* (Chin, Rhodes et al. 2005; Moore, Fu et al. 2007; Chen, Nikolaitchik et al. 2009). The auto-complementary nature of the DIS supports the initiation of Watson–Crick base pairing between the two HIV-1 RNA molecules and thus generating a “kissing loop” (Clever, Wong et al. 1996; Paillart, Westhof et al. 1997; Kieken, Paquet et al. 2006) structure. The most common DIS sequence is GCGCGC in subtype B and GUGCAC in subtype A, C and G of HIV-1 strains.

Furthermore, the SL2 loop containing the SD (splicing domain), a motif of nine nucleotides, CUG-GUGAGU, where the dash between nucleotides represent the cleavage site, which is considered as major splice donor site (O'Reilly, McNally et al. 1995). It is located in the upper part of a short stem-loop. This means that all HIV-1 transcripts are cleaved at this point by the spliceosome except the full-length RNA. The SL3 loop also called psi (Ψ), which is the major site of packaging, has been considered for a long time the only essential loop for packaging (Lever, Gottlinger et al. 1989; Kuzembayeva, Dilley et al. 2014). More recent studies have shown that several sequences upstream of SL3, including the SL1 loop, were also essential for a

specific encapsidation of genomic RNA (Ekram W. Abd El-Wahab, Redmond P. Smyth et al. 2014). Finally, SL4 loop contains the AUG start codon of Gag (Nikolaitchik, Dilley et al. 2013).

A.4. The U3 region

The U3 region at 3' end composed of approximately 450 nucleotides and contains the signals required for the regulation of transcription of proviral DNA into viral RNA with the help of transcription machinery of the host cell (Gaynor 1992).

There are other non-coding regions within the viral genome:

The PPT (Poly purine Tract) and PPTC (Poly purine Tract central) are purine-rich domains of the RNA genome. The 3' PPT is located immediately upstream of U3 sequence of the 3' LTR of the proviral genome, while the PPTC is located in the open reading frame of the pol gene (Charneau, Alizon et al. 1992). The RNase H activity of reverse transcriptase degrades the viral genomic RNA during the synthesis of double-stranded DNA, with the exception of two purine rich sequences which serve as primers for the synthesis of the (+) strand DNA.

RRE (Rev Responsive Element) is composed of 351 nucleotides, consists of several sequences of stem-loops and is located in the *env gene*. It interacts with the Rev protein of HIV-1, which facilitates nuclear export of non- or semi-spliced viral transcripts (Felber, Hadzopoulou-Cladaras et al. 1989).

B. The coding region

The coding region of HIV-1 is much more complex than in other retroviruses. In addition to the classic three genes *gag*, *pol* and *env*, it encodes for other viral proteins like Tat, Rev, Nef, Vif, Vpr and Vpu (Figure 8).

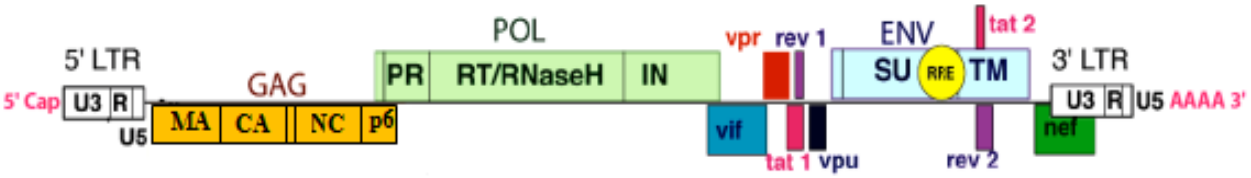

Figure 8: Landmarks of the HIV-1 genome. Genetic organization of HIV-1 genome. Positions of 5' Cap, 3' polyadenylation tail, LTRs and RRE are indicated; ORFs are shown as rectangles. (Paillart, Shehu-Xhilaga et al. 2004).

2.3 Viral protein synthesis

Eukaryotic translation begins with the recruitment of the small ribosomal subunit (40S subunit) on the mRNA and its movement until it reaches and localizes the initiation codon (the initiation step) in a favorable *Kosak* context (A/G)CCAUG. Next step corresponds to the elongation phase where the ribosome decodes the mRNA and links residues in order to get the protein translation. This elongation stops when the ribosome reads one of three possible termination codons (UGA, UAA or UAG) (Alkalaeva, Pisarev et al. 2006). This final step corresponds to the ribosome recycling for the next round of translation (Pisarev, Hellen et al. 2007).

As for cellular mRNA, viral RNAs are capped at their 5' extremity and poly- adenylated at their 3' end. These two phenomenons are required for efficient mRNA translation initiation by the 5' cap-dependent initiation mechanism. Translation starts with interaction of eIF2-tRNA^{Met} with the 43S pre-initiation complex (40S ribosome subunit + eIFs). This complex later interacts with the 5'-capped RNA via eIF4F. This latter factor is a DEAD-box RNA helicase that unwinds RNA structures of the 5'UTR, initiating ribosomal scanning till the AUG codon. The 60S large ribosomal subunit can then join to the 40S ribosomal subunit and thus assembling an 80S ribosome. This 80S complex is competent for the elongation step (Pestova, Lomakin et al. 2000).

Nevertheless, for viruses and in particular for HIV, the limiting process during its RNA translation is its folded structure and the length of 5'UTR. To overcome this difficulty, internal initiation takes place at the level of the internal ribosome entry site (IRES)-mediated translation initiation site (Balvay, Soto Rifo et al. 2009). In this case, the 43S pre-initiation complex containing eIF4G and eIF4A binds directly into internal stem loop initiating the scanning to the initiation codon. All viral proteins are synthesized on free polysomes in the cytoplasm except for the precursor Env p160, which is synthesized in the rough endoplasmic reticulum (RER).

2.3.1 Viral structural proteins

A. Gag protein

Gag protein will be described in later sections of thesis.

B. The viral envelope protein (Env)

The *Env* protein is expressed as the precursor gp160 from a bi-cistronic mono-spliced mRNA. Like all surface glycoproteins, *Env* is synthesized in the RER and migrates through the Golgi apparatus where it undergoes glycosylation. Subsequent maturation processing yields the gp120 surface subunit [SU] and gp41 *trans*-membranous subunit [TM] (Checkley, Luttge et al. 2011). The gp120 exists as a trimer located on the surface of the infected cells and of the virions, where it is linked non-covalently to the gp41 (Figure 9).The gp120 harbors five hypervariable regions, V1-V5 interspersed with five constant regions (C1 to C5). On the other hand, gp41 is composed of an N-terminal ectodomain, which contains the fusion peptide, a *trans*-membrane domain, and a C-terminal intravirion segment that interacts with MA (Figure 9)(Checkley, Luttge et al. 2011).

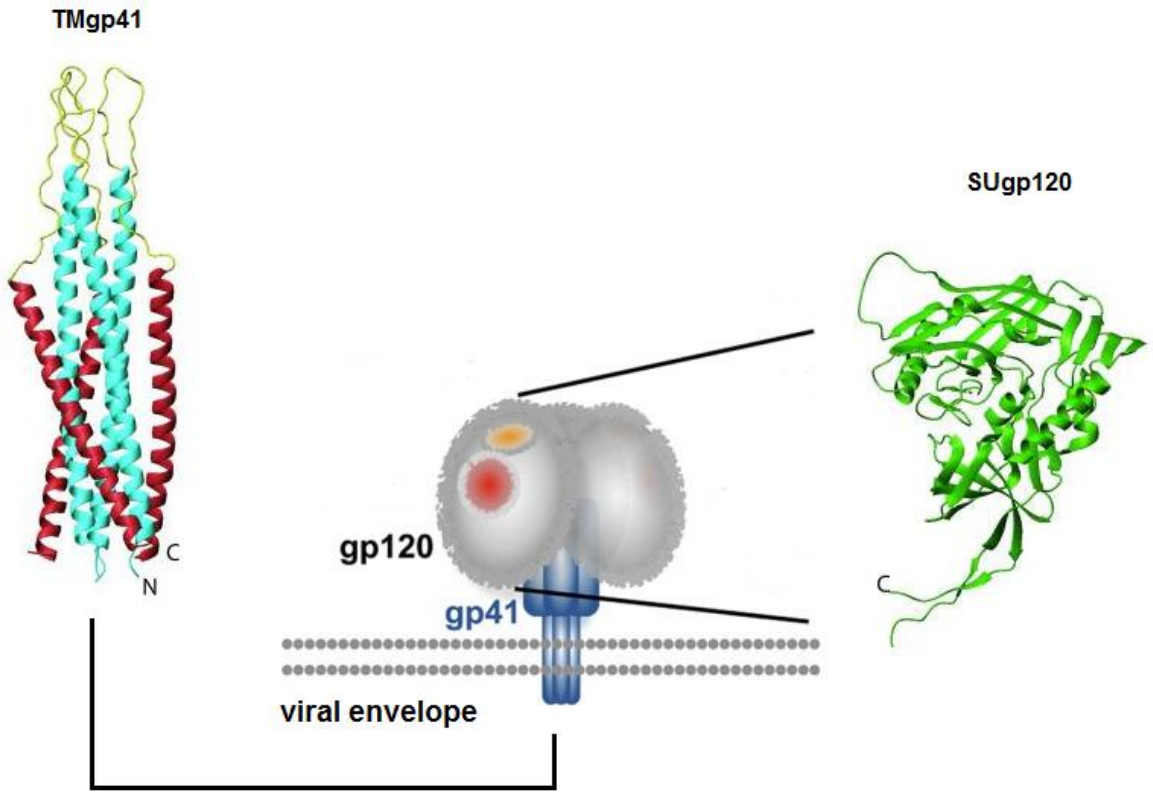

Figure 9: Structure of envelope proteins of HIV-1 (Caffrey 2011; Guttman, Kahn et al. 2012).HIV-1 Membrane proteins oligomerize in heterotrimeric. The three-dimensional structures represent a SUgp120 surface subunit of HIV-1 of one hand and the ectodomain of the transmembrane subunit under TMgp41 VIS in other hand.

2.3.2 The viral enzymes

2.3.2.1 The viral protease

It is a member of the aspartyl protease family, is expressed as a *Gag-Pol* fusion protein and is released by an autocatalytic mechanism. HIV-1 protease activity is required for cleavage of the *Gag* and *Gag-Pol* polyprotein precursors during virion maturation. The functional form of the protease enzyme is an asymmetrical homodimer stabilized by four-stranded antiparallel β-sheets formed by N- and C- terminal β-strands connected to each other by a β-turn and forms a flexible flap on top of the catalytic site (Figure 10)(Das, Prashar et al. 2006).

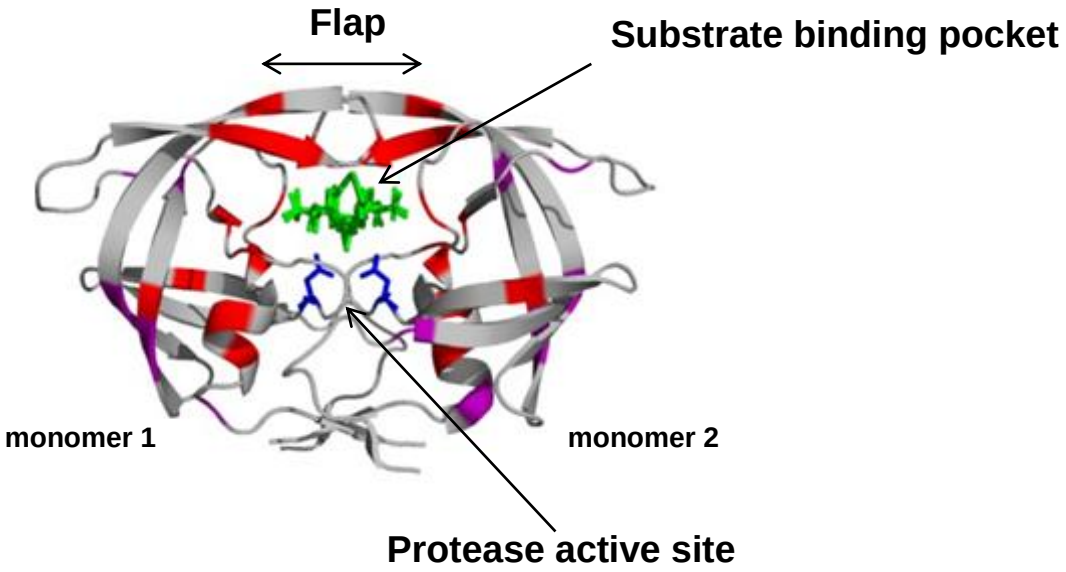

Figure 10: Crystal structure of HIV-1 protease. Structure of the HIV-1 protease in its functional form. The catalytic site composed of two Asp residues is shown in blue. In the binding pocket, there is a polypeptide substrate shown in green. (Lee, Potempa et al. 2012).

2.3.2.2 The viral reverse transcriptase (RT)

This enzyme is encoded by the *pol* gene, and is initially packaged into virions as a *Gag-Pol* precursor (Herschhorn and Hizi 2010). Its proteolytic cleavage primarily produces a homodimer of two p66 molecules each containing both a polymerase and an RNase H domain. The RNase H domain is subsequently removed by proteolysis from one of the subunits giving the mature p51/p66 RT heterodimer. The polymerase domain is composed of four subdomains known as the "fingers", "palm", "thumb", and "connection" which connects the polymerase and RNase H domains (Figure 11). RT has RNA-dependent and DNA-dependent polymerase activities and

acts to catalyze the process of reverse transcription to convert the viral genome into a double-stranded DNA. The RNase H activity removes the original RNA template from the first DNA strand to allow the synthesis of the complementary DNA strand. However, RT has high error and mutation rates during synthesis of proviral DNA due to absence of 3'→5'exonucleolytic proofreading activity (Hu and Hughes 2012).

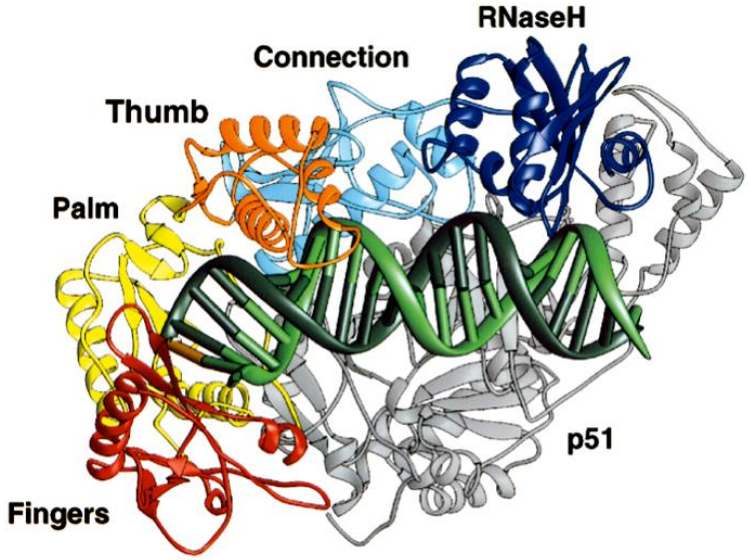

Figure 11: The structure of the HIV-1 RT catalytic complex. The polymerase active site is on the left and the RNase H domain on the right. The domains of p66 are in color: fingers (red), palm (yellow), thumb (orange), connection (cyan), and RNase H (blue); p51 is in gray. In the two chains, the domains have very different relative orientations. The DNA template strand (light green) contains 25 nucleotides, and the primer strand (dark green), 21 nucleotides. The incoming dNTP is in gold (Huang, Chopra et al. 1998).

2.3.2.3 The viral integrase (IN)

HIV integrase mediates the insertion of the HIV proviral DNA into the genomic DNA and is a 32 kDa protein product derived from the C-terminal portion of the *pol* gene (Ciuffi and Bushman 2006). The three-dimensional structure of the full-length HIV-1 integrase has been resolved by means of X-ray crystallography (Figure 12).The structure of IN contains three canonical domains connected by flexible linkers: an N-terminal HH-CC zinc-binding domain, a central catalytic core domain and a C-terminal DNA-binding domain (Karki, Tang et al. 2004; Cherepanov, Maertens et al. 2011).

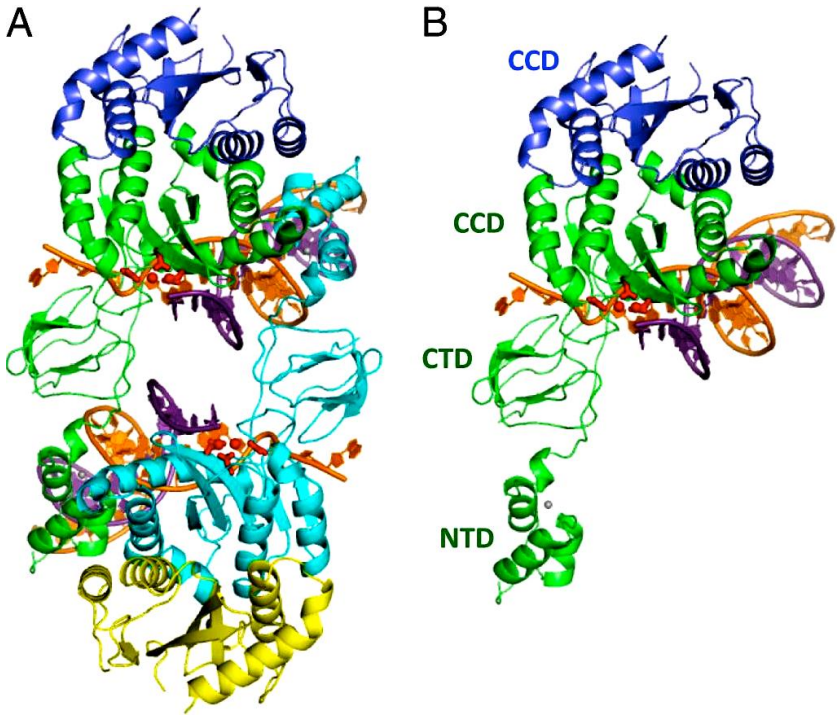

Figure 12: Architecture of the HIV-1 intasome. (A) The inner subunits of the IN tetramer, comprising residues 1–270 and engaged with viral DNA, are green and cyan; outer IN CCDs (residues 56–202) are blue and yellow. The reactive and non-transferred DNA strands are magenta and orange, respectively. Red sticks, side chains of inner monomer active site residues; red and gray spheres, Mn and Zn ions, respectively. **(B)** Resection of the upper IN dimer from A highlights the part of the model analogous to the PFV crystallographic asymmetric unit. Locations of canonical IN domains are indicated (Cherepanov, Maertens et al. 2011).

Several studies have shown the importance of the interaction of cellular cofactors with integrase for viral integration and infectivity. Among them, it has been shown a stable and functional complex between the wild-type full-length integrase and the cellular cofactor LEDGF/p75 that shows enhanced in vitro integration activity compared with the integrase alone (Michel, Crucifix et al. 2009). By using mass spectrometry and cryo-EM it was shown that the functional unit comprises two asymmetric integrase dimers and two LEDGF/p75 molecules (Michel, Crucifix et al. 2009). One integrase molecule performs the catalytic reaction, whereas the other one positions the viral DNA in the active site of the opposite dimer, shedding the light on the integration mechanism.

2.3.3 Viral regulatory and auxiliary proteins

2.3.3.1 The trans-activator of the transcription (Tat)

Tat is an RNA binding protein that acts as a *trans* activator of viral transcription (Pugliese, Vidotto et al. 2005) and can be found in two forms of 72 or 101 amino acids from two coding exon. The structure of Tat consists of four domains: the cysteine-rich segment, the core, a basic segment rich in arginine responsible for TAR recognition and binding, and a glutamine rich segment (Tahirov, Babayeva et al. 2010) (Figure 13). It is responsible for enhancing expression of some cellular factors including tumor necrosis factor beta (TNF-β), and transforming growth factor beta. On the other hand, it acts to suppress the expression of other cellular genes including bcl-2 and the chemokine, MIP-1α (Pugliese, Vidotto et al. 2005).

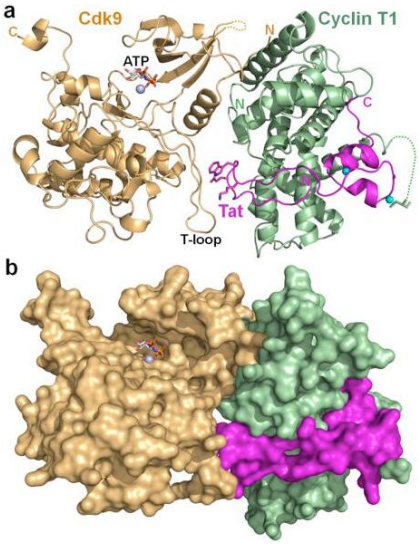

Figure 13: Overall structure of the Tat/PTEFb/ATP complex. (**a**)Ribbon representation and (**b**) surface representation of the Tat/PTEFb-ATP structure. Cdk9 is light orange, Cyclin T1 is pale green and Tat is magenta. The side chains of the Cdk9-interacting residues of Tat, Cys261 of Cyclin T1, and ATP analog are drawn as sticks, and the zinc and magnesium atoms are drawn as cyan and light blue spheres, respectively. The dashed lines represent the missing link between Lys88 and Gly35 of Cdk9 and between Leu252 and Cys261 of Cyclin T1 (Tahirov, Babayeva et al. 2010)

Furthermore, as far its functions are concern, Tat is considered to stimulate the RTion reaction through its ability to chaperone the annealing of the primer tRNA onto the viral RNA (Kameoka, Morgan et al. 2002) as well as the first cDNA strand transfer (Guo, Kameoka et al. 2003). It has been reported that Tat exhibits potent nucleic acid chaperone activities similar to those of the HIV-1 nucleocapsid protein NCp7 (Godet, Boudier et al. 2012) and of the Flaviviridae core protein (Ivanyi-Nagy, Lavergne et al. 2008), which is mediated by the basic 44-61 peptide sequence (Kuciak, Gabus et al. 2008; Boudier, Storchak et al. 2010).

2.3.3.2 The viral regulatory protein (Rev)

The protein Rev is a 13-kDa (116 residues) sequence-specific RNA binding protein and is trafficked into the nucleus after its synthesis in the cytoplasm. It is involved in the nuclear export of HIV unspliced and singly-spliced mRNAs by binding to the RRE (Suhasini and Reddy 2009). This Rev-mediated nuclear export enhances the encapsidation efficiency of RRE-containing lentiviral vector RNAs up to 200-fold, irrespective of whether RNAs have been spliced or not (Grewe, Ehrhardt et al. 2012). By using X-ray crystallography, three-dimensional structures of HIV-1 Rev and the multimeric RNA-protein complex that forms on the RRE has already been revealed (Fig. 14). It shows that Rev can form homo-tetramers and contains three functional domains: an arginine-rich RNA binding domain, a multimerization domain and an effector domain harboring an NES (Hammarskjold 2011).

a) **b)**

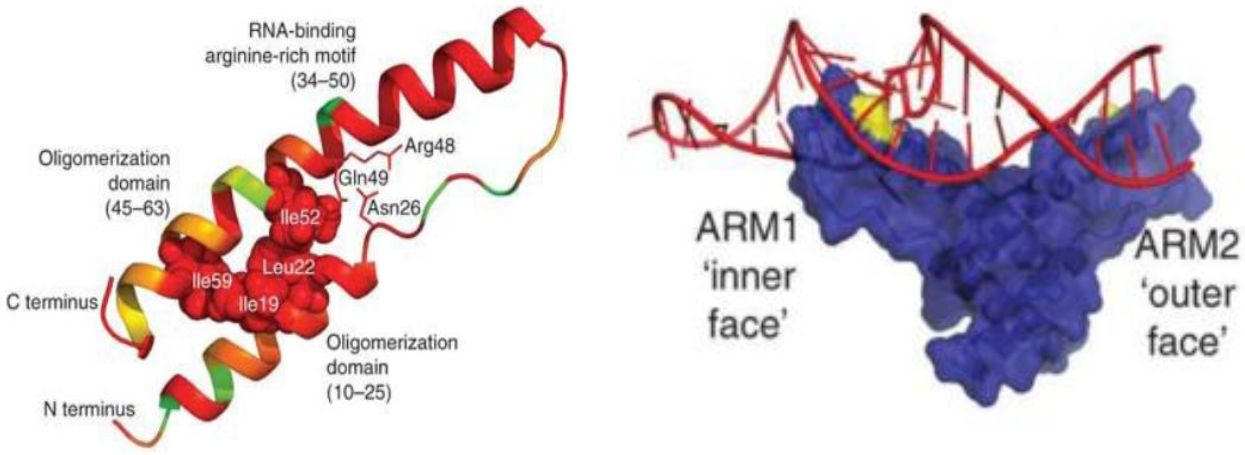

Figure 14: Structure of the Rev Dimer. (**a**) The folded core of a Rev monomer with its functional domains is shown. The amino acids prominent in mediating the core structure are specified. The different colors of the ribbon indicate amino acid conservation among 1201 HIV-1 isolates in the Los Alamos Sequence Database, with green representing the least conservation (26%) and red the highest (100%). **(b)** Model of the Rev dimer interacting with a model Rev Response Element (RRE) stem IIB binding site (Hammarskjold 2011).

2.3.3.3 The viral negative factor (Nef)

Nef is a 27-kDa protein and undergoes post-translational modification by phosphorylation and N-terminal myristoylation (Figure 15). It is encoded by a single exon that extends into the 3' LTR of a multispliced mRNA. At later stages of viral life cycle, it is cleaved by the viral protease

after packaging during virion maturation, however the relevance of this event is not clear (Turner and Summers 1999).

Nef plays a major role in the evolution of viral infection towards an immunodeficiency syndrome. It promotes virus dissemination by releasing virus from infect cells and by increasing cell/cell transfer of virions. However, it takes part in avoiding super-infection by down-regulating HIV-1 receptors like CD4 from plasma membrane (Laguette, Bregnard et al. 2010).

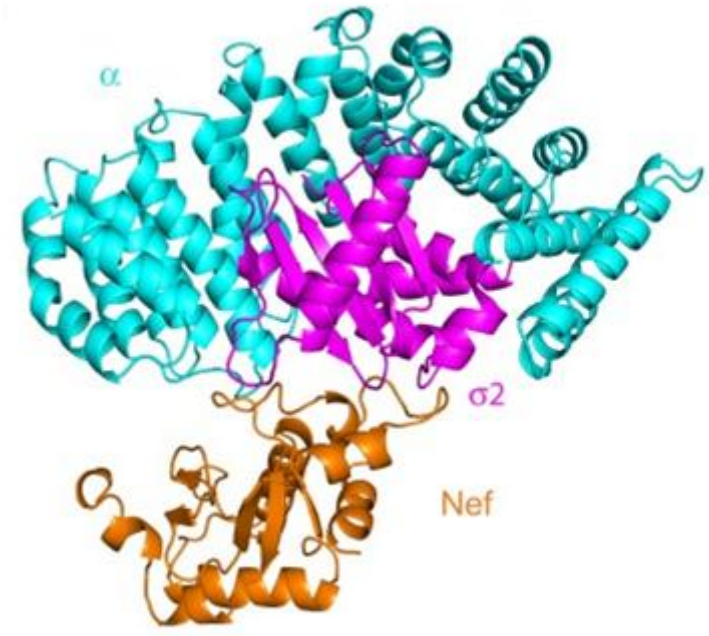

Figure 15: Three-dimensional structure of the complex formed between the Nef protein of HIV-1 and AP-2. Nef (orange) binds to the alpha subunits (cyan) and sigma 2 (magenta) of AP-2. (Ren X 2014).

2.3.3.4 The viral protein R (Vpr)

This protein is composed of 96 amino acids and about 12.7 kDa (Fritz, Briant et al. 2010). Vpr performs its functions over many steps in the retroviral cycle, particularly during the early phase where it may be involved in the fidelity of reverse transcription. Furthermore, Vpr is part of PIC and participate in the transit of the proviral DNA into the nucleus through its two NLS (Guenzel, Herate et al. 2014). Although the nuclear import of viral DNA process is still uncertain, it appears that Vpr is involved, especially in quiescent cells or macrophages cells latent kind, maintaining the PIC near nuclear pores (NPC) through its interaction with nucleoporin hCG1 (Le

Rouzic, Mousnier et al. 2002). Furthermore, it has recently been shown that Vpr is capable of reorganizing dsDNA more compactly (Lyonnais, Gorelick et al. 2013). Finally, Vpr also has the property to destabilize the nuclear membranes in the cell medium (Piller, Ewart et al. 1999; de Noronha, Sherman et al. 2001; Brugger, Glass et al. 2006), suggesting that Vpr may participate in passive PIC transit through the disturbed areas of the nuclear membrane (Figure 16).

NMR studies were performed to obtain the structure of Vpr and its various fragments, in different solvent condition, due to the aggregation prone of the protein and it was observed that the protein contains three helical domains (Figure 16). The first α-helix D17-H33, seems to be responsible for nuclear import and virion incorporation, the second α-helix, W38-Y50 appears to be responsible for the oligomerization of Vpr and the third α-helix, W54-R77, derives the nuclear transport and amplification of viral replication in non-dividing cells (Morellet, Roques et al. 2009). The protein adopts the same secondary and three-dimensional conformation, a similar orientation of the three amphipathic α-helices folding around a hydrophobic core, in pure H_2O as in presence of CH_3CN. Structure revealed that the three successive α-helices are mutually oriented to promote lipophilic interactions between the hydrophobic amino acid side chains of helix I, helix II and helix III (Morellet, Bouaziz et al. 2003).

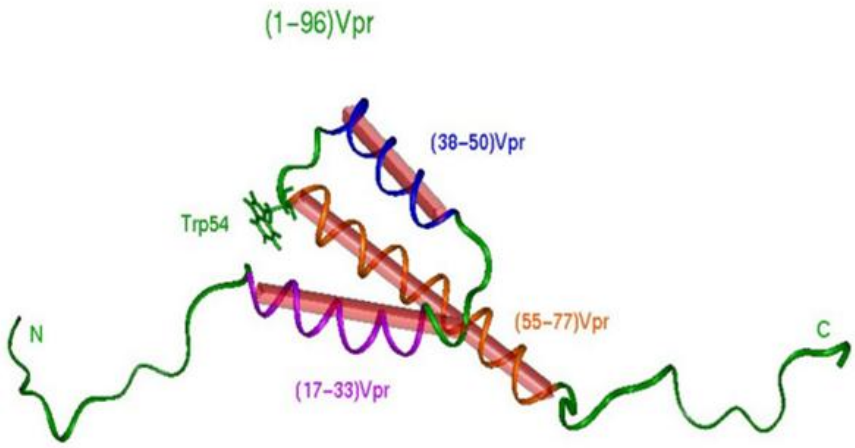

Figure 16: Three-dimensional structure of the HIV-1 Vpr protein (Morellet, Bouaziz et al. 2003). Alpha helices are colored in pink, orange and blue. The Trp54 residue responsible for interactions with cellular proteins is also highlighted.

Furthermore, it is considered as a regulatory protein that is incorporated in particles along the budding. This incorporation depends on NCp7 and p6 domains of Gag (de Rocquigny, Petitjean et al. 1997; Bachand, Yao et al. 1999). Interestingly, this incorporation is highly sensitive to the Vpr oligomerisation. In fact, Vpr was shown to form dimers and trimers in the cytoplasm and in

the nucleus (Fritz, Didier et al. 2008) that are essential for Gag recognition (Fritz, Briant et al. 2010; Fritz, Dujardin et al. 2010).

Among the range of functions of the Vpr protein, the Vpr-dependent G2 arrest activity was extensively explored since its discovery (He, Choe et al. 1995; Jowett, Planelles et al. 1995; Refaeli, Levy et al. 1995; Rogel, Wu et al. 1995). HIV-1 LTR was shown more active in the G2 phase, implying that the G2 arrest may confer a favorable cellular environment for efficient transcription of HIV-1(Goh, Rogel et al. 1998). The mechanism whereby Vpr indices G2 arrest involved many different pathways such as p34cdc2/cyclinB(Goh, Rogel et al. 1998), formation of a complex with p53 and sp1 transcription factor(Wang, Mukherjee et al. 1995; Sawaya, Khalili et al. 1998). More recently, the interaction of Vpr with the structure-specific endonuclease (SSE) regulator SLX4 complex (SLX4com) has been shown crucial for the G2-arrest activity (Laguette, Bregnard et al. 2014).

2.3.3.5 The viral protein U (Vpu)

It is a 16-kDa protein found as an integral membrane phosphoprotein primarily localized in the internal membranes of the cell (Maldarelli, Chen et al. 1993). The structure of Vpu consists of a hydrophobic NTD that functions both as signal and membrane anchor peptide, and a hydrophilic CTD, which protrudes into the cytoplasm (Figure 17). However, the 3-D structure of the full-length HIV-1 Vpu has not yet been determined (Dube, Bego et al. 2010).

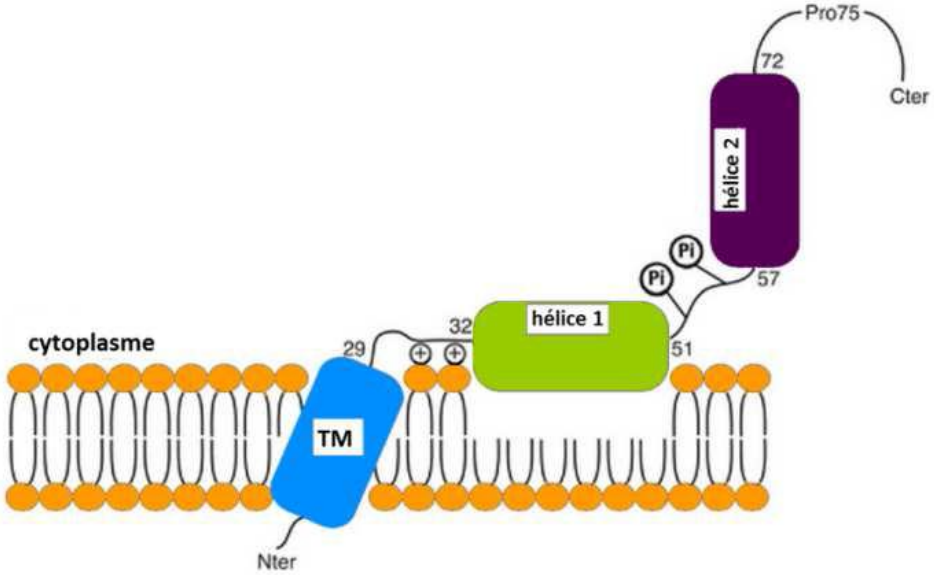

Figure 17: Schematic representation of the structure of the HIV-1 Vpu protein of (Bour and Strebel 2003). Vpu has a transmembrane domain (TM) and a cytoplasmic domain composed of two regions arranged in alpha helices.

This protein displays two major functions during HIV-1 replication cycle. Firstly, Vpu targets the newly synthesized CD4 receptor to the proteasomal degradation (Willey, Maldarelli et al. 1992). Secondly, it favors the egress of viral particles from most human cell types through counteracting the inhibitory effect of BST2 (Neil, Zang et al. 2008; Van Damme, Goff et al. 2008). More recently, Vpu was shown to down-regulate cell surface expression of two additional mediators of the immune response: the lipid-antigen presenting protein CD1d expressed by antigen-presenting cells (Moll, Andersson et al. 2010) and the natural killer cells ligand NTB-A (Shah, Sowrirajan et al. 2010).

2.3.3.6 The viral infectivity factor (Vif)

It is a 32 kDa basic protein that being produced during the late phase of the viral life cycle (Henriet, Mercenne et al. 2009). About 60-100 molecules per virion are packaged *via* an interaction with viral gRNA and the precursors *Gag/Gag-Pol*. It is found essential for the viral pathogenesis and replication in peripheral blood lymphocytes, macrophages, and certain non-permissive cell lines (Henriet, Mercenne et al. 2009). A three-dimensional structural model for Vif is available, that was constructed by a comparative modeling based on two templates (VHL and NarL) used to construct its C-terminal and N-terminal domains (Figure 18)(Lv, Liu et al. 2007). In vitro, Vif was shown to oligomerize to form dimers, trimmers and tetramers (Yang, Sun et al. 2001; Auclair, Green et al. 2007), possibly mediated by the region from positions 151 to 164 amino acids (Yang, Sun et al. 2001; Yang, Gao et al. 2003).

Initially, Vif has been shown to interact with Gag *in vitro* as well as in infected cells (Bouyac, Courcoul et al. 1997). Later on, the interaction was investigated further by using two-hybrid assay and it was observed that Vif can interact with nucleocapsid proteins of Gag. It was revealed that amino-terminal (1-22 aa) and central (77-100 aa) regions of Vif are essential for its interaction with Gag. On the other hand, Gag requires a 35-amino acid region of the protein bridging the MA(p17)-CA(p24) junction for its interaction with Vif (Syed and McCrae 2009). In addition, oligomerization of Vif is not critical for Gag recognition, but the interaction between these two proteins leads to the redistribution of Vif protein at the plasma membrane, which likely mediates Vif incorporation into nascent virions (Batisse, Guerrero et al. 2013; Ludovic Richert 2015).

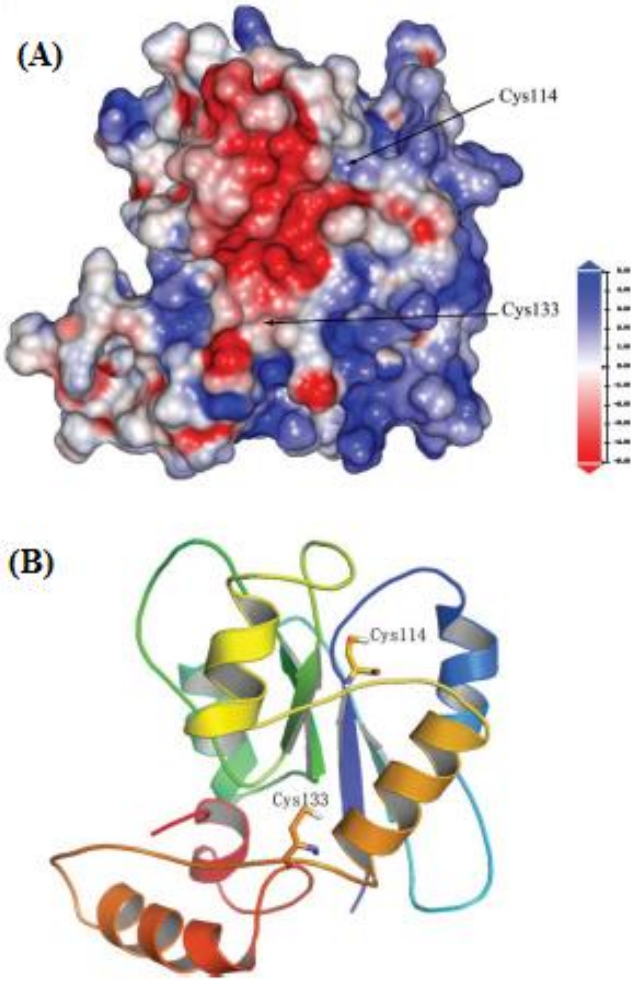

Figure 18: (A) Solid surface of Vif showing a negatively charged concave patch. Coloring is according to the electrostatic potential at the surface calculated with DELPHI. (B) 3D structure of VIF from the same viewpoint as (A); a three-dimensional model of VIF was constructed by comparative modeling based on two templates, VHL and NarL, which were used to construct the C-terminal domain and N-terminal domain of Vif respectively (Lv, Liu et al. 2007).

The main function of Vif concerns its interaction with APOBEC3 family to an E3 ubiquitin ligase complex for polyubiquitylation and proteasomal degradation. During this process Vif adopts a noval structural fold that determines Vif stability and interaction with cellular proteins and motifs driving Vif homodimerization. Both of these functions are essential in Vif functionality and HIV-infection (Batisse, Guerrero et al. 2013; Salter, Morales et al. 2014).

3. Assembly of the viral particles

3.1 Gag protein:

Gag is encoded in the Gag-pol gene and is 55 kDa polyprotein. A translational frame-shift in the 3′ region of Gag regulates the expression of either Gag or the fusion protein Gag-Pol (Karn and Stoltzfus 2012). It has been shown that Gag alone is able to mediate the assembly of immature VLPs.

Gag consists of a series of globular, α-helical domains connected by flexible linkers. It contains five proteolytic sites that are cleaved by the viral PR during maturation to generate three proteins: Matrix (MA), Capsid (CA) and Nucleocapsid (NC) and three peptides: SP1, SP2 and p6 (Figure 19). Processing of Gag leads to the nucleocapsid condensation. After binding to nucleic acids, NCp15, a proteolytic intermediate of NC, was processed at its C-terminus by PR, yielding premature NC (NCp9) followed by mature NC (NCp7), through the consecutive removal of p6 and SP1. This allows NC co-aggregation with its single-stranded nucleic acid substrate. Thus, the interchangeable roles of HIV-PR and RT, by controlling the NC architecture during the steps of condensation and dismantling, engage in a successive nucleoprotein-remodeling process. This process is among the common features developed by mobile genetic elements to ensure successful replication (Mirambeau, Lyonnais et al. 2007).

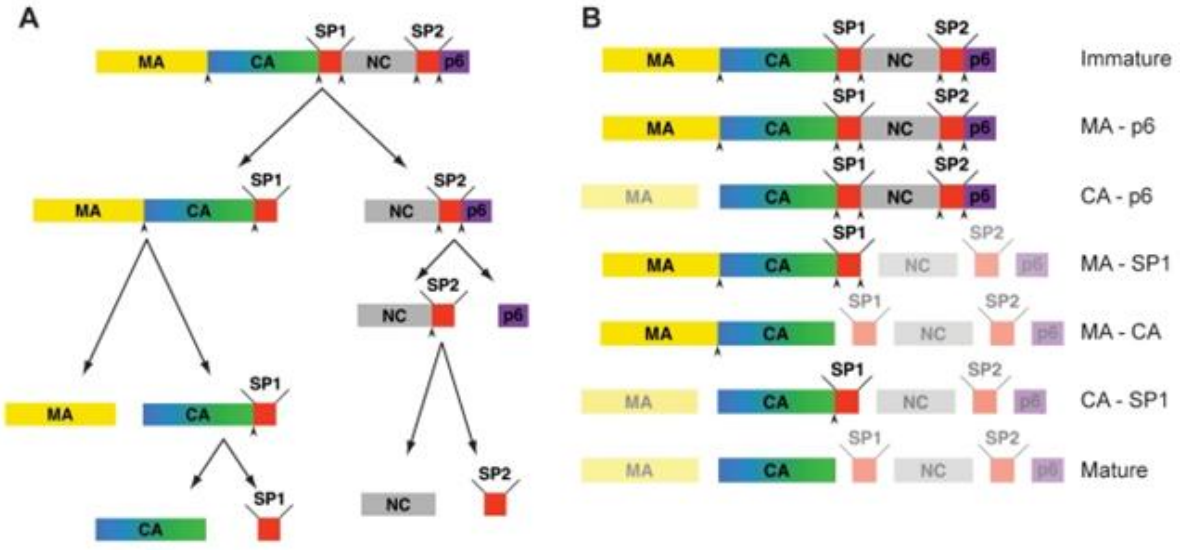

Figure 19: Steps in HIV-1 proteolytic maturation, and variants analyzed. A) Schematic outline of the proteolytic cleavages which take place in Gag during the HIV-1 maturation process. Arrowheads indicate proteolytic sites before cleavage. The order of cleavage events shown is based on the rates of cleavage in vitro as described in (Pettit, Moody et al. 1994). B) Schematic representation of Gag after completion of cleavage for each variant analyzed. The non-cleaved products due to the inactivation of the proteolytic sites are highlighted. Mutated and therefore uncleaved processing sites are indicated by an arrowhead (de Marco, Muller et al. 2010)

By using Small-angle scattering, Gag has been found highly flexible protein, with the domains moving freely around the flexible linkers (Datta, Curtis et al. 2007). This flexibility is particularly prominent for the linker between MA and CA. This flexibility makes the Gag polyprotein difficult to study in its entirety using structural biology methods, still a good amount of knowledge has been retrieved by studying individual constituent domains in isolation.

(A)

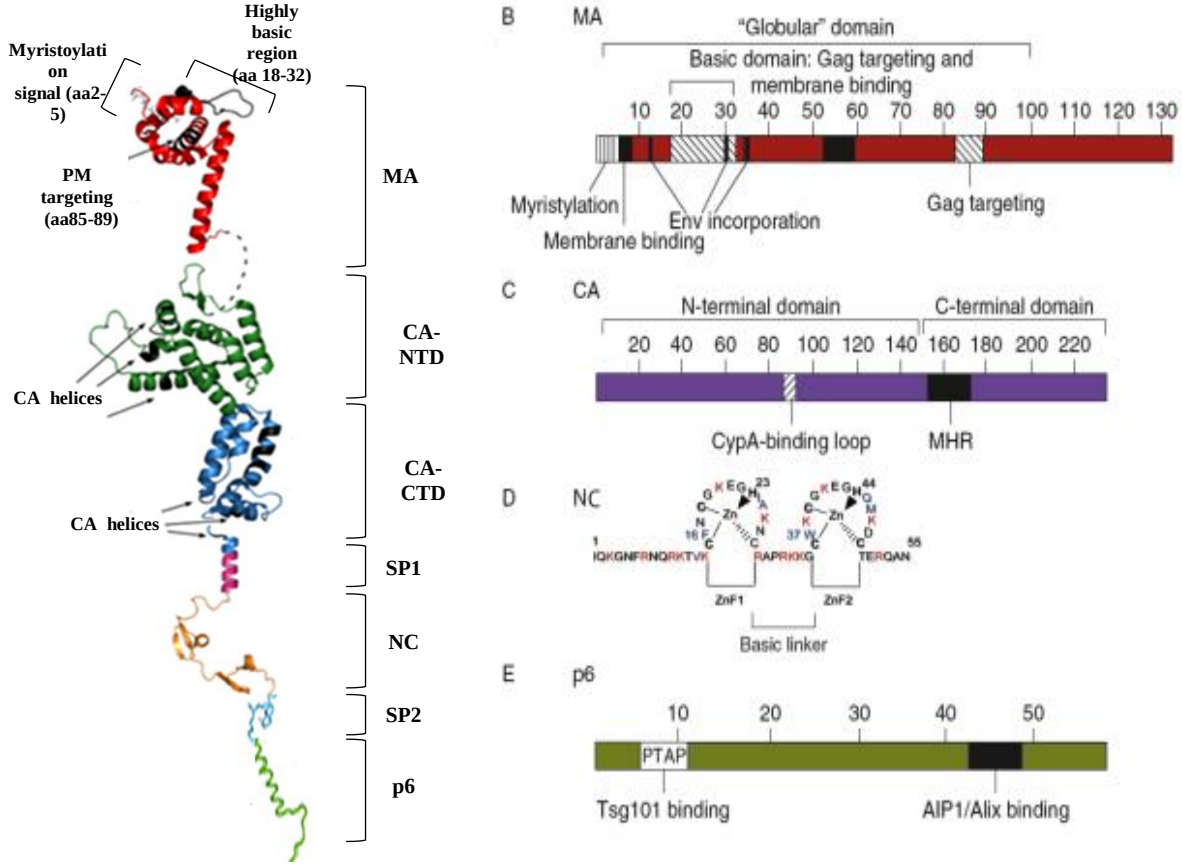

Figure 20: Schematic representation of Gag and its constituent domains. (A) Positions of myristoylated matrix (MA), capsid (CA), nucleocapsid (NC), and p6 domains, and the spacer peptides SP1 and SP2 within the uncleaved Gag are indicated. **(B)** MA. Domains contributing to virus assembly, membrane binding, Gag targeting, post-entry steps, and Env incorporation are shown. The region of MA which forms the main globular domain is indicated, the position of the highly basic domain near the N terminus is shown. **(C)** CA. The N-terminal ''core'' and C-terminal ''dimerization'' domains are indicated. The Cyp-A binding loop and MHR are shown. **(D)** NC. The amino acid sequence is indicated and the two zinc-finger domains are shown. **(E)** p6. The two currently recognized major functional domains are shown: the N-terminal region involved in virus release and the C-terminal Vpr-interacting sequence. Amino acid positions are shown over each diagram. Adapted from (Adamson and Freed 2007).

3.1.1 Matrix protein: architect of Membrane Targeting

132 amino acid long structural matrix protein is derived from the N-terminal myristoylated end of the Gag (MAp15) (Figure 21B) and remains attached with the inner surface of the viral envelope in the mature particle (Chukkapalli and Ono 2011). HIV-1 MA folds into a compact core domain, consisting largely of 5 α-helices, two short 3 α-helical stretches and a three-stranded mixed β-sheet (Figure 21A) (Verli, Calazans et al. 2007). This protein exists in a monomeric state in solution, but crystallizes as trimmers that can be correlated with the formation of higher-order MA structures required for its function in the viral life cycle.

As myristoylation is essential for efficient membrane binding and assembly, the N-terminus of MA domain plays a major role in Gag targeting to the cytoplasmic leaflet of the PM (Bryant and Ratner 1990; Yuan, Yu et al. 1993; Freed, Orenstein et al. 1994; Zhou, Parent et al. 1994; Saad, Miller et al. 2006). The N-terminal myristic acid moiety (Bryant and Ratner 1990; Saad, Miller et al. 2006) and a highly basic region on the surface of MA (residues 16–31) (Yuan, Yu et al. 1993; Zhou, Parent et al. 1994) are required for membrane association (Hermida-Matsumoto and Resh 2000; Ono, Orenstein et al. 2000). The myristoyl moiety of MA is thought to exist in either an exposed or a sequestered conformation which is in analogy to other myristoylated proteins (Tang, Loeliger et al. 2004). It has been suggested that most of myristoylated proteins regulate membrane association through a myristoyl switch mechanism, in case of Gag, a concentration-dependent oligomerisation triggered the myristoyl switch and facilitate membrane binding (Tang, Loeliger et al. 2004). This allosteric conformational change that exposes the myristoyl moiety of Gag due to the interaction of MA and $PI(4,5)P_2$, (Saad, Miller et al. 2006). $PI(4,5)P_2$ is a inositol phospholipid found on the cytosolic leaflet of the PM and is a major determinant for PM targeting by a number of cytoplasmic peripheral PM proteins (Behnia and Munro 2005).

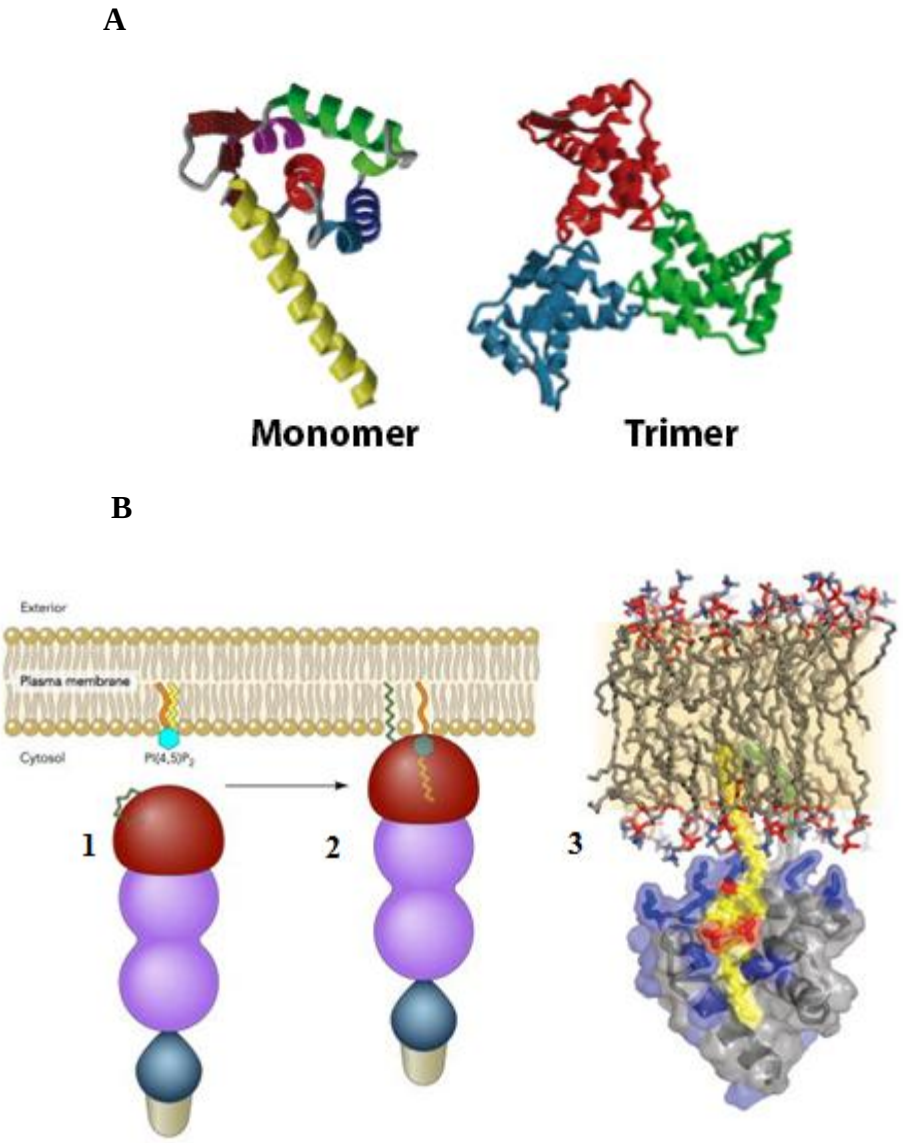

Figure 21: A. Three-dimensional structure of HIV-1 MA monomer and trimer as determined by X-ray crystallography. The putative membrane binding surface of the trimer is shown. **B. Model of membrane binding by MA**. **1:** the NH2-terminal myristic acid moiety (green) of MA is depicted in its sequestered conformation. $PI(4,5)P_2$ embedded in the inner leaflet of the PM lipid bilayer is shown with its (orange) and (yellow) acyl chains in the lipid bilayer. **2:** binding between MA and $PI(4,5)P_2$ leads to the flipping out of the myristate moiety into an exposed conformation with its subsequent insertion into the lipid bilayer, and the extrusion of the 2′acyl chain from the lipid bilayer and its sequestration by MA. **3:** during the formation of the complex between HIV-1 MA and $PI(4,5)P_2$, the 2′-unsaturated acyl chain of $PI(4,5)P_2$ (yellow) binds to the hydrophobic cleft in MA and the myristyl group (green) of MA inserts into the lipid bilayer (Balasubramaniam and Freed 2011).

The MA domain is highly basic, harbors an NTD HBR (Highly Basic Region) and could function by interacting directly with the viral RNA as shown by *in vitro* nucleic acid binding assays (Steeg and Vogt 1990; Purohit, Dupont et al. 2001; Cai, Huang et al. 2010; Alfadhli,

McNett et al. 2011). Virions lacking GagNC were shown to incorporated significant amount of viral RNA suggesting that MA was involved in the recognition of RNA (Ott, Coren et al. 2005).

3.1.2 Capsid protein: Major Structural Element

The CA protein is main brick of architect that is required for Gag-Gag interactions in the immature shell as well as in the mature particles and comprises two independent domains (NTD & CTD) separated by a flexible linker (Figure 22).The structure of the individual CA-CTD and CA-NTD has been resolved recently, by using cryoelectron microscopy (cryo-EM) and cryotomography and NMR spectroscopy (Briggs and Krausslich 2011; Yeager 2011).

The immature capsid shell is arranged in a lattice formed by Gag hexamers stabilized by a six helix bundle of SP1 peptides and are joined through CTD dimer interface, whereas the residues of the NTD contribute to intra-hexamer and/or inter-hexamer interactions (Mateu 2009). Furthermore, mature HIV-1 CA adopts a cone-shaped shell forming a curved hexagonal lattice arranged in a fullerene-type geometry consisting of ~250 hexameric subunits with a 90-100 Å inter subunit spacing (Fig. 21) (Briggs and Krausslich 2011; Yeager 2011).

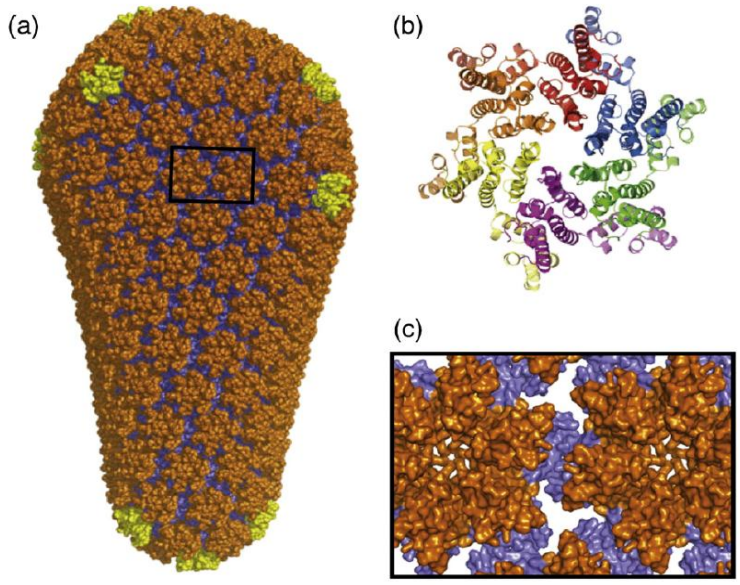

Figure 22: The architecture of the mature HIV-1 core. (a) Pseudo atomic model of an HIV-1 core showing the fullerene cone architecture, with the 12 pentamers highlighted in yellow. (b) Structure of the hexamer formed by the N-terminal domains of CA, showing the 18-helix bundle. (c) A higher magnification of the boxed region in(a) illustrating the6-fold interactions of the N-terminal domains (orange) and the 2-fold interactions of the C-terminal domains (blue) (Briggs and Krausslich 2011; Yeager 2011).

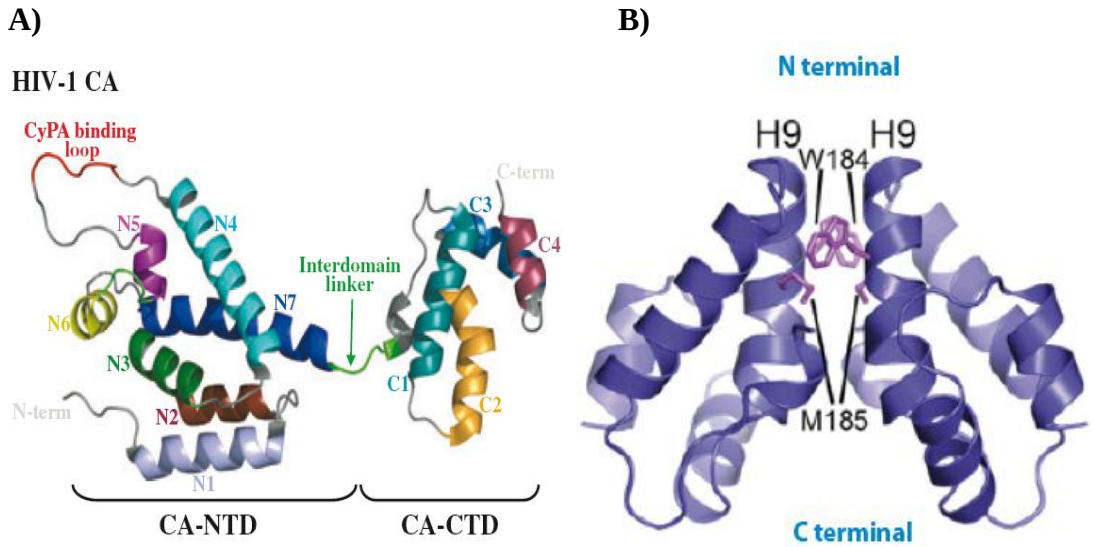

Figure 23: (A) X-ray crystal structure of HIV-1 CA. Helices N1–N7 in the CA-NTD and C1–C4 in the CA-CTD, the CyPA-binding loop (red) and inter domain linker (green) are indicated (Mascarenhas and Musier-Forsyth 2009). **(B) 3-D structure of the CA-CA dimer formed upon proteolytic cleavage of the MA-CA junction.** The amino-terminal β- hairpin, which forms only after proteolysis, mediates CA-CA interactions facilitating capsid core condensation during virus maturation (Yeager 2011).

3.1.3 The nucleocapsid protein (NCp7)

Main architect in Recognition and Binding of Viral Genome (reviewed in (Darlix, de Rocquigny et al. 2014))

The HIV nucleocapsid (NCp7) protein harbors two conserved “CCHC domains" (Cys-X2-Cys-X4-His- X4-Cys; where X is a variable amino acid residue) forming the zinc-finger (ZF) motifs (Figure 24B) that contains a zinc ion each and is flanked on either side by linker harboring highly basic residues (RAPRKKG) (Figure 24) (Morellet, Jullian et al. 1992; Muriaux and Darlix 2010; Darlix, Godet et al. 2011). Enriched literature data showed that the NTD-ZF1 is essential for genome recognition, whereas the CTD-ZF2 would be more involved in viral assembly and the early stages of viral replication (Houzet, Morichaud et al. 2008).

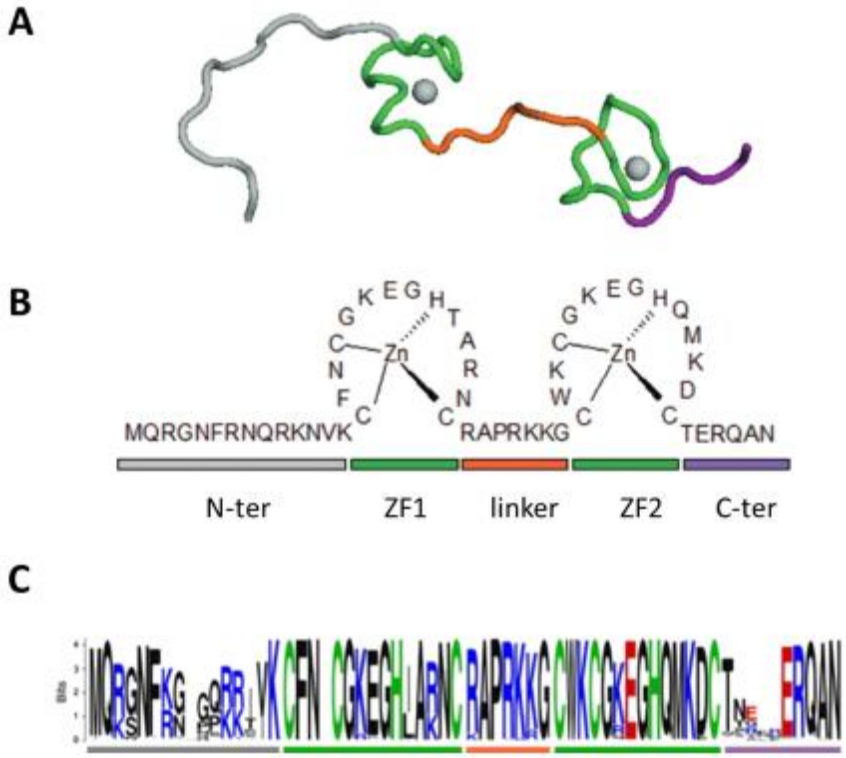

Figure 24: Structure and sequence of the HIV-1 NCp7 (adapted from (Godet and Mely 2010; Godet, Boudier et al. 2012). (A) Three-dimensional structure (PDB 1AAF) and (B) Sequence of NCp7. The zinc fingers (ZF) are shown in green, the basic linker is shown in orange and the N-ter domains and unstructured C-ter are shown in gray and magenta, respectively. (C) Identification of variables and conserved residues of NCp7 of HIV-1, resulting in the alignment of 3120 sequences base data HIV LANL (http://www.hiv.lanl.gov/).

GagNC of HIV-1 is essential during many key processes both during the early steps of the viral life cycle as the mature GagNC protein and during the late steps as domain of the precursor Gag (Mirambeau, Lyonnais et al. 2010):

i) It helps in the recognition and specific packaging the viral genomic RNA (gRNA) (Later described in details) (Darlix, Godet et al. 2011).

ii) it entirely coats and protects the genome forming a compact ribonucleoprotein (RNP) complex in the viral particle maturation, with a very high degree of occupancy (1:5 nt up to 1:1) (Darlix, Lapadat-Tapolsky et al. 1995)

vii) It participates to viral DNA integration as shown by cDNA integration *in vitro* (Carteau, Batson et al. 1997). Additionally, it has been shown that GagNC and Integrase cooperate to ensure protection of the inverted repeat sequences ‘‘ir’’at both ends of the LTR (Bampi, Jacquenet et al. 2004).

iii) it drives directly or indirectly the incorporation in nascent particles of cellular APOBEC3G (Alce and Popik 2004), viral protein Vif (Huvent, Hong et al. 1998; Bardy, Gay et al. 2001), and Vpr (Bachand, Yao et al. 1999).

iv) it has a RNA chaperon property essential to enhance dimerization of viral RNA (Darlix, Gabus et al. 1990; De Rocquigny, Gabus et al. 1992) and its conversion into a more compact and stable form, a process known as ‘‘RNA maturation’’ (Feng, Copeland et al. 1996; Muriaux, De Rocquigny et al. 1996).

3.1.3.1 Nucleic acid chaperone activity during the replication cycle:

Nucleic acid chaperones have the ability to direct structural rearrangements of secondary structures of nucleic acids (DNA and RNA) via rapid iterative on and off binding to the nuclei acid. Such a binding mode helps nucleic acids to overcome ‘kinetically trapped inactive states’ in order to rapidly reach the most stable conformation (Herschlag 1995; Kovacs, Rakacs et al. 2009). This chaperone activity of nucleic acids is essential during reverse transcription, by inducing hybridization $tRNA^{Lys3}$ to the viral RNA, by increasing the speed of the reverse transcriptase and activating strongly the transfer of strands (Levin, Guo et al. 2005; Godet, de Rocquigny et al. 2006; Ramalanjaona, de Rocquigny et al. 2007; Rein, Datta et al. 2011; Darlix, de Rocquigny et al. 2014). This activity consists of three steps: interaction with target nucleic acids, destabilization of strands and hybridization of complementary strands. The NCp7-chaperoned folding of NAs has been characterized by both a NA destabilizing activity and a complementary strand annealing activity (Reviewed in (Godet and Mely 2010)). The destabilizing activity of GagNC appears to be weak and strongly dependent on the NA stability, resulting in a transient melting of ‘weak spots’ within the NA. The locally transiently-melted areas allow conformational sampling, resulting in the selection of stable conformations. On the other hand, the ability of NCp7 to efficiently screen repulsive charges and aggregate NAs, mainly through its basic residues, strongly enhances the limiting nucleation step during annealing of complimentary NAs. Thus, the destabilizing activity of NCp7 depends essentially on zinc fingers (Beltz, Clauss et al. 2005) while the hybridization and condensation activities

depend essentially from basic parts surrounding the CCHC motifs (De Rocquigny, Gabus et al. 1992; Williams, Rouzina et al. 2001) (Figure 24 B).

Furthermore, Gag protein has also a chaperone activity but that seems less efficient than the one of GagNC (Rein 2010; Wu, Datta et al. 2010). Interestingly, it has been shown that this chaperone activity was increased with the maturation products of Gag NCp15, NCp9 and NCp7 (Wu, Datta et al. 2010; Wang, Naiyer et al. 2014).

Conversely, the Gag protein interacts strongly with nucleic acids and this affinity decreases in the different maturation products. This suggests a model in which in the early stages of assembly, Gag protein requires a strong affinity to recognize and interact with the genomic RNA. Then, during maturation by the viral protease, this affinity decreases in the benefit of the chaperone activity promoting reverse-transcription (Mirambeau, Lyonnais et al. 2010; Godet, Boudier et al. 2012).

3.1.4 The protein p6: Recruiter of Cellular Budding Machinery

p6 is a small proline-rich protein of 6 kDa and is located at the C terminus of Gag. It is separated from GagNC by SP2 (Figure 20E). As the N terminus of this domain is encoded by sequences that direct translational frame shift into the overlapping pol gene (Klein, Reed et al. 2007), thus, it is absent from the Gag-Pol precursor. This deletion results in impaired virus release (Gottlinger 2001).

The p6 domain contains two highly conserved the P(T/S)AP and LXXLF motifs at its N and C termini, respectively. The NTD, also called assembly or “L” late domain is involved in the viral budding (Morita and Sundquist 2004; Yeager 2011). LXXLF is also considered as late domain as well as is needed for the incorporation of Vpr protein into the assembling virions (Gottlinger 2001). Next, this domain is necessary for recruiting the ESCRT-I component TSG101 (Later described in details). Interestingly, these motifs are also found in many viruses such as ebola, RSV, Marburg, Mason-Pfizer monkey virus, bovine leukemia virus, Human T-cell leukemia virus type 1, etc (Strack, Calistri et al. 2000; Herrington, Coates et al. 2015).

3.1.5 SP1 (p2) & SP2 (p1)

SP1 and SP2 are two small spacer peptides, cleaved during viral particle maturation and separates CA with NC, and NC with p6, respectively (Figure 20). These peptides influence precursor polyprotein processing and viral morphogenesis which is required to produce fully infectious virions (Gottlinger 2001; Klein, Reed et al. 2007). However, their precise functions are controversial. With a possibility that SP1 can function as a molecular switch region that controls the transition from sphere to cone, it also contributes with CA to the interface of Gag-Gag multimerization (Morellet, Demene et al. 1998; Morellet, Druillennec et al. 2005; Datta, Temeselew et al. 2011).

3.2 Gag assembly and trafficking

A generally accepted model for HIV-1 assembly stipulates that the genomic RNA acts as a scaffolding platform onto which Gag molecules bind *via* GagNC, then kick-starting assembly by CA-CA interaction (Ott, Coren et al. 2009; Kutluay and Bieniasz 2010; Fogarty, Chen et al. 2011; O'Carroll, Soheilian et al. 2013). This, in turn causes the binding of N-terminal myristyl switch of Gag MA or binding of the RNA-bound Gag oligomers (Lindwasser and Resh 2001; Ono, Ablan et al. 2004; Saad, Miller et al. 2006; Li, Dou et al. 2007) to either the plasma membrane (PM) (Neil, Eastman et al. 2006; Welsch, Keppler et al. 2007; Jouvenet, Bieniasz et al. 2008; Ivanchenko, Godinez et al. 2009) or to endosomes (Grigorov, Arcanger et al. 2006; Perlman and Resh 2006; Joshi, Ablan et al. 2009; Lehmann, Milev et al. 2009).

Gag alone is required for the viral assembly, this assembly occurring either at the level of the PM (Ono 2009), or in intracellular vesicles like multivesicular bodies (MVB) (Nydegger, Foti et al. 2003; Dong, Li et al. 2005; Grigorov, Arcanger et al. 2006; Perlman and Resh 2006). It was observed that both mechanisms of Gag assembly and trafficking are cell line dependent, indicating that the cellular context has a major influence on the mechanism of Gag assembly and trafficking (reviewed in (Balasubramaniam and Freed 2011)).

Mutational analysis revealed that only MA, CA and NC are required for Gag assembly while the p6 domain was shown more essential for budding and release. MA governs the targeting to the membrane either by its myristate and HBR, CA contains residues critical for Gag-Gag interaction and GagNC is responsible for viral genomic RNA packaging as well as non-specific

interaction of RNA. In line with this, replacement of the HIV-1 GagNC domain by a leucine zipper protein dimerization (or trimerization) domain that allows Gag-Gag contact does not impair virus assembly and release, albeit with no detectable viral RNA.

This retroviral Gag oligomerization and trafficking were obtained by mainly using molecular imaging for recent review (Chojnacki and Muller 2013; de Rocquigny, Gacem et al. 2013; de Rocquigny, El Meshri et al. 2014). Gag-Gag interactions at the level of the PM were first visualized by two photon imaging, using Rous sarcoma virus (RSV) followed by studies onto HIV-1 Gag. Therefore, a fluorescent reporter was localized to the C terminus of Gag (gives rise to abnormal immature virus structures (Larson, Johnson et al. 2005)) or between MA and CA. In this latter case, when co-expressed with wild-type Gag, infectious virus particles are assembled with apparently normal morphology (Muller, Daecke et al. 2004; Hubner, Chen et al. 2007). As far as HIV-1 is concern, Gag-Gag interaction was confirmed using an approach similar to FRET, where Gag fluorescent chimeras were expressed in Mel JuSo cells (human melanoma cell line) (Derdowski, Ding et al. 2004), HeLa cells (Jouvenet, Bieniasz et al. 2008; Hogue, Hoppe et al. 2009) and epithelial 293T cells (Hubner, Chen et al. 2007). Alternatively, another strategy was also used by following interactions with FLIM. The FLIM technique measures the fluorescence decay of a chromophore at each pixel or group of pixels of the cell, allowing determining the fluorescence lifetime (τ) (see Mat and Met for details on FRET FLIM). This strategy was applied to follow the fluorescence lifetime of FlAsH linked to HIV-1 Gag-TC (Fritz, Dujardin et al. 2010). Gag oligomerization was followed by the decrease in the fluorescence lifetime of FlAsH, due to its self-quenching and/or exciton coupling (Lakowicz 1980; Krishnamoorthy, Duportail et al. 2002). The studies were performed by using Hela cells, transfected by a plasmid encoding for Gag-TC, (see in material and methods) that showed Gag accumulation at the level of the PM and the dropping of FlAsH lifetime to 2.57 ns (Figure 26, panel 2, blue pseudo color), as compared to 3.52 ns of the control experiments.

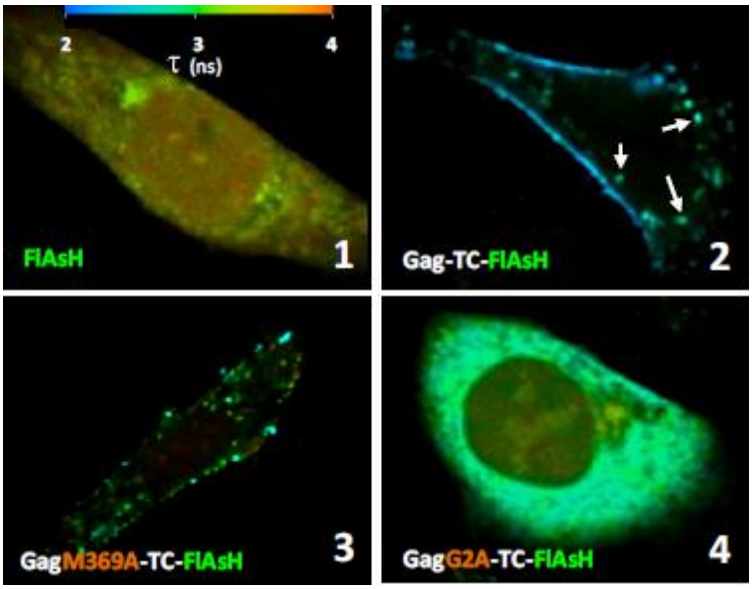

Figure 25: Gag-Gag interaction monitored by FLIM. HeLa cells were transfected by a plasmid encoding for Gag-TC (Rudner, Nydegger et al. 2005). 24 hours post- transfection, cells were labeled with the FlAsH derivative (Fritz, Dujardin et al. 2010). Then, two-photon FLIM images were recorded and measured lifetimes were imaged using an arbitrary color scale. (top of panel 1). Panel 1, control naive HeLa cells incubated with FlAsH. The chromophore is homogeneously distributed with an average lifetime of 3.52 ns. Panel 2: HeLa cell expressing Gag-TC. The close proximity of Gag-TC-FlAsH molecules decreases their fluorescence lifetime to 2.52 ns, reflecting Gag multimerization. Gag-containing dots with an intermediate lifetime (green color) might correspond to Gag oligomers. Panel 3: Substitution of methionine 369 in the SP1 spacer for alanine (GagM369A-TC) severely impairs Gag assembly, as shown by the 3.08 ns fluorescence lifetime value obtained for this mutant. Panel 4: HeLa cell transfected with the GagG2A-TC mutant. The substitution of Gly for Ala hampers membrane anchoring of Gag. The fluorescence lifetime homogenously distributed throughout the cytoplasm is equal to 2.87 ns indicating that myristylation-defective Gag can oligomerize but does not form high molecular weight structures. This figure is adapted from fig 3 of (Hugues de Rocquigny* 2012)

Similar FRET studies were performed to determined that SP1 (Krausslich, Facke et al. 1995; Accola, Ohagen et al. 2000), has a severe impact on Gag-Gag FRET (Liang, Hu et al. 2003; von Schwedler, Stray et al. 2003; Hogue, Hoppe et al. 2009), while membrane-defective Gag can still oligomerize in the cytoplasm (Lee, Liu et al. 1999; Morikawa, Hockley et al. 2000; Derdowski, Ding et al. 2004; Li, Dou et al. 2007). The use of this technique to determine the role of GagNC in Gag-Gag interaction was developed during my thesis but with Gag-eGFP and Gag-mCherry and is presented in the results.

Next, investigations were performed to determine the place of Gag oligomer formation inside cell. Furthermore, to address the question of whether VLPs detected at the surface of *HeLa* cells resulted from Gag clusters arriving from the cytoplasm or from Gag molecules assembling at the PM (Ruthardt, Lamb et al. 2011), Total Internal Reflection Fluorescence (TIRF) and wide-field

(WF) microscopy were used (Ivanchenko, Godinez et al. 2009). WF images were recorded in the green channel with an excitation of the photoconverted Gag-EOS at 488 nm, while TIRF images were recorded in the red channel with an excitation at 516 nm, after a pulse at 405 nm (Figure 26). By following, the emission of Gag-EOS in green and red channel, it was concluded that VLP formation at the surface of *HeLa* cells likely resulted from the accumulation of Gag oligomers coming from the cytoplasm.

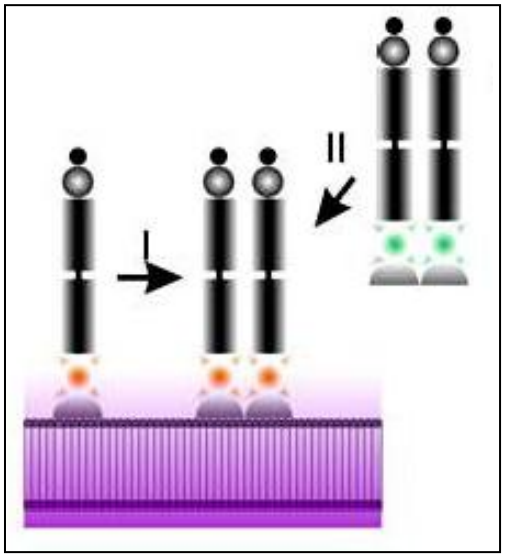

Figure 26: VLP assembly results from the recruitment of cytosolic Gag clusters. Photoconversion scheme and intracellular localization of Gag-EOS chimera proteins. The green spheres correspond to the non-photoconverted form of Gag-EOS (λexc= 488 nm and λem=516 nm) observable in the epifluorescence mode. The red spheres correspond to the photoconverted form of Gag-EOS (λexc= 516 nm and λem=581 nm) after a photoconversion pulse at 405 nm in the TIRF mode. Gag coming from the cytoplasm (II) will be detected in the green channel while Gag already anchored at the plasma membrane (I) prior to the 405 nm pulse will be detected in the red channel. This figure is adapted from fig 3 of (Hugues de Rocquigny* 2012).

Finally, recent data using TIRF microscopy approach have allowed to track the appearance/disappearance of the viral particle into the plasma membrane. These data, obtained from HeLa cells, show that a first population of viral particles appear/disappear with very short time (5-10 sec.) and their co-localisation with the endosomal marker CD63 suggest their internalization by endocytosis (Jouvenet, Bieniasz et al. 2008). A second population is described with appearance of Gag kinetics about ten minutes followed by a longer period of about 25 minutes which can correspond to either an assembly at the PM from a cytosolic fraction of Gag or re-internalization of Gag in the cytoplasm (Jouvenet, Bieniasz et al. 2008; Ivanchenko, Godinez et al. 2009). Thus, the step of localisation of Gag to the membrane and budding could

be influenced by a balance between the extracellular release of Gag as a viral particle and its internalization into the cell by endocytosis.

Additionally, in *in vitro* conditions, MA and NC domains of monomeric Gag bind to gRNA and adopts a U shape conformation that brings these two domains closer (Datta, Curtis et al. 2007). To achieve the process of condensation, then MA recruits and interacts tightly with $PI(4,5)P_2$ of the PM. During this interaction with phosphoinositol, the abovementioned U shape of Gag is reverted back to non-bended conformation and form rode like structure. This leads to the strengthening of Gag-Gag interactions at the membrane, establishing a dense condensation of Gag:gRNA complexes (Parent and Gudleski 2011; Rein, Datta et al. 2011). (Figure 27)

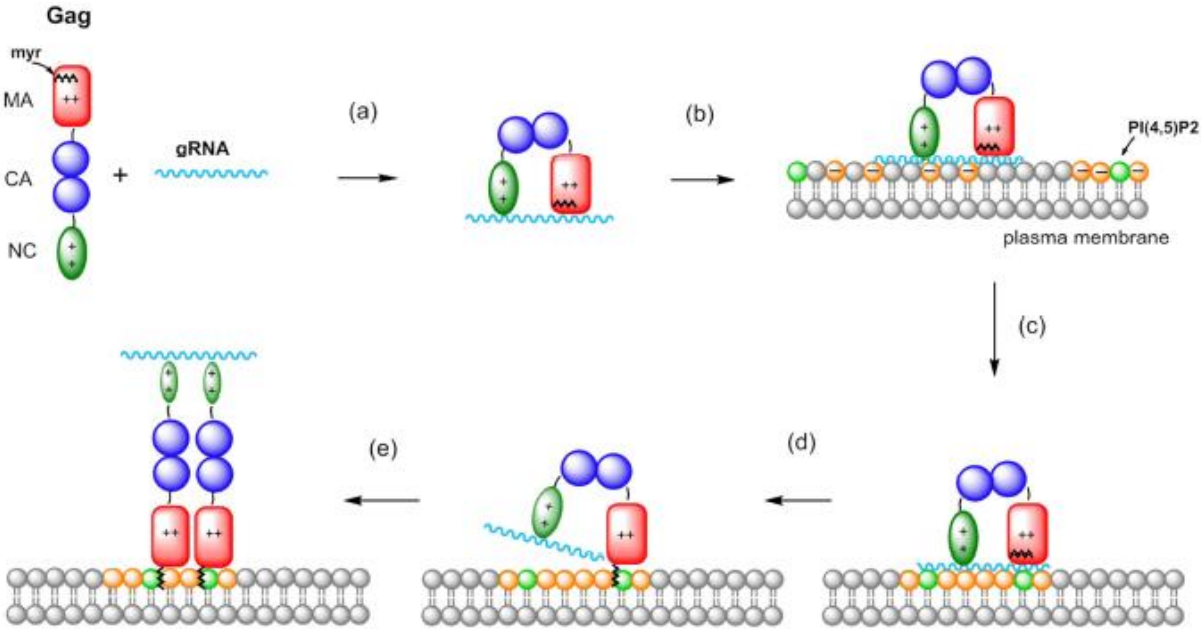

Figure 27: Proposed mechanism for NC-promoted binding of Gag to the plasma membrane. (a) Newly made Gag polyprotein binds to the gRNA via its NC and MA domains, so that it adopts a bent conformation. (b) The Gag-gRNA complex also interacts with the plasma membrane via its MA and NC domains. (c) The NC domain recruits negatively charged lipids, including $PI(4,5)P_2$, that form an acidic lipid-enriched microdomain. (d) The MA domain recognizes $PI(4,5)P_2$, which results in the exposure of the previously sequestered myristyl group that inserts into the cytoplasmic leaflet of the PM. As a consequence of this anchoring of MA into the PM, MA dissociates from the gRNA. (e) Without the support of MA, the bent conformation is released and the Gag molecule adopts a rod-shaped conformation (Kempf, Postupalenko et al. 2014).

However, it remains to be determined if this U-structure is also found in cells as well mechanism involved behind this phenomenon. There is a possibility that we may differ with the in vitro findings as in cells Gag can co-opts a host protein that either prevents Gag from adopting the folded-over form, or facilitates conversion from the folded-over to the extended form.

In addition to this, as conformational studies have only been performed with myr(−)GagΔp6, the effect of highly unstructured p6 domain in these folded-over conformations needs to be tested. More recently, Mckinstry et al., have managed to purify full length Gag (myr(-)Gag) and could be crucial in answering these questions (McKinstry, Hijnen et al. 2014).

3.3 Gag-RNA specific recognition for packaging

Schematically, two types of Gag-RNA interactions are described. Initially, non-specific interactions with either cellular RNA or genomic RNA; this interaction drives Gag oligomerisation during the assembly and also allows a RNA wrapping to protect the viral genome from protease attack. Secondly, a more specific interaction has been described between the 5'UTR and the GagNC domain of the Gag polyprotein. Extensive studies delineate various positions of the UTR recognized by GagNC such as TAR (Kanevsky, Chaminade et al. 2005), SL1, SL2 and SL3 (Darlix, Gabus et al. 1990; Clever, Sassetti et al. 1995; Amarasinghe, De Guzman et al. 2000; Houzet, Paillart et al. 2007).

Despite the abundance of studies, still there exist many unsolved issues related to the molecular interactions responsible for selective gRNA packaging. The HIV-1 genome packaging is a highly specific and selective mechanism and has been shown to involve direct binding of packaging signal (Ψ) and the nucleocapsid domain (NC) of the retroviral Gag precursor (Berkowitz, Fisher et al. 1996; D'Souza and Summers 2005; Lever 2007; Lu, Heng et al. 2011). It is interesting to know that, despite the relative scarcity of the unspliced viral RNA (usually <1% of total RNA), it is strongly favored over abundant cellular RNAs and viral spliced mRNA species. Moreover, unspliced RNA is more efficiently packaged compare to spliced RNA despite a number of common packaging signals shared by the two RNAs namely: TAR, Poly-A, PBS and the DIS (Paillart, Shehu-Xhilaga et al. 2004; Lu, Heng et al. 2011).

Recently, Ekram W et al. demonstrated that the primary Gag binding site on the gRNA consists of the internal loop and the lower part of Stem-loop 1 (SL1). Along with, a double regulation by the upstream and downstream nucleotide sequences of SL1 ensures specific binding of Gag to the gRNA. The region upstream of SL1, which is present in all HIV-1 RNAs, prevent binding to SL1, but this negative effect is counteracted by sequences downstream of SL4, which are unique to the gRNA (Ekram W. Abd El-Wahab, Redmond P. Smyth et al. 2014).

3.3.1 Role of NC region of Gag in recognition for packaging

It has been shown that the zinc fingers are critical in intracellular trafficking of Gag (Grigorov, Decimo et al. 2007) and in the recognition of cellular partners during budding (Popov, Popova et al. 2008; Dussupt, Javid et al. 2009). Additionnaly, mutations in NCp7 result in late RTion suggesting that NCp7 *via* its role in the Gag-Gag interactions can control temporally triggering of the reverse transcription (Didierlaurent, Houzet et al. 2008; Houzet, Morichaud et al. 2008).

All evidences from *in vivo* and *in vitro* studies showed that the specific interaction between viral genome and Gag is mainly displayed by its nucleocapsid domain (NC)(D'Souza and Summers 2005; Lever 2007; Muriaux and Darlix 2010; Rein 2010; Lu, Heng et al. 2011; Rein, Datta et al. 2011). First it has been shown that GagNC displays a strong preference for viral RNA and RNAs containing the Ψ site (Berkowitz, Luban et al. 1993; Dannull, Surovoy et al. 1994; Luban and Goff 1994; Geigenmuller and Linial 1996). Impairing zinc-binding caused an increased ratio of spliced to unspliced vRNA in virus particles and replacement of a single zinc-coordinating residue with a non-zinc coordinating one can lead to assembly of virus particles lacking vRNA (Gorelick, Henderson et al. 1988; Aldovini and Young 1990; Gorelick, Nigida et al. 1990; Berkowitz, Luban et al. 1993; Poon, Wu et al. 1996; Schmalzbauer, Strack et al. 1996; Damgaard, Dyhr-Mikkelsen et al. 1998; Cruceanu, Urbaneja et al. 2006; Wu, Datta et al. 2010). These results suggest that the specificity of interaction with the gRNA is provided by the zinc fingers that helps in discriminating viral genomic RNA from spliced RNA species (Aldovini and Young 1990; Zhang, Qian et al. 1998; Accola, Strack et al. 2000).

3.3.2 Gag-mediated RNA dimerization and packaging

As shown on (Figure 7), an overlap can be seen between the cis-acting elements required for RNA dimerization, that are extended downstream Gag ORF, and the transacting elements i.e. Gag to achieve specific packaging of the viral RNA genome. Thus, the RNA elements important for packaging of HIV-1 genomic RNA, have been mapped to the highly conserved and structured 5' untranslated region and furthermore, extends into the Gag coding sequence (Lever, Gottlinger et al. 1989; Aldovini and Young 1990; Clavel and Orenstein 1990; Luban and Goff 1991; Buchschacher and Panganiban 1992; Hayashi, Shioda et al. 1992; Luban and Goff 1994; McBride and Panganiban 1997). Moreover, this region that is essential for RNA packaging (SL1 to SL4) (Clever, Sassetti et al. 1995; McBride and Panganiban 1997) also overlaps the region

required for RNA dimerization. In fact, this dimerization occurs in the cytoplasm (Moore, Fu et al. 2007) before the encapsidation process suggesting that this dimerisation process also participates to the selection of the viral RNA among the cellular RNAs (Nikolaitchik, Dilley et al. 2013).

3.4 Viral RNA nuclear transport and packaging

3.4.1 Role of nuclear trafficking of Gag in genome packaging

Unfortunately, the mechanisms related to the transport of HIV-1 gRNA throughout the cell to the assembly site at the PM are poorly understood. However, two mechanisms have been described for cytoplasmic transport of cellular mRNAs like active transport along the cytoskeleton or passive diffusion (Gaudin, de Alencar et al. 2013).

In the first case, RNA was shown to move along with viral Gag *via* endosomal trafficking pathways for reaching the sites of assembly at the PM (Basyuk, Galli et al. 2003; Swanson and Malim 2006; Lehmann, Milev et al. 2009; Molle, Segura-Morales et al. 2009). This hypothesis becomes more prominent with the fact that the *Psi* domain within the gRNA directs its targeting to a perinuclear/centrosomal site where it interacts with Gag prior to an eventual transport to the assembly site, and that its absence leads to inappropriate subcellular localization (Poole, Strappe et al. 2005; Swanson and Malim 2006). Additionally, some specific cellular factors were also reported to direct viral structural proteins and gRNA to the site of assembly including like the Rab family of small GTPases (Rey, Canon et al. 1996), Staufen (hStau), a double stranded non sequence specific RNA binding protein (Mouland, Mercier et al. 2000; Chatel-Chaix, Clement et al. 2004).

In contrast, diffusion/trapping model was proposed using total internal reflection fluorescence microscopy (TIRF) (Ivanchenko, Godinez et al. 2009; Jouvenet, Simon et al. 2009; Jouvenet, Simon et al. 2011). Using this approach combined with fluorescently labeled and photoconvertible HIV-1 components, it was shown that a complex of few Gag molecules (<12) and a viral RNA dimer targets the PM with subsequent irreversible anchoring, while displaying lateral mobility in the plane of the PM. This phenomenon ceases as further Gag molecules accumulate till reaching the critical number required for complete virion assembly (Jouvenet, Simon et al. 2009). However, without Gag, the gRNA was found to be highly diffusing moving

in and out near the PM. Additionally, mutations interfering with Gag multimerization and assembly, resulted in dissociation of the gRNA after being anchored at the PM. In line with this model, the group of Wei-Shau Hu et al recently shows that HIV RNA lacks directionality when moving in the cytoplasm suggesting a diffusive movement and intact cytoskeletal structure was not needed for this motion (Chen, Grunwald et al. 2014).

3.5 Role of GagNC in assembly (reviewed in (de Rocquigny, El Meshri et al. 2014))

Early 90s, the NC domain of Gag was shown involved in Gag assembly and release of particles. In fact, mutation of residues involved in zinc chelation (CCHC domain) or mutating the aromatic residues Phenylalanine16 and Tryptophan 37 of the ZFs caused a large decrease in particle production (Gorelick, Henderson et al. 1988; Aldovini and Young 1990; Dorfman, Luban et al. 1993). Next, studies were carried out using the two-hybrid systems (Franke, Yuan et al. 1994) and recombinant baculoviruses (Carriere, Gay et al. 1995) it was observed that the smallest domain identified for Gag oligomer formation was encompassing the C-terminal domain (CTD) of CA (Wills and Craven 1991; Strambio-de-Castillia and Hunter 1992) and GagNC.

Next, even though other domains in the matrix (Hong and Boulanger 1993; Mammano, Ohagen et al. 1994), and the spacer peptide1 SP1 (Krausslich, Facke et al. 1995) were found essential for Gag assembly (Gottlinger 2001; Adamson and Freed 2007), the mechanism whereby the GagNC participates in Gag assembly lies in the interaction between GagNC and nucleic acids. This interplay appears to contribute to assembly by tethering Gag molecules onto the RNA promoting Gag–Gag interaction (Burniston, Cimarelli et al. 1999; Cimarelli and Luban 2000; Ott, Coren et al. 2009). To model homotypic GagNC interactions driven by the RNA and GagNC, GagNC was substituted for the *bacillus subtilisis* Apo MTRB protein that endowed protein-protein interaction and formation of particles at levels similar to the wt Gag was determined (Antson, Otridge et al. 1995). This suggests the essential role of GagNC was to make protein-protein contacts.

These results were re-confirmed by the use of a Gag construct where GagNC was substituted by the leucine zipper of human CREB DNA binding domain (Gag-ZIP) (Zhang, Qian et al. 1998; Chang, Chang et al. 2008; Wang, Marshall et al. 2013) or where GagNC was replaced by the Coat protein of the MS2 RNA bacteriophage (Dykeman, Grayson et al. 2011). In all cases, viral

particles can be formed by a recombinant Gag in the absence of a specific RNA partner (O'Carroll, Soheilian et al. 2013). Moreover, the impact of NC on Gag-Gag interaction was tested using the ability of wt Gag to rescue non-myristylated Gag at the PM (Morikawa, Hinata et al. 1996; Ono, Demirov et al. 2000; Li, Dou et al. 2007; Kawada, Goto et al. 2008). Since non-myristylated Gag proteins do not interact with membranes, different N-myristly defective mutants like ΔNC Gag and ΔCA-CTD labeled mutants were co-transfected with wt Gag. No FRET was observed with the Myr$^-$ΔCA-CTD Gag mutant which is in agreement with the observations on homotypic complexes and thus confirming the key role of the CA-CTD domain in Gag oligomerization. Similar results Myr$^-$ΔNC Gag mutants were obtained indicating that the NC domain is required for Gag–Gag interactions in the absence of membrane binding.

3.5.1 Assembly of recombinant Gag in vitro

To gain insights into the process of assembly, *in vitro* systems have been generated that recapitulate capsid formation outside the context of the cell by using purified recombinant Gag at high concentrations (~1mg/ml, or 20 μM) in buffer known as HIV-1 myr(−)GagΔp6. More recently, Mckinstry et al., have managed to purify full length Gag (myr(-)Gag) and could be crucial in answering these questions (McKinstry, Hijnen et al. 2014). By using myr(−)GagΔp6 it was shown that Gag is in a monomer-dimer equilibrium in solution, while (myr(-)Gag) showed that it exist in trimeric form (Ekram W. Abd El-Wahab, Redmond P. Smyth et al. 2014).

By using this *in vitro* approach it was established that Gag can assemble spontaneously in presence of nucleic acid, i.e. un-catalyzed and without the input of energy, still there are a number of key differences between the recombinant assembly system and the intracellular environment (Ellis 2001). Another set of studies has been performed in assembly of newly synthesized Gag using cell extracts, such as rabbit reticulocyte extract (Sakalian, Parker et al. 1996; Spearman and Ratner 1996) or wheat germ extract (Lingappa, Hill et al. 1997; Singh, Hill et al. 2001; Zimmerman, Klein et al. 2002), and by linking Gag assembly to translation. It was observed that the cell-free assembly system closely recapitulates the process of assembly that occurs in cells (Lingappa, Hill et al. 1997; Singh, Hill et al. 2001).

Further, studies revealed that capsid assembly in the cell-free system is energy-dependent, that ATP hydrolysis and not just ATP binding was likely required. This energy requirement is post-translational and therefore separate from the well-understood requirement for energy during

translation (Lingappa, Hill et al. 1997). This energy-dependent in cells implies that the mechanism of assembly in cells differs from the spontaneous assembly observed with recombinant Gag *in vitro* and also supported by the energy-dependence of retroviral capsid assembly in the cell-free system and in cells (Weldon, Parker et al. 1998; Dooher and Lingappa 2004), and by the identification of an ATP-binding protein, ABCE1, that facilitates assembly in cells (Zimmerman, Klein et al. 2002).

3.6 Incorporation of other viral components

Other cellular and viral components important for the assembly and infectivity of virus, are incorporated into the particle during assembly namely, cellular $tRNA_3^{Lys}$ (50-100 molecules/virion) (Isel, Ehresmann et al. 2010), several viral proteins including: Vpr (100-200 molecules/virion), Vif (10-100 molecules/virion), and Nef (5-70 molecules/virion). A number of cellular proteins are incorporated into viral particles including: Cyp-A (~250 molecules/virion), Hsp70 present at 1:25 Gag molecules, LysRS, TSG101, Ubiquitin, APOBEC3G, INI1/HSNF5, Staufen, UNG2, HLA-II, ICAM-1 (CD54), annexins and tetraspanins (Coffin JM 1997; Ott 2008; Balasubramaniam and Freed 2011). Furthermore, the interaction between the GagNC and the packaging domain of the gRNA allows further contacts between the viral RNA and $tRNA^{Lys3}$/LysRS facilitating thereby the annealing of the $tRNA^{Lys3}$ to the PBS (Kaminska, Shalak et al. 2007; Kleiman, Jones et al. 2010; Kobbi, Octobre et al. 2011).

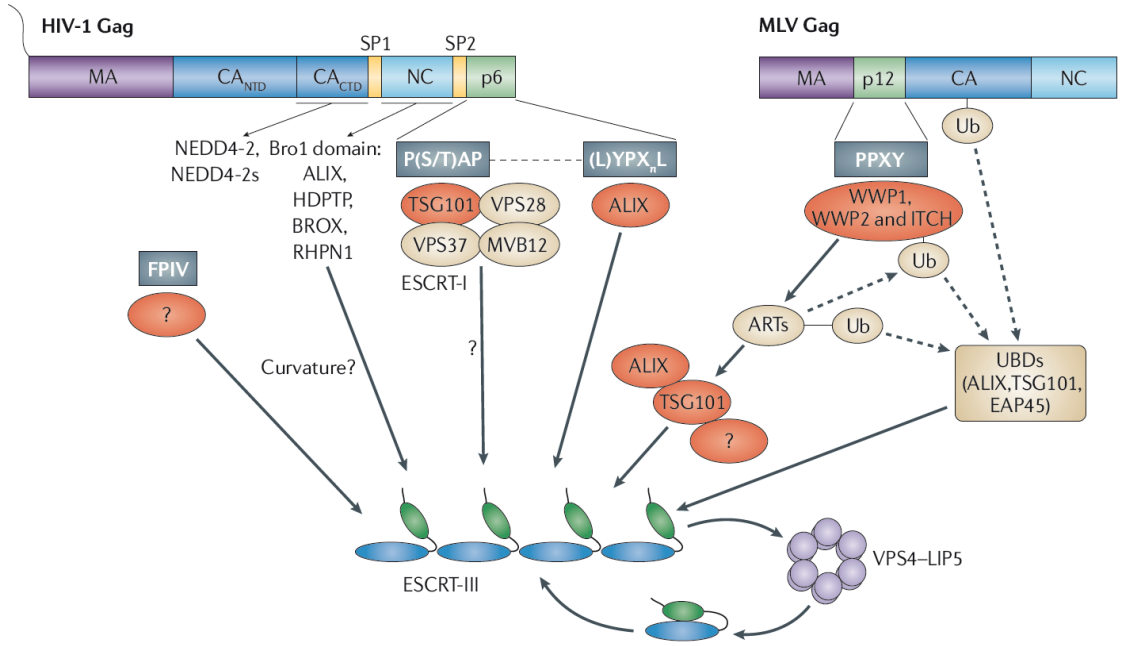

Figure 28: HIV-1 budding and release. Recruitment of host factors by L-domains. Late-budding domains (L-domains) encoded by enveloped viruses (grey boxes in the figure) recruits the ESCRT machinery through direct interactions with adaptor proteins in this pathway (red). Every known L-domain requires components of the core ESCRT machinery, such as ESCRT-III and vacuolar protein sorting-associated protein 4 (VPS4), to facilitate the final separation of virions from the infected cell. Auxiliary interactions that have been described HIV-1 Gag with the NEDD4-2 and NEDD4-2s isoforms and with Bro1 domain-containing proteins are shown (Marcello, Zoppe et al. 2001).

3.7 Virus particle budding and release

The terminal stage of the viral life cycle starts with budding and the assembled viral particle induce a membrane fission event to completely separate the viral envelope from the infected cell surface (Weiss and Gottlinger 2011). To catalyze this egress, the virus hijacks the host ESCRT pathway (Morita and Sundquist 2004; Bieniasz 2009). In cell, ESCRT (endocytic sorting complex required for trafficking) factors are implicated in membrane fission reactions to release vesicles into endosomal multivesicular bodies and to separate daughter cells along the cytokinesis (Sundquist and Krausslich 2012). ESCRT factors belong from the VPS system, composed of proteins called class E, grouped into five major complexes: HRS-STAM complex, ESCRT-0, ESCRT-I, ESCRT-II and ESCRT-III as well as the accessory proteins VPS4 and ALIX (Fig. 28) (Martin-Serrano and Neil 2011). As mentioned earlier, impaired viral particle release takes place when defects in HIV-1 p6 domain occur (Figure 29). With the help of its two different domains referred as "late domain" motifs, Gag p6 recruit early-acting ESCRT factors

(Morita and Sundquist 2004; Bieniasz 2009; Carlton and Martin-Serrano 2009; Usami, Popov et al. 2009) by mainly two and possibly three different pathways:

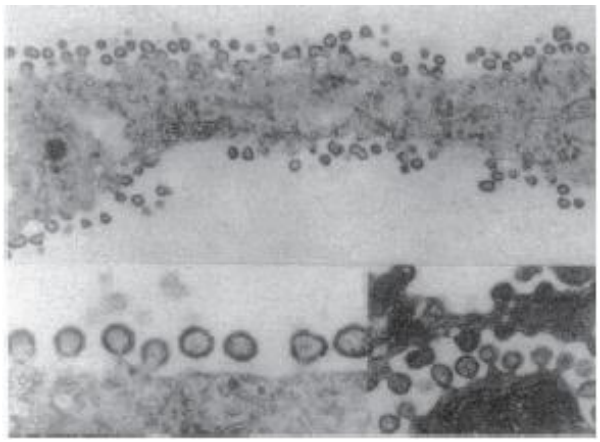

Figure 29: HIV-1 p6 mutants have a pronounced defect in release. Electron microscopy image of HIV-1 virions that carry mutations in p6 Gag. The membrane of both host cell and nascent virion remain connected through a thin membranous stalk. Adapted from (Gottlinger, Dorfman et al. 1991).

3.7.1 Gag-TSG101 pathway

The primary pathway involves the late "L" domain of Gag (PTAP motif of p6), which recruits and binds directly to Tsg101 (Tumor susceptibility gene 101), a subunit of ESCRT-I, heterotetramer that also contains VPS28, VPS37 and MVB12 (Martin-Serrano and Neil 2011; Weiss and Gottlinger 2011). Tsg101 was originally identified in neoplasia associated after its functional inactivation in murine fibroblasts (Li and Cohen 1996). A variety of nuclear, microtubule, and mitotic spindle abnormalities have been observed in cell line that are deficient in TSG101 (SL6) (Li and Cohen 1996; Xie, Li et al. 1998; Zhong, Chen et al. 1998). SL6 cells that are deficient in Tsg101 show defective endosomal trafficking (Babst, Odorizzi et al. 2000). TSG101 contains various sub domains notably an ubiquitin (Ub) conjugase (E2) - like domain that lacks the active-site Cys residue crucial to Ub conjugation (Figure 30) (Pornillos, Alam et al. 2002). The PTAP motif interacts with the amino-terminal of this domain (Garrus, von Schwedler et al. 2001; Martin-Serrano, Zang et al. 2001; VerPlank, Bouamr et al. 2001). On the other hand, the C-terminal region of Tsg101 contains a binding site for Vps28, and an upstream coiled-coil domain may bind Vps37 (Bishop and Woodman 2001; Katzmann, Babst et al. 2001; Martin-Serrano, Zang et al. 2003). These three proteins, Vps28, Vps37 and Tsg101, form a complex called ESCRT-1 (Figure 28). Interestingly, this PTAP motif is also found in various proteins

known to recruit ESCRT-I to endosomal membranes notably the human HRS (Bouamr, Houck-Loomis et al. 2007). Thus, in HIV, the PTAP domain of p6 mimics a cellular ESCRT-I recruiting motif and plays a role in virus budding.

Mutations in the PTAP motif disrupt this interaction (Demirov, Ono et al. 2002). Moreover, It has been shown by (Garrus, von Schwedler et al. 2001) by using small interfering RNAs that inhibition of TSG101 expression markedly impairs HIV-1 virus production. Similarly (Demirov, Ono et al. 2002), also demonstrated that overexpression of the N-terminal domain of TSG101 (TSG-5′) dramatically reduces virus release by blocking at the level of virus budding (Garrus, von Schwedler et al. 2001; Demirov, Ono et al. 2002). This blocking was found specific to HIV-1, as MLV release was unaffected by either TSG101 underexpression or TSG-5′ overexpression. In addition to that, it has also been shown that p6 ubiquitination promotes the interaction of Gag with TSG101 (VerPlank, Bouamr et al. 2001; Pornillos, Alam et al. 2002; Freed 2003);(reviewed in (Freed 2002)).

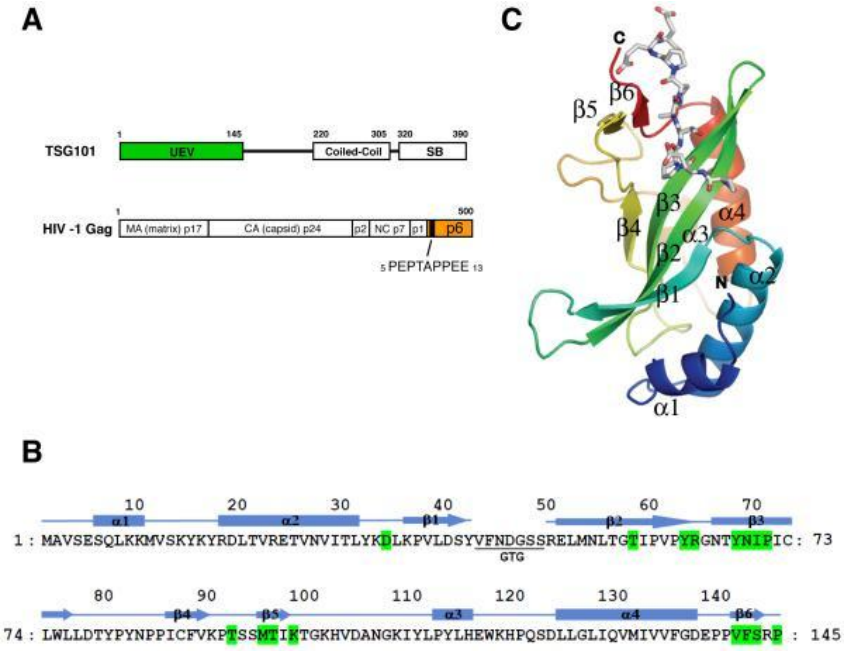

Figure 30: Structure of TSG101 UEV and HIV-1 p6 peptide. (A) Schematic representations of human TSG101 and HIV-1 Gag. Abbreviations within TSG101 are: UEV (ubiquitin E2 variant) and SB (‘steadiness’ box). Viral protease cleavage sites are indicated by vertical lines and the names of resulting proteins are shown. The location of the PTAP peptide in p6 Gag is indicated. (B) Amino acid sequence and secondary structure of TSB101 UEV. The residues involved in PTAP peptide binding are colored in green. (C) Overall structure of TSG101 UEV and HIV p6 peptide. The Tsg101 UEV sequence consists of 145 amino acid residues. The location of β sheets and α helices are shown in the sequence and secondary structure. The position of the beta hairpin tongue is indicated. Residues in green are important for binding to the p6 PTAP peptide. Modified from (Im, Kuo et al. 2010).

3.7.2 Gag-Alix pathway

A secondary late domain of p6 YPXL/LXXLF binds the ESCRT factor ALIX to initiate second budding pathway known as Alix-pathway. The YPXL late domain contributes significantly to HIV-1 replication but is less critical compare to the PTAP motif in most cell types (Fujii, Munshi et al. 2009; Eekels, Geerts et al. 2011). Moreover, this motif YPXL has never been found in mammalian partners.

Alix interacts with the C-terminal helical regions of the CHMP4 proteins of ESCRT-III components (Martin-Serrano, Yarovoy et al. 2003; Strack, Calistri et al. 2003; von Schwedler, Stuchell et al. 2003). It is a modular protein that possesses a banana-shaped N-terminal Bro1 domain, a V-shaped middle domain, and a C-terminal PRR (Fisher, Chung et al. 2007) domain. Bro1 domain binds membranes and induces negative curvature through their convex surfaces (Kim, Sitaraman et al. 2005) (Figure 31) while the V domain binds to $LYPx_n$ L-type L domains via a hydrophobic pocket on one of its arms (Fisher, Chung et al. 2007; Lee, Joshi et al. 2007; Zhai, Fisher et al. 2008), thus linking HIV-1 Gag directly to the CHMP4/ESCRT-III membrane fission complex. Additionally, Alix has potential to bridge ESCRT-I and ESCRT-III through a possible binding between the UEV domain of TSG101 and PSAP motif of the ALIX PRR (Martin-Serrano, Yarovoy et al. 2003; Strack, Calistri et al. 2003; von Schwedler, Stuchell et al. 2003; Ku, Bendjennat et al. 2014) domain.

The $LYPx_n$ L-type L domain in HIV-1 p6 has a much lower affinity for ALIX (Zhai, Fisher et al. 2008) as compare to PTAP-TSG101, thus suggesting that HIV-1 budding depends primarily on the TSG101 binding site, and the ALIX binding site plays an auxiliary role (Fisher, Chung et al. 2007). However, the role of the p6 ALIX binding site in particle release becomes critical in case of "minimal" HIV-1 Gag that lacks certain MA and CA NTD sequences (Strack, Calistri et al. 2003), which suggests that assembly defects can to some extent be compensated by the presence of an optimal L domain.

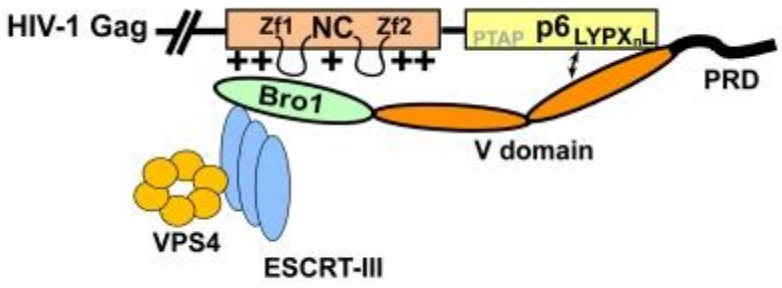

Figure 31: Model for GagNC cooperation with the PTAP/Tsg101 and LYPXnL/Alix budding pathways. Role of GagNC in the LYPXnL/Alix pathway: GagNC interacts with the Bro1 domain of Alix through its N-terminal basic residues and zinc fingers to recruit the essential downstream budding machinery components, ESCRT-III and VPS4, to promote virus egress. (Dussupt, Javid et al. 2009)

Interestingly, it has been found that ALIX also interacts with the NC domain of Gag through its Bro1 domain (Popov, Popova et al. 2008; Dussupt, Javid et al. 2009), through conserved zinc finger motifs and on basic residues within GagNC (Popov, Popova et al. 2008; Sette, Dussupt et al. 2012) as well as disruption of this interaction impaired ALIX-mediated HIV-1 budding. This also brings a notion that the viral RNA may serve as a bridging factor due to the ability of GagNC to interact with it.

3.7.3 Gag-NEDD4L pathway

A third type of L domain, PPXY (found in RSV, MLV, HTLV and MPMV, but not in HIV) can engage NEDD4 ubiquitin ligase. However, we cannot exclude the role of NEDD4 during HIV-1 budding from cells as there is relatively low ESCRT-I levels. Interaction between the carboxy-terminal domain of GagCA and the NEDD4L can help ESCRT to assemble (Chung, Morita et al. 2008; Usami, Popov et al. 2008; Weiss, Popova et al. 2010) and thus can also rescue the budding of HIV-1 L-domain mutants (Ono and Freed 2004; Weiss and Gottlinger 2011).

4. HIV Budding

HIV-1 budding and release are essential for spreading viral infection. The virus usurps the host ESCRT pathway to terminate Gag polymerization and catalyze release of vesicles by membrane fission reactions (Sundquist and Krausslich 2012).

In essence, TSG101/ESCRT-I, ALIX and possibly NEDD4L functions by recruiting downstream ESCRT-III and VPS4 complexes, which in turn mediate membrane fission and recycling of ESCRT factor V. As illustrated in (Figure 32), entire ESCRT assembly process, in presence of ALIX, takes approximately 10 minutes and occurs in multiple stages, with a gradual and concomitant buildup of the Gag and ALIX proteins, followed by short (∼2 min) bursts of ESCRT-III and VPS4 recruitment immediately prior to virus budding (Sundquist and Krausslich 2012).This budding process is aided by CHMP4 subunits, possibly in complex with CHMP2 and other ESCRT-III proteins, to form inwardly spiraling filaments within the neck of the budding virus. These filaments may create closed "domes" that constrict the opposing membranes and promote fission (Sundquist and Krausslich 2012).

As far as virus release is concern, it seems that VPS4 plays an active role in it (Baumgartel, Ivanchenko et al. 2011; Elia, Sougrat et al. 2011; Jouvenet, Simon et al. 2011), as ESCRT-III recruitment alone is insufficient for virus release (Jouvenet, Simon et al. 2011). It is possible that VPS4 helps to promote the formation of abovementioned ESCRT-III dome and/or removal of ESCRT-III subunits from the dome, thereby destabilizing hemi-fission intermediates and thus helps to drive fission to completion (Sundquist and Krausslich 2012).

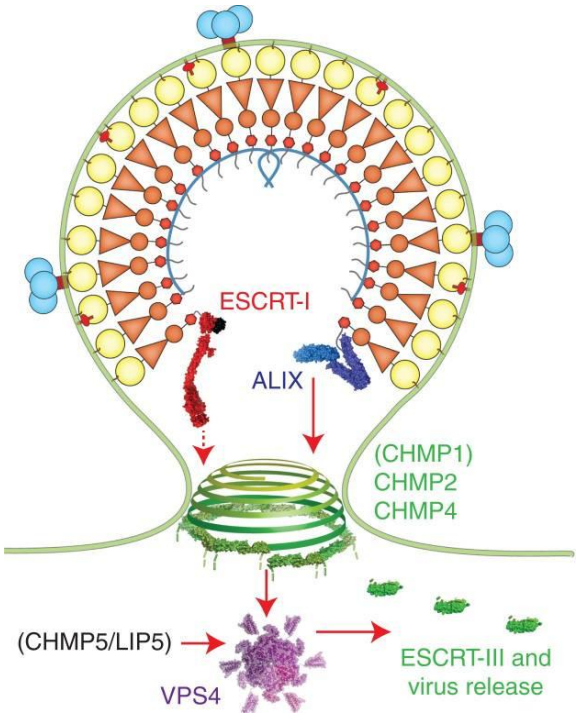

Figure 32: Schematic representation of the essential core ESCRT machinery during budding. Late domain motifs within p6Gag binds directly to the UEV domain of the TSG101 subunit of the heterotetrameric ESCRT-I complex (red, with bound ubiquitin in black) and the V domain of ALIX (blue) to recruit the ESCRT-III proteins of the CHMP1, CHMP2, and CHMP4 families (green), which apparently polymerize into a "dome" that promotes closure of the membrane neck. Due to these interactions, VPS4 ATPases also get recruited that completes the membrane fission reaction and uses the energy of ATPase to release the ESCRT-III from the membrane and back into the cytoplasm (Sundquist and Krausslich 2012).

5. Cellular partners interacting with Gag via NC domain

Several cellular partners of Gag have been identified that interact with Gag via NCp7 domain, including the actin protein (Ott, Coren et al. 1996), Staufen -1 (Mouland, Mercier et al. 2000; Chatel-Chaix, Clement et al. 2004) and several other proteins (Ptak, Fu et al. 2008). However, the role of all the proteins, interacting with Gag, is not fully determined. Here we presented a list of known proteins, and their functions in the replication cycle, that interact with Gag via NC domain in Table 1:

Interaction Parameter / Cellular partner	Function of the protein in the cell	Involved domain/Specificity	Role of the interaction	Technique used	Ref.
AIP1 = Alix (Apoptosis linked gene 2 -interacting protein X)	Promotes viral egress and membrane fission events.	NC and p6	virus budding	GST pull down	(Popov, Popova et al. 2008)
AP-2 (Clathrin-associated Adaptor Protein 2)	Associated to the plasma membrane and responsible of endocytosis	Junction MA-CA	AP-2 plays a role in regulating assembly and release during late phase of replication	GST pull down	(Batonick, Favre et al. 2005)
Actin	actin microfilaments: an essential component of the cytoskeleton	NC	Interaction of Gag/actin could play a role in assembly and/or other stages of the replication cycle	Co-IP, in vitro protein binding assay	(Rey, Canon et al. 1996; Liu, Dai et al. 1999; Wilk, Gowen et al. 1999)

AGO2 (Argonaute 2)	Role in repression mediated by RNA interference		Gag turns away the function of Ago2 that play a role in virus replication	Co-IP (not found by two-hybrid)	(Bouttier, Saumet et al. 2012)
EF1α (Elongation Factor 1- α)	component of the translational machinery, delivering amino-tRNA to ribosomes	MA and NC	EF1α allows incorporation of tRNA into virions and its interaction with Gag prevents translation, consistent with the previous model where the inhibition of translation by accumulation of Gag allows the release of the RNA from polysomes and favor encapsidation in viral particles	Two-hybrid	(Cimarelli and Luban 1999)
HP68= ABCE1 (ATP-Binding	Inhibits the ribonuclease L (which has antiviral properties) and has an	basic residues (NC) HIV-1	Facilitating the capsid assembly process.	Co-IP GST-pull down	(Lingappa, Dooher et al. 2006)

Cassette protein E1)	antiapoptotic and protumoral role				
Kif4 (Kinesin superfamily protein)	Motor protein regulating movements of multiple cellular components	(N-terminal matrix) Gag	Role in delivering retroviral Gag polyproteins to the plasma membrane.	two-hybrid Co-IP GST pull down	(Kim, Tang et al. 1998)
Lyric (HIV-inducible gene)	-Implicated in HIV associated neuropathy. - signaling pathway. - antiapoptotic effects, tumorigenesis.	MA and NC	Regulates viral infectivity	CoIP , Tandem affinity purification (TAP)	(Engeland, Oberwinkler et al. 2011)
RPL7 (human ribosomal protein)	- interfering with the translation from distinct mRNAs in vitro and in vivo. - Translational regualtion of gene expression. - Co-regulator of nuclear receptor-mediated transcription.	- (NC) Gag/RPL7 - Independent of its multimerization and localization at the membrane.	would regulate the balance between translation/packaging during late stages of viral replication : to demonstrate	two-hybrid Co-IP FRET/ FLIM Biacord	(unpublished data)

Stau (Staufen)	Role in RNA localization, translation and mRNA decay.	NC	Staufen-1 influences the multimerization of Gag.	Co-IP BRET	(Abrahamyan, Chatel-Chaix et al. 2010)
TSG101 (human tumor susceptibility gene 101)	- Component of the endosomal sorting complex ESCRT-I - sorting of ubiquitinated cargo into small vesicles that but into the lumen of multivesicular bodies (MVBs).	NC and p6	Release of infectious virions and facility of viral budding.	Yeast two-hybrid GST pull down	(Garrus, von Schwedler et al. 2001; Chamontin, Rassam et al. 2015)
Nuc (Nucleolin)	- Shuttle between the nucleus and cytoplasm. - Ribosome biogenesis and assembly.	NC and CA	can potently inhibit virus assembly	Two-hybrid GST pull down	(Bacharach, Gonsky et al. 2000)

Table 1: List of cellular proteins which are interacts with Gag mainly via its NCp7 domain.

Research Aim

The Gag structural polyprotein of HIV-1 orchestrates viral particle assembly in producer cells, in a process that requires two platforms, the genomic RNA on the one hand and a membrane with a lipid bilayer, on the other. Gag is formed composed of matrice (MA), capsid (CA), nucleocapsid (NCp7) containing two invariant CCHC zinc fingers and p6 domains which are essential for the formation of infectious viral particles. GagNC, in addition to its role as chaperone, was also shown essential in Gag assembly by virtue of its interaction with a wide range of nucleic acids thanks to numerous basic residues distributed throughout the protein. This nonspecific binding mode seems to contribute to the assembly by tethering Gag molecules onto the RNA generating a molecular crowding that in turn promotes Gag-Gag interactions.

Based on this knowledge, the aim of the thesis was to describe the role of the NC domain as part of Gag (GagNC) in Gag-Gag interaction that is essential for the assembly of the particles and also the role of Gag (NC) along the budding notably using quantitative fluorescent microscopy. During the course of our studies we divide our aims into these categories:

1- The first aim of the thesis was to analyse the influence of the NC zinc finger (ZF) on the intracellular localization and assembly of HIV-1 Gag. Therefore, we used fluorescent Gag derivatives such as Gag-eGFP and Gag-mcherry, where the fluorophore was inserted next to the MA domain and monitored the assembly of Gag by the two photon fluorescence lifetime imaging microscopy (FLIM) based fluorescence energy transfer (FRET) and by the time laps epifluorescence microscopy. Detailed analyses of FRET images revealed a homogenous distribution of Gag-Gag complex in cells with a progressive concentration of ordered Gag oligomers underneath the plasma membrane (PM) favouring a model where Gag oligomerization in the cytoplasm precedes virus assembly at the PM. In this model, the absence of NC domain results in i) an accumulation of Gag as large aggregates that are dispersed in the cytoplasm, ii) a decrease of Gag-Gag condensation and iii) a delay for Gag-Gag complexes in reaching the PM. Thus GagNC is involved directly through protein-protein interaction or indirectly by its virtue to interact with RNA to the formation and the trafficking of Gag in the cell.

2- Next, as a result of first aim of thesis, the monitoring of Gag assembly as function of time revealed a large decrease of VLPs at the level of the PM which is in agreement with data

showing a defect in Gag, in the supernatant of cell expressing GagΔNC (grigorv 2007, hogue et al 2009). Taking into account the importance of TSG101 in Gag budding, our second aim was to determine the role of GagNC in the TSG101 pathway. For this, cells were transfected with HA-TSG101 together with plasmids expressing Gag or Gag mutants that are formed by deleting either the zinc finger motifs or the entire GagNC domain. Results were compared with cell co-expressing TSG101 and Gag-L6I7, in which PTAP sequence was substituted for LIAP (Freed et al 2003) or GagΔp6. Using a series of experiments including immunoprecipitation, confocal fluorescent microscopy and FLIM-FRET, we found that NC alone or in the context of Gag, interacts directly with TSG101 and could participate with p6 in the recruitment of ESCRT-I budding pathway of HIV-1.

Materials and Methods

1. Materials

1.1. Cell line

HeLa cells: are the first immortal cell line of human origin and named after HEnrietta LAcks. Isolated in 1951, these adherent cells derived from metastases and were taken from a patient with cervix cancer.

293T cells: lineage constitute a derivative of human epithelial kidney cells transformed with adenovirus E1A, which also expresses the SV40 T antigen for the episomal replication of plasmids containing the SV40 origin and the promoter region.

1.2. Plasmids

Table 1: List of plasmids used in my thesis:

Plasmid	Resistance gene	Tag	Promoteur	Provenance
eGFP	Kanamycine		CMV	
Gag-TC	Ampicilline	/	CMV	Dr. D.Ott (National Cancer Institute, Frederick, Maryland, USA)
Gag-eGFP	Ampicilline	C-terminal (MA)	CMV	Dr.V.Goldshmidt
Gag-mCherry	Ampicilline	C-terminal (MA)	CMV	Dr.V.Goldshmidt
Gag-ΔZF1-TC	Ampicilline	/	CMV	Dr.V.Goldshmidt
Gag-ΔZF2-TC	Ampicilline	/	CMV	Dr.V.Goldshmidt
Gag-ΔZF1Δ ZF2-TC	Ampicilline	/	CMV	Salah EL Meshri
Gag-ΔNCp7-TC	Ampicilline	/	CMV	Salah EL Meshri
Gag-Δp6-TC	Ampicilline	/	CMV	Salah EL Meshri
Gag-L6i7-TC	Ampicilline	/	CMV	Salah EL Meshri
Gag-eGFP-ΔZF1	Ampicilline	C-terminal (MA)	CMV	Salah EL Meshri
Gag-eGFP-ΔZF2	Ampicilline	C-terminal (MA)	CMV	Salah EL Meshri
Gag-eGFP-ΔZF1Δ ZF2	Ampicilline	C-terminal (MA)	CMV	Salah EL Meshri
Gag-eGFP-ΔNCp7	Ampicilline	C-terminal (MA)	CMV	Salah EL Meshri
Gag-eGFP-Δp6	Ampicilline	C-terminal (MA)	CMV	Salah EL Meshri

Gag-mCherry-ΔZF1	Ampicilline	C-terminal (MA)	CMV	Salah EL Meshri
Gag-mCherry-ΔZF2	Ampicilline	C-terminal (MA)	CMV	Salah EL Meshri
Gag-mCherry-ΔZF1Δ ZF2	Ampicilline	C-terminal (MA)	CMV	Salah EL Meshri
Gag-mCherry-ΔNCp7	Ampicilline	C-terminal (MA)	CMV	Salah EL Meshri
Gag-mCherry-Δp6	Ampicilline	C-terminal (MA)	CMV	Salah EL Meshri
eGFP-TSG	Kanamycine	N-terminal	CMV	NIH AIDS Reagent Program
HA-TSG	Ampicilline	N-terminal	CMV	NIH AIDS Reagent Program
GagG2A-TC	Ampicilline	/	CMV	Dr J.V. Fritz
NCp7-mCherry	Ampicilline	C-terminal	CMV	Dr.V.Goldshmidt
NCp7-eGFP	Ampicilline	C-terminal	CMV	Dr. V.Goldshmidt
NCp7-ΔZF1-eGFP	Ampicilline	C-terminal	CMV	IGBMC
NCp7-ΔZF2-eGFP	Ampicilline	C-terminal	CMV	Dr.V.Goldshmidt
NCp7-ΔZF1ΔZF2-eGFP	Ampicilline	C-terminal	CMV	Dr.V.Goldshmidt

1.3. Primary and secondary antibodies

Table 2: List of different primary antibodies used

Name	Species	Provider	Reference	Fluorophore or enzyme	Mono / Polyclonal	Application / dilution
Anti-p24 Gag	Mouse	NIH	6521	/	Monoclonal	WB 1/10000
Anti-p24 Gag	Rabbit	abcam	32352	/	Monoclonal	WB 1/10000
Anti-HA	Rabbit	abcam		/	Polyclonal	IP 4µg/mg WB 1/4000
Anti-eGFP	Mouse	proteintech	66002-1-Ig	/	Monoclonal	WB 1/4000
Anti-TSG101	Rabbit	abcam	Ab30871	/	Polyclonal	WB 1/250
Anti-HA	Mouse	abcam		/	Monoclonal	WB 1/10000
Anti-GAPDH	Mouse	millipore	MAB374	/	Monoclonal	WB 1/5000
Anti-mCherry	Rabbit	abcam		/	Polyclonal	WB 1/1000
Anti-RPS7	souris	abcam	57637	/	Monoclonal	WB 1/500
Anti-RPS14	lapin	abcam	50390	/	Polyclonal	WB 1/400
Anti-Flag	souris	sigma	F1804	/	Monoclonal	WB 1/4000

Table 3: List of different secondary antibodies used

Name	Species	Provider	Reference	Fluorophore or enzyme	Mono / Polyclonal
Anti- mouse HRP		Promega	W402B	HRP	WB 1/10000
Anti- rabbit HRP		Promega	W401B	HRP	WB 1/10000
Anti- Rabbit	Goat	invitrogen		Alexa fluor 488	IF 1/2000
Anti-Mouse	Goat	invitrogen	A110111	Alexa fluor 568	IF 1/2000
protein A		invitrogen	101023	HRP	WB 1/15000

1.4. Oligonucleotides

Synthetic oligodeoxyribonucleotide (ODN) were purchased from Sigma-Aldrich. The sequences of these oligonucleotide primers used in my thesis are described in the table below:

Table 4: The oligonucleotides used for mutagenesis are phosphorylated at the 5 ' end.

Name	Sequence 5 'to 3'
Mut Gag-deltaZF1--Fwd	CGCGCCCCCCGCAAGAAGGGCTGC
Mut Gag-deltaZF1--Rev	CTTGACGGTCTTCCGCTGGTTGCG
Mut Gag-deltaZF2--Fwd	ACCGAGCGCCAGGCCAACTTCCTG
Mut Gag-deltaZF2--Rev	GCCCTTCTTGCGGGGGGCGCGCTTG
Mut Gag-deltaNCp7--Fwd	TTCCTGGGCAAGATCTGGCC
Mut Gag-deltaNCp7--Rev	CATGATGGTCGCCGGGTTC
Mut Gag-Δp6-Fwd	GGCAACTTCCTGTAAAGCCGCCCCGAG
Mut Gag-Δp6-Rev	GGGGCGGCCCTTGTAGCTGGGCC
Mut Gag-L6i7-Fwd	CGCCCCGAGCTAATCGCCCCCCCCGAG
Mut Gag-L6i7-Rev	GCTCGCAGGAAGTTGCCGGG

1.5. Competent bacteria

The Escherichia coli DH5α competent bacteria are prepared in the laboratory and were used to amplify plasmids. Several mutations are found in the genotype of the bacterium. Examples include mutations that *endA1* and *recA1* which respectively leads to inactivation of an intracellular endonuclease thus allowing greater protection of foreign plasmid DNA and allows the elimination of homologous recombination. The bacteria are stored at -80 ° C in TB buffer (10 mM Hepes, 250 mM CaCl2, 25 mM KCl, 55mM MnCl2, pH 6.7) containing 2% DMSO.

Ultra competent bacteria from New England's Biolabs (NEB 5-alpha #C2987H) were also used to amplify PCR products from cloning.

2. Methods

2.1. Transformation of competent bacteria and purification of plasmid DNA

After slow thawing of the E. coli DH5α bacteria in ice, 50 µL of the competent bacteria were incubated with 1ng of plasmid of interest, in ice for 30min. The tube containing the mixture is then placed at 42 ° C for 45 seconds, and then immediately transferred back to ice for 10 minutes. This step is known as thermal shock (heat shock) and is a crucial step during exogenous plasmid transformed. After that, 950µl of sterile LB medium (tryptone 10 g / L, yeast extract 5 g / L, NaCl 5g / L, pH 7 - DifcoTM LB, Lennox) were added. The bacteria are then placed in the incubator at 37 ° C for one hour. Finally, the bacteria are plated on Petri dishes containing LB agar medium (agar: 15 g / L - DifcoTM agar LB, Lennox) and the antibiotic which has the resistance gene in plasmid of interest and placed at 37 ° C overnight.

Ampicillin and kanamycin are used at final concentrations of 100µg/mL and 50µg/mL respectively.

The second day, the colonies having a thrust on the culture medium is inoculated into 3 ml of LB medium with antibiotic for 8 to 10 hours. This 3ml pre-culture is used to inoculate 150 ml of LB medium containing antibiotics and cultured at 37 ° C for 14 to 16 hours.

Purification of plasmid DNA is carried through the KIT Nucleobond Xtra Midi Plus® (Macherey-Nagel) and DNA concentrations were measured by using nanodrop.

2.2. Cell Culture: Passage of Hela cells, 293T

HeLa and 293T cells were grown in flasks of 75cm^2 in DMEM solution, Glutamax (*Dulbecco's Modification of Eagle's Medium*) developed by Harry Eagle in 1959. This medium contains amino acids (L-Threonine, L Glutamine), salts (potassium chloride and magnesium sulfate), vitamins (folic acid, nicotinamide, and riboflavin), glucose and organic supplements such as pyruvate. It is supplemented with fetal calf serum or 10% FCS and 5 ml mixture of antibiotics, names as S/P, like penicillin (100 IU/ml) and streptomycin (100 IU/ml). Serum would be used as cell growth factors which they need to proliferate and antibiotics are used to prevent bacterial contamination.

The first step was to remove the culture medium. Then the cells were washed with 10 mL of 1X PBS (Phosphate Buffered Saline 10X: KH_2PO_4 1.44g/L NaCl 9 g/L, $NaHPO_4$ 7.95 g/L, pH 7.4). After removal of PBS, 2 to 3 mL of 1X trypsin was added. Due to the action of the enzyme cells will be separated from plastic wall of the culture flask. The flask is then placed in the incubator for 2 to 5 minutes at 37 ° C (optimum temperature action of trypsin) in a humid atmosphere with 5% CO_2. After checking the proper action of enzyme on the optical bench microscope, 7-8 mL of DMEM, for inhibiting the action of trypsin, was added. The cells were recovered by pipetting and then placed in a 15 mL Falcon tube and then centrifuged for 5 minutes at 1100 rpm. The supernatant is then removed and the cell pellet was suspended in 10 mL of fresh DMEM solution and numbers of cells were counted by using a Neubauer cell (Figure 33):

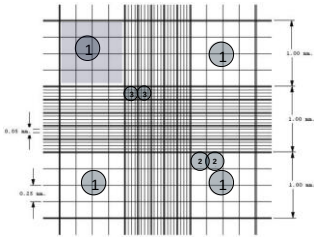

Figure 33: Cell Neubauer (According www.celeromics.com)

The area of the single square is denoted by 1mm^2 and the volume by 0.1 mm^3 = 1.10^{-4} ml. Thus, to count the cells, the undermentioned formula was used:

$$\text{Cell concentration} = \left(\frac{\text{Total cells counted}}{\text{Number of square}}\right) * 10\,000$$

$1x10^6$ cells were then placed in a $75cm^2$ flask in 20mL DMEM solution with (P/S + 10% FCS). The cells were finally placed in incubator at 37 ° C in a humid atmosphere of 5% CO_2.

2.3. Cell transfection

The transfection of HeLa or 293T cells is carried out by using a Polyplus jetPEI™ kit and a solution of 150 mM NaCl. Polyethyleneimine (JetPEI) is a polycationic agent which binds to DNA and allows the migration of DNA through the cell wall in a few steps. During this process, the polycation binds to the phosphate bone of negative DNA and make complexes. The complex formed is positive and is able to bind to the plasma membrane of negative polysaccharides. Once attached to the membrane, the complex is endocytosed. Moreover, JetPEI has sponge like properties which help its merger with the endosome and thereby inactivating the acidic hydrolases that could be responsible for DNA degradation. Then the polycation-DNA complex leaves the endosome, and goes to the nucleus to be transcribed.

The transfection of HeLa cells were performed in 6/12-wells plates or µ-Dish 35mm Ibidi (BioValley) (Table 5).

After, coverslip of 18 mm in diameter were deposited at the bottom of each well of 6/12-wells (except µ-Dish 35mm Ibidi, where the surface is pretreated to make it sterile and to improve cell adhesion). The slides were then sterilized by the addition of 70% ethanol for 5 minutes, then successive washing steps were performed by using solutions containing 1X PBS (1 x 2 mL) and two washes with DMEM (2 x 2 mL). The cells were seeded according to the calculated amount and are placed at 37 ° C (5% CO_2) for 24 hours.

For each test sample, two Eppendorf tubes are prepared according to specific methods detailed in Table 5:

		Number of adherent cells to deposit	Maximum amount of DNA (µg)	Volume DNA (µL)	Volume NaCl (µL)	Volume jetPEI® (µL)
12 wells plate	tube 1	80 000 - 100 000	/	/	46	4
	tube 1'		2	**X**	50-**X**	/
6-well plates or µ-Dish ^{35mm}Ibidi	tube 1	200 000 - 300 000	/	/	94	6
	tube 1'		3	**Y**	100-**Y**	/

Table 5: Number of HeLa cells to be deposited in the wells and conditions of use jetPEI® used for transfection of HeLa cells

The complexes were prepared by using volumes of plasmid DNA (X and Y) of interest and twice the volume of JetPEI® as compared to DNA.

The transfection experiment was conducted simultaneously by preparing two eppendorfs tubes at the same time. After a short incubation period of less than 5 minutes, the contents of tube 1 is added to the contents of the tube 1' (and not the reverse), vortexed for 15 seconds and further incubated for 20 minutes at room temperature. The content of tube was then deposited on seeded cells. After brief manual stirring of the well plate, the cells were returned to 37 ° C (5% CO_2) and allowed to incubate for the time necessary for the experiment (usually 12 to 24 hours for imaging experiments and 48 hours for co -IP). To prevent excessive cell toxicity due to the presence of JetPEI, it is important to change the medium of the culture after 5-6 hrs with fresh DMEM.

2.4. Fixation by PFA (paraformaldehyde)

In order to stabilize the structures (antigens) as close as possible to their live appearance, water-insoluble molecules (cross-linking) were used to block the enzyme systems.

The fixer used in the laboratory is a non-coagulating fixative: paraformaldehyde $(CH_2O)n$ (insoluble polymer of formaldehyde from the group of aldehydes). It reacts essentially with proteins and amino acids, and allows the formation of methylene bridges which acts as water-insoluble barrier.

Fixation of HeLa cells

Fixation of the cells is generally performed 12-24h post-transfection, in several stages. After removal of the DMEM medium, the wells containing the cells were washed 2 times with 1X PBS (2 times 1 ml/well). Then they were fixed with 2 ml of 4% PFA for 10 min at room temperature under constant stirring and dark. Three successive washings of 5 minutes each, with 2 ml of 1X PBS, were then conducted.

Two options are possible:

- When cell were transfected with plasmids expressing fluorescent proteins, coverslip are mounted on slide using a drop of mounting medium (consisting of DAPI-Fluoromount-G and Fluoromount-G 50/50). The coverslip must be in contact with the mounting medium for at least 16 hours. Then we can proceed to microscopic observations, after gently surrounding the coverslip with nail-polish to prevent contamination and other movements during the observations.

- Either performs immunofluorescence.

2.5. Immunofluorescence of HeLa cells

Immunofluorescence allows observation of the expressed proteins (endogenous or overexpressed following transfection by a plasmid) cell by confocal microscopy.

After washes with 1X PBS previously described, the cells were permeabilized with 2 mL of 0.2% Triton (diluted in 1X PBS) for 10 minutes at room temperature under stirring and dark. The cells are then washed three times with 1X PBS with a gap of 5 each. Blocking of non-specific sites were performed by using 2% BSA (Bovine Serum Albumin) for 1 hour stirring under dark. After washing with 1X PBS, 50 µl of solution containing primary antibody diluted in 4% BSA solution (Table 2) is directly deposited on parafilm. The coverslips on which HeLa cells are adhered, is gently transferred on the drop of diluted antibody. Incubation lasts for 1 hour at room temperature in the dark. Two successive washings for slides with 1X PBS were then performed. Coverslips were transferred again to a secondary antibody solution, diluted in 4% BSA solution (Table 3) thus, in the similar way as for the primary antibody and incubation was performed for

40 minutes in dark. Finally, the cells were washed three times with 1X PBS before their mounting with Fluoromount medium (SouthernBiotech).

2.6. Confocal Microscopy

The cellular localization of the proteins of interest coupled to fluorophores (eGFP, mCherry, Alexa Fluor and ReAsH) were visualized using a confocal microscope having a laser as a light source.

The exciting monochromatic laser beam is reflected by a dichroic mirror for reflecting only the selected wavelengths. The beam then enters the sample after being focused by a lens which, in this case, acts as a condenser. The laser delivers energy to the optical fluorochromes on impact, thus allowing them to move on an electronic layer of stronger energy. Fluorochromes naturally return to their ground state, emitting rays of lower energy. The wavelength of the emitted fluorescent light being greater than the excitation wavelength, the emitted light can pass through the dichroic mirror. Through a variable diaphragm ("pinhole") located in the focal plane of the lens of the optical tube, it is possible to select the rays emitted by a single plane of the preparation. The rays are then detected by the photomultiplier, which will convert the photonic signal to an amplified digital signal. A point by point image is reconstructed by the computer, by using received signals. Image acquisition is done by computer using the Leica software. The images obtained, once captured, are analyzed using the commercial ImageJ software.

The microscope used is a laser scanning confocal microscope Leica SPE-TC II (G objective 63X oil immersion).

2.7. FRET (Förster / fluorescence resonance energy transfer)

During my PhD, the FRET-FLIM measurements were perform to visualized Gag/Gag interactions and oligomerizations in fixed or live HeLa cells. To study Gag-Gag oligomerization by FRET-FLIM, cells were transfected by Gag proteins tagged by eGFP (donor) and mCherry or ReAsH (acceptor) (Figure 34), and we monitor the fluorescence lifetime of the donor at each pixel of the image.

FRET is a non-radiative process where the energy of a donor fluorophore (ex: eGFP) in the excited state is transferred to an adjacent acceptor fluorophore (ex mCherry or ReAsH). It is possible in the presence of an overlap between the emission spectrum of the donor and the

absorption spectrum of acceptor (Figure 34) and also requires that the distance between the donor and acceptor should be less than 5-8 nm (Förster distance) with a favorable orientation. These conditions of energy transfer between the donor and acceptor are only possible if the labeled proteins are very close and exclude random interactions (Figure 34). FRET can be carried out with various (donor, acceptor) couples, the most popular being eGFP as a donor and either mCherry or mRFP as acceptor (Tramier, Zahid et al. 2006; Fritz, Didier et al. 2008; Albertazzi, Arosio et al. 2009; Padilla-Parra, Auduge et al. 2009; Boutant, Didier et al. 2010; Fritz, Dujardin et al. 2010; McGinty, Stuckey et al. 2011; Batisse, Guerrero et al. 2013; Carillo, Bennet et al. 2013).

There are three major approaches for measuring FRET i) by fluorescence intensity measurements, ii) by the photobleaching of acceptor (acceptor photobleaching), and iii) by fluorescence lifetime (FLIM). FILM microscopy is the most robust approach to follow FRET in the live cells. We used this approach based on the Time-correlated single-photon counting (TCSPC) that acquire fluorescent lifetime decay of donor for each pixel of an image. In contrast to fluorescence intensity, the fluorescence lifetime is an absolute parameter that does not depend on the instrumentation or the local concentration of the fluorescent molecules (Wachsmuth, Waldeck et al. 2000). The image was obtained in scanning mode microscopy. Therefore, the FRET efficiency at each pixel can be directly determined from the decrease of the fluorescence lifetime of the donor in comparison to its natural lifetime.

In practice, the donor fluorophore is excited by a pulsed laser, and its fluorescence decay is recorded by TCSPC to measure its fluorescence lifetime. The variation of the lifetime of the donor in the presence of the acceptor can calculate the efficiency of energy transfer through the equation:

$$E = 1 - \frac{\tau(ad)}{\tau(d)}$$

Where τ (d) is the lifetime of the donor alone and τ (ad) is the lifetime of the donor in the presence of the acceptor.

The imaging fluorescence lifetime measurements are performed over a home-made scanning microscope using a two-photon excitation. This setup, developed in the laboratory (Azoulay, Clamme et al. 2003; Clamme, Azoulay et al. 2003; Clamme, Krishnamoorthy et al. 2003;

Ludovic Richert 2015) consists of an inverted fluorescence microscope Olympus IX70 with a water objective lense (60X, Numerical aperture = 1.2). The fluorophores are excited by femtosecond pulsed laser (Insight Spectra Physics) which delivers pulses of 100fs between 680 and 1300nm. The fluorescence emitted by the sample is recorded with the avalanche Photodiode (APD) coupled to a TCSPC board (SPC 830). This system allows obtaining images in which the contrast is given by the lifetime of the fluorescence of eGFP and intensity images. The raw data is analyzed using commercial software (Image SPC, BH). A fluorescence lifetime image is generated by using a color scale reflecting the fluorescence lifetime by color (for example shorter lifetime in blue and longer lifetime in red) at each pixel. Thus a reconstruct of the observed cell life are done and allow the determination of the presence of interactions between two proteins exists or not. We considered that a minimum of 5% of FRET is needs to proof interactions between the two tagged proteins and exclude random interactions.

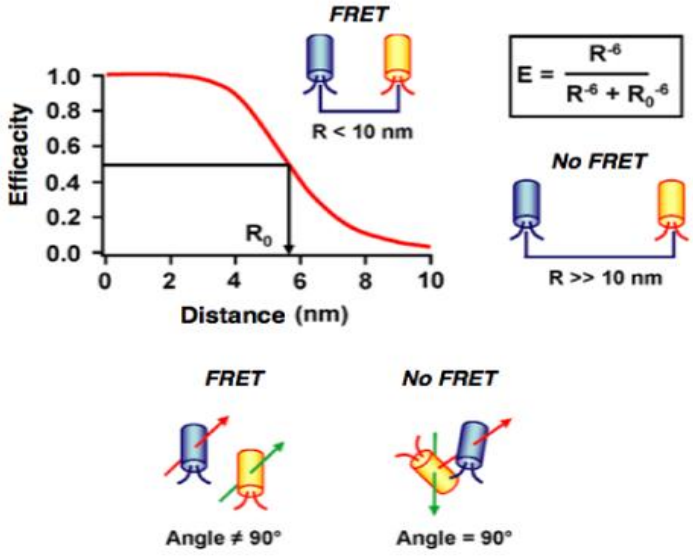

Figure 34: Principle of the FRET-FLIM.

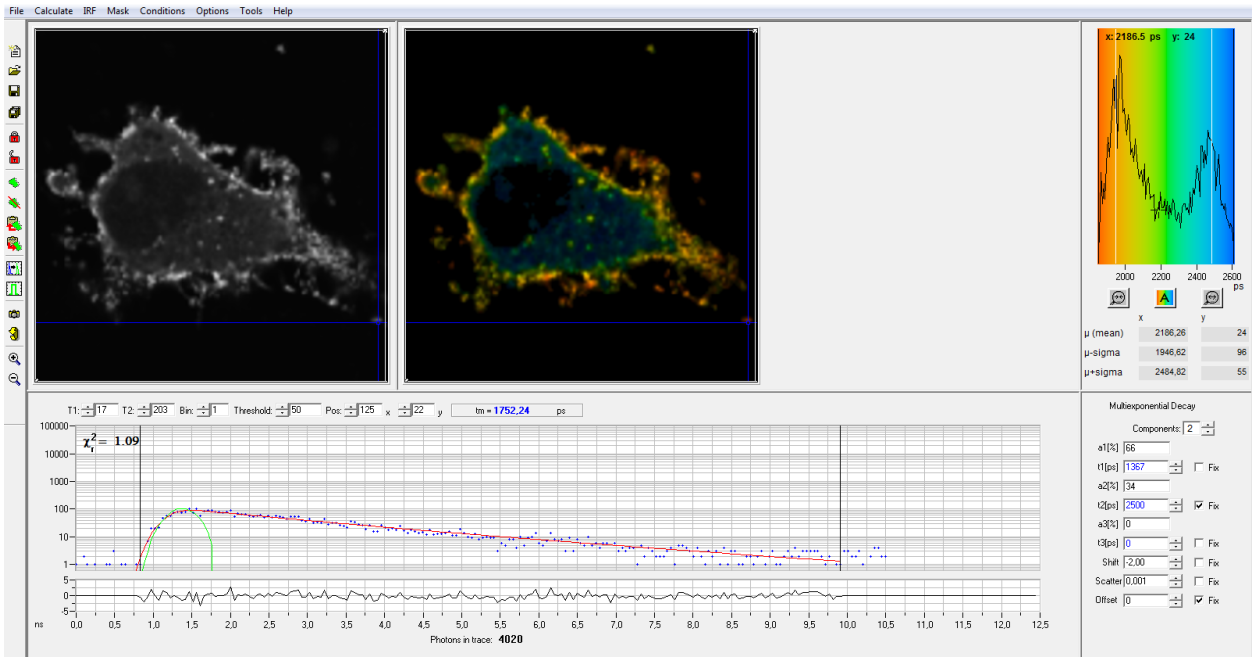

Figure 35: Two component analysis of FLIM images of cells expressing Gag/Gag-eGFP/ Gag-mCherry in a 7/1/2 ratio at 12 h or 24 h post transfection. The fluorescence decays in each pixel were analysed using a bi-exponential model, with a long-lived component τ2 fixed to the lifetime of free eGFP (2.5 ns). The τ1 and α1 values were converted into a colour code ranging from blue (0.1 ns, 0 %) to red (2 ns, 100 %). All images were recorded using 50 × 50 μm scale and 128 × 128 pixels.

As shown in the above image, we observe two lifetime values in our experimental conditions. The lower lifetime values at the plasma membrane (yellow color) compared to the cytoplasm suggests (green to blue color) that either the eGFP and mCherry tags are closer to each other in the oligomers (giving a higher FRET efficiency) or that a higher fraction of Gag proteins are in oligomeric form at the membrane (Figure 35). The time-resolved decays of Gag-eGFP ± Gag-mCherry were analyzed by a two component model function.

$$F(t) = \alpha_1 e^{\frac{-t}{\tau_1}} + \alpha_2 e^{\frac{-t}{\tau_2}}$$

Where, τ1 and τ2 are short-lived and long-lived lifetime, respectively. Additionally, α1 and α2 are corresponding populations of short and long-lived lifetime species, respectively.

2.8. Protein Assay

The Bradford assay is a spectroscopic assay to measure the concentration of protein in solution using colorimetry. This assay is based on the fact that Coomassie blue (G250) absorbance change when it interacts with the basic amino acids (arginine in particular) or aromatic proteins.

Bradford solution is obtained by mixing 1 ml of the "BioRad Protein Assay" solution with 4mL of milliQ water. 200 µL this Coomassie blue solution is then deposited into the wells of a 96 well plate (200 µL / well). To establish standard curve, a solution of BSA (Bovine Serum Albumin) was diluted to one-tenth in Tris buffer and an increasing amount of BSA is then placed in the wells of a 96 well plate (Figure 36). Similarly, solutions containing proteins (cell lysate) are also diluted to 1/20 in Tris and 10 µl of this protein solution are then used (Figure 36).

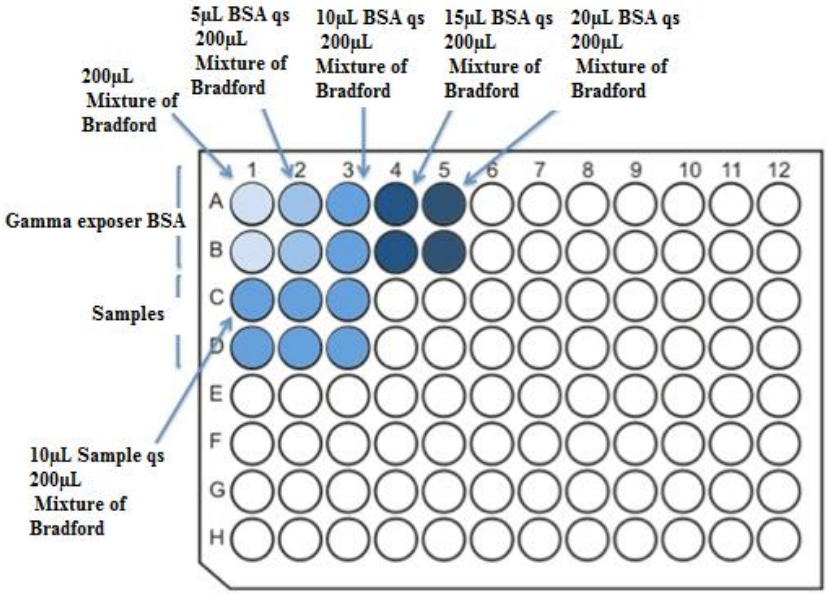

Figure 36: 96 wells plate for a Bradford assay,

For example, 3 samples the absorbance at 595nm is obtained by the spectrofluorimeter safas FLX-Xenius. The optical densities obtained are used to calculate the protein concentration of the samples and thus determine the amount of protein.

2.9. Co-immunoprecipitation

Three wells of a 6-well plate were transfected with the same sample. 48 hours post-transfection the DMEM medium is removed from the wells by a water pump. Then, the cells are rinsed with 1 mL of 1X PBS, trypsinized by adding 1 ml of trypsin (1X) and incubated at 37 ° C for 2 to 3

minutes. Then, 2 ml of DMEM medium is added and the total volume of the three wells, corresponding to the sinlge sample, is transferred into one 15 ml Falcon tube. The recovered cells were centrifuged at 14,000 rpm for 3 min. Then, the supernatant is aspirated and the pellet is lysed by the addition of 1mL of sample lysis buffer (10mM Tris HCl, 150mM NaCl, 1mM EDTA, 1% NP40, 0.05% SDS) containing protease inhibitors (Complete Mini, EDTA-free Protease Inhibitor Cocktail Tablets, Roche) for 30 minutes at 4°C to be then transferred to Eppendorf tubes and centrifuged for 10 minutes at 4°C at 14,000 rpm. The supernatant is recovered and the amount of total protein was assayed by the Bradford method. The supernatant is divided into two parts (as Figure 37): 20 micrograms of protein are used in 'input' and 1 mg of total proteins is used for immunoprecipitation (IP).

'The input' which shows that the protein of interest is present in the lysate before immunoprecipitation was also checked. The proteins of the 'input' are directly denatured for 5 min at 95 ° C in a solution of 1X Laemmli (Tris-HCl 250 mM, 100% glycerol, 20% SDS, 5 mg of bromophenol blue) containing 100 mM DTT.

For the IP, proteins were incubated with 1 µg of the antibody of interest (anti-Gag p24, anti-HA or anti-TSG101) and stirred for 2 hours on a wheel at 4 ° C. Meanwhile, protein A coated (Dynabeads) magnetic beads (by 50µL for each sample) were washed in 1X PBS (700µl) and then equilibrated by two successive washes in NP40 buffer (described above). To separate the beads from washing solutions, the tubes are placed on a magnetic rack. The prepared beads are incubated with the IP tubes and placed on the wheel under stirring at 4 ° C for one hour. Using the magnetic rack,beads are then washed three times with 500 µL of NP40 lysis buffer, taken up in a solution composed of 50 µL of Laemmli and DTT (32.5 µL H_2O, 5µL DTT, 12.5µL 4X Laemmli) and denatured for 5 minutes at 95 ° C. Storage takes place at -20 ° C prior to analysis by Western blot (Figure 37).

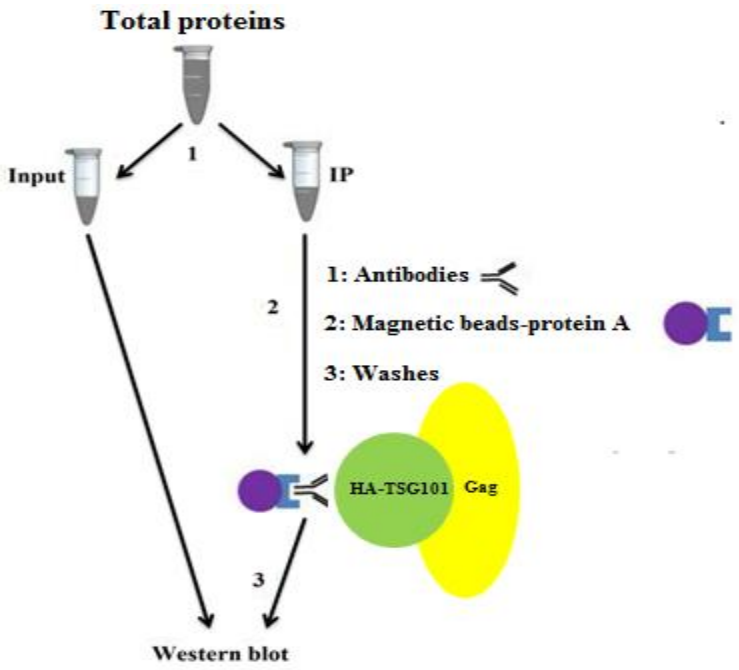

Figure 37: The principle of co-immunoprecipitation

2.10. Western blot

The proteins are separated by electrophoresis on polyacrylamide gel 12% or 8% (depending on the size of the proteins to be) in a migration buffer (15.14 g Tris, 72.05 g of glycine, 20% SDS, pH 8.8, diluted to one-tenth, qs 500 mL milliQ water). The samples were loaded into the wells of the gel (stacking gel) and then separated (Separating gel) according to their molecular mass by applying a current of 110 volts (0.05 A) for two hours. The proteins are then transferred onto a PVDF membrane (polyvinylidene fluoride), previously activated with methanol. The transfer is done in a liquid medium (15.14 g Tris, 72.05 g of glycine diluted to one-tenth with 20% ethanol, qs 500 mL MilliQ water), on ice and under a current of 80 volts for two hours with stirring. The recovered membrane is placed for one hour in a 50 mL Falcon tube, containing 10 mL of a solution of TBS-T (Tris-buffered saline-0.05% Tween 20) containing 3% casein (Biorad). This blocking step can saturate the membrane. It is then incubated with the primary antibody diluted in the same buffer (dilution depends on the antibody used) overnight at 4°C or for one hour at room temperature (Table 2A). Then the membrane was washed 3 time for 10 minutes with 10 mL of TBS-T and incubated for one hour at room temperature with a secondary antibody coupled to HRP (horseradish peroxidase) (Table 2B). For exposure, two 50 mL Falcon tubes

were prepared, tube A containing 17 µL of coumaric acid (90 mM), 40 µL of luminol (250 mM), 400 µL of 1 M Tris, pH 8.5 and 3.5 ml of water and tube B containing 2.5µL hydrogen peroxide, 400 µL of 1 M Tris, pH 8.5 and 3.6 mL of water. These two tubes were mixed and the solution is deposited on the membrane for one minute and then removed. The membrane is placed in a cassette and the exposure is made in the darkroom or using camera-las4000 GE Healthcare without requiring the cassette. The peroxidase catalyzes the oxidation of luminol in the presence of H_2O_2. Luminol returned to its reduced state by emitting photon (chemiluminescence) that were analyzed in LAS4000. The membrane can be reused for other proteins detected after three washes of 10 min each with TBS-T, it is dehybridized with 10 mL of a solution 'restore most western blot stripping buffer' (ThermoScientific) for 15 min at room temperature under constant stirring. The membrane is then washed 3×10 min in TBS-T and placed under agitation. Then, the steps of blocking and incubation with the solutions containing the primary and secondary antibodies as described above are restarted.

2.11. Mutagenesis

To perform all mutants of Gag, we design primer as mentioned before. For that, I used the protocol of "Site-Directed Mutagenesis Kit" which consists of three steps:

-The first step is a PCR reaction (see Table 5) for the amplification of the plasmid to be mutated with their phosphorylated primers whose design is as shown in (Figure 38).

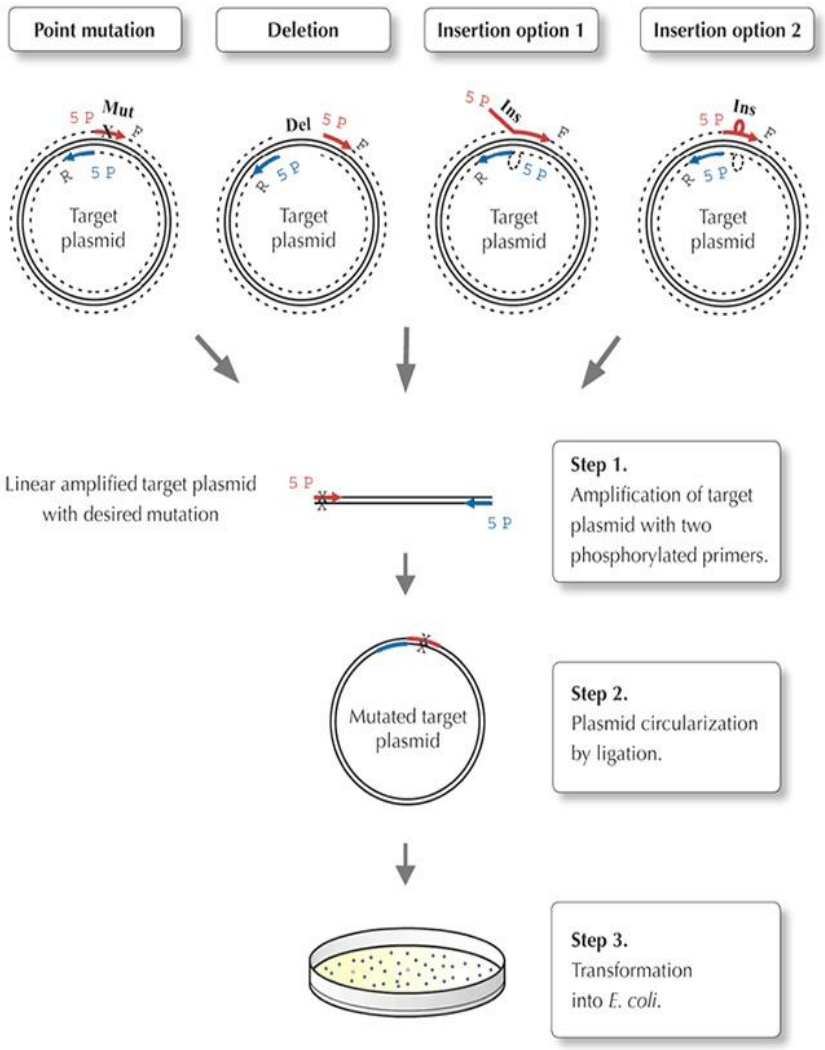

Figure 38: Schematic representation of different mutations

Component	Final volume of the reaction 50µL	Final concentration
H_2O	Add to 50µL	
5x phusion HF Buffer	10µl	1x
10mM dNTPs	1µl	200µM each
primer A	2.5 µl	10µM
primer B	2.5 µl	10µM
Template DNA	x µl	1 ng
Phusion Hot Start II DNA Polymerase (2U/µL)	0.5µl	0.02 U/µl

Table 6: Mutagenesis Reaction

Amplification is carried out using a thermocycler with the undermentioned program (Figure 39). The sequences of the primers used, are given in Table 4.

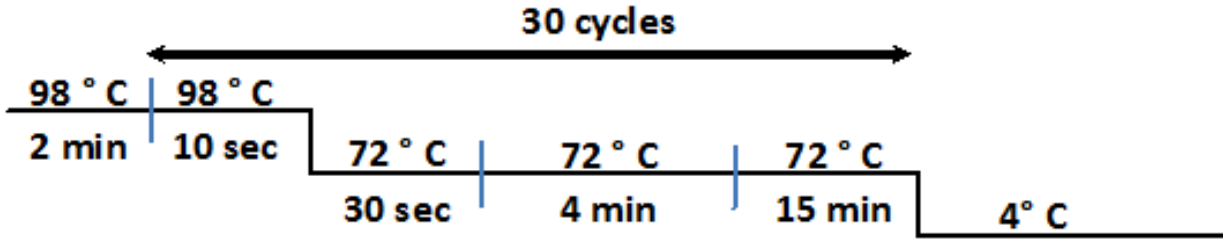

Figure 39: Thermocycler of PCR.

- Single step of annealing the PCR product with T4 DNA ligase.

- Circularized of transformation DNA in ultra-competent bacteria (NEB), then verification of the mutation by sequencing of the plasmid.

2.12. ReAsH/FlAsH Staining

For live/fixed-cell imaging we also used TC-FlAsH/ReAsH expression tag-based fluorescence technique. It is ideal for protein localization or real-time protein production studies, though its versatility offers a range of benefits.

FlAsH is a fluorescein derivative and contain two arsenic atoms at a set distance from each other. ReAsH is based on resorufin and has been similarly modified. Both on them are virtually non-fluorescent when bound to ethane dithiol (EDT). The biarsenical labeling reagents FlAsH-EDT2 and ReAsH-EDT2 become fluorescent after binding to the recombinant proteins containing the tetracysteine (TC) motif Cys-Cys-Pro-Gly-Cys-Cys (Figure 40).

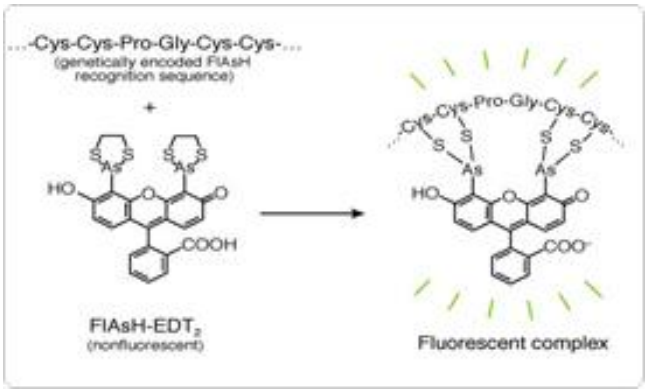

Figure 40: Mode of action of FlAsH and ReAsH

The undermentioned solutions were prepared and the pointwise protocol was followed:

-OPTI-MEM+GlutaMAX 1x (invitrogene): Store the solution at 4°C. Use it at RT for labelling.

- Flash 1.25µM: stock Flash 800x (1x =1.25µM), dilute 1.25µl of pure Flash in 2ml of *OPTI-MEM+GlutaMAX* 1x (depends on the volume).

- BAL wash Buffer (2, 3-mercaptopropanol): dilute 64µl of BAL pure in 6.4ml of *OPTI-MEM+GlutaMAX* 1x should be handled under the hood.

Protocol for Labelling

Before labelling media was removed and undermentioned steps were performed:

- Rince 2 times by 2 ml of *OPTI-MEM+GlutaMAX* 1x.
- Remove *OPTI-MEM+GlutaMAX* 1x, add 500µl of ReAsH/FlAsH.
- Incubate 1h at 37°C.
- Rince with 2 ml *of OPTI-MEM+GlutaMAX* 1x.
- Incubate 10min with 1ml of BAL wash buffer (BAL/ *OPTI-MEM+GlutaMAX* 1x) at RT in dark atmosphere.
- Rince with *OPTI-MEM+GlutaMAX* 1x.

For non-fixed cells, microscopic observation could be performed immediately or after several hours. In the later case, the *OPTI-MEM+GlutaMAX* were replaced by cell culture medium (DMEM,) and cells were placed again at 37°C. At the time of observation, DMEM was again replaced by *OPTI-MEM+GlutaMAX* 1x and observations were made.

Results and Discussion

Chapter 1:

Role of the Nucleocapsid Domain in HIV-1 Gag Oligomerization and Trafficking to the Plasma Membrane

The first aim of this work was to analyse the influence of the NC zinc finger (ZF) on the intracellular localization and assembly of HIV-1 Gag. Therefore, we used fluorescent Gag derivatives such as Gag-eGFP and Gag-mcherry, where the fluorophore was inserted next to the MA domain. The monitoring of protein-protein interaction in cellular context can be performed by different techniques such as by fluorescence spectroscopy that needs to extract proteins, by intensity after photobleaching or radiometric images but with many controls (cross talk, filters, level of expression….). All these approaches were used to monitor Gag-Gag interaction and a review was published to compare all this techniques (publication 1). Nevertheless, to get rid of these drawbacks, during my thesis, Gag assembly was directly visualized by using the FLIM approach combined with FRET. This technique measures the fluorescence decay of the donor at each pixel of the image and from the decay function, an average fluorescence lifetime is derived. Moreover, using a multi-exponential decay analysis, the fluorescent lifetime and the amplitude are obtained to determine the presence of interacting and non interacting population of proteins.

Using this approach, detailed analyses of FRET images revealed a homogenous distribution of Gag-Gag complex in cells with a progressive concentration of ordered Gag oligomers underneath the plasma membrane (PM) favouring a model where Gag oligomerization in the cytoplasm precedes virus assembly at the PM. In this model, the absence of NC domain results i) in an accumulation of Gag as large aggregates that are dispersed in the cytoplasm, ii) in lowering of Gag-Gag condensation and iii) in a delay for Gag-Gag complexes in reaching the PM. Thus NC is involved directly through protein-protein interaction or indirectly by its virtue to interact with RNA to the formation and the trafficking of Gag in the cell.

Publication 1:

Role of the nucleocapsid region in HIV-1 Gag assembly as investigated by quantitative fluorescence-based microscopy

Virus Research 193 (2014) 78–88

Contents lists available at ScienceDirect

Virus Research

journal homepage: www.elsevier.com/locate/virusres

Review

Role of the nucleocapsid region in HIV-1 Gag assembly as investigated by quantitative fluorescence-based microscopy

Hugues de Rocquigny**, Salah Edin El Meshri, Ludovic Richert, Pascal Didier, Jean-Luc Darlix, Yves Mély*

UMR 7213 CNRS, Laboratoire de Biophotonique et Pharmacologie, Faculté de Pharmacie, 74 route du Rhin, F-67401 Illkirch, France

ARTICLE INFO

Article history:
Available online 9 July 2014

Keywords:
HIV
NC
Microscopy
Fluorescence
Assembly
FRET-FLIM
Gag

ABSTRACT

The Gag precursor of HIV-1, formed of the four proteic regions matrix (MA), capsid (CA), nucleocapsid (NC) and p6, orchestrates virus morphogenesis. This complex process relies on three major interactions, NC-RNA acting as a scaffold, CA-CA and MA-membrane that targets assembly to the plasma membrane (PM). The characterization of the molecular mechanism of retroviral assembly has extensively benefited from biochemical studies and more recently an important step forward was achieved with the use of fluorescence-based techniques and fluorescently labeled viral proteins. In this review, we summarize the findings obtained with such techniques, notably quantitative-based approaches, which highlight the role of the NC region in Gag assembly.

Contents

1. Introduction

The HIV-1 Pr55 Gag polyprotein precursor is formed of four structural domains that are from the N- to the C-terminus, the matrix (MA), capsid (CA), nucleocapsid (NC) and p6, which upon processing by the viral protease (PR) during virion maturation gives rise to MAp17, CAp24, NCp7 and p6 structural proteins present in infectious virions (Mirambeau et al., 2010). Gag orchestrates HIV virion formation (Adamson and Freed, 2007; Balasubramaniam and Freed, 2011; Bell and Lever, 2013) by initially undergoing oligomerization upon its binding to the genomic RNA acting as a scaffold (Fogarty et al., 2011; Kutluay and Bieniasz, 2010; O'Carroll et al., 2013). Then the Gag–genomic RNA (gRNA) oligomers interact with a second platform corresponding to the plasma membrane (PM) (Ivanchenko et al., 2009; Jouvenet et al., 2008; Neil et al., 2006) or an endosomal membrane (Basyuk et al., 2003; Dong et al., 2005; Grigorov et al., 2006; Kemler et al., 2010; Lehmann et al., 2009; Molle et al., 2009; Nydegger et al., 2003; Pelchen-Matthews et al., 2003; Perlman and Resh, 2006). However viral assembly on internal membranes was challenged by the mild effect of endosomal traffic on virus production (Jouvenet et al., 2006) as well as by electron microscopy on macrophage showing that internal organelles

* Corresponding author. Tel.: +33 3688 542 63.
** Corresponding author. Tel.: +33 3688 541 03.
E-mail addresses: hderocquigny@unistra.fr (H. de Rocquigny), yves.mely@unistra.fr (Y. Mély).

http://dx.doi.org/10.1016/j.virusres.2014.06.009
0168-1702/

containing viral particles possibly correspond to deep invaginations of the plasma membrane (Welsch et al., 2007) or to an extensive tubular network (Bennett et al., 2009).

The process of Gag oligomerization is driven by series of homotypic interactions, involving the CA and SP1 regions (Datta et al., 2011; Gamble et al., 1997; Morellet et al., 2005; Pornillos et al., 2009, 2011; von Schwedler et al., 2003) and additionally MA (Hill et al., 1996). Once Gag oligomers are formed, the N-terminus of MA with the myristate and the stretch of basic residues becomes accessible, which in turn anchors the Gag oligomers to the PM (Adamson and Freed, 2007; Ono et al., 2000) via interactions with negatively charged lipids, notably phosphatidyl inositol (4,5) biphosphate (Li et al., 2007; Lindwasser and Resh, 2001; Ono et al., 2004; Perez-Caballero et al., 2004; Saad et al., 2006). Last, Gag molecules assembling at the PM form viral particles that are ultimately released in the extracellular milieu (Derdowski et al., 2004; Fritz et al., 2010; Hogue et al., 2009; Hubner et al., 2007; Ivanchenko et al., 2009; Jouvenet et al., 2008; Larson et al., 2003). The NC domain plays a key role in Gag assembly by recruiting the genomic RNA or cellular RNAs, that act as a scaffold for the binding of Gag molecules, their oligomerization and ultimately formation of the viral core (Bolinger et al., 2010; Burniston et al., 1999; Cimarelli and Luban, 2000; Muriaux et al., 2001; Ott et al., 2009; Housset et al., 1993). Also binding of Gag molecules to the RNA results in the neutralization of NC positive charges and NC-NC interaction that cause a molecular crowding phenomenon prevailing in the viral core (Tanchou et al., 1995). Moreover, both the basic part (Lingappa et al., 2006) and the NC zinc fingers (Chatel-Chaix et al., 2008; Milev et al., 2010) were shown to recruit a number of cellular proteins such as ABCE 1 and Stauffen which influence Gag oligomerisation (for a review (Muriaux and Darlix, 2010)). The NC domain of Gag was also shown to hijack members of the ESCRT (endosomal sorting complexes required for transport) machinery which turned out to be necessary for viral particles budding (Dussupt et al., 2009; Popov et al., 2008, 2009). In fact dynamic imaging analyses support an assembly model (Chojnacki and Muller, 2013) where Gag molecules initially appear as small cytoplasmic clusters which next traffic to the PM, and are ultimately released as viral particles in the extracellular milieu (Derdowski et al., 2004; Fritz et al., 2010; Hogue et al., 2009; Hubner et al., 2007; Ivanchenko et al., 2009; Jouvenet et al., 2008; Larson et al., 2003). The aim of this report is to review the role of NC in Gag oligomerization and assembly as monitored by quantitative fluorescence microscopy.

2. NC and Gag assembly

The finding that the NC domain of Gag was involved in Gag assembly and the release of particles dated back to the early 90s. This was originally observed by estimating the amount of cell-free CAp24 protein as compared to that in transfected cells (Dorfman et al., 1993). In fact, single point mutations of the Cystein or Histidine residues involved in zinc chelation by the $CX_2CX_4HX_2C$ (CCHC) zinc finger (ZF) caused a large decrease in particle production. Similarly mutating the aromatic residues Phenylalanine16 and Tryptophan 37 of the ZFs to alanine caused a reduction in the production of viral particles. Taken together, these findings suggested that NC was directly involved in Gag assembly and the production of viral particles. The same phenotype was observed for RSV (Dupraz and Spahr, 1992) since the expression of a ΔNC mutant Gag in comparison with wild-type (wt) RSV Gag was increased in the producer cells together with an accumulation of Gag processed intermediates and the absence of particles in the supernatant (Bennett et al., 1993).

To correlate such a Gag assembly defect with the absence of homotypic interactions, studies were carried out using the two-hybrid system (Franke et al., 1994) and recombinant baculoviruses (Carriere et al., 1995). Results obtained with the two-hybrid system indicated that the smallest domain identified for Gag oligomer formation was encompassing the C-terminal domain (CTD) of CA (Strambio-de-Castillia and Hunter, 1992; Wills and Craven, 1991) and NC. The involvement of NC was unexpected since mutating the CCHC zinc fingers had minimal effects on the level of Gag production (Aldovini and Young, 1990; Gorelick et al., 1988). Nonetheless, these results were entirely consistent with the fact that HIV NC was able to direct assembly once fused to a truncated RSV Gag mutant defective for assembly (Bennett et al., 1993). In the baculovirus system, Gag was expressed in recombinant baculovirus-infected cells and the formation of VLPs was investigated by means of complementation assays. The latter were based on the ability of wt Gag to rescue assembly-defective Gag mutants (Hogue et al., 2009; Lee and Linial, 1995; Park and Morrow, 1992). By co-expressing wt Gag with series of truncated Gag mutants, it was found that domains in the matrix (Hong and Boulanger, 1993; Mammano et al., 1994), the CA and the spacer peptide1 SP1 (Krausslich et al., 1995) were essential for Gag assembly in agreement with experiments carried out in mammalian cells (Adamson and Freed, 2007; Gottlinger, 2001). Interestingly, a region overlapping the SP1-NC junction with most of NC was also found to be essential for Gag assembly.

In this context, how does NC participate in Gag assembly? the role of NC would be linked to its interplay with nucleic acids. In fact, the NC domain of Gag interacts with RNAs and DNAs with a preference for the viral PSI RNA packaging sequence (Clever et al., 1995, 2000; Lochrie et al., 1997), which drives the selective packaging of the genomic RNA into the assembling viral particle (Chen et al., 2009; Hu et al., 2003; Paillart et al., 2004; Gorelick et al., 1999), reviewed in (Balasubramaniam and Freed, 2011; Resh, 2005). In HIV-1, the specificity for the Psi-containing genomic RNA is mediated by the two NC zinc fingers (Gorelick et al., 1993, 1996; Gorelick et al., 1988, 1990; Tanchou et al., 1995, 1998). Moreover NC is also able to interact non specifically with a wide variety of nucleic acids via its numerous basic residues flanking the ZF's (Ottmann et al., 1995; Poon et al., 1996). This non specific binding mode appears to contribute to assembly by tethering Gag molecules onto the RNA promoting Gag–Gag interaction (Burniston et al., 1999; Cimarelli et al., 2000; Ott et al., 2009). Due to this, the RNA molecule is viewed as a scaffold driving Gag assembly from the nucleation step up to the formation of large Gag ensembles and ultimately the viral particles that are released by budding at the PM.

But as proposed by another model, Gag assembly would result from homotypic NC interactions. Indeed, substituting NC for the bacillus subtilisis ApoMTRB protein domain resulted in the formation of particles at levels similar to the wt Gag (Antson et al., 1995). Since the ApoMTRB protein forms high-order oligomers (Antson et al., 1995), it was assumed that the essential role of NC was its ability to make protein-protein contacts. To confirm this, a Gag–ZIP construct where NC was substituted by the leucine zipper of human CREB DNA binding domain was expressed (Chang et al., 2008; Wang et al., 2013; Zhang et al., 1998) and shown to release viral particles resembling wt particles (Crist et al., 2009; Zhang et al., 1998). Along this line, a Gag construct with a leucine zipper unable to make homodimers did not lead to an efficient production of particles (Accola et al., 2000; Zhang et al., 1998). In addition, in vitro GagZip does not bind nucleic acids at 0.15 M NaCl (Crist et al., 2009) in agreement with the fact that GagZip particles did not contain any RNA (Crist et al., 2009; Zhang et al., 1998). A Gag construct where NC was replaced by the Coat protein of the MS2 RNA bacteriophage was also designed (Dykeman et al., 2011). The coat protein interacts with the bacteriophage RNA through the specific recognition of small RNA hairpins located close to the 5′ end of the MS2 genomic RNA (Stockley et al., 1995). It was found that cells expressing the Gag–MS2 released high levels of virus-like particles (VLP) that did not contain RNA. Taken together, these studies favor the notion that

viral particles can be formed by a recombinant Gag in the absence of a specific RNA partner (O'Carroll et al., 2013).

3. Implications of NC in Gag–Gag interaction as viewed by fluorescence microscopy

In order to study homotypic Gag interactions by fluorescence microscopy in cells, HIV, RSV (Larson et al., 2003) and FIV (Kemler et al., 2010) Gag polyproteins were tagged with a fluorescent reporter protein (Fig. 1 a) or with complementary nonfluorescent fragments of the Venus protein that become fluorescent when they are brought together (Milev et al., 2010). For current applications, the well characterized derivatives of natural fluorescent proteins such as the enhanced green fluorescence protein (eGFP) and related proteins proved to be good candidates (Chojnacki and Muller, 2013; Shaner et al., 2005). These proteins are well suited for lifetime imaging since they are naturally fluorescent in the visible range and can be expressed as chimeric proteins with the protein of interest in target cells and organisms. However, due to their rather large size and the propensity of some of them to oligomerize, fluorescent proteins may affect the biological properties of the proteins of interest.

In early studies, the green fluorescent protein (GFP) of *Aequorea victoria* or its derivatives was fused to the Gag C-terminus. The expressed Gag–GFP chimeric proteins were found to be localized throughout the cytoplasm (Perrin-Tricaud et al., 1999) and at the cell PM (Hermida-Matsumoto and Resh, 2000) but electron microscopy revealed aberrant morphological maturation (Pornillos et al., 2003). Recently, two groups engineered Gag–GFP recombinants where the eGFP was inserted close to the C-terminus of MA (Fig. 1a). Viruses obtained with these recombinant proteins were shown to resemble wt viruses with respect to Gag localization, particle morphology and infectivity (Hubner et al., 2007; Muller et al., 2004).

To minimize the size of the fluorescent tag, a 12-amino-acid tetracysteine sequence was inserted at different positions in HIV-1 Gag, notably at its the C-terminus, as well as downstream of MA (Gousset et al., 2008; Rudner et al., 2005) NC or CA (Pereira et al., 2011). This tag interacts with high affinity with a membrane-permeable biarsenical fluorescein derivative, FlAsH (4,5-bis(1,3,2-dithiarsolan-2-yl) fluorescein -FlAsH-EDT2) or its red analog ReAsH (4,5-bis(1,3,2-dithiarsolan-2-yl) resorufin -ReAsH-EDT2)(Adams et al., 2002; Griffin et al., 1998). Addition of this tag to Gag did not interfere with Gag localization and assembly at the PM, virus infectivity and packaging of the viral Vpr protein (Fritz et al., 2010; Gousset et al., 2008; Pereira et al., 2011; Perlman and Resh, 2006; Rudner et al., 2005; Turville et al., 2008).

All these Gag-based recombinants were developed with the aim of investigating Gag distribution and trafficking throughout the replication cycle and to examine Gag–Gag homotypic interactions in a cellular context. Among the various fluorescent techniques to study protein-protein interactions, Gag–Gag interactions were followed by BRET using energy transfer between Gag-*Renilla reniformis* luciferase and Gag–YFP (Chatel-Chaix et al., 2007) and by bimolecular fluorescence complementation assay (BiFC) in the cytoplasm and at the plasma membrane (Milev et al., 2010). Both techniques are endowed with high signal to noise ratio, but are only semi-quantitative, being based on fluorescence intensity measurements. One other of the most powerful techniques to investigate such interactions is Förster Resonance Energy Transfer (FRET), which consists in a non radiative energy transfer between a fluorescent donor and an acceptor when they are less than 8–10 nm apart, a distance corresponding to intermolecular protein–protein interactions (Bastiaens and Squire, 1999; Day et al., 2001; Voss et al., 2005). Thus, FRET measurements can provide a direct evidence for a physical interaction between the labeled proteins with high spatial and temporal resolutions. For FRET monitoring, plasmids coding

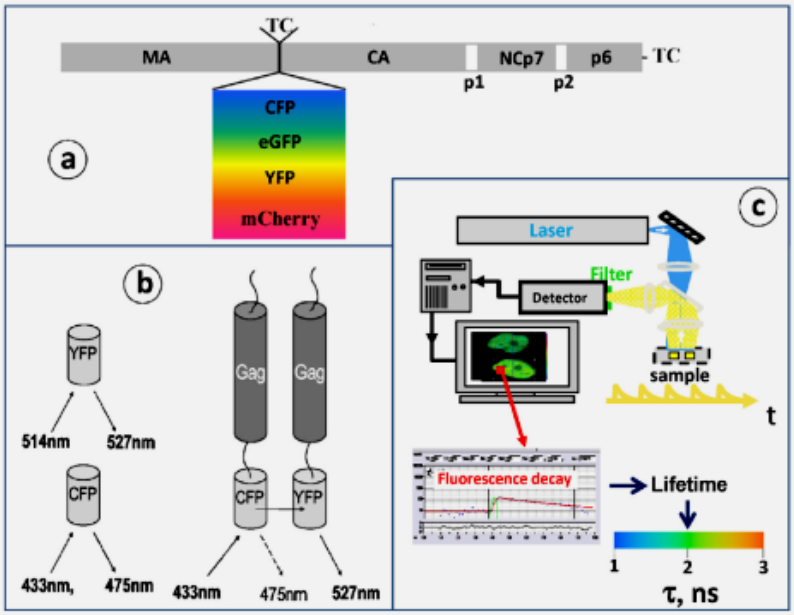

Fig. 1. Schematic representation of Gag fusion proteins and the principle of FRET measurements by intensity or lifetime. (a) A fluorescent protein was inserted at the C-terminus or downstream of the MA domain of Gag (Chojnacki and Muller, 2013). TC corresponds to the tetracysteine motif that tightly interacts with the FlAsH or ReAsH probes (Griffin et al., 1998). (b) Principle of FRET measurements based on donor/acceptor emission intensities (adapted from (Derdowski et al., 2004)). Excitation and emission wavelengths of free YFP and CFP proteins are indicated. Energy transfer on Gag–CFP interaction with Gag–YFP resulted in a decrease of CFP emission (dotted arrow) and an increase of YFP emission (solid arrow). (c) Principle of the two-photon excitation scanning microscope used for FLIM measurements (Fritz et al., 2008). At each pixel, the collected fluorescence intensity decay is analyzed to provide a fluorescence lifetime that is converted into a given color, according to an arbitrary color code.

for CFP (or GFP) and YFP (or mCherry) are co-expressed (Fig. 1b) (Derdowski et al., 2004; Hogue et al., 2009; Hubner et al., 2007; Kemler et al., 2010; Larson et al., 2003) allowing to measure (i) a decrease in the donor fluorescence intensity and (ii) a proportional increase in the acceptor fluorescence intensity. Since fluorescence intensities are relative measurements that depend notably on the local concentrations of the fluorescence tags and the instrument settings the changes in fluorescence intensities accompanying FRET can only be monitored in solution where the concentrations of the donor and acceptor can be controlled. In cells, FRET monitoring is much more tedious. The simplest approach to determine the loss in donor fluorescence due to FRET is to measure the recovery of donor fluorescence after a selective photobleaching of the acceptor. Though apparently simple in its concept, this method is difficult to apply since it needs to find the proper conditions to fully bleach the acceptor without compromising the emission of the donor or the cell viability. Moreover, this method only monitors the amount of donor bound by acceptor, which is influenced by the local ratio of acceptor to donor molecules. Alternatively, the FRET can be determined using fluorescence signals from direct donor fluorescence, direct acceptor fluorescence, and acceptor fluorescence due to FRET that are converted into measures of molecule concentration and FRET efficiency (Hogue et al., 2009; Hoppe et al., 2002).

However, this method is cumbersome, requiring multiple images of the same sample collected with various combinations of excitation and emission wavelengths, as well as measurements with model systems in order to take into account several parameters (i) the cross talk of the fluorophores into each other's detection channel, (ii) the ratio of the extinction coefficients of the two fluorophores, and (iii) the relationship between the increase in acceptor fluorescence due to FRET to the decrease in donor fluorescence due to FRET.

A more straightforward and simpler approach to study Gag–Gag oligomerization by FRET is to use the fluorescence lifetime imaging (FLIM) technique (Fig. 1c), which monitors the fluorescence lifetime of the donor at each pixel of the image. In contrast to fluorescence intensity, the fluorescence lifetime is an absolute parameter that does not depend on the instrumentation or the local concentration of the fluorescent molecules (Wachsmuth et al., 2000). Therefore, the FRET efficiency at each pixel can be directly determined from the decrease of the fluorescence lifetime of the donor in comparison with its natural lifetime. FLIM can be carried out with various (donor, acceptor) couples, the most popular being eGFP as a donor and either mCherry or mRFP as acceptor (Albertazzi et al., 2009; Batisse et al., 2013; Boutant et al., 2010; Carillo et al., 2013; Fritz et al., 2008, 2010; McGinty et al., 2011; Padilla-Parra et al., 2009; Tramier et al., 2006).

The use of the various FRET-based approaches to investigate Gag–Gag interactions and notably the role of NC in Gag oligomerization is reviewed below.

4. NC of RSV Gag is involved in Gag oligomerization and plasma membrane localization

Gag–Gag interactions in a cellular context were originally studied with RSV Gag labeled at the C-terminus with CFP or YFP (Larson

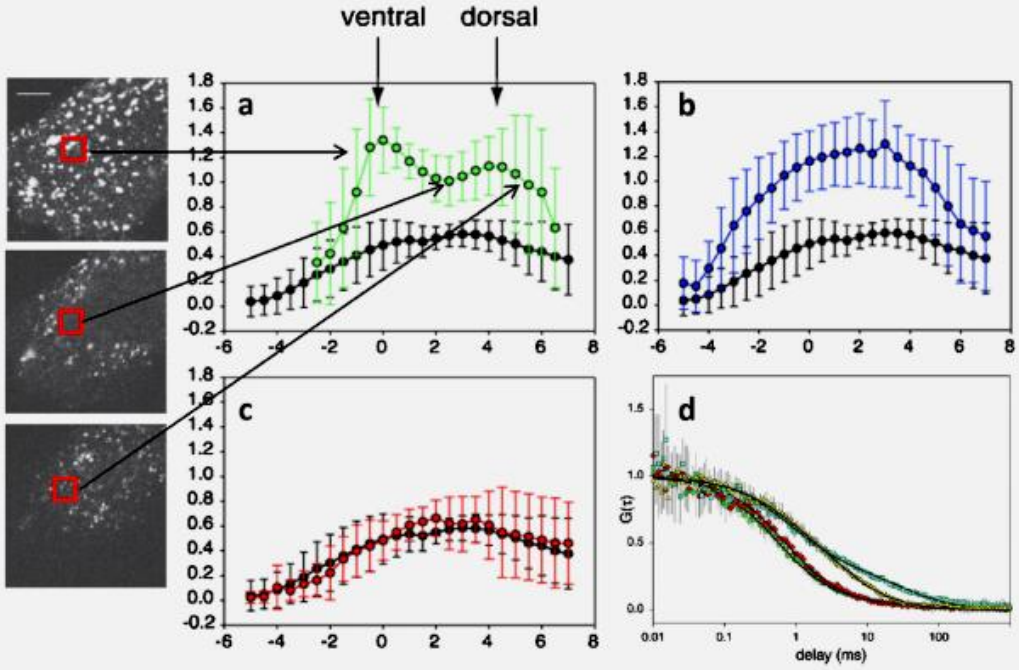

Fig. 2. FRET and FCS measurements of RSV Gag–CFP/Gag–YFP interaction. Histograms a to c correspond to the plots of the FRET values (vertical axe) for the various z planes (horizontal axe) of cells co-expressing: (a) Gag–CFP/YFP (black circles) and Gag–CFP/Gag–YFP (green circles); (b) Gag–CFP/YFP (black circles) and GagΔMBD-CFP/GagΔMBD-YFP (blue circles); (c) Gag–CFP/YFP (black circles) and GagΔNC-CFP/GagΔNC-YFP (red circles). The zero value on the *x*-axis corresponds to the contact zone of the cell ventral surface with the coverslip. Negative and positive *x*-axis values correspond to *z* positions below and above the coverslip, respectively. At each *z* position (0.5 μm), the FRET value was calculated as a ratio of yellow to cyan intensity and was corrected from bleedthrough, background and photobleaching as described in Larson et al. (2003). Images on the left are from the ventral position (0.0 μm), at 2.0 μm and at the top of the cell (4.5 μm). Two photon excitation was at 830 nm to maximize CFP absorption. (d) Normalized autocorrelation curves G(τ) of Gag–GPF (yellow triangles) and GagΔNC-GFP (red diamonds) from intracellular FCS measurements on live DF-1 cells. GFP alone (green circles) and PM-GFP (cyan squares) were used to respectively characterize free cytoplasmic diffusion and at the PM. Each curve is an average of five 10-s curves, and the error bars are the measured SD. G(τ) values are normalized to G(0) = 1 for display. Each curve is fitted (black lines) using a 3D diffusion model with two components. Excitation wavelength was at 910 nm.

This figure was adapted from Figs. 4 and 6 of Larson et al. (2003).

et al., 2003). Through 2-photon excitation of the donor, CFP and YFP intensities were recorded in a series of z planes at 0.5 μm interval throughout the cells. For each *z*-plane, a FRET value was calculated as the ratio of yellow to blue emissions (Fig. 2, panel a). A basal FRET value was observed in cells co-expressing Gag–CFP and YFP (black circles), as a consequence of the cross talk between CFP and YFP emissions. When FRET was monitored on cells expressing both Gag–CFP and Gag–YFP, significantly higher FRET values were observed (open green circles). Interestingly, the FRET value displayed two maxima at positions corresponding to the ventral and dorsal surfaces of the cells. Moreover, images recorded at these two positions showed a punctuate staining pattern indicating that these two FRET maxima probably corresponded to assembling and budding viral particles (Fig. 2, left images). FRET was also observed in the middle of the cell, suggesting that RSV Gag–Gag interactions initiate in the cytoplasm before Gag oligomers migrate toward the cell periphery (Larson et al., 2003).

A similar study was carried out with Gag–CFP and Gag–YFP chimeric protein mutants deleted of their membrane binding domain (MBD). Even though the bimodal aspect of the FRET distribution was abolished (Fig. 2, panel b), the still high FRET values highlighted that RSV Gag oligomerization does not require the docking of RSV Gag to the PM. Next, this approach was applied to GagΔNC mutants, where the NC domain of Gag was removed (Fig. 2, panel c). The low FRET values observed with this mutant clearly indicated that Gag–Gag interactions were abolished upon NC deletion. Thus, NC turns out to be a critical domain for RSV Gag assembly.

RSV Gag–Gag interactions were also investigated by fluorescence correlation spectroscopy (FCS) (Larson et al., 2003). This technique characterizes the dynamic motions of fluorescent molecules (or molecular complexes) diffusing through the subfemtoliter observation volume of a confocal or a two-photon microscope. By calculating the autocorrelation curves from the intensity fluctuations observed in this volume, several physical parameters, such as the diffusion time, local concentration, and molecular brightness can be extracted (Wachsmuth et al., 2000). Using this technique, the GFP protein was shown to freely diffuse in the cytoplasm with a diffusion coefficient $D = 26\ \mu m^2/s$ (Fig. 2d, green dots). Anchoring of GFP to the PM through a signal peptide dramatically decreased its diffusion constant to a value of $0.48\ \mu m^2/s$ (Fig. 2d, cyan squares) (Pyenta et al., 2001).

Autocorrelation curves of Gag–GFP chimeric proteins revealed the presence of two populations (Fig. 2d, yellow triangles). Half of the molecules diffused ($D = 23\ \mu m^2/s$) as free GFP proteins while the remaining population diffused with an intermediate diffusion coefficient of $3.2\ \mu m^2/s$, that is thought to be associated to Gag-containing complexes diffusing in the cytosol. Interestingly, analysis of the autocorrelation curves of GagΔNC-GFP showed that a large proportion of these proteins diffuses like free GFP proteins (96% with a D value of $21\ \mu m^2/s$) emphasizing that, in the RSV model, the NC domain is necessary for Gag assembly (Larson et al., 2003).

5. Implication of the NC domain in HIV-1 Gag assembly

5.1. Investigation by steady state spectroscopy in solution

Similarly to RSV Gag, assembly of HIV-1 particles was studied by monitoring Gag–Gag interactions by FRET. To that end, chimeric Gag proteins were designed with CFP or YFP coupled at their C-terminal end (Derdowski et al., 2004). In a first attempt, membrane and cytosolic fractions were analyzed by fluorescence spectroscopy using an excitation of the CFP-labeled proteins (Fig. 3). The maximum emission wavelength of Gag–CFP was centered at 470 nm

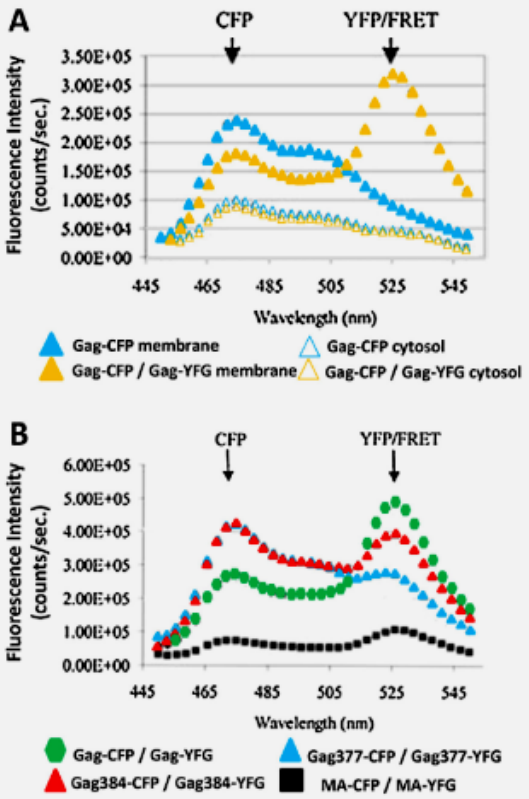

Fig. 3. HIV-1 Gag interactions as monitored by FRET in solution. (A) Fluorescence spectra of membrane and cytosolic fractions of 293T cells isolated by ultracentifugation through an iodixanol gradient (Derdowski et al., 2004). Membrane (closed symbols) and cytosolic (open symbols) fractions were obtained from cells expressing Gag–CFP (blue triangle) or Gag–CFP/Gag–YFP (yellow triangle). A large increase of YFP emission was observed upon formation of Gag–CFP/Gag–YFP complexes. (B) Fluorescence spectra of lysates of 293T cells expressing Gag–CFP/Gag–YFP (green diamond), Gag384-CFP/Gag384-YFP (red triangle), Gag377-CFP/Gag377-YFP (blue triangle), and MA-CFP/MA-YFP (black square). Excitation wavelength was at 433 nm.

both in the cytosolic (empty blue triangle) and in the membrane (closed blue triangle) fractions (Fig. 3A). When Gag–CFP was co expressed with Gag–YFP, the emission spectrum revealed a second peak around 525 nm in the membrane fraction, indicating an efficient FRET (closed orange triangle, Fig. 3A). In contrast, nearly no FRET was observed in the cytosolic fraction of the same cells (empty orange triangle), supporting the view that membranes and notably the PM is required for Gag assembly. To validate the importance of the PM for Gag–Gag interactions, chimeric Gag proteins were mutated so that their N-terminus could not be myristylated (Bryant and Ratner, 1990; Gottlinger et al., 1989). Only a low energy transfer was observed in the membrane fractions when Myr⁻Gag–CFP and Myr⁻Gag–YFP were co-expressed (not shown), further supporting the key role of the PM in Gag assembly.

To evaluate the role of the I domain (residues 378–384) corresponding to the N-terminal region of NC (Adamson and Freed, 2007; Cimarelli et al., 2000; Hubner et al., 2007; Sandefur et al., 1998), truncated Gag molecules containing a stop codon at position 377 or 384 were fused to CFP and YFP and expressed in 293 T cells. As shown in Fig. 3B, cells co-expressing Gag containing the I domain exhibited spectrum similar to the wt Gag (compare green diamonds and red triangles) in contrast to constructs lacking the I domain (blue triangle). These results were confirmed by the group of Chen who studied Gag–Gag interactions by FRET in cells expressing all viral proteins (Hubner et al., 2007), indicating that the I domain

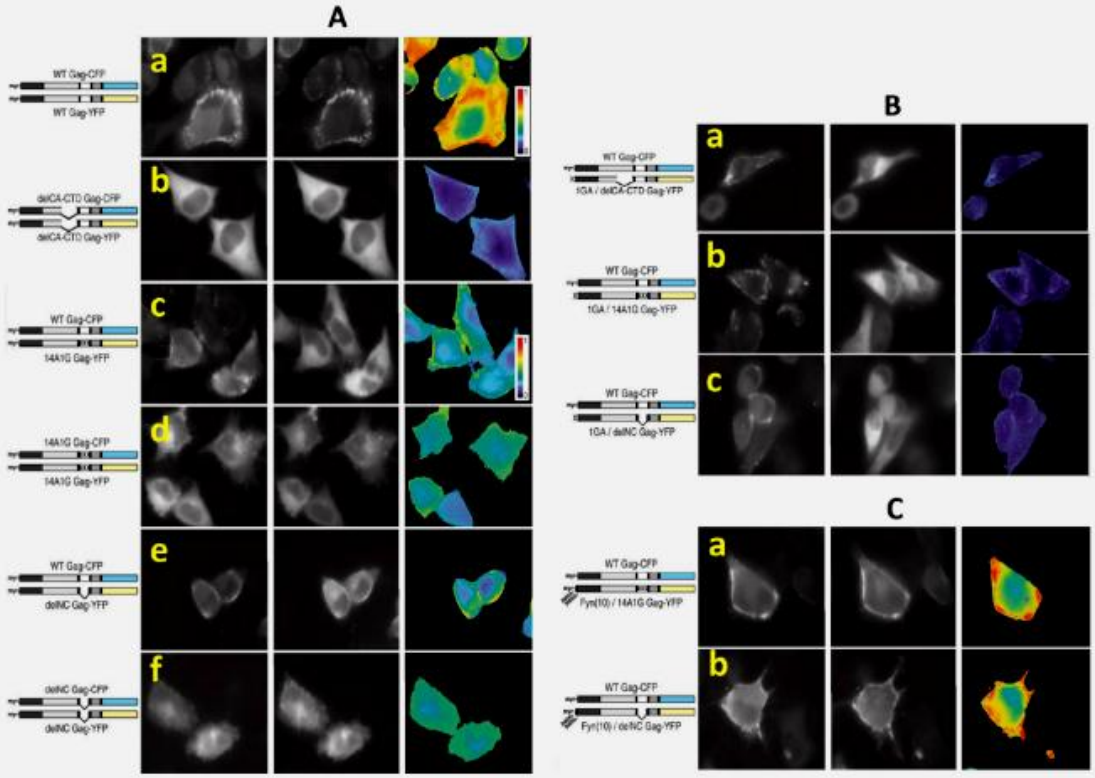

Fig. 4. HIV-1 Gag assembly visualized by FRET microscopy. Homotypic and heterotypic interactions of CFP- and YFP-labeled Gag derivatives were monitored by wide-field fluorescence microscopy and analyzed by the FRET stoichiometry method (Hoppe et al., 2002). (A) Homotypic interactions of wt Gag (panel a), Gag mutants deleted of the CA domain (panel b), Gag with mutations of the NC basic residues (panel d) or NC deletion (panel f) and heterotypic interactions (i.e. Gag–YFP construct contains a mutation, but the Gag–CFP construct does not) with Gag constructs mutated at the level of NC basic residues (panel c), or Gag constructs with NC deletion (panel e). Note that mutation and deletion of NC have a similar impact on Gag–Gag interactions. (B) Heterotypic interactions of wt Gag with mutated Gag harboring two modifications. In addition to be Myr-, the mutant Gag's were either deleted of their CA CTD domain (panel a), mutated on the NC basic residues (panel b) or deleted of their NC domain (panel c). Note that a strong impact of NC deletion was observed on Gag–Gag interactions in the absence of myristate. (C) Heterotypic interactions of wt Gag proteins with Gag constructs containing constitutive enhanced membrane binding (Fyn(10)) together with mutations of NC basic residues (panel a) or deletion of NC domain (panel b). Note that the constitutive binding to the PM rescued the interaction of Gag NC mutant with Gag.
This figure was adapted from Figs. 3, 5 and 6 from Hogue et al. (2009).

is required for proper Gag assembly (Briggs and Krausslich, 2011; Sundquist and Krausslich, 2012).

5.2. Investigation by epifluorescence microscopy

To further analyze the contribution of NC in Gag assembly, Hogue et al. used the FRET stoichiometry method based on calibrated spectral analysis of epifluorescence microscopy images (Hogue et al., 2009; Hoppe et al., 2002). Chimeric Gag proteins coupled at their C-terminus with CFP and YFP were expressed in HeLa cells. High levels of FRET between Gag–CFP and Gag–YFP (Fig. 4A, row a) appeared to be associated with puncta at the PM, while moderate FRET levels appeared diffuse throughout the cell. This confirmed that Gag olimerization starts in the cytoplasm and subsequently the PM plays a major role in Gag assembly. In contrast, nearly no FRET was observed with constructs deleted of the CA-CTD domain (Fig. 4, row b), indicating a major role of this domain in Gag/Gag interactions.

Next, the effect of NC mutations on Gag oligomerization was assessed by examining interactions between wt Gag–CFP and mutated Gag–YFP proteins where either all 15 basic amino acids were replaced by neutral residues (14A1G Gag) (Cimarelli et al., 2000) or where most of the NC domain was deleted (delNC Gag). These mutated Gag constructs were expressed as CFP and YFP derivatives for homotypic interactions, or together with wt Gag–CFP for heterotypic interactions. As depicted in Fig. 4 A (rows c to f), intermediate FRET values were obtained with all NC mutants (green colors) indicating that the NC domain had less influence on Gag–Gag interactions than the CA-CTD domain (Fig. 4A, row b). Higher FRET values were observed for heterotypic interactions (rows c and e) as compared to homotypic interactions (rows d and f), in line with the ability of wt Gag proteins to rescue NC-mutated Gag proteins in the assembly process (Lee and Linial, 1995; Park and Morrow, 1992).

However, as mutations in NC are known to also influence Gag membrane binding (Burniston et al., 1999; Grigorov et al., 2007; Ott et al., 2009), the decrease in FRET observed with the Gag NC mutants could partly arise from a defect in Gag membrane association (Hubner et al., 2007). To evaluate the effect of membrane binding on Gag–Gag interactions, the authors took advantage of the ability of wt Gag to rescue non myristylated Gag at the PM (Kawada et al., 2008; Li et al., 2007; Morikawa et al., 1996; Ono et al., 2000). Along this line, since nonmyristylated Gag proteins did not interact with membranes, they reasoned that the interaction between Myr^+ and Myr^- Gag proteins mainly relies on protein-protein interactions. Therefore, 14A1G Gag, delNC Gag and delCA-CTD Gag mutants were further modified by substituting alanine for glycine 2 to render them N- myristyl defective. These

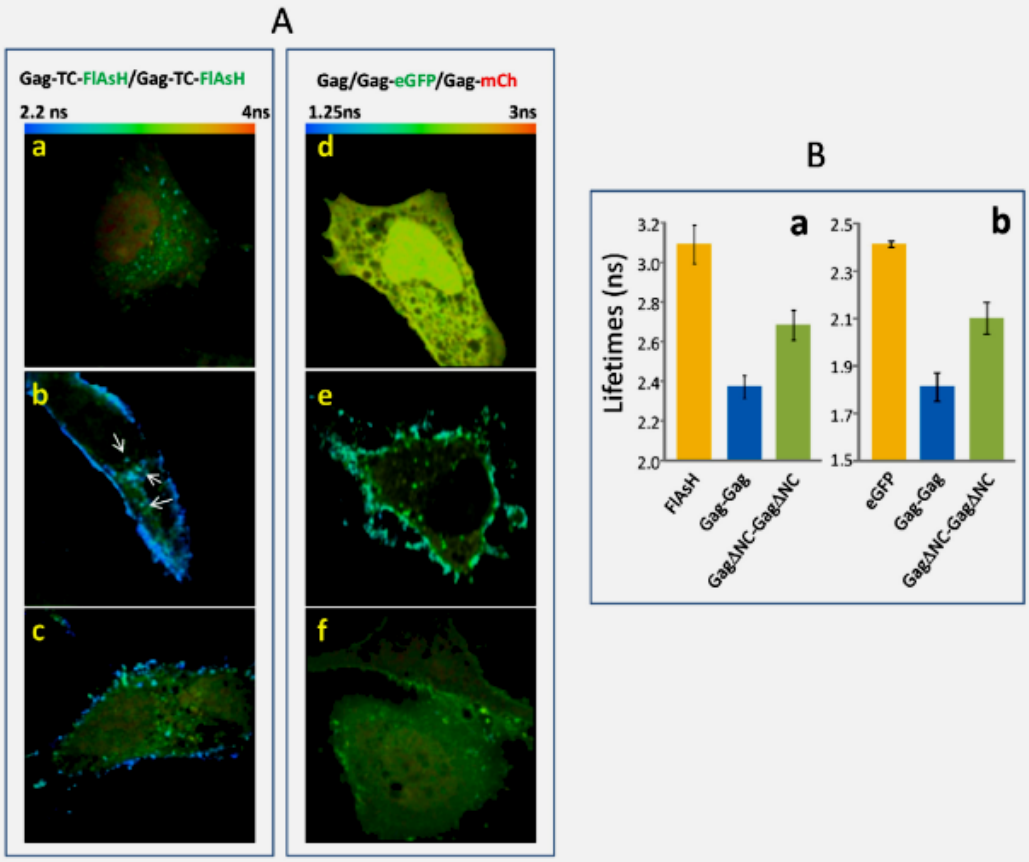

Fig. 5. HIV-1 Gag assembly imaged by FLIM. (A) FLIM images of cells expressing Gag–TC and labeled by -FlAsH (left) and cells expressing Gag–eGFP and Gag–mCherry (right). Since FlAsH and eGFP exhibit different lifetimes, the lifetime color scales on the top of panels a and d are different. (a) FlAsH chromophore alone, (b) Gag–TC-FlAsH, (c) GagΔNC-TC-FlAsH, (d) eGFP, (e) Gag/Gag–eGFP/Gag–mCherry and (f) GagΔNC/GagΔNC-eGFP/GagΔNC-mCherry. (B) Histograms representing the mean lifetime values of FlAsH (a) and eGFP (b) determined from measurements on at least 30 cells. FLIM measurements were performed using the time-correlated single-photon counting technique on a two-photon microscope (Azoulay et al., 2003; Clamme et al., 2003). Excitation at 900 nm was provided by a mode-locked titanium-sapphire laser (Tsunami, Spectra Physics). Photons were collected using a short-pass filter with a cut-off wavelength of 680 nm and a band-pass filter of 520 ± 17 nm and were directed to a fiber-coupled APD (SPCM-AQR-14-FC, Perkin Elmer) connected to a SPC830 electronic card (Becker & Hickl, Germany). Data were analyzed using the SPCImage V2.8 software (Becker & Hickl, Germany).

Myr⁻ defective Gag's were co-transfected with wt Gag to evaluate heterotypic interactions. As expected, no FRET was observed with the Myr⁻ del CA-CTD Gag mutant (Fig. 4B, row a), in agreement with the observations on homotypic complexes (Fig. 4A, row b). This confirmed the key role of the CA-CTD domain in Gag oligomerization. With Myr⁻ 14A1G Gag and Myr⁻ delNC Gag mutants, no FRET was detected in contrast to the observations with the same Myr⁺ Gag constructs (compare Fig. 4A, rows c-f with Fig. 4B, rows b and c), indicating that the NC domain is required for Gag–Gag interactions in the absence of membrane binding. Thus, the NC and the CA-CTD domains are most probably involved at the nucleation step of Gag oligomerization in the cytoplasm.

To further determine the effect of membrane binding on the ability of Gag mutants to multimerize, constitutively membrane binding Gag derivatives were used. In these mutants, membrane binding was enhanced by a 10-residue exogenous triple-acylation signal derived from Fyn kinase [Fyn(10)] at their N-termini. No FRET was detected between wt Gag–CFP and YFP-labeled Fyn(10)-delCA-CTD Gag (data not shown), further indicating that the Gag multimerization defect observed in CA-CTD mutants results from defective Gag–Gag interactions and not from a secondary effect via membrane binding. Interestingly, near wt levels of FRET were recorded when Gag–CFP was co-expressed with YFP-labeled Fyn(10)-14A1G Gag (Fig. 4C, row a) or Fyn(10)- delNC Gag (Fig. 4C, row b). These results show that enhanced membrane binding can rescue the interaction of Gag NC mutants with Gag, indicating a possible compensatory effect between Gag membrane binding and NC-mediated Gag oligomerization (for recent reviews (Waheed and Freed, 2009; Yandrapalli et al., 2014).

5.3. *Gag assembly investigated by fluorescence lifetime imaging microscopy*

Gag assembly was further investigated by FLIM, using TC-tagged Gag proteins or a combination of eGFP- and mCherry-labeled Gag proteins (Fig. 5A, panels a–f). In the case of Gag–TC proteins, the fluorescence signal was obtained through complexation by the TC sequence of the cell permeant FlAsH probes added to the cell. Interestingly, Gag–Gag interaction brings in close proximity the FlAsH probes resulting into self-quenching and/or formation of ground state dimers or oligomers (exciton coupling) (Bernacchi and Mely, 2001). This in turn resulted in changes in the fluorescence lifetime of FlAsH that could be used to monitor the assembly of Gag–TC proteins by FLIM (Fritz et al., 2010). Thus, as presented in Fig. 5 the fluorescence lifetime value of FlAsH incubated with non transfected cells was 3.1 ± 0.1 ns (Fig. 5A, panel a and Fig. 5B, histogram

a), but dropped to 2.37 ± 0.05 ns when FlAsH was bound to Gag–TC at the PM (Fig. 5A, panel b and Fig. 5B, histogram a). In addition, dots (white arrows) with intermediate lifetimes were observed in the cytoplasm, confirming that Gag oligomers form in this compartment. To further explore the role of NC in Gag assembly, a GagΔNC-TC mutant where the NC domain of Gag was fully deleted, was designed. In the presence of FlAsH, both a decreased accumulation of GagΔNC-TC at the PM (Fig. 5A, panel c) and a lower change in the FlAsH lifetime (Fig. 5B, histogram a) as compared to Gag–TC were observed, indicating that NC deletion impacted both the binding and the efficient assembly of Gag at the PM. Though the FlAsH/TC methodology is highly attractive due to the small size of the TC label that does not affect the functions of Gag, its application is tedious due to the fluorescence background and the cytotoxicity generated by free FlAsH molecules.

These drawbacks are avoided when fluorescent proteins are used in a FRET/FLIM approach. The most popular couple of FRET donor/acceptor is eGFP/mCherry. Indeed, eGFP is frequently used as a donor since it is characterized by a high quantum yield and a simple mono-exponential fluorescence decay (Pepperkok et al., 1999). mCherry is a convenient acceptor since its absorption spectrum nicely overlaps the fluorescence spectrum of eGFP, giving a large Förster R_0 distance (where the transfer efficiency is 50%) of about 54 Å (Merzlyak et al., 2007). Moreover, in contrast to other red proteins, mCherry is monomeric and maturates rapidly. The main drawback of the eGFP/mCherry couple is the large size of these fluorescent proteins that can alter the properties of the proteins of interest. As aforementioned, a minimal alteration of the Gag assembly process was obtained when the reporter proteins were inserted downstream of MA and when Gag–eGFP and Gag–mCherry were co-expressed with an excess of non labeled Gag (Hubner et al., 2009; Muller et al., 2004). When expressed alone in HeLa cells, eGFP is diffuse in the cell and shows a lifetime of 2.41 ± 0.08 ns (Fig. 5A, panel d). When Gag–eGFP was expressed in HeLa cells, a strong accumulation was observed at the PM with a lifetime of 2.38 ± 0.05 ns, indicating that the intracellular distribution of Gag was not altered by eGFP and that the eGFP lifetime was not affected by its fusion to Gag (data not shown).

As expected, in the presence of Gag–mCherry, the fluorescence lifetime of Gag–eGFP dropped to 1.81 ± 0.06 ns (Fig. 5A, panel e and B, histogram b), which corresponded to an average FRET efficiency of 25%. As with Gag–TC/FlAsH, dots with intermediate lifetime values of 2 to 2.2 ns were observed in the cytoplasm, confirming that Gag oligomerization starts in the cytoplasm (Fritz et al., 2010; Hubner et al., 2007; Kutluay and Bieniasz, 2010). FLIM measurements on cells expressing GagΔNC-eGFP together with GagΔNC-mCherry showed a decreased accumulation of Gag at the PM (Fig. 5A, panel f), together with a lower FRET efficiency (13%, 5B, histogram b). Thus, both the TC/FlAsH and eGFP/mCherry tags provide very consistent data, clearly showing that the NC domain of Gag is required for efficient Gag assembly at the PM. Moreover, the nearly identical images obtained with the two types of labeling strongly suggest that both labeling strategies preserve the properties and functions of Gag in the virus assembly process.

6. Conclusion

As summarized here, fluorescence-based techniques notably quantitative fluorescence microscopy techniques appear to be very useful to decifer the mechanisms and the role of the Gag domains in retrovirus assembly. A key advantage of such techniques when combined with FRET is that they allow to directly visualize and evidence Gag–Gag interactions in a cellular context. Comparison of Fig. 5A, panels b and e with Fig. 4A – row a – further revealed that the FLIM approach provides a much better contrast than that based on epifluorescence microscopy. As a result, the sub-structures at the PM and in the cytoplasm where Gag assembly takes place are directly visible by FLIM. This is related to the fact that the measured lifetimes directly report on the FRET efficiency, while complex image analyses and quantifications are required to monitor the FRET efficiency in the other approach. In addition, being confocal in nature, the FLIM shows a much better signal to noise ratio than epifluorescence microscopy. Last, the FLIM is well suited for live cells, so that dynamic events and reactions can be monitored. Taken together, the use of such fluorescent approaches indicates that the NC domain of Gag is an important determinant for HIV-1 and RSV viral assembly, probably not as critical as the CA-CTD domain in HIV-1 Gag since its deletion completely abolishes virus assembly. Moreover, a clear relationship was established between NC- mediated Gag–Gag interactions and Gag localization at the PM. As it presently stands combining advanced techniques such as FLIM, FCS and super-resolution techniques with appropriately designed Gag mutant and fusion proteins should result in major advances in the understanding of the sophisticated choregraphy of HIV-1 virus assembly and particle production.

Acknowledgements

Thanks are due to Institut National sur la Santé Et la Reherche Médicale (INSERM), Centre National Recherche Scientifique (CNRS), Agence National Recherche sur le SIDA (ANRS) (2012-14. CSS2), SIDACTION (AI22-1-01963) and Unistra for constant support. This work was also supported by the European Project THINPAD "Targeting the HIV-1 Nucleocapsid Protein to fight Antiretroviral Drug Resistance" (FP7 – grant agreement 601969).

References

Accola, M.A., Strack, B., Gottlinger, H.G., 2000. Efficient particle production by minimal Gag constructs which retain the carboxy-terminal domain of human immunodeficiency virus type 1 capsid-p2 and a late assembly domain. J. Virol. 74, 5395–5402.

Adams, S.R., Campbell, R.E., Gross, L.A., Martin, B.R., Walkup, G.K., Yao, Y., Llopis, J., Tsien, R.Y., 2002. New biarsenical ligands and tetracysteine motifs for protein labeling in vitro and in vivo: synthesis and biological applications. J. Am. Chem. Soc. 124, 6063–6076.

Adamson, C.S., Freed, E.O., 2007. Human immunodeficiency virus type 1 assembly, release, and maturation. Adv. Pharmacol. (San Diego, Calif.) 55, 347–387.

Albertazzi, L., Arosio, D., Marchetti, L., Ricci, F., Beltram, F., 2009. Quantitative FRET analysis with the EGFP-mCherry fluorescent protein pair. Photochem. Photobiol. 85, 287–297.

Aldovini, A., Young, R.A., 1990. Mutations of RNA and protein sequences involved in human immunodeficiency virus type 1 packaging result in production of noninfectious virus. J. Virol. 64, 1920–1926.

Antson, A.A., Otridge, J., Brzozowski, A.M., Dodson, E.J., Dodson, G.G., Wilson, K.S., Smith, T.M., Yang, M., Kurecki, T., Gollnick, P., 1995. The structure of trp RNA-binding attenuation protein. Nature 374, 693–700.

Azoulay, J., Clamme, J.P., Darlix, J.L., Roques, B.P., Mely, Y., 2003. Destabilization of the HIV-1 complementary sequence of TAR by the nucleocapsid protein through activation of conformational fluctuations. J. Mol. Biol. 326, 691–700.

Balasubramaniam, M., Freed, E.O., 2011. New insights into HIV assembly and trafficking. Physiology (Bethesda) 26, 236–251.

Bastiaens, P.I., Squire, A., 1999. Fluorescence lifetime imaging microscopy: spatial resolution of biochemical processes in the cell. Trends Cell Biol. 9, 48–52.

Basyuk, E., Galli, T., Mougel, M., Blanchard, J.M., Sitbon, M., Bertrand, E., 2003. Retroviral genomic RNAs are transported to the plasma membrane by endosomal vesicles. Dev. Cell 5, 161–174.

Batisse, J., Guerrero, S.X., Bernacchi, S., Richert, L., Godet, J., Goldschmidt, V., Mely, Y., Marquet, R., de Rocquigny, H., Paillart, J.C., 2013. APOBEC3G Impairs the Multimerization of the HIV-1 Vif Protein in Living Cells. J. Virol. 87, 6492–6506.

Bell, N.M., Lever, A.M., 2013. HIV Gag polyprotein: processing and early viral particle assembly. Trends Microbiol. 21, 136–144.

Bennett, A.E., Narayan, K., Shi, D., Hartnell, L.M., Gousset, K., He, H., Lowekamp, B.C., Yoo, T.S., Bliss, D., Freed, E.O., et al., 2009. Ion-abrasion scanning electron microscopy reveals surface-connected tubular conduits in HIV-infected macrophages. PLoS Pathog. 5, e1000591.

Bennett, R.P., Nelle, T.D., Wills, J.W., 1993. Functional chimeras of the Rous sarcoma virus and human immunodeficiency virus gag proteins. J. Virol. 67, 6487–6498.

Bernacchi, S., Mely, Y., 2001. Exciton interaction in molecular beacons: a sensitive sensor for short range modifications of the nucleic acid structure. Nucleic Acids Res. 29, E62–62.

Bolinger, C., Sharma, A., Singh, D., Yu, L., Boris-Lawrie, K., 2010. RNA helicase A modulates translation of HIV-1 and infectivity of progeny virions. Nucleic Acids Res. 38, 1686–1696.

Boutant, E., Didier, P., Niehl, A., Mely, Y., Ritzenthaler, C., Heinlein, M., 2010. Fluorescent protein recruitment assay for demonstration and analysis of in vivo protein interactions in plant cells and its application to Tobacco mosaic virus movement protein. Plant J. 62, 171–177.

Briggs, J.A., Krausslich, H.G., 2011. The molecular architecture of HIV. J. Mol. Biol. 410, 491–500.

Bryant, M., Ratner, L., 1990. Myristoylation-dependent replication and assembly of human immunodeficiency virus 1. Proc. Natl. Acad. Sci. U. S. A. 87, 523–527.

Burniston, M.T., Cimarelli, A., Colgan, J., Curtis, S.P., Luban, J., 1999. Human immunodeficiency virus type 1 Gag polyprotein multimerization requires the nucleocapsid domain and RNA and is promoted by the capsid-dimer interface and the basic region of matrix protein. J. Virol. 73, 8527–8540.

Carillo, M.A., Bennet, M., Faivre, D., 2013. Interaction of proteins associated with the magnetosome assembly in magnetotactic bacteria as revealed by two-hybrid two-photon excitation fluorescence lifetime imaging microscopy Forster resonance energy transfer. J. Phys. Chem. B 117, 14642–14648.

Carriere, C., Gay, B., Chazal, N., Morin, N., Boulanger, P., 1995. Sequence requirements for encapsidation of deletion mutants and chimeras of human immunodeficiency virus type 1 Gag precursor into retrovirus-like particles. J. Virol. 69, 2366–2377.

Chang, C.Y., Chang, Y.F., Wang, S.M., Tseng, Y.T., Huang, K.J., Wang, C.T., 2008. HIV-1 matrix protein repositioning in nucleocapsid region fails to confer virus-like particle assembly. Virology 378, 97–104.

Chatel-Chaix, L., Boulay, K., Mouland, A.J., Desgroseillers, L., 2008. The host protein Staufen1 interacts with the Pr55Gag zinc fingers and regulates HIV-1 assembly via its N-terminus. Retrovirology 5, 41.

Chen, J., Nikolaitchik, O., Singh, J., Wright, A., Bencsics, C.E., Coffin, J.M., Ni, N., Lockett, S., Pathak, V.K., Hu, W.S., 2009. High efficiency of HIV-1 genomic RNA packaging and heterozygote formation revealed by single virion analysis. Proc. Natl. Acad. Sci. U. S. A. 106, 13535–13540.

Chojnacki, J., Muller, B., 2013. Investigation of HIV-1 assembly and release using modern fluorescence imaging techniques. Traffic (Copenhagen, Denmark) 14, 15–24.

Cimarelli, A., Luban, J., 2000. Human immunodeficiency virus type 1 virion density is not determined by nucleocapsid basic residues. J. Virol. 74, 6734–6740.

Cimarelli, A., Sandin, S., Hoglund, S., Luban, J., 2000. Basic residues in human immunodeficiency virus type 1 nucleocapsid promote virion assembly via interaction with RNA. J. Virol. 74, 3046–3057.

Clamme, J.P., Azoulay, J., Mely, Y., 2003. Monitoring of the formation and dissociation of polyethylenimine/DNA complexes by two photon fluorescence correlation spectroscopy. Biophys. J. 84, 1960–1968.

Clever, J., Sassetti, C., Parslow, T.G., 1995. RNA secondary structure and binding sites for gag gene products in the 5′ packaging signal of human immunodeficiency virus type 1. J. Virol. 69, 2101–2109.

Clever, J.L., Taplitz, R.A., Lochrie, M.A., Polisky, B., Parslow, T.G., 2000. A heterologous, high-affinity RNA ligand for human immunodeficiency virus Gag protein has RNA packaging activity. J. Virol. 74, 541–546.

Crist, R.M., Datta, S.A., Stephen, A.G., Soheilian, F., Mirro, J., Fisher, R.J., Nagashima, K., Rein, A., 2009. Assembly properties of human immunodeficiency virus type 1 Gag-leucine zipper chimeras: implications for retrovirus assembly. J. Virol. 83, 2216–2225.

Datta, S.A., Temeselew, L.G., Crist, R.M., Soheilian, F., Kamata, A., Mirro, J., Harvin, D., Nagashima, K., Cachau, R.E., Rein, A., 2011. On the role of the SP1 domain in HIV-1 particle assembly: a molecular switch? J. Virol. 85, 4111–4121.

Day, R.N., Periasamy, A., Schaufele, F., 2001. Fluorescence resonance energy transfer microscopy of localized protein interactions in the living cell nucleus. Methods 25, 4–18.

Derdowski, A., Ding, L., Spearman, P., 2004. A novel fluorescence resonance energy transfer assay demonstrates that the human immunodeficiency virus type 1 Pr55Gag I domain mediates Gag–Gag interactions. J. Virol. 78, 1230–1242.

Dong, X., Li, H., Derdowski, A., Ding, L., Burnett, A., Chen, X., Peters, T.R., Dermody, T.S., Woodruff, E., Wang, J.J., et al., 2005. AP-3 directs the intracellular trafficking of HIV-1 Gag and plays a key role in particle assembly. Cell 120, 663–674.

Dorfman, T., Luban, J., Goff, S.P., Haseltine, W.A., Gottlinger, H.G., 1993. Mapping of functionally important residues of a cysteine-histidine box in the human immunodeficiency virus type 1 nucleocapsid protein. J. Virol. 67, 6159–6169.

Dupraz, P., Spahr, P.F., 1992. Specificity of Rous sarcoma virus nucleocapsid protein in genomic RNA packaging. J. Virol. 66, 4662–4670.

Dussupt, V., Javid, M.P., Abou-Jaoude, G., Jadwin, J.A., de La Cruz, J., Nagashima, K., Bouamr, F., 2009. The nucleocapsid region of HIV-1 Gag cooperates with the PTAP and LYPXnL late domains to recruit the cellular machinery necessary for viral budding. PLoS Pathog. 5, e1000339.

Dykeman, E.C., Grayson, N.E., Toropova, K., Ranson, N.A., Stockley, P.G., Twarock, R., 2011. Simple rules for efficient assembly predict the layout of a packaged viral RNA. J. Mol. Biol. 408, 399–407.

Fogarty, K.H., Chen, Y., Grigsby, I.F., Macdonald, P.J., Smith, E.M., Johnson, J.L., Rawson, J.M., Mansky, L.M., Mueller, J.D., 2011. Characterization of cytoplasmic Gag–gag interactions by dual-color z-scan fluorescence fluctuation spectroscopy. Biophys. J. 100, 1587–1595.

Franke, E.K., Yuan, H.E., Bossolt, K.L., Goff, S.P., Luban, J., 1994. Specificity and sequence requirements for interactions between various retroviral Gag proteins. J. Virol. 68, 5300–5305.

Fritz, J.V., Didier, P., Clamme, J.P., Schaub, E., Muriaux, D., Cabanne, C., Morellet, N., Bouaziz, S., Darlix, J.L., Mely, Y., et al., 2008. Direct Vpr–Vpr interaction in cells monitored by two photon fluorescence correlation spectroscopy and fluorescence lifetime imaging. Retrovirology 5, 87.

Fritz, J.V., Dujardin, D., Godet, J., Didier, P., De Mey, J., Darlix, J.L., Mely, Y., de Rocquigny, H., 2010. HIV-1 Vpr oligomerization but not that of Gag directs the interaction between Vpr and Gag. J. Virol. 84, 1585–1596.

Gamble, T.R., Yoo, S., Vajdos, F.F., von Schwedler, U.K., Worthylake, D.K., Wang, H., McCutcheon, J.P., Sundquist, W.I., Hill, C.P., 1997. Structure of the carboxyl-terminal dimerization domain of the HIV-1 capsid protein. Science 278, 849–853.

Gorelick, R.J., Henderson, L.E., Hanser, J.P., Rein, A., 1988. Point mutants of Moloney murine leukemia virus that fail to package viral RNA: evidence for specific RNA recognition by a "zinc finger-like" protein sequence. Proc. Natl. Acad. Sci. U. S. A. 85, 8420–8424.

Gorelick, R.J., Nigida Jr., S.M., Bess Jr., J.W., Arthur, L.O., Henderson, L.E., Rein, A., 1990. Noninfectious human immunodeficiency virus type 1 mutants deficient in genomic RNA. J. Virol. 64, 3207–3211.

Gorelick, R.J., Chabot, D.J., Rein, A., Henderson, L.E., Arthur, L.O., 1993. The two zinc fingers in the human immunodeficiency virus type 1 nucleocapsid protein are not functionally equivalent. J. Virol. 67, 4027–4036.

Gorelick, R.J., Chabot, D.J., Ott, D.E., Gagliardi, T.D., Rein, A., Henderson, L.E., Arthur, L.O., 1996. Genetic analysis of the zinc finger in the Moloney murine leukemia virus nucleocapsid domain: replacement of zinc-coordinating residues with other zinc-coordinating residues yields noninfectious particles containing genomic RNA. J. Virol. 70, 2593–2597.

Gorelick, R.J., Fu, W., Gagliardi, T.D., Bosche, W.J., Rein, A., Henderson, L.E., Arthur, L.O., 1999. Characterization of the block in replication of nucleocapsid protein zinc finger mutants from moloney murine leukemia virus. J. Virol. 73, 8185–8195.

Gottlinger, H.G., 2001. The HIV-1 assembly machine. AIDS (London, England) 15 (Suppl 5), S13–S20.

Gottlinger, H.G., Sodroski, J.G., Haseltine, W.A., 1989. Role of capsid precursor processing and myristoylation in morphogenesis and infectivity of human immunodeficiency virus type 1. Proc. Natl. Acad. Sci. U. S. A. 86, 5781–5785.

Gousset, K., Ablan, S.D., Coren, L.V., Ono, A., Soheilian, F., Nagashima, K., Ott, D.E., Freed, E.O., 2008. Real-time visualization of HIV-1 GAG trafficking in infected macrophages. PLoS Pathog. 4, e1000015.

Griffin, B.A., Adams, S.R., Tsien, R.Y., 1998. Specific covalent labeling of recombinant protein molecules inside live cells. Science 281, 269–272.

Grigorov, B., Arcanger, F., Roingeard, P., Darlix, J.L., Muriaux, D., 2006. Assembly of infectious HIV-1 in human epithelial and T-lymphoblastic cell lines. J. Mol. Biol. 359, 848–862.

Grigorov, B., Decimo, D., Smagulova, F., Pechoux, C., Mougel, M., Muriaux, D., Darlix, J.L., 2007. Intracellular HIV-1 Gag localization is impaired by mutations in the nucleocapsid zinc fingers. Retrovirology 4, 54.

Hermida-Matsumoto, L., Resh, M.D., 2000. Localization of human immunodeficiency virus type 1 Gag and Env at the plasma membrane by confocal imaging. J. Virol. 74, 8670–8679.

Hill, C.P., Worthylake, D., Bancroft, D.P., Christensen, A.M., Sundquist, W.I., 1996. Crystal structures of the trimeric human immunodeficiency virus type 1 matrix protein: implications for membrane association and assembly. Proc. Natl. Acad. Sci. U. S. A. 93, 3099–3104.

Hogue, I.B., Hoppe, A., Ono, A., 2009. Quantitative fluorescence resonance energy transfer microscopy analysis of the human immunodeficiency virus type 1 Gag–Gag interaction: relative contributions of the CA and NC domains and membrane binding. J. Virol. 83, 7322–7336.

Hong, S.S., Boulanger, P., 1993. Assembly-defective point mutants of the human immunodeficiency virus type 1 Gag precursor phenotypically expressed in recombinant baculovirus-infected cells. J. Virol. 67, 2787–2798.

Hoppe, A., Christensen, K., Swanson, J.A., 2002. Fluorescence resonance energy transfer-based stoichiometry in living cells. Biophys. J. 83, 3652–3664.

Housset, V., De Rocquigny, H., Roques, B.P., Darlix, J.L., 1993. Basic amino acids flanking the zinc finger of Moloney murine leukemia virus nucleocapsid protein NCp10 are critical for virus infectivity. J. Virol. 67, 2537–2545.

Hu, W.S., Rhodes, T., Dang, Q., Pathak, V., 2003. Retroviral recombination: Review of genetic analyses. Front. Biosci. 8, D143–D155.

Hubner, W., Chen, P., Del Portillo, A., Liu, Y., Gordon, R.E., Chen, B.K., 2007. Sequence of human immunodeficiency virus type 1 (HIV-1) Gag localization and oligomerization monitored with live confocal imaging of a replication-competent, fluorescently tagged HIV-1. J. Virol. 81, 12596–12607.

Hubner, W., McNerney, G.P., Chen, P., Dale, B.M., Gordon, R.E., Chuang, F.Y., Li, X.D., Asmuth, D.M., Huser, T., Chen, B.K., 2009. Quantitative 3D video microscopy of HIV transfer across T cell virological synapses. Science 323, 1743–1747.

Ivanchenko, S., Godinez, W.J., Lampe, M., Krausslich, H.G., Eils, R., Rohr, K., Brauchle, C., Muller, B., Lamb, D.C., 2009. Dynamics of HIV-1 assembly and release. PLoS Pathog. 5, e1000652.

Jouvenet, N., Neil, S.J., Bess, C., Johnson, M.C., Virgen, C.A., Simon, S.M., Bieniasz, P.D., 2006. Plasma membrane is the site of productive HIV-1 particle assembly. PLoS biology 4, e435.

Jouvenet, N., Bieniasz, P.D., Simon, S.M., 2008. Imaging the biogenesis of individual HIV-1 virions in live cells. Nature 454, 236–240.

Kawada, S., Goto, T., Haraguchi, H., Ono, A., Morikawa, Y., 2008. Dominant negative inhibition of human immunodeficiency virus particle production by the nonmyristoylated form of gag. J. Virol. 82, 4384–4399.

Kemler, I., Meehan, A., Poeschla, E.M., 2010. Live-cell coimaging of the genomic RNAs and Gag proteins of two lentiviruses. J. Virol. 84, 6352–6366.

Krausslich, H.G., Facke, M., Heuser, A.M., Konvalinka, J., Zentgraf, H., 1995. The spacer peptide between human immunodeficiency virus capsid and nucleocapsid proteins is essential for ordered assembly and viral infectivity. J. Virol. 69, 3407–3419.

Kutluay, S.B., Bieniasz, P.D., 2010. Analysis of the initiating events in HIV-1 particle assembly and genome packaging. PLoS Pathog. 6, e1001200.

Larson, D.R., Ma, Y.M., Vogt, V.M., Webb, W.W., 2003. Direct measurement of Gag–Gag interaction during retrovirus assembly with FRET and fluorescence correlation spectroscopy. J. Cell Biol. 162, 1233–1244.

Lee, P.P., Linial, M.L., 1995. Inhibition of Wild-Type Hiv-1 Virus Production by a Matrix Deficient Gag Mutant. Virology 208, 808–811.

Lehmann, M., Milev, M.P., Abrahamyan, L., Yao, X.J., Pante, N., Mouland, A.J., 2009. Intracellular transport of human immunodeficiency virus type 1 genomic RNA and viral production are dependent on dynein motor function and late endosome positioning. J. Biol. Chem. 284, 14572–14585.

Li, H., Dou, J., Ding, L., Spearman, P., 2007. Myristoylation is required for human immunodeficiency virus type 1 Gag–Gag multimerization in mammalian cells. J. Virol. 81, 12899–12910.

Lindwasser, O.W., Resh, M.D., 2001. Multimerization of human immunodeficiency virus type 1 Gag promotes its localization to barges, raft-like membrane microdomains. J. Virol. 75, 7913–7924.

Lingappa, J.R., Dooher, J.E., Newman, M.A., Kiser, P.K., Klein, K.C., 2006. Basic residues in the nucleocapsid domain of Gag are required for interaction of HIV-1 gag with ABCE1 (HP68), a cellular protein important for HIV-1 capsid assembly. J. Biol. Chem. 281, 3773–3784.

Lochrie, M.A., Waugh, S., Pratt Jr., D.G., Clever, J., Parslow, T.G., Polisky, B., 1997. In vitro selection of RNAs that bind to the human immunodeficiency virus type-1 gag polyprotein. Nucleic Acids Res. 25, 2902–2910.

Mammano, F., Ohagen, A., Hoglund, S., Gottlinger, H.G., 1994. Role of the major homology region of human immunodeficiency virus type 1 in virion morphogenesis. J. Virol. 68, 4927–4936.

McGinty, J., Stuckey, D.W., Soloviev, V.Y., Laine, R., Wylezinska-Arridge, M., Wells, D.J., Arridge, S.R., French, P.M., Hajnal, J.V., Sardini, A., 2011. In vivo fluorescence lifetime tomography of a FRET probe expressed in mouse. Biomed. Opt. Exp. 2, 1907–1917.

Merzlyak, E.M., Goedhart, J., Shcherbo, D., Bulina, M.E., Shcheglov, A.S., Fradkov, A.F., Gaintzeva, A., Lukyanov, K.A., Lukyanov, S., Gadella, T.W., et al., 2007. Bright monomeric red fluorescent protein with an extended fluorescence lifetime. Nat. Methods 4, 555–557.

Milev, M.P., Brown, C.M., Mouland, A.J., 2010. Live cell visualization of the interactions between HIV-1 Gag and the cellular RNA-binding protein Staufen1. Retrovirology 7, 41.

Mirambeau, G., Lyonnais, S., Gorelick, R.J., 2010. Features, processing states, and heterologous protein interactions in the modulation of the retroviral nucleocapsid protein function. RNA Biol. 7, 724–734.

Molle, D., Segura-Morales, C., Camus, G., Berlioz-Torrent, C., Kjems, J., Basyuk, E., Bertrand, E., 2009. Endosomal trafficking of HIV-1 gag and genomic RNAs regulates viral egress. J. Biol. Chem. 284, 19727–19743.

Morellet, N., Druillennec, S., Lenoir, C., Bouaziz, S., Roques, B.P., 2005. Helical structure determined by NMR of the HIV-1 (345–392)Gag sequence, surrounding p2: implications for particle assembly and RNA packaging. Protein Sci. 14, 375–386.

Morikawa, Y., Hinata, S., Tomoda, H., Goto, T., Nakai, M., Aizawa, C., Tanaka, H., Omura, S., 1996. Complete inhibition of human immunodeficiency virus Gag myristoylation is necessary for inhibition of particle budding. J. Biol. Chem. 271, 2868–2873.

Muller, B., Daecke, J., Fackler, O.T., Dittmar, M.T., Zentgraf, H., Krausslich, H.G., 2004. Construction and characterization of a fluorescently labeled infectious human immunodeficiency virus type 1 derivative. J. Virol. 78, 10803–10813.

Muriaux, D., Mirro, J., Harvin, D., Rein, A., 2001. RNA is a structural element in retrovirus particles. Proc. Natl. Acad. Sci. U. S. A. 98, 5246–5251.

Muriaux, D., Darlix, J.L., 2010. Properties and functions of the nucleocapsid protein in virus assembly. RNA Biol. 7, 744–753.

Neil, S.J., Eastman, S.W., Jouvenet, N., Bieniasz, P.D., 2006. HIV-1 Vpu promotes release and prevents endocytosis of nascent retrovirus particles from the plasma membrane. PLoS Pathog. 2, e39.

Nydegger, S., Foti, M., Derdowski, A., Spearman, P., Thali, M., 2003. HIV-1 egress is gated through late endosomal membranes. Traffic (Copenhagen, Denmark) 4, 902–910.

O'Carroll, I.P., Soheilian, F., Kamata, A., Nagashima, K., Rein, A., 2013. Elements in HIV-1 Gag contributing to virus particle assembly. Virus Res. 171, 341–345.

Ono, A., Demirov, D., Freed, E.O., 2000. Relationship between human immunodeficiency virus type 1 Gag multimerization and membrane binding. J. Virol. 74, 5142–5150.

Ono, A., Ablan, S.D., Lockett, S.J., Nagashima, K., Freed, E.O., 2004. Phosphatidylinositol (4,5) bisphosphate regulates HIV-1 Gag targeting to the plasma membrane. Proc. Natl. Acad. Sci. U. S. A. 101, 14889–14894.

Ott, D.E., Coren, L.V., Shatzer, T., 2009. The nucleocapsid region of human immunodeficiency virus type 1 Gag assists in the coordination of assembly and Gag processing: role for RNA–Gag binding in the early stages of assembly. J. Virol. 83, 7718–7727.

Ottmann, M., Gabus, C., Darlix, J.L., 1995. The central globular domain of the nucleocapsid protein of human immunodeficiency virus type 1 is critical for virion structure and infectivity. J. Virol. 69, 1778–1784.

Padilla-Parra, S., Auduge, N., Lalucque, H., Mevel, J.C., Coppey-Moisan, M., Tramier, M., 2009. Quantitative comparison of different fluorescent protein couples for fast FRET-FLIM acquisition. Biophys. J. 97, 2368–2376.

Paillart, J.C., Shehu-Xhilaga, M., Marquet, R., Mak, J., 2004. Dimerization of retroviral RNA genomes: an inseparable pair. Nat. Rev. 2, 461–472.

Pelchen-Matthews, A., Kramer, B., Marsh, M., 2003. Infectious HIV-1 assembles in late endosomes in primary macrophages. J. Cell. Biol. 162, 443–455, Epub 2003 Jul 2028.

Park, J., Morrow, C.D., 1992. The nonmyristylated Pr160gag-pol polyprotein of human immunodeficiency virus type 1 interacts with Pr55gag and is incorporated into viruslike particles. J. Virol. 66, 6304–6313.

Pepperkok, R., Squire, A., Geley, S., Bastiaens, P.I., 1999. Simultaneous detection of multiple green fluorescent proteins in live cells by fluorescence lifetime imaging microscopy. Curr. Biol. 9, 269–272.

Pereira, C.F., Ellenberg, P.C., Jones, K.L., Fernandez, T.L., Smyth, R.P., Hawkes, D.J., Hijnen, M., Vivet-Boudou, V., Marquet, R., Johnson, I., et al., 2011. Labeling of multiple HIV-1 proteins with the biarsenical-tetracysteine system. PLOS ONE 6, e17016.

Perez-Caballero, D., Hatziioannou, T., Martin-Serrano, J., Bieniasz, P.D., 2004. Human immunodeficiency virus type 1 matrix inhibits and confers cooperativity on gag precursor–membrane interactions. J. Virol. 78, 9560–9563.

Perlman, M., Resh, M.D., 2006. Identification of an intracellular trafficking and assembly pathway for HIV-1 gag. Traffic (Copenhagen, Denmark) 7, 731–745.

Perrin-Tricaud, C., Davoust, J., Jones, I.M., 1999. Tagging the human immunodeficiency virus gag protein with green fluorescent protein. Minimal evidence for colocalisation with actin. Virology 255, 20–25.

Poon, D.T.K., Wu, J., Aldovini, A., 1996. Charged amino acid residues of human immunodeficiency virus type 1 nucleocapsid p7 protein involved in RNA packaging and infectivity. J. Virol. 70, 6607–6616.

Popov, S., Popova, E., Inoue, M., Gottlinger, H.G., 2008. Human immunodeficiency virus type 1 Gag engages the Bro1 domain of ALIX/AIP1 through the nucleocapsid. J. Virol. 82, 1389–1398.

Popov, S., Popova, E., Inoue, M., Gottlinger, H.G., 2009. Divergent Bro1 domains share the capacity to bind human immunodeficiency virus type 1 nucleocapsid and to enhance virus-like particle production. J. Virol. 83, 7185–7193.

Pornillos, O., Higginson, D.S., Stray, K.M., Fisher, R.D., Garrus, J.E., Payne, M., He, G.P., Wang, H.E., Morham, S.G., Sundquist, W.I., 2003. HIV Gag mimics the Tsg101-recruiting activity of the human Hrs protein. J. Cell Biol. 162, 425–434.

Pornillos, O., Ganser-Pornillos, B.K., Kelly, B.N., Hua, Y., Whitby, F.G., Stout, C.D., Sundquist, W.I., Hill, C.P., Yeager, M., 2009. X-ray structures of the hexameric building block of the HIV capsid. Cell 137, 1282–1292.

Pornillos, O., Ganser-Pornillos, B.K., Yeager, M., 2011. Atomic-level modelling of the HIV capsid. Nature 469, 424–427.

Pyenta, P.S., Holowka, D., Baird, B., 2001. Cross-correlation analysis of inner-leaflet-anchored green fluorescent protein co-redistributed with IgE receptors and outer leaflet lipid raft components. Biophys. J. 80, 2120–2132.

Resh, M.D., 2005. Intracellular trafficking of HIV-1 Gag: how Gag interacts with cell membranes and makes viral particles. AIDS Rev. 7, 84–91.

Rudner, L., Nydegger, S., Coren, L.V., Nagashima, K., Thali, M., Ott, D.E., 2005. Dynamic fluorescent imaging of human immunodeficiency virus type 1 gag in live cells by biarsenical labeling. J. Virol. 79, 4055–4065.

Saad, J.S., Miller, J., Tai, J., Kim, A., Ghanam, R.H., Summers, M.F., 2006. Structural basis for targeting HIV-1 Gag proteins to the plasma membrane for virus assembly. Proc. Natl. Acad. Sci. U. S. A. 103, 11364–11369.

Sandefur, S., Varthakavi, V., Spearman, P., 1998. The I domain is required for efficient plasma membrane binding of human immunodeficiency virus type 1 Pr55Gag. J. Virol. 72, 2723–2732.

Shaner, N.C., Steinbach, P.A., Tsien, R.Y., 2005. A guide to choosing fluorescent proteins. Nat. Methods 2, 905–909.

Stockley, P.G., Stonehouse, N.J., Murray, J.B., Goodman, S.T.S., Talbot, S.J., Adams, C.J., Liljas, L., Valegard, K., 1995. Probing sequence-specific RNA recognition by the bacteriophage-Ms2 coat protein. Nucleic Acids Res. 23, 2512–2518.

Strambio-de-Castillia, C., Hunter, E., 1992. Mutational analysis of the major homology region of Mason-Pfizer monkey virus by use of saturation mutagenesis. J. Virol. 66, 7021–7032.

Sundquist, W.I., Krausslich, H.G., 2012. HIV-1 assembly, budding, and maturation. Cold Spring Harb. Perspect. Med. 2, a006924.

Tanchou, V., Gabus, C., Rogemond, V., Darlix, J.L., 1995. Formation of stable and functional HIV-1 nucleoprotein complexes in vitro. J. Mol. Biol. 252, 563–571.

Tanchou, V., Decimo, D., Pechoux, C., Lener, D., Rogemond, V., Berthoux, L., Ottmann, M., Darlix, J.L., 1998. Role of the N-terminal zinc finger of human immunodeficiency virus type 1 nucleocapsid protein in virus structure and replication. J. Virol. 72, 4442–4447.

Tramier, M., Zahid, M., Mevel, J.C., Masse, M.J., Coppey-Moisan, M., 2006. Sensitivity of CFP/YFP and GFP/mCherry pairs to donor photobleaching on FRET determination by fluorescence lifetime imaging microscopy in living cells. Microsc. Res. Technol. 69, 933–939.

Turville, S.G., Aravantinou, M., Stossel, H., Romani, N., Robbiani, M., 2008. Resolution of de novo HIV production and trafficking in immature dendritic cells. Nat. Methods 5, 75–85.

von Schwedler, U.K., Stray, K.M., Garrus, J.E., Sundquist, W.I., 2003. Functional surfaces of the human immunodeficiency virus type 1 capsid protein. J. Virol. 77, 5439–5450.

Voss, T.C., Demarco, I.A., Day, R.N., 2005. Quantitative imaging of protein interactions in the cell nucleus. Biotechniques 38, 413–424.
Wachsmuth, M., Waldeck, W., Langowski, J., 2000. Anomalous diffusion of fluorescent probes inside living cell nuclei investigated by spatially-resolved fluorescence correlation spectroscopy. J. Mol. Biol. 298, 677–689.
Waheed, A.A., Freed, E.O., 2009. Lipids and membrane microdomains in HIV-1 replication. Virus Res. 143, 162–176.
Wang, F., Marshall, C.B., Ikura, M., 2013. Transcriptional/epigenetic regulator CBP/p300 in tumorigenesis: structural and functional versatility in target recognition. Cell. Mol. Life Sci. 70, 3989–4008.
Welsch, S., Keppler, O.T., Habermann, A., Allespach, I., Krijnse-Locker, J., Krausslich, H.G., 2007. HIV-1 buds predominantly at the plasma membrane of primary human macrophages. PLoS Pathog. 3, e36.
Wills, J.W., Craven, R.C., 1991. Form, function, and use of retroviral gag proteins. AIDS (London, England) 5, 639–654.
Zhang, Y., Qian, H., Love, Z., Barklis, E., 1998. Analysis of the assembly function of the human immunodeficiency virus type 1 gag protein nucleocapsid domain. J. Virol. 72, 1782–1789.

Publication 2:

Role of the Nucleocapsid Domain in HIV-1Gag Oligomerization and Trafficking to the Plasma Membrane: A Fluorescence Lifetime Imaging Microscopy Investigation

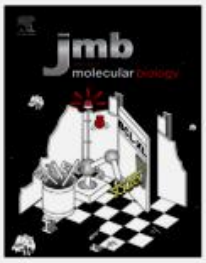

Role of the Nucleocapsid Domain in HIV-1 Gag Oligomerization and Trafficking to the Plasma Membrane: A Fluorescence Lifetime Imaging Microscopy Investigation

Salah Edin El Meshri, Denis Dujardin, Julien Godet, Ludovic Richert, Christian Boudier, Jean Luc Darlix, Pascal Didier, Yves Mély and Hugues de Rocquigny

Laboratoire de Biophotonique et Pharmacologie, *UMR 7213 CNRS, Faculté de Pharmacie, Université de Strasbourg, 74, Route du Rhin, 67401 Illkirch Cedex, France*

Correspondence to Yves Mély and Hugues de Rocquigny: *yves.mely@unistra.fr; hderocquigny@unistra.fr*
http://dx.doi.org/10.1016/j.jmb.2015.01.015
Edited by E. O. Freed

Abstract

The Pr55 Gag of human immunodeficiency virus type 1 orchestrates viral particle assembly in producer cells, which requires the genomic RNA and a lipid membrane as scaffolding platforms. The nucleocapsid (NC) domain with its two invariant CCHC zinc fingers flanked by unfolded basic sequences is thought to direct genomic RNA selection, dimerization and packaging during virus assembly. To further investigate the role of NC domain, we analyzed the assembly of Gag with deletions in the NC domain in parallel with that of wild-type Gag using fluorescence lifetime imaging microscopy combined with Förster resonance energy transfer in HeLa cells. We found that, upon binding to nucleic acids, the NC domain promotes the formation of compact Gag oligomers in the cytoplasm. Moreover, the intracellular distribution of the population of oligomers further suggests that oligomers progressively assemble during their trafficking toward the plasma membrane (PM), but with no dramatic changes in their compact arrangement. This ultimately results in the accumulation at the PM of closely packed Gag oligomers that likely arrange in hexameric lattices, as revealed by the perfect match between the experimental Förster resonance energy transfer value and the one calculated from the structural model of Gag in immature viruses. The distal finger and flanking basic sequences, but not the proximal finger, appear to be essential for Gag oligomer compaction and membrane binding. Moreover, the full NC domain was found to be instrumental in the kinetics of Gag oligomerization and intracellular trafficking. These findings further highlight the key roles played by the NC domain in virus assembly.

Introduction

In human immunodeficiency virus type 1 (HIV-1) producer cells, virus assembly is orchestrated by the Pr55 Gag (also referred to as Gag) polyprotein precursor composed of four structural domains, the N-terminal matrix (MA), the capsid (CA), the nucleocapsid (NC) and p6. During and/or soon after assembly, Gag molecules undergo maturation by the viral protease generating the MAp17, CAp24, NCp7 and p6 proteins found in infectious mature virions [1,2]. A generally accepted model for HIV-1 assembly stipulates that the genomic RNA acts as a scaffolding platform onto which Gag molecules bind via NC, then kick-starting assembly [3–6]. This, in turn, causes the N-terminal myristyl switch of Gag MA and binding of the RNA-bound Gag oligomers [7–10] to either the plasma membrane (PM) [11–14] or endosomes [15–18]. Previous dynamic imaging analyses support an assembly model where Gag molecules first appear as small cytoplasmic clusters that then traffic to the PM and are ultimately released as viral particles [11,12,19–23].

Several Gag domains are involved in oligomer formation [24], notably, the MA domain that contains two signals critical for PM targeting and anchoring of Gag, namely, the N-terminal myristyl and a stretch of basic residues [24,25], and can form trimers [26]. Moreover, the CA domain is the major driving force for Gag oligomerization [27,28] together with SP1 corresponding to a short stretch of residues linking the CA and NC domains [29–31]. The NC domain

also participates in Gag oligomerization and assembly by recruiting the genomic RNA [6,32–34]. In addition, NC influences the intracellular localization of Gag since deletion or point mutations can cause Gag diffusion throughout the cytoplasm and its accumulation as intracellular aggregates [16,35].

This prompted us to investigate by fluorescence lifetime imaging microscopy (FLIM) with Förster non-radiative energy transfer [Förster resonance energy transfer (FRET)] the influence of NC mutations on Gag oligomerization and localization in HeLa cells co-expressing Gag, Gag-eGFP and Gag-mCherry. There is a high level of FRET not only at the PM but also in the cytoplasm, indicating that formation of compact Gag oligomers already starts in this compartment. Deletion of the two zinc fingers or of the complete NC resulted in a diffuse cellular localization of Gag, with a large decrease of FRET suggesting that the NC domain is critical for Gag compaction. Interestingly, deletion of a single NC zinc finger had a limited impact on FRET efficiency but strongly slowed down the assembly process. Taken together, our observations indicate that the highly conserved NC zinc fingers play an important role in Gag oligomerization and trafficking of the Gag oligomers from the cytoplasm to the PM and ultimately their binding to the PM.

Results

Cellular localization of wild-type Gag and of zinc finger mutants soon after synthesis

In a previous work, the wild-type (wt) Gag and NC mutants of Gag with either the complete NC deletion (GagΔNC) or that of the first, the second or both zinc fingers (GagΔZF1, GagΔZF2 and GagΔZF1ΔZF2) were transiently expressed in 293T cells, and 24 h later, their expression was assessed by means of immunofluorescence microscopy [35]. Different patterns of Gag localization were found, clearly indicating that each NC zinc finger has an impact on Gag localization and assembly. Our aim was to investigate by FLIM-FRET Gag–Gag interactions for the wt protein and its NC mutants in order to better understand whether these phenotypes resulted from a defect in Gag oligomerization.

To this end, we constructed a series of plasmid DNA expressing either wt Gag or NC deletion mutants and their fusion proteins with eGFP or mCherry reporter protein inserted upstream of CA [20,36] (Fig. 1a) and transfected it into HeLa cells. Location of the reporter gene and the co-transfection of these constructs together with those expressing non-labeled Gag proteins were shown to only slightly affect the virus morphology, Gag localization and Gag budding [11,12,36–38]. Expression of the unlabeled (Fig. 1b) and labeled (Fig. S1) Gag derivatives was checked by Western blotting. In previous studies investigating Gag distribution and assembly, cells were observed at 24 h or even days after DNA transfection [21–23,35,39,40]. However, Gag expression can be detected as early as ~10 h post-transfection [41], which prompted us to monitor first by confocal microscopy the time course of Gag assembly at 12 h and 24 h post-transfection. Images a–e (left column) and f–j (right column) of Fig. 1c represent the main staining phenotype observed for each Gag derivative at 12 h or 24 h post-transfection, respectively. Gag-expressing cells (Fig. 1c-A) displayed punctuate and diffuse staining in the cytoplasm and an accumulation at or near the PM. There was an important accumulation of Gag at the PM at 24 h together with a slight cytoplasmic staining (Fig. 1c-F). Noticeably, this accumulation of Gag observed by direct Gag-eGFP (or Gag-Cherry) imaging is different from that obtained using anti-Gag antibodies. In fact, our approach using eGFP-tagged Gag permits an improved detection of Gag at the PM as compared to immunofluorescence microscopy, probably due to the fact that Gag oligomerization was shown to hide several Gag epitopes [22,42].

For the GagΔZF1 and GagΔZF2 mutants, in which either the proximal or the distal NC zinc finger was deleted, we observed a diffuse staining pattern at 12 h (Fig. 1c-B and c-C) in the cytoplasm and only a partial accumulation at the PM as compared to wt Gag. At 24 h, inline with the data of Grigorov *et al.* [35], a similar phenotype was observed (Fig. 1c-G and c-H) while about 20% of the cells displayed a phenotype similar to the wt. In addition, these two Gag NC deletion mutants were found to partially accumulate in the nucleoplasm and in the nucleoli in about 30% of the cells. This localization was not previously observed probably due to the immunostaining procedure, which is not suited for nuclear antigen detection.

We next examined the localization of the GagΔZF1ΔZF2 mutant where the two zinc fingers were removed, leaving only the basic domains flanking the two zinc fingers, and of GagΔNC where the entire NC sequence was deleted. At 12 h post-transfection, these Gag mutants were found diffuse in the cytoplasm, accumulating as large aggregates and only slightly at the PM (Fig. 1c-D and c-E). At 24 h, an increase in the accumulation of the Gag mutants at the PM was observed, this accumulation being more pronounced for GagΔZF1ΔZF2 (Fig. 1c-I and c-J) suggesting that the basic domains flanking the zinc fingers could play a role in the trafficking of Gag to the PM. Moreover, ring-like structures resembling giant unilamellar vesicles and possibly corresponding to the section of tubular structures (Fig. 1c-E, c-I and c-J, white arrows) were regularly observed for these Gag NC deletion mutants as described in Ref. [35].

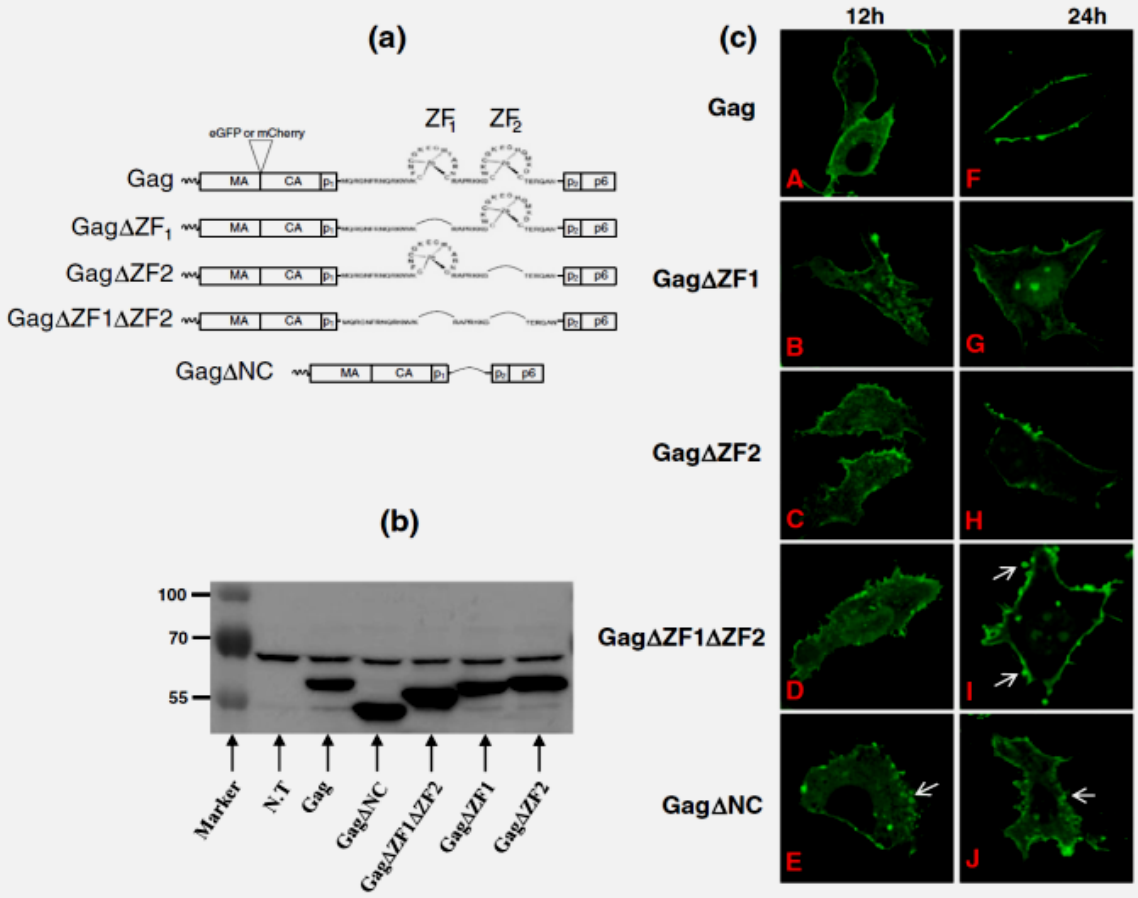

Fig. 1. Western blotting and confocal microscopy of HIV-1 Gag and Gag derivatives. (a) Sequences of HIV-1 Gag derivatives used in this study. NC is represented by its sequence while MA, CA, p1, p2 and p6 domains are shown as black boxes. Deletion of each zinc finger is symbolized by a bridge that links the flanking basic sequences. eGFP or mCherry reporter proteins are inserted upstream of CA. (b) Western blot analysis of the HIV-1 Gag derivatives used in this study. HeLa cells were transfected with 1 μg of plasmid and harvested 24 h post-transfection. A total of 30 μg protein were heat denatured, loaded on an SDS-PAGE and immunodetected using an anti-p24 Gag monoclonal antibody. The Gag derivatives had the expected molecular weights. (c) Confocal microscopy of HeLa cells expressing eGFP-labeled wt Gag, GagΔZF1, GagΔZF2, GagΔZF1ΔZF2 or GagΔNC. For each Gag derivative, HeLa cells were transfected with 0.8 μg of plasmid expressing the non-labeled Gag derivative and 0.2 μg of plasmid expressing the eGFP-labeled Gag counterpart. Cells were fixed by 1.5% of PFA, 12 h or 24 h post-transfection, and analyzed by confocal microscopy. Each panel shows the major observed phenotype. White arrows show ring-like structures likely corresponding to the section of tubular structures.

Gag oligomerization and progressive accumulation of Gag oligomers at the PM

To further analyze the intracellular Gag oligomerization, we used the FLIM technique to monitor the FRET between eGFP- and mCherry-labeled Gag proteins [43]. The eGFP was used as the donor since it exhibits a high quantum yield (0.6) and a mono-exponential fluorescence decay (2.4 ns) [44]. The mCherry was used as the acceptor since its absorption spectrum overlaps the fluorescence spectrum of eGFP, giving a large Förster R_0 distance (where the transfer efficiency is 50%) of about 54 Å [45]. FRET between eGFP and mCherry only occurs when they are less than 8 nm apart, a distance corresponding to intermolecular protein–protein interactions [46–48]. By measuring the fluorescence decay at each pixel of the cell, the FLIM technique allows extracting the fluorescence lifetime (τ) that, in contrast to fluorescence intensity, does not depend on the instrumentation or the concentration of fluorophores. FRET occurrence is associated to a shortening of the donor fluorescence lifetime. Therefore, FLIM images built up using false-color lifetime encoded pixels directly describe the spatial distribution of Gag–Gag interactions.

As controls, cells expressing eGFP (data not shown) or Gag/Gag-eGFP (ratio of 0.8:0.2) were imaged to determine the intrinsic fluorescence lifetime of Gag-eGFP at 12 h and 24 h post-transfection (Fig. 2a and b). The fluorescence decay of eGFP fused to Gag (2.31 ± 0.05 ns; Fig. 2e and f, black curves) was similar to that of free eGFP (2.39 ± 0.08 ns; data not shown), suggesting that eGFP fluorescence was not modified by its fusion to Gag or upon Gag assembly. Co-expression of free mCherry did not further change Gag-eGFP lifetime (Fig. S2a), ruling out short-range interactions between Gag-eGFP and free mCherry.

Next, cells expressing Gag/Gag-eGFP/Gag-mCherry (ratio of 0.7:0.1:0.2) were imaged by FLIM. Using a mono-exponential model to analyze the fluorescence decays in each pixel, we observed, at 12 h post-transfection, a bimodal distribution of the lifetimes with peaks centered at 1.8 ns and 2.4 ns (Fig. S2b). While the 1.8 ns evidenced the existence of FRET, the 2.4 ns peak suggested that a fraction of the Gag-eGFP proteins was monomeric or in the form of small oligomers where Gag-mCherry was absent. To take this species heterogeneity into account, we analyzed the fluorescence decays with a two components model: $F(t) = \alpha_1 e^{-t/\tau_1} + \alpha_2 e^{-t/\tau_2}$ where the long-lived lifetime τ_2 was fixed at the lifetime of free eGFP (2.4 ns), while the short component τ_1 and the populations (α_1 and α_2) associated with the two lifetimes were allowed to float. By so doing, it was possible to determine the distribution of the short component and its population thus giving access to the fraction of interacting proteins. As depicted in Fig. 2c, at 12 h post-transfection, τ_1 was homogeneously distributed all over the cell indicating that Gag oligomerization already occurred in the cytoplasm [49]. The average value of τ_1 was 1.45 ± 0.1 ns (Fig. 2e, red curve), yielding an average FRET efficiency of 41% [see Materials and Methods, Eq. (1), and Fig. 3b-A]. This strong FRET efficiency suggests that Gag molecules are closely packed in the oligomers, enabling a close proximity between the eGFP and mCherry tags. Moreover, the amplitude of the τ_1 component, that is, the fraction of Gag undergoing FRET, increased from 20% to 75% as shown by the colored gradient from the cytoplasm to the PM, indicating a spatial enrichment in the population of oligomers toward the PM. This progressive enrichment is emphasized in the enlargement of the PM region and the corresponding distribution profile of α_1 values as a function of the distance to the PM (Fig. 2g).

At 24 h post-transfection, Gag-eGFP proteins were mainly concentrated at the PM, showing a narrow distribution of their τ_1 values, with an average of 1.2 ± 0.1 ns (Fig. 2d and f, red curve). This value corresponding to a FRET efficiency of 50% was significantly different from the average value measured at 12 h post-transfection (Fig. 3b-A),

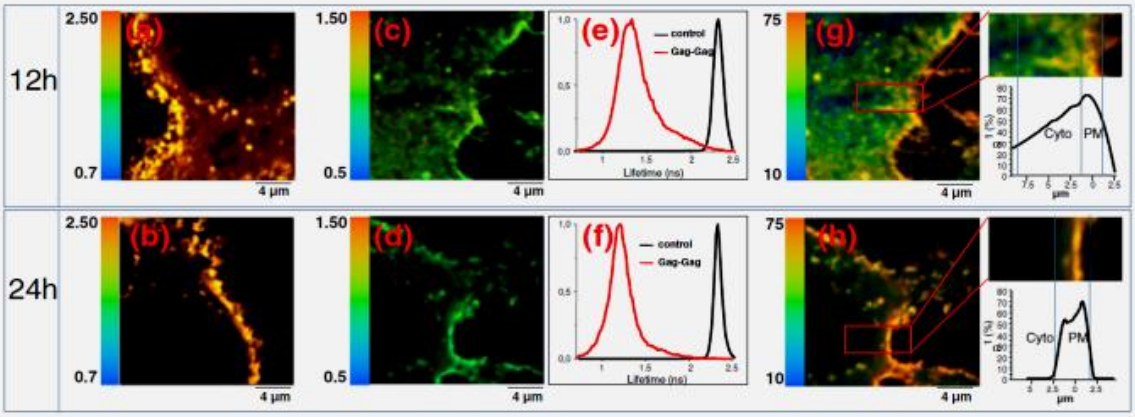

Fig. 2. HIV-1 Gag assembly monitored by FRET-FLIM. Cells were transfected with DNA constructs encoding Gag/Gag-eGFP (in a ratio 0.8:0.2) or Gag/Gag-eGFP/Gag-mCherry (in a ratio 0.7:0.1:0.2). Cells were fixed by 1.5% of PFA and analyzed by FLIM, 12 h (upper row) or 24 h (lower row) post-transfection. FLIM measurements were carried out using a 20 µm × 20 µm scale and 256 pixels × 256 pixels as settings (Nyquist–Shannon criteria). (a and b) HeLa cells expressing Gag/Gag-eGFP proteins. The fluorescence lifetime of Gag-eGFP was determined by using a single-exponential model and its value was converted into a color code, ranging from blue (0.7 ns) to red (2.5 ns). (c–h) FLIM of HeLa cells expressing Gag/Gag-eGFP/Gag-mCherry proteins using a bi-exponential model with a long-lived lifetime component τ_2 fixed to the lifetime of free eGFP (2.4 ns). (c and d) FLIM image showing the values of the short-lived lifetime τ_1 (corresponding to the Gag-eGFP proteins undergoing FRET) converted into an arbitrary color code ranging from 0.5 to 1.5 ns. (e and f) Distribution of τ_1 values, expressed in nanoseconds. (g and h) FLIM images corresponding to (c) and (d), showing the values of the amplitude α_1 of the short-lived lifetime τ_1, using a color code ranging from blue (10%) to red (75%). The insets in (g) and (h) correspond to the enlargement of the region delimited by the red rectangles, as well as the distribution of α_1 values as a function of the distance to the PM.

suggesting a further compaction of Gag oligomers with time and/or an increase in the oligomer size so that the number of acceptor molecules in close proximity to each donor increases. In addition, the homogeneous large population (up to 75%) associated with the τ_1 component (see homogeneous orange color in the enlargement panel of Fig. 2h and the gaussian distribution of α1 around the PM) showed that almost all Gag-eGFP proteins undergo FRET at the PM, as expected from the extended polymerization of Gag polyproteins required to form new viral particles [24].

Taken together, our data indicate that Gag oligomers can already form in the cytoplasm. Moreover, the spatial enrichment in the population of oligomers from the cytoplasm to the PM suggests that, during their trafficking toward the membrane, monomers or small oligomers may progressively assemble with already formed oligomers. This results in the progressive accumulation of closely packed Gag oligomers at the PM leading to the formation of new viral particles. Noticeably, bright internal dots characterized by a large τ_1 population, and thus a strong accumulation of Gag, were

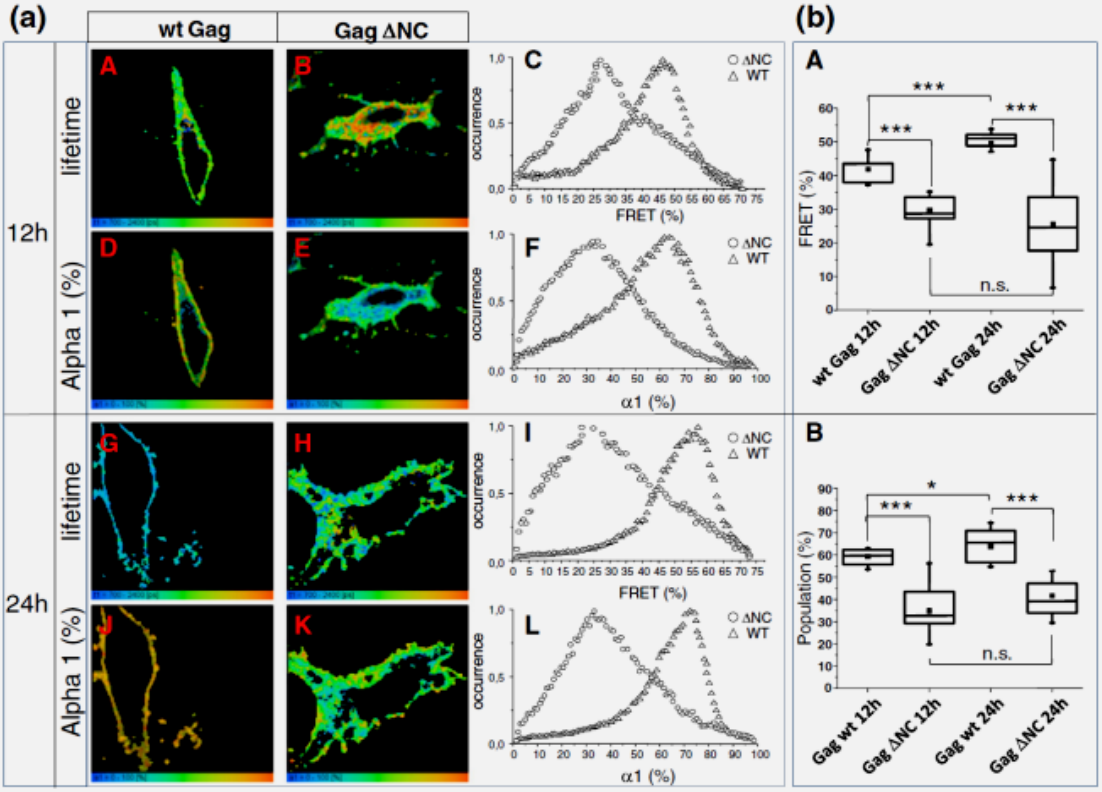

Fig. 3. Impact of NC deletion on Gag–Gag interactions as monitored by FLIM. Cells were transfected with DNA constructs encoding Gag or GagΔNC with their eGFP- and mCherry-labeled counterparts (ratio of 0.7:0.1:0.2) and analyzed by FLIM at 12 h or 24 h post-transfection. The fluorescence decays were measured in each pixel and analyzed by using a bi-exponential model with a long-lived lifetime component τ_2 fixed to the lifetime of free eGFP (2.4 ns). The τ_1 and α_1 values were converted into a color code ranging from blue (0.7 ns, 0%) to red (2.4 ns, 100%). All images were acquired using a 50 μm × 50 μm scale and 128 pixels × 128 pixels. (a) FLIM image showing the values of the short-lived lifetime τ_1 (corresponding to the Gag-eGFP proteins undergoing FRET) of representative HeLa cells expressing Gag/Gag-eGFP/Gag-mCherry (a-A) or GagΔNC/GagΔNC-eGFP/GagΔNC-mCherry (a-B) at 12 h post-transfection. (a-C) Normalized distribution of FRET efficiencies from $N = 150$ cells expressing wt Gag (triangle) or GagΔNC (circle). (a-D and a-E) FLIM images corresponding to (a-A) and (a-B), showing the values of the amplitude α_1 of the short-lived lifetime τ_1. (a-F) Normalized distribution of α_1 values from $N = 150$ cells expressing wt Gag (triangle) or GagΔNC (circle). (a-G) to (a-L) correspond to (a-A) to (a-F), but at 24 h post-transfection. (b) Box-and-whiskers plot depicting the FRET efficiency (b-A) and FRET population (b-B) of wt Gag or GagΔNC at 12 h and 24 h post-transfection. The boxes define the interquartile range that extends from the 25th to the 75th percentile, whereas the horizontal lines show the median values and square the mean. The whiskers correspond to 1.5 times the interquartile range. The FRET efficiencies and populations were calculated using the average lifetime values from at least 150 cells in three independent experiments. For the statistical analysis, a student *t*-test was performed ($^*p < 0.05$ and $^{***}p < 10^{-3}$).

observed in the cytoplasm both at 12 h and at 24 h, suggesting a local assembly of Gag proteins independently from the assembly of Gag at the PM [27].

The NC domain is required for Gag oligomerization and intracellular trafficking

In order to examine the role of the NC domain in Gag oligomerization, we transfected cells with DNA constructs expressing Gag, Gag-eGFP or Gag-mCherry proteins where the NC domain was deleted (GagΔNC). As for the wt, transfection was carried out with a mixture of plasmids expressing non-labeled GagΔNC and its eGFP- and mCherry-tagged counterparts at a ratio of 0.7:0.1:0.2. FLIM-FRET experiments were performed at 12 h (Fig. 3a-A to Fa-) and 24 h post-transfection (Fig. 3a-G to a-L). As for the native Gag, a two-exponential model was used for the analysis of the fluorescent decays at each pixel of the image, with the τ_2 value fixed at 2.4 ns.

At 12 h post-transfection, GagΔNC showed a diffuse pattern in the cytoplasm, with higher τ_1 values compared to wt Gag, as it could be seen from the warmer colors in the FLIM image for the mutant (Fig. 3a, compare a-A and a-B). As a consequence, the average FRET value was shifted from 41% for wt Gag to 29% for GagΔNC (Fig. 3a-C, triangle and circle, respectively, and Fig. 3b-A), indicating that the average distance between the fluorescent tags was larger in GagΔNC oligomers than in Gag oligomers, likely as a result of less packed oligomers. Meanwhile, the population undergoing FRET decreased from 60% for wt Gag to 32% for GagΔNC (Fig. 3a-F, triangle and circle, respectively, and Fig. 3b-B), indicating that less oligomers were formed with the Gag mutant.

Interestingly, at 24 h post-transfection, the intracellular distribution of GagΔNC (Fig. 3a-H), the average FRET value (25%; Fig. 3a-I, circle) and the population undergoing FRET (40%; Fig. 3a-L, circle) were similar to those at 12 h post-transfection (Fig. 3b-A and b-B), indicating that the initially formed GagΔNC oligomers did not evolve with time.

Thus, deletion of the NC domain of Gag strongly reduced the ability of Gag to form oligomers, also resulting in less dense oligomers. Moreover, these GagΔNC oligomers did not grow and get more compact with time, and at the same time, they did not traffic toward the PM and accumulate at the PM.

Role of the NC zinc fingers in Gag oligomerization

To delineate the role of the zinc fingers in Gag assembly, we deleted either one or both in the GagΔZF1, GagΔZF2 and GagΔZF1ΔZF2 mutants, respectively. At 12 h post-transfection, GagΔZF1 and GagΔZF2 exhibited similar τ_1 values and thus similar distribution of FRET values (Fig. 4a and b), with an average FRET value of 39% and 35%, for GagΔZF1 and GagΔZF2, respectively (Fig. 5a, compare triangles with magenta and green curves). The average FRET value of both mutants was similar to that of the wt Gag (Fig. 5b, compare black, magenta and green box-and-whiskers plots) although a broader distribution of values could be noted for the mutants. Thus, deletion of one NC finger did not prevent the formation of tightly packed oligomers but provided more heterogeneous populations of these oligomers. In contrast, a strong decrease of Gag oligomers undergoing FRET was observed with a drop from 60% for the wt Gag to 40% for the two mutants (Fig. 5c and d), suggesting that the formation of oligomers was less efficient with the two Gag zinc finger mutants at early expression time. At 24 h post-transfection, a significant increase of the FRET efficiency was observed for GagΔZF1 (46%; Fig. 5e, magenta line, and Fig. 5f, magenta box), giving an average FRET value similar to that of wt Gag (Fig. 5e, triangles; Fig. 5f, black box). However, even though an increase of the average FRET value was noticed for GagΔZF2 between 12 and 24 h (43%), this value remained significantly below that of the wt Gag at 24 h (Fig. 5e and f, green line and box). Thus, deletion of the distal but not the proximal zinc finger significantly altered the ability of Gag to form closely packed oligomers or decreased the size of the oligomers so that less mCherry acceptor molecules could decrease the lifetime of the eGFP donor molecules. The increase in FRET efficiency for these two NC mutants at 24 h was accompanied by a strong increase in the population of oligomers undergoing FRET, an average value of 52% being reached for both mutants (Fig. 5g and h, green and magenta lines and boxes). Nevertheless, this value was significantly below 65% obtained for wt Gag (Fig. 5h), indicating that deletion of one zinc finger did not prevent Gag oligomerization but reduced its efficiency so that Gag assembly at the PM was delayed. Taken together, our data with the two zinc finger mutants revealed that each mutant has a much lower impact on Gag oligomerization than GagΔNC, indicating that the two fingers are somewhat redundant. Nevertheless, the impact on Gag assembly was somewhat stronger when the distal zinc finger was deleted as compared to the proximal finger, suggesting that the former plays a more important role in the assembly process.

For the GagΔZF1ΔZF2 mutant, where both zinc fingers have been deleted, the average FRET values (29% and 34% ,respectively, for 12 and 24 h) and the population associated with the oligomers undergoing FRET (31% and 34%, respectively, for 12 h and 24 h) were found to be similar to those obtained with the GagΔNC mutant (Fig. 4c, f, i and l and Fig. 5, compare circles and dark blue curves and box plots). Moreover, it was interesting to note that, in contrast to GagΔZF1 or GagΔZF2, these values did not change between 12 h and 24 h post-transfection.

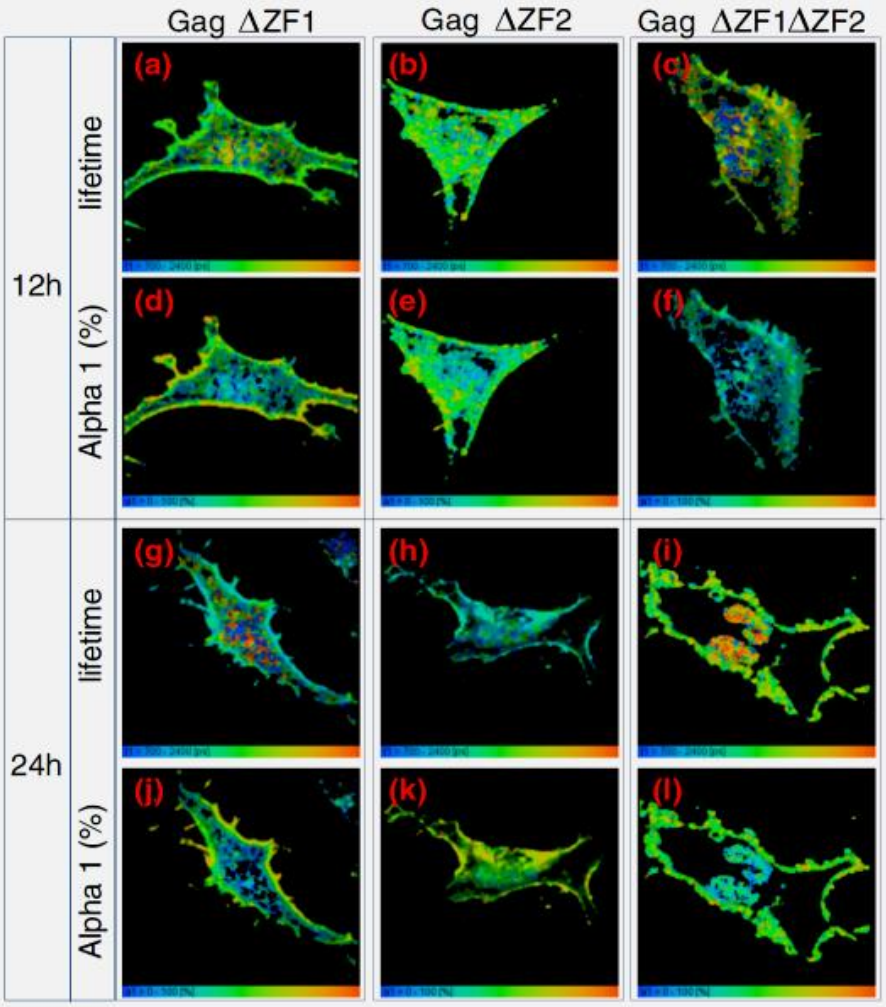

Fig. 4. Impact of zinc finger deletion on Gag–Gag interactions, as monitored by FLIM. Cells were transfected with DNA constructs encoding GagΔZF1, GagΔZF2 and GagΔZF1ΔZF2 with their eGFP- and mCherry-labeled counterparts (ratio of 0.7:0.1:0.2) and analyzed by FLIM at 12 h or 24 h post-transfection. The fluorescence decays were measured and analyzed, as described in Fig. 3. The τ_1 and α_1 values were converted into a color code, as described in Fig. 3. All images were acquired using a 50 μm × 50 μm scale and 128 pixels × 128 pixels. (a–f) FLIM image showing the values of the short-lived lifetime τ_1 (a–c) and its amplitude (d–f) of representative HeLa cells expressing GagΔZF1/GagΔZF1-eGFP/GagΔZF1-mCherry (a and d), GagΔZF2/GagΔZF2-eGFP/GagΔZF2-mCherry (b and e) and GagΔZF1ΔZF2/GagΔZF1ΔZF2-eGFP/GagΔZF1ΔZF2-mCherry (c and f). (g) to (l) correspond to (a) to (f), but at 24 h post-transfection.

Thus, deletion of both NC zinc fingers caused a strong reduction in the ability of Gag to form closely packed oligomers, showing that the fingers are critical for this activity.

Taken together, our data show that both zinc fingers play a critical role in Gag oligomerization, notably in the formation of the highly packed oligomers that are required for the efficient and rapid assembly of Gag at the PM. The two zinc fingers show a certain level of redundancy but do not seem equivalent, with a somewhat more important role for the distal finger.

NC zinc fingers are necessary for the rapid formation of Gag aggregates

To confirm the role of the NC zinc fingers in the kinetics of Gag oligomerization, we performed time-lapse microscopy experiments to monitor Gag assembly early after its synthesis. To that end, we microinjected plasmids encoding the different eGFP-tagged Gag constructs into the nuclei of HeLa cells. Subsequently, eGFP fluorescence was monitored every 2 min by time-lapse microscopy to monitor Gag accumulation in the cytoplasm. Time zero was defined

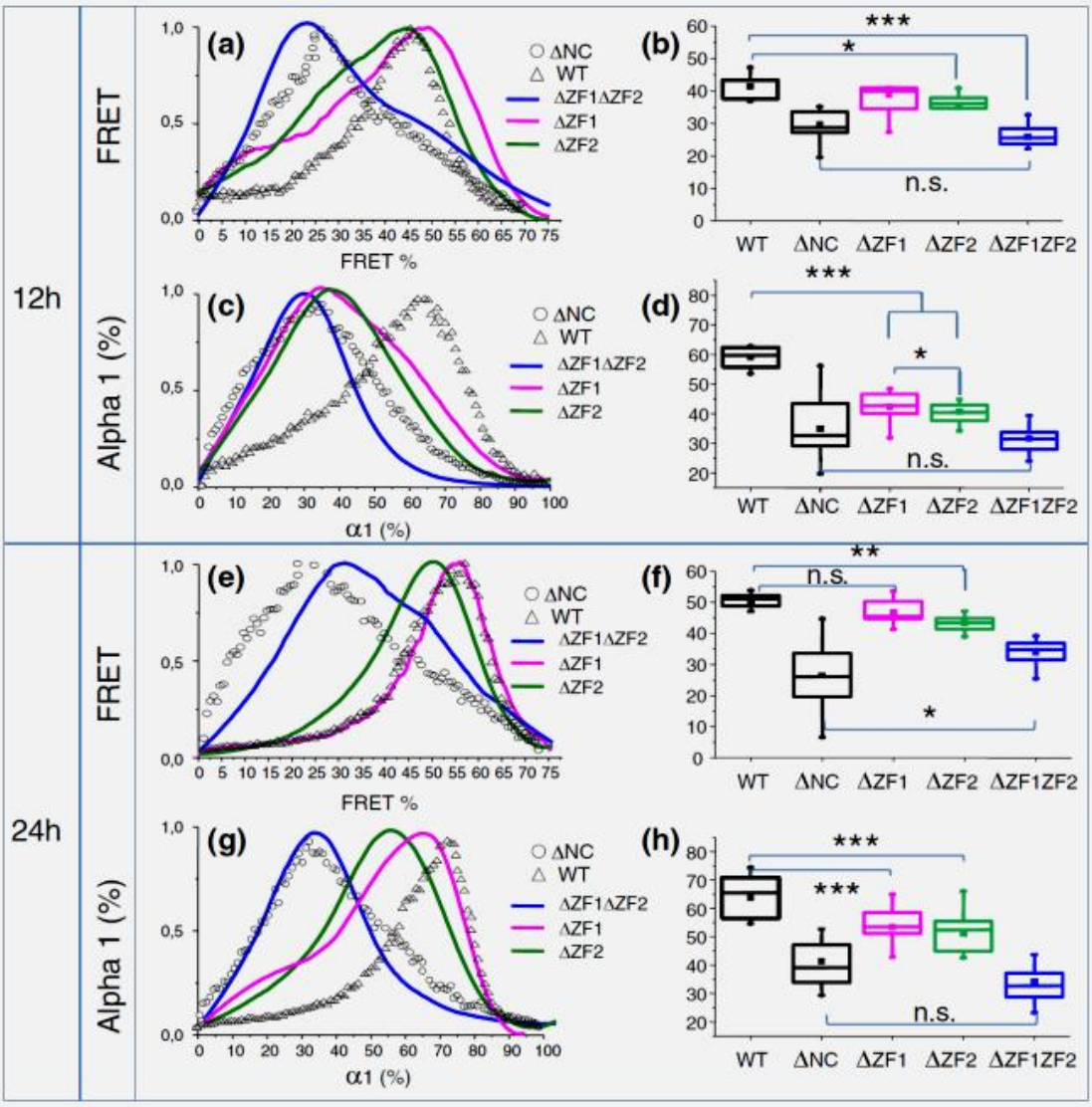

Fig. 5. Distribution of FRET efficiencies and populations for the Gag NC mutants. Distribution of the FRET efficiencies (a and e) and populations (c and g) for wt Gag (triangles), GagΔNC (circles), GagΔZF1 (magenta), GagΔZF2 (green) and GagΔZF1ΔZF2 (blue) at 12 h (a and c) and 24 h (e and g) post-transfection. The FRET efficiencies and populations were determined for at least 150 cells in three independent experiments, as described in Fig. 3. Box-and-whiskers plots of the FRET efficiencies (b and f) and populations (d and h) at 12 h (b and d) and 24 h (f and h) post-transfection. The box-and-whiskers plots are shown as in Fig. 3. Student tests were performed to compare the FRET efficiencies and populations (*$p < 0.05$ and ***$p < 10^{-3}$).

as the time where the Gag fluorescence signal appeared in the cytoplasm, above the fluorescent background (typically 30–60 min after microinjection). A progressive fluorescence increase was then observed until the first Gag aggregates were observed (Fig. 6, arrows and insets). Interestingly, a remarkably constant time of about 20 min was observed for the wt Gag between the initial detection of eGFP fluorescence and the first detectable Gag aggregates at or close to the PM (Fig. 6a and b). This delay that will be referred to as the "assembly time" was then used as an indicator for the efficiency of Gag particle formation. We next examined the effects of deleting the zinc fingers on the kinetics of Gag assembly. Expression of GagΔZF1, GagΔZF2 or GagΔZF1ΔZF2 mutants resulted in a significant delay in the assembly time as compared to wt Gag (34, 42 and 38 min, respectively; Fig. 6b). This confirmed the role of both

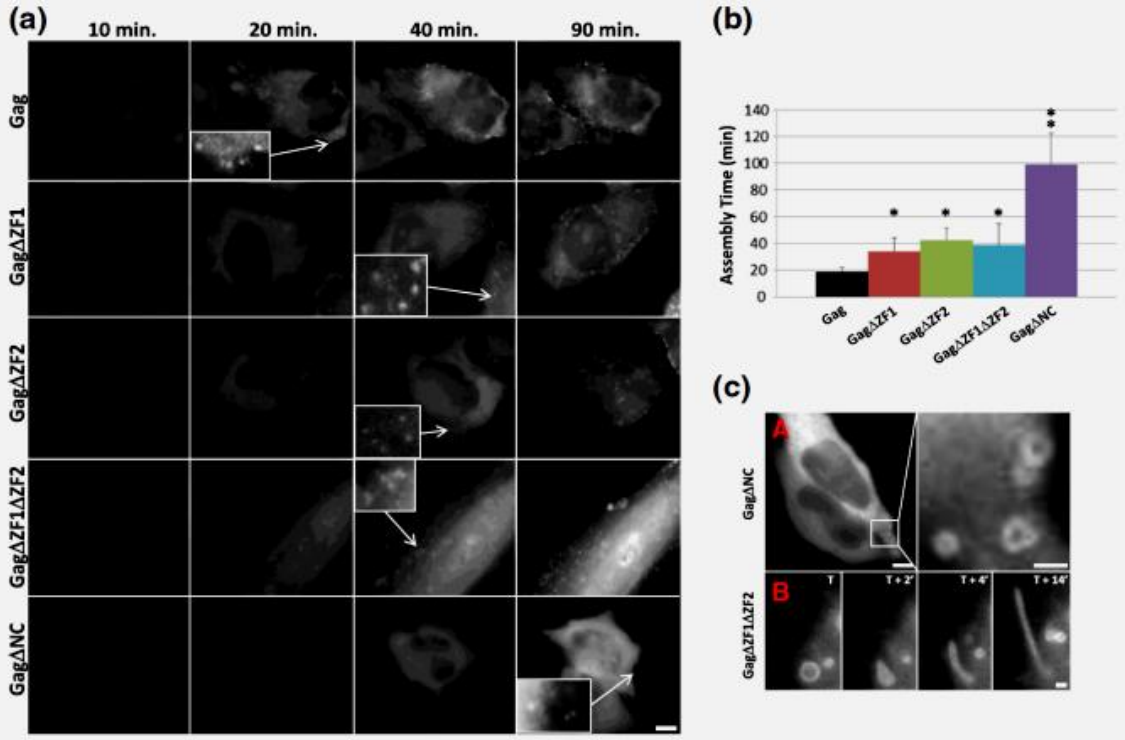

Fig. 6. Role of the NC domain in the kinetics of Gag assembly. (a) Time-lapse microscopy of cells microinjected in the nucleus with DNA encoding for wt Gag/Gag-eGFP (ratio of 0.8:0.2) or Gag mutants with their eGFP-labeled counterpart (ratio of 0.8:0.2). Each column displays cells at the indicated time after appearance of the initial eGFP emission. Insets represent magnified cell regions displaying Gag aggregates at the PM. Scale bars represent 5 μm. (b) Mean assembly time for the various Gag derivatives. This parameter describes the average delay between the appearance of the initial eGFP signal and the detection of the first Gag aggregates at or close to the PM. With the use of ANOVA associated to Tukey's multiple comparison tests, significant differences ($p < 0.05$) were observed between wt Gag (19 ± 3 min, $n = 29$) and GagΔZF1 (35 ± 10 min, $n = 30$), GagΔZF2 (42 ± 9 min, $n = 18$), GagΔZF1ZF2 (40 ± 15 min, $n = 18$) and GagΔNC (100 ± 20 min, $n = 20$). For cells expressing GagΔNC, Gag particles were only observed in 16 out of 20 cells within the time frame of the experiment (180 min). (c) Representative examples of ring-like and tubular structures in cells expressing GagΔNC (top panels) and GagΔZF1ZF2 (bottom panels). The time increment (min) during the progression of the tubular extension is indicated. Scale bars represent 5 μm (upper left panel) and 1 μm (other panels).

NC zinc fingers in the efficient assembly of Gag at or close to the PM. Interestingly, the complete deletion of NC caused a far more important delay in Gag assembly (about 100 min), highlighting the role of the basic domains of NC in the assembly process by comparing it with the GagΔZF1ΔZF2 mutant. With GagΔNC, 20% of the transfected cells did not show any Gag aggregates at or close to the PM within the time frame of the experiment (3 h). Noticeably, some Gag aggregates were observed to adopt ring-like structures in cells expressing GagΔNC mutants (Fig. 6c-A and inset) and GagΔZF1ΔZF2. These rings of 0.6–1.5 μm in diameter may represent cross-sections of growing tubular structures as shown for GagΔZF1ZF2 (Fig. 6c-B).

In conclusion, the kinetics of Gag assembly relies, at least in part, on the NC domain suggesting a role in Gag trafficking from the cytoplasm to the PM.

Discussion

The HIV-1 Gag polyprotein is a key player in virus assembly due to its ability to form oligomers in the cytoplasm [5,16,22,23] and at the PM [11,12,41,50]. In this study, Gag assembly was visualized by the FLIM-FRET methodology that monitors at each pixel the fluorescence lifetime of eGFP used as a FRET donor. Since the fluorescence lifetime does not depend on the instrumentation or the local concentration of the fluorescent molecules [51,52], this methodology is more straightforward than the fluorescence-intensity-based methods that were previously used to monitor Gag assembly [19–22,42]. Furthermore, through a two-exponential analysis, the FLIM-FRET approach provided the unique possibility to discriminate Gag monomers or small oligomers from larger Gag oligomers and to monitor their

spatiotemporal distribution in cells. By so doing, we found that, at 12 h post-transfection (Fig. 2c and d), compact Gag oligomers can already form in the cytoplasm and do not undergo important structural changes at the PM. However, our data do not allow discriminating between the bent and extended conformations of Gag proteins [3,53], since closely packed oligomers may likely form with both conformations.

Moreover, from the amplitudes associated to the short-lived lifetime, a clear gradient from the inner to the periphery of the cell was perceived (Fig. 2g), indicating that Gag monomers progressively assemble into oligomers during their traffic toward the membrane. As a result of this progressive assembly and traffic, the Gag oligomers accumulate at the PM so that, at 24 h post-transfection, nearly all Gag proteins are assembled at the PM. Moreover, the further decrease in the short-lived lifetime value at 24 h as compared to 12 h suggested a further compaction of Gag proteins at the PM with time and/or an increase in the size of the Gag ensembles at the PM.

Since Gag molecules were reported to be arranged in hexameric lattices in immature virus particles [54,55], we next checked whether the FRET efficiency values observed at 24 h at the PM were consistent with this structural model, by comparing them with the theoretical FRET value calculated from the structural model. Since the fluorescent proteins are localized upstream of the N-terminus of CA (CA-NTD), we focused on the structure of the Gag lattice at this level. In the Gag lattice, each CA-NTD domain interacts with five neighboring other ones (magenta ribbons in Fig. 7a and magenta dots in Fig. 7b) [56] at a distance of 43.4 Å from its two closest neighbors in the same hexamer and of 22–23 Å from the closest neighbors in the surrounding hexamers (Fig. 7b). Four additional CA-NTD domains (Fig. 7b, blue circles) are at a distance (50–65 Å) compatible with FRET. All other CA-NTD domains being at more than 80 Å (Fig. 7a, gray ribbons; Fig. 7b, gray dots) will minimally contribute to the FRET efficiency and thus are not taken into account in the calculations. Assuming a minimum inter-dye distance of 40 Å, as

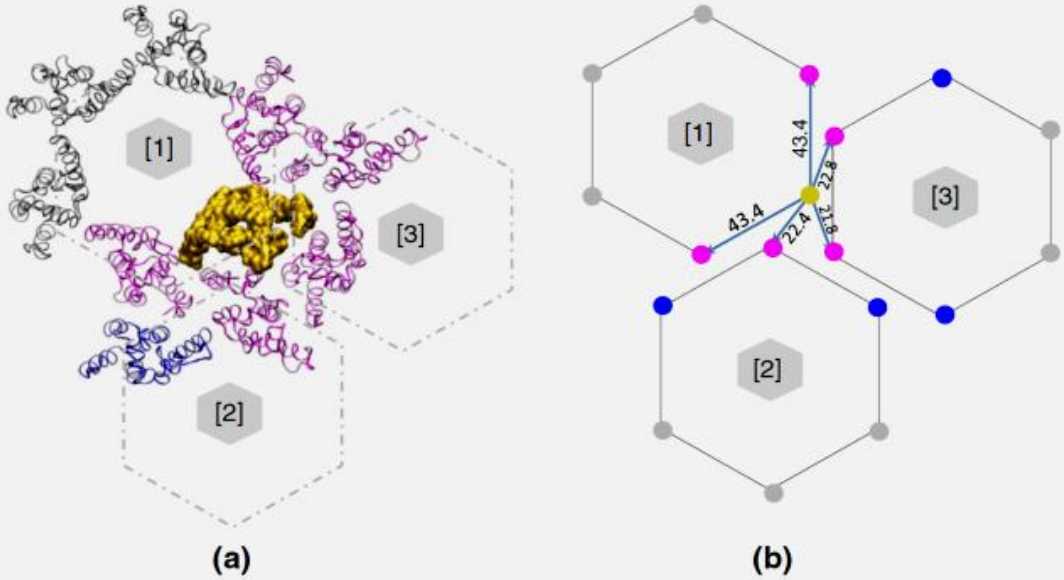

Fig. 7. Structural model for predicting the FRET efficiencies between fluorescent Gag proteins at the PM. (a) Three-dimensional structure of the N-terminal part of the CA domain (CA-NTD) from PDB ID 4USN [56]. This part of Gag was selected because the eGFP and mCherry labels were inserted upstream CA-NTD. This view is from the top of the CA-NTD domain and shows the hexagonal arrangement of the Gag lattice. To calculate the theoretical FRET efficiency from this structural model, we selected one of the CA-NTD domain of the hexameric unit [1] (gold surface). The CA-NTD domains of the hexameric units [1], [2] and [3], interacting with the selected CA-NTD, are in magenta. The other CA-NTD domains located at a distance compatible with FRET are in blue and the CA-NTD domains too far from the domain in gold to provide significant FRET are in gray. (b) Scheme of the three hexameric structures. Distances between the N-terminal Met142 residue of the CA-NTD domain in gold and the corresponding residues of the closest CA-NTD domains (magenta) are indicated. Distances between the gold and blue dots vary from 50 to 65 Å. We indicated 6-fold symmetry axes by gray hexagons.

a consequence of the size of the fluorescent proteins [57], and resampling Gag-eGFP, Gag-mCherry and wt Gag positions according to their respective concentrations (10%, 20% and 70%, respectively), we found an average FRET efficiency of 52%, using Eq. (1) and the distances given in Fig. 7b. This FRET efficiency calculated from the structural model is in excellent agreement with the measured FRET efficiency (50%), reflecting that the Gag organization measured by FLIM-FRET at 24 h at the PM closely matches that in immature viral particles.

Both Gag oligomerization and accumulation at the PM were largely altered by deleting the NC domain or its two zinc fingers (Figs. 3 and 4), confirming the key role of NC in Gag assembly [6,58–60] and accumulation at the PM [9,42,61]. As NC deletion strongly reduces the binding of Gag to nucleic acids [62], the key role of NC in Gag assembly is likely related to its ability to form with nucleic acids a scaffold for Gag oligomerization. This NC-induced scaffolding is instrumental for the Gag proteins to pack closely together and bind efficiently to the PM. The residual FRET observed with both GagΔNC and GagΔZF1ΔZF2 mutants all over the cell suggests that these Gag mutants likely oligomerize as a result of CA–CA interactions [28] with some possible contribution of MA–RNA interaction (for a recent review, see Ref. [63]) but are unable to form compact Gag oligomers. Moreover, as these highly packed Gag oligomers are already observed in the cytoplasm 12 h after transfection with wt Gag, nucleic acid binding to Gag may start shortly after Gag expression and may constitute thus an early step in viral assembly. The distal zinc finger was found to be more important than the proximal one in bringing Gag molecules in close proximity on the nucleic acid platform (Fig. 5a and e). Since the NC domain of Gag was recently suggested to electrostatically interact with negatively charged phospholipids in the initial step of Gag binding to the PM [64], this may additionally explain the poor binding of the GagΔNC mutant to the PM. Moreover, the more extended binding of the GagΔZF1ΔZF2 mutant as compared to GagΔNC at the PM (Figs. 3 and 4) is inline with the contribution of the basic domains of NC in Gag binding to the PM [34,65,66]. Finally, the large amount of viral particles (Fig. 6a) together with the high FRET efficiencies (Fig. 4g and h) observed for GagΔZF1 and GagΔZF2 at the PM indicate that proper binding of Gag to the PM can be achieved when the basic domains and one of the two zinc fingers of NC are present.

NC also contributes to the rapid trafficking of the Gag oligomers to the membrane as shown by the major difference between GagΔNC and wt Gag (Fig. 6b). This probably results from the loss of the NC-mediated interactions of Gag with cytoskeleton proteins (actin/tubulin) [67,68] and cellular motor proteins such as KIF4 [69], which are required for Gag trafficking. Interestingly, a much smaller delay in Gag assembly was observed with the GagΔZF1ΔZF2, GagΔZF1 and GagΔZF2 mutants (Fig. 6b), suggesting that the interactions of Gag with the cellular partners involved in Gag trafficking are mediated through both the zinc fingers and the flanking basic sequences.

In conclusion, our data clearly indicate that Gag proteins form compact oligomers in the cytoplasm, likely as a result of both CA–CA interactions and NC-promoted binding to nucleic acids. The oligomers progressively assemble and thus likely grow in size by trafficking from the cytoplasm toward the membrane, but with no dramatic changes in their compact arrangement. The NC domain also favors the binding of Gag oligomers to the PM and the proper timing of viral particle assembly at the PM, likely as a result of its interaction with cell proteins involved in Gag trafficking. While the proximal zinc finger appears dispensable for oligomer compaction and membrane binding, the distal finger and the flanking basic domains appear critical for these properties. Finally, the full NC sequence appears important for the proper timing of Gag assembly.

Materials and Methods

Plasmid DNA

The human-codon-optimized $Pr55^{Gag}$ encoding plasmid and pNL4-3^{EGFP} were kindly provided by David E. Ott (National Cancer Institute at Frederick, Maryland) and B. Muller (Abteilung Virologie, Universitatklinikum Heidelberg, Germany), respectively [23,36,39,70]. This latter plasmid was used to PCR amplify the sequence encoding for Gag-eGFP. The DNA product was inserted in pcDNA under the control of the CMV promoter and eGFP was substituted for mCherry by PCR. Juncture sequences surrounding eGFP are 5′ ccggcaacagcagccagggatcc-MA/eGFP-atggt//caaggaatt-eGFP/MA-gtgagccagaac-taccccatcgtgcagaacctgcagggccag-MA/CA-atggtgcac caggccatcagccccgcacc 3′. Juncture sequences surrounding mCherry are as follows: 5′ agccagggatcc-MA/mCherry-atggt gag//gaattc-mCherry/MA-gtgagccagaactaccccatcgtgca gaacctgcagggccag-MA/CA-atggtgcacca 3′. GagΔZF1, GagΔZF2, GagΔZF1ΔZF2 and GagΔNC (Fig. 1a) deletion mutants were constructed by PCR-based site-directed mutagenesis following the supplier's protocol using Gag-eGFP, Gag-mCherry or Gag as substrate (Stratagene). The integrity of all plasmid constructs was assessed by DNA sequencing.

Cell culture and plasmid transfection

We cultured 10^5 HeLa cells (from American Type Culture Collection, reference CCL-2 Amp, HeLa; cervical adenocarcinoma; human) in 6-well plates containing an 18-mm coverslips (μ-Dish IBIDI; Biovalley, France) in Dulbecco's modified Eagle's medium supplemented with 10% fetal calf serum (Invitrogen Corporation, Cergy Pontoise, France) and 1% of an antibiotic mixture (penicillin/streptomycin; Invitrogen Corporation) at 37 °C in a 5% CO_2 atmosphere. HeLa

cells were transfected using jetPEI™ (Life Technologies, Saint Aubin, France) with a mixture of plasmids coding for Gag-eGFP, Gag-mCH and wt Gag at the ratios indicated in the text. These conditions allowed the production of infectious particles [36].

Western blotting

We treated 5×10^5 HeLa cells transfected with 1 μg of plasmid DNA expressing Gag or Gag derivatives with trypsin and resuspended them in ice-cold lysis buffer [1% Triton X-100, 100 mM NaF, 10 mM NaPPi and 1 mM Na_3VO_4 in PBS (phosphate-buffered saline) supplemented with a complete anti-protease cocktail from Roche, Meylan, France]. After sonication and centrifugation, protein concentration was assessed by a Bradford assay (Xenius, Safas, Monaco). We reduced 30 μg of total proteins with 10 mM DTT containing loading buffer (Laemmli, Bio-Rad), heat denatured and electrophoresed on 12% SDS-PAGE gel. Subsequently, proteins were transferred onto a polyvinylidene difluoride membrane (Amersham, Orsay, France) and blots were probed with mouse monoclonal antibody anti-CAp24 Gag (reference 6521 #24-4; AIDS Reagent Program, Division of AIDS, National Institute of Allergy and Infectious Diseases, National Institutes of Health, from Dr. Michael H. Malim) or anti-eGFP (Proteintech, reference 66002-1) or rabbit polyclonal anti-mCherry (GeneTex, reference GTX59788). After several washings, secondary anti-mouse or anti-rabbit antibodies conjugated to the horseradish peroxidase were added to the membrane and proteins were visualized by the chemiluminescent ECL system (Amersham) on a LAS 4000 apparatus.

Confocal microscopy

At 12 h and 24 h post-transfection, the cells were extensively washed, fixed with a 1.5% paraformaldehyde/PBS (pH 7.4) solution and kept in PBS at 4 °C until observation with a Leica SPE equipped with a 63× 1.4NA oil immersion objective (HXC PL APO 63×/1.40 OIL CS). The eGFP images were obtained by scanning the cells with a 488-nm laser line and a 500- to 555-nm band-pass for emission. For the mCherry images, a 561-nm laser line was used with a 570- to 625-nm band-pass.

Fluorescence lifetime imaging microscopy

The experimental setup for FLIM measurements was as previously described [70]. Briefly, time-correlated single-photon counting FLIM measurements were performed on a homemade two-photon excitation scanning microscope based on an Olympus IX70 inverted microscope with an Olympus 60× 1.2NA water immersion objective operating in the descanned fluorescence collection mode [71,72]. Two-photon excitation at 900 nm was provided by a mode-locked titanium-sapphire laser (Tsunami; Spectra Physics) or an Insight DeepSee (Spectra Physics) laser. Photons were collected using a set of two filters: a short pass filter with a cutoff wavelength of 680 nm (F75-680; AHF, Germany) and a band-pass filter of 520 ± 17 nm (F37-520; AHF, Germany). The fluorescence was directed to a fiber-coupled APD (SPCM-AQR-14-FC; Perkin Elmer), which was connected to a time-correlated single-photon counting module (SPC830; Becker & Hickl, Germany). Typically, the samples were continuously scanned for about 60 s to achieve the appropriate photon statistics in order to investigate the fluorescence decays. Moreover, to reach the Nyquist–Shannon sampling criteria, we carried out FLIM measurements using 20 μm × 20 μm scale and 256 pixels × 256 pixels. Data were analyzed using a commercial software package (SPCImage v2.8; Becker & Hickl, Germany).

For FRET experiments with eGFP, the FRET efficiency (E) was calculated according to:

$$E = 1 - \frac{\tau_{DA}}{\tau_D} = \frac{1}{1 + (R/R_0)^6} \quad (1)$$

where τ_{DA} is the lifetime of the donor in the presence of the acceptor and τ_D is the lifetime of the donor in the absence of the acceptor, R is the distance between donor and acceptor and R_0 is the Förster distance.

Prediction of the FRET efficiencies

The inter-CA-NTD distances were calculated from the 4USN structure using the Visual Molecular dynamics software[†] [56]. Distances refer to the space separating the two N-terminal α-carbon atoms (methionine residues) of a CA-NTD pair. Estimations of the theoretical fluorescence lifetime were calculated using R statistical software version 3.0.1[‡]. Fluorophores positions were resampled 10^5 times. Fluorescence lifetime of eGFP in the presence of n acceptors was defined as $1/[(1/\tau) + \Sigma k_i \tau_i]$ in which τ is the fluorescence lifetime of eGFP and k_t is the transfer rate defined for a given distance. The average lifetime was calculated as the sum of the different lifetimes weighted by their frequency of occurrence.

Plasmid DNA microinjection

For microinjection experiments, subconfluent HeLa cells plated on glass coverslips were mounted in a Ludin Chamber (Life Imaging Services, Basel, Switzerland). The cells were then placed on a Leica DMIRE2 microscope equipped with a control system of 37 °C, 5% CO_2 (Life Imaging Services). The abovementioned plasmids encoding for the different Gag constructs (a mixture of 75% Gag/25% Gag-eGFP) were microinjected into the nucleus at 0.1 μg/μL, along with a fluorescent microinjection reporter solution (0.5 μg/μL rhodamine dextran; Invitrogen), using a Femtojet/InjectMan NI2 microinjector (Eppendorf). The coordinates of several microinjected cells were memorized using a Märzhäuser (Wetzlar, Germany) automated stage piloted by the Leica FW4000 software. Images were then acquired with a 100× HCX PL APO (1.4 NA) objective every 2 min during 3 h using a Leica DC350FX CCD camera piloted by the FW4000 software. Time-lapse movies were then analyzed using the MetaMorph (Molecular Devices, Sunnyvale, USA) and ImageJ (National Institutes of Health, USA) softwares to determine the first time at which the GFP signal appears, as well as that at which Gag aggregates appear at or close to the PM.

Supplementary data to this article can be found online at http://dx.doi.org/10.1016/j.jmb.2015.01.015.

Acknowledgments

This work was supported by the European Project THINPAD "Targeting the HIV-1 Nucleocapsid Protein to Fight Antiretroviral Drug Resistance" (FP7 Grant Agreement 601969), French ANRS (National Agency for AIDS Research) and Sidaction. We thank the AIDS Reagent Program for providing anti-Gag (reference 6521 #24-4), Romain Vauchelles and Philippe Carl for technical support and Edouard Troesch for recombinant plasmid DNAs.

Received 9 December 2014;
Received in revised form 26 January 2015;
Accepted 27 January 2015
Available online 30 January 2015

Keywords:
FRET-FLIM;
HIV-1;
Gag;
oligomer;
NC

†http://www.pdb.org.
‡http://www.R-project.org/.

Abbreviations used:
FRET, Förster resonance energy transfer; FLIM, fluorescence lifetime imaging microscopy; HIV-1, human immunodeficiency virus type 1; PM, plasma membrane; wt, wild type.

References

[1] Summers MF, Karn J. Special issue: structural and molecular biology of HIV. J Mol Biol 2011;410:489–90.
[2] Sundquist WI, Krausslich HG. HIV-1 assembly, budding, and maturation. Cold Spring Harbor Perspect Med 2012;2: a006924.
[3] O'Carroll IP, Soheilian F, Kamata A, Nagashima K, Rein A. Elements in HIV-1 Gag contributing to virus particle assembly. Virus Res 2013;171:341–5.
[4] Fogarty KH, Chen Y, Grigsby IF, Macdonald PJ, Smith EM, Johnson JL, et al. Characterization of cytoplasmic Gag-Gag interactions by dual-color z-scan fluorescence fluctuation spectroscopy. Biophys J 2011;100:1587–95.
[5] Kutluay SB, Bieniasz PD. Analysis of the initiating events in HIV-1 particle assembly and genome packaging. PLoS Pathog 2010;6:e1001200.
[6] Ott DE, Coren LV, Shatzer T. The nucleocapsid region of human immunodeficiency virus type 1 Gag assists in the coordination of assembly and Gag processing: role for RNA-Gag binding in the early stages of assembly. J Virol 2009;83: 7718–27.
[7] Saad JS, Miller J, Tai J, Kim A, Ghanam RH, Summers MF. Structural basis for targeting HIV-1 Gag proteins to the plasma membrane for virus assembly. Proc Natl Acad Sci U S A 2006;103:11364–9.
[8] Ono A, Ablan SD, Lockett SJ, Nagashima K, Freed EO. Phosphatidylinositol (4,5) bisphosphate regulates HIV-1 Gag targeting to the plasma membrane. Proc Natl Acad Sci U S A 2004;101:14889–94.
[9] Li H, Dou J, Ding L, Spearman P. Myristoylation is required for human immunodeficiency virus type 1 Gag–Gag multimerization in mammalian cells. J Virol 2007;81:12899–910.
[10] Lindwasser OW, Resh MD. Multimerization of human immunodeficiency virus type 1 Gag promotes its localization to barges, raft-like membrane microdomains. J Virol 2001;75: 7913–24.
[11] Jouvenet N, Bieniasz PD, Simon SM. Imaging the biogenesis of individual HIV-1 virions in live cells. Nature 2008;454: 236–40.
[12] Ivanchenko S, Godinez WJ, Lampe M, Krausslich HG, Eils R, Rohr K, et al. Dynamics of HIV-1 assembly and release. PLoS Pathog 2009;5:e1000652.
[13] Neil SJ, Eastman SW, Jouvenet N, Bieniasz PD. HIV-1 Vpu promotes release and prevents endocytosis of nascent retrovirus particles from the plasma membrane. PLoS Pathog 2006;2:e39.
[14] Welsch S, Keppler OT, Habermann A, Allespach I, Krijnse-Locker J, Krausslich HG. HIV-1 buds predominantly at the plasma membrane of primary human macrophages. PLoS Pathog 2007;3:e36.
[15] Perlman M, Resh MD. Identification of an intracellular trafficking and assembly pathway for HIV-1 gag. Traffic 2006;7:731–45.
[16] Grigorov B, Arcanger F, Roingeard P, Darlix JL, Muriaux D. Assembly of infectious HIV-1 in human epithelial and T-lymphoblastic cell lines. J Mol Biol 2006;359:848–62.
[17] Lehmann M, Milev MP, Abrahamyan L, Yao XJ, Pante N, Mouland AJ. Intracellular transport of human immunodeficiency virus type 1 genomic RNA and viral production are dependent on dynein motor function and late endosome positioning. J Biol Chem 2009;284:14572–85.
[18] Joshi A, Ablan SD, Soheilian F, Nagashima K, Freed EO. Evidence that productive human immunodeficiency virus type 1 assembly can occur in an intracellular compartment. J Virol 2009;83:5375–87.
[19] Larson DR, Ma YM, Vogt VM, Webb WW. Direct measurement of Gag–Gag interaction during retrovirus assembly with FRET and fluorescence correlation spectroscopy. J Cell Biol 2003;162:1233–44.
[20] Hubner W, Chen P, Del Portillo A, Liu Y, Gordon RE, Chen BK. Sequence of human immunodeficiency virus type 1 (HIV-1) Gag localization and oligomerization monitored with live confocal imaging of a replication-competent, fluorescently tagged HIV-1. J Virol 2007;81:12596–607.
[21] Hogue IB, Hoppe A, Ono A. Quantitative fluorescence resonance energy transfer microscopy analysis of the human immunodeficiency virus type 1 Gag–Gag interaction: relative contributions of the CA and NC domains and membrane binding. J Virol 2009;83:7322–36.
[22] Derdowski A, Ding L, Spearman P. A novel fluorescence resonance energy transfer assay demonstrates that the human immunodeficiency virus type 1 Pr55Gag I domain mediates Gag–Gag interactions. J Virol 2004;78:1230–42.
[23] Fritz JV, Dujardin D, Godet J, Didier P, De Mey J, Darlix JL, et al. HIV-1 Vpr oligomerization but not that of Gag directs the interaction between Vpr and Gag. J Virol 2010;84:1585–96.
[24] Adamson CS, Freed EO. Human immunodeficiency virus type 1 assembly, release, and maturation. Adv Pharmacol 2007;55: 347–87.

[25] Ono A, Demirov D, Freed EO. Relationship between human immunodeficiency virus type 1 Gag multimerization and membrane binding. J Virol 2000;74:5142–50.
[26] Hill CP, Worthylake D, Bancroft DP, Christensen AM, Sundquist WI. Crystal structures of the trimeric human immunodeficiency virus type 1 matrix protein: implications for membrane association and assembly. Proc Natl Acad Sci U S A 1996;93:3099–104.
[27] Balasubramaniam M, Freed EO. New insights into HIV assembly and trafficking. Physiology (Bethesda) 2011;26:236–51.
[28] Briggs JA, Krausslich HG. The molecular architecture of HIV. J Mol Biol 2011;410:491–500.
[29] Datta SA, Temeselew LG, Crist RM, Soheilian F, Kamata A, Mirro J, et al. On the role of the SP1 domain in HIV-1 particle assembly: a molecular switch? J Virol 2011;85:4111–21.
[30] Morellet N, Druillennec S, Lenoir C, Bouaziz S, Roques BP. Helical structure determined by NMR of the HIV-1 (345-392) Gag sequence, surrounding p2: implications for particle assembly and RNA packaging. Protein Sci 2005;14:375–86.
[31] Bharat TA, Castillo Menendez LR, Hagen WJ, Lux V, Igonet S, Schorb M, et al. Cryo-electron microscopy of tubular arrays of HIV-1 Gag resolves structures essential for immature virus assembly. Proc Natl Acad Sci U S A 2014;111:8233–8.
[32] Cimarelli A, Luban J. Human immunodeficiency virus type 1 virion density is not determined by nucleocapsid basic residues. J Virol 2000;74:6734–40.
[33] Muriaux D, Mirro J, Harvin D, Rein A. RNA is a structural element in retrovirus particles. Proc Natl Acad Sci U S A 2001;98:5246–51.
[34] Burniston MT, Cimarelli A, Colgan J, Curtis SP, Luban J. Human immunodeficiency virus type 1 Gag polyprotein multimerization requires the nucleocapsid domain and RNA and is promoted by the capsid-dimer interface and the basic region of matrix protein. J Virol 1999;73:8527–40.
[35] Grigorov B, Decimo D, Smagulova F, Pechoux C, Mougel M, Muriaux D, et al. Intracellular HIV-1 Gag localization is impaired by mutations in the nucleocapsid zinc fingers. Retrovirology 2007;4:54.
[36] Muller B, Daecke J, Fackler OT, Dittmar MT, Zentgraf H, Krausslich HG. Construction and characterization of a fluorescently labeled infectious human immunodeficiency virus type 1 derivative. J Virol 2004;78:10803–13.
[37] Larson DR, Johnson MC, Webb WW, Vogt VM. Visualization of retrovirus budding with correlated light and electron microscopy. Proc Natl Acad Sci U S A 2005;102:15453–8.
[38] Lampe M, Briggs JA, Endress T, Glass B, Riegelsberger S, Krausslich HG, et al. Double-labelled HIV-1 particles for study of virus-cell interaction. Virology 2007;360:92–104.
[39] Rudner L, Nydegger S, Coren LV, Nagashima K, Thali M, Ott DE. Dynamic fluorescent imaging of human immunodeficiency virus type 1 gag in live cells by biarsenical labeling. J Virol 2005;79:4055–65.
[40] Perez-Caballero D, Hatziioannou T, Martin-Serrano J, Bieniasz PD. Human immunodeficiency virus type 1 matrix inhibits and confers cooperativity on gag precursor-membrane interactions. J Virol 2004;78:9560–3.
[41] Jouvenet N, Neil SJ, Bess C, Johnson MC, Virgen CA, Simon SM, et al. Plasma membrane is the site of productive HIV-1 particle assembly. PLoS Biol 2006;4:e435.
[42] Ono A, Waheed AA, Joshi A, Freed EO. Association of human immunodeficiency virus type 1 gag with membrane does not require highly basic sequences in the nucleocapsid: use of a novel Gag multimerization assay. J Virol 2005;79:14131–40.
[43] Padilla-Parra S, Auduge N, Lalucque H, Mevel JC, Coppey-Moisan M, Tramier M. Quantitative comparison of different fluorescent protein couples for fast FRET-FLIM acquisition. Biophys J 2009;97:2368–76.
[44] Pepperkok R, Squire A, Geley S, Bastiaens PI. Simultaneous detection of multiple green fluorescent proteins in live cells by fluorescence lifetime imaging microscopy. Curr Biol 1999;9:269–72.
[45] Merzlyak EM, Goedhart J, Shcherbo D, Bulina ME, Shcheglov AS, Fradkov AF, et al. Bright monomeric red fluorescent protein with an extended fluorescence lifetime. Nat Methods 2007;4:555–7.
[46] Bastiaens PI, Squire A. Fluorescence lifetime imaging microscopy: spatial resolution of biochemical processes in the cell. Trends Cell Biol 1999;9:48–52.
[47] Day RN, Periasamy A, Schaufele F. Fluorescence resonance energy transfer microscopy of localized protein interactions in the living cell nucleus. Methods 2001;25:4–18.
[48] Voss TC, Demarco IA, Day RN. Quantitative imaging of protein interactions in the cell nucleus. Biotechniques 2005;38:413–24.
[49] Fogarty KH, Berk S, Grigsby IF, Chen Y, Mansky LM, Mueller JD. Interrelationship between cytoplasmic retroviral Gag concentration and Gag-membrane association. J Mol Biol 2014;426:1611–24.
[50] Jouvenet N, Simon SM, Bieniasz PD. Imaging the interaction of HIV-1 genomes and Gag during assembly of individual viral particles. Proc Natl Acad Sci U S A 2009;106:19114–9.
[51] Wachsmuth M, Waldeck W, Langowski J. Anomalous diffusion of fluorescent probes inside living cell nuclei investigated by spatially-resolved fluorescence correlation spectroscopy. J Mol Biol 2000;298:677–89.
[52] de Rocquigny H, El Meshri SE, Richert L, Didier P, Darlix JL, Mely Y. Role of the nucleocapsid region in HIV-1 Gag assembly as investigated by quantitative fluorescence-based microscopy. Virus Res 2014;193C:78–88.
[53] Munro JB, Nath A, Farber M, Datta SA, Rein A, Rhoades E, et al. A conformational transition observed in single HIV-1 Gag molecules during *in vitro* assembly of virus-like particles. J Virol 2014;88:3577–85.
[54] Bharat TA, Davey NE, Ulbrich P, Riches JD, de Marco A, Rumlova M, et al. Structure of the immature retroviral capsid at 8 Å resolution by cryo-electron microscopy. Nature 2012;487:385–9.
[55] Briggs JA, Riches JD, Glass B, Bartonova V, Zanetti G, Krausslich HG. Structure and assembly of immature HIV. Proc Natl Acad Sci U S A 2009;106:11090–5.
[56] Schur FK, Hagen WJ, Rumlova M, Ruml T, Muller B, Krausslich HG, et al. Structure of the immature HIV-1 capsid in intact virus particles at 8.8 Å resolution. Nature 2015;517:505–8.
[57] Ormo M, Cubitt AB, Kallio K, Gross LA, Tsien RY, Remington SJ. Crystal structure of the *Aequorea victoria* green fluorescent protein. Science 1996;273:1392–5.
[58] Johnson MC, Scobie HM, Ma YM, Vogt VM. Nucleic acid-independent retrovirus assembly can be driven by dimerization. J Virol 2002;76:11177–85.
[59] Cimarelli A, Sandin S, Hoglund S, Luban J. Basic residues in human immunodeficiency virus type 1 nucleocapsid promote virion assembly via interaction with RNA. J Virol 2000;74:3046–57.
[60] Crist RM, Datta SA, Stephen AG, Soheilian F, Mirro J, Fisher RJ, et al. Assembly properties of human immunodeficiency virus type 1 Gag-leucine zipper chimeras: implications for retrovirus assembly. J Virol 2009;83:2216–25.

[61] Ono A, Freed EO. Plasma membrane rafts play a critical role in HIV-1 assembly and release. Proc Natl Acad Sci U S A 2001;98:13925–30.
[62] Berkowitz RD, Ohagen A, Hoglund S, Goff SP. Retroviral nucleocapsid domains mediate the specific recognition of genomic viral RNAs by chimeric Gag polyproteins during RNA packaging *in vivo*. J Virol 1995;69:6445–56.
[63] Alfadhli A, Barklis E. The roles of lipids and nucleic acids in HIV-1 assembly. Front Microbiol 2014;5:253.
[64] Kempf N, Postupalenko V, Bora S, Didier P, Arntz Y, de Rocquigny H, et al. The HIV-1 nucleocapsid protein recruits negatively charged lipids to ensure its optimal binding to lipid membranes. J Virol 2015;89:1756–67.
[65] Sandefur S, Varthakavi V, Spearman P. The I domain is required for efficient plasma membrane binding of human immunodeficiency virus type 1 Pr55Gag. J Virol 1998;72: 2723–32.
[66] Jones CP, Datta SAK, Rein A, Rouzina I, Musier-Forsyth K. Matrix domain modulates HIV-1 Gag's nucleic acid chaperone activity via inositol phosphate binding. J Virol 2011;85: 1594–603.
[67] Liu B, Dai R, Tian CJ, Dawson L, Gorelick R, Yu XF. Interaction of the human immunodeficiency virus type 1 nucleocapsid with actin. J Virol 1999;73:2901–8.
[68] Jolly C, Mitar I, Sattentau QJ. Requirement for an intact T-cell actin and tubulin cytoskeleton for efficient assembly and spread of human immunodeficiency virus type 1. J Virol 2007;81:5547–60.
[69] Martinez NW, Xue X, Berro RG, Kreitzer G, Resh MD. Kinesin KIF4 regulates intracellular trafficking and stability of the human immunodeficiency virus type 1 Gag polyprotein. J Virol 2008;82:9937–50.
[70] Fritz JV, Didier P, Clamme JP, Schaub E, Muriaux D, Cabanne C, et al. Direct Vpr-Vpr interaction in cells monitored by two photon fluorescence correlation spectroscopy and fluorescence lifetime imaging. Retrovirology 2008; 5:87.
[71] Clamme JP, Azoulay J, Mely Y. Monitoring of the formation and dissociation of polyethylenimine/DNA complexes by two photon fluorescence correlation spectroscopy. Biophys J 2003;84:1960–8.
[72] Azoulay J, Clamme JP, Darlix JL, Roques BP, Mely Y. Destabilization of the HIV-1 complementary sequence of TAR by the nucleocapsid protein through activation of conformational fluctuations. J Mol Biol 2003;326:691–700.

Chapter 2:

The role of NCp7 domain of HIV-1 Gag in regulating trafficking of Tumor susceptibility gene 101

In this article, we monitored the impact of NCp7 domain on the trafficking of Tumor susceptibility gene 101 (TSG101). We first validated that the removal of p6 domain of Gag results in a dramatic decrease of Gag-TSG101 interaction by immune-precipitation and FRET-FLIM. By using similar techniques, we found that the NCp7 alone or as a domain of Gag (GagNC) was required for Gag to interact with TSG101 suggesting an interplay between NC and L domain of Gag in the process of viral budding and release. The NCp7 mediated interaction between Gag and TSG101 necessitates at least one of the two zinc fingers since removal of a singular zinc finger within GagNC or within NCp7 does not impact the interaction with TSG101. Next, by analyzing amplitudes associated to the short-lived lifetime in the cytoplasm, in vesicles and at the PM, it was concluded that Gag is the main driving force for TSG101 trafficking. Moreover, the removal of RNA does not abrogate Gag-TSG101 interaction and thus, this NC-TSG101 interaction seems highly contrasted to the interaction of NC and Bro 1 occurring in the LYPXnL pathway. This leaves to imply that the two mechanisms maybe not redundant but rather that the NC could recruit simultaneously both TSG101 and ALIX proteins in order to best optimize the chances of the virus to bud. This brings to a hypothesis which implies that the two mechanisms, Gag/TSG101 and Gag/ALIX, maybe not redundant but concordant, in a way that the NC could recruit simultaneously both TSG101 and ALIX proteins in order to best optimize the chances of the virus to bud.

In summary, we have used a series of biochemical assays to underline the role of NCp7 domain of Gag for the recruitment of TSG101. These approaches have provided evidences that the complex formation of Gag-TSG101 get strengthened by direct interaction of TSG101 with either free NC or NC as GagNC and by the virtue of GagNC, Gag trafficking is responsible for the docking of TSG101 to the PM.

Publication 3:

Influence of the nucleocapsid region of the HIV-1 Gag polyprotein precursor on the trafficking of the Tumor susceptibility gene 101.

Influence of the nucleocapsid region of the HIV-1 Gag polyprotein precursor on the recruitment and trafficking of the Tumor susceptibility gene 101.

Authors : Salah Edin El Meshri[1], E.Boutant[1], Audrey Thomas[2], Vivet Boudout[3], Ludovic Richert[1], Yves Mély[1], Delphine Muriaux [2] and Hugues de Rocquigny *

[1] Laboratoire de Biophotonique et Pharmacologie, UMR 7213 CNRS, Faculté de Pharmacie, Université de Strasbourg, 74, Route du Rhin, 67401 ILLKIRCH Cedex, France.

6. 2 Membrane Domains and Viral Assembly, CNRS UMR-5236, Centre d'étude d'agents Pathogènes et Biotechnologies pour la Santé, 1919 route de Mende - 34293 Montpellier cedex 5, France.

3 Architecture et Réactivité de l'ARN, Université de Strasbourg, CNRS, IBMC, 15 Rue R. Descartes, 67084 Strasbourg Cedex

**** Corresponding author**

Tel : +33 (0)3 90 24 41 03 Fax : +33 (0)3 90 24 43 12

e-mail: hderocquigny@unistra.fr

Abbreviations:

FRET: Fluorescence Resonance Energy Transfer; FLIM: Fluorescence Lifetime Imaging Microscopy; WB: Western Blotting; HIV-1: Human Immunodeficience Virus type 1; ZF: zinc finger; eGFP: enhanced Green Fluorescent Protein ; IP: immunoprecipitation

Running title: Role of HIV-1 NCp7 in PTAP pathway.

Abstract

The human immunodeficiency virus type 1 (HIV-1) Gag polyprotein precursor orchestrates viral particle assembly and directs virus budding by recruiting the cellular endosomal sorting complex required for transport (ESCRT) machinery. This is accomplished by two short motifs in the C-terminal p6 region of Gag, namely PTAP and LYPXnL, referred to as the 'late assembly domains' that bind the cellular sorting factors TSG101 and ALIX. The influence of the NC domain of Gag on p6 PTAP/TSG101 interaction and function was analyzed by immunoprecipitation and FLIM-FRET experiments. Investigating the interaction of Gag mutated in NC and p6 with TSG101 showed that both NC zinc fingers are required to strengthen the Gag-TSG101 interaction. In addition we provide evidences that NC-mediated Gag trafficking is responsible for the docking of TSG101 to the plasma membrane. These findings highlight the key role played by the NC region of Gag in the recruitment of the ESCRT machinery and thus in virions budding.

Introduction

The human immunodeficiency virus type 1 (HIV-1) Gag polyprotein is composed of four domains, that are the matrix (MA), capsid (CA), nucleocapsid (NC) flanked by SP1 and SP2 and p6, all involved in viral particle assembly and budding (Sundquist and Krausslich 2012). This complex process takes place soon after Gag synthesis where the MA region targets Gag oligomers to the plasma membrane (PM) through the interaction of its N terminal myristate and several basic residues located close to the N terminus. The CA region notably its C-terminal domain (CTD) together with SP1 is the major player in Gag oligomerization, further facilitated by the basic NC region interacting with the genomic RNA and considered to be the initial assembly plateform (Muriaux and Darlix 2010). At least, the C terminus of Gag corresponding to p6 is required for the incorporation of the accessory protein Vpr. This protein also contains two short sequences PTAP (Gottlinger et al. 1991; Huang et al. 1995) and $LYPX_nL$ (Puffer et al. 1997; Strack et al. 2003) referred to as the 'late assembly domains' which binds TSG101 and ALIX (Garrus et al. 2001; Martin-Serrano et al. 2001; VerPlank et al. 2001; Strack, Calistri et al.

2003; von Schwedler et al. 2003). These sorting proteins which belong to the cellular ESCRT machinery are transiently recruited at the HIV-1 budding site to facilitate membrane fission and viral particle egress (Bleck et al. 2014; Prescher et al. 2015). In that respect, the Tsg101/Gag-PTAP interaction is considered to be the major determinant for HIV-1 particle release (Bieniasz 2006; Sundquist and Krausslich 2012). Tsg101 is a member of the ESCRT-1 complex that initiates the sorting of surface proteins into multivesicular bodies (MVB) with the help of ESCRT-III and the activity of VPS4 AAA-type ATPase. Either depletion or over-expression of TSG101 blocked HIV-1 budding and particle release (Garrus, von Schwedler et al. 2001; Demirov et al. 2002; Goila-Gaur et al. 2003). Moreover, it has been shown that the interaction of TSG101 and the PTAP motif is mediated by the N-terminal ubiquitin (Ub) conjugase (E2) -(UEV) like domain of TSG101(Pornillos et al. 2002).

As far as the role of PTAP is concerned, recent studies suggested that this motif facilitates virus budding and release in a context-dependent manner where an optimal activity requires its positioning near GagNC. This implies that it cooperates with other Gag regions to achieve an efficient viral release (Yuan et al. 2000; Strack et al. 2002; Martin-Serrano et al. 2003). In line with this, addition of the NCp7-p1 (NCp9) region to the GagΔp6-Leucine zipper (Gag Z) was found to turn it into a transdominant negative inhibitor of the ESCRT pathway. This clearly shows that NCp9 should play an important role in the ESCRT-dependent HIV-1 particle release (Popova et al. 2010). In support of this, mutating the basic residues of NC results in an inhibition of Gag particles release (Cimarelli et al. 2000; Ott et al. 2003; Ott et al. 2005), confirming that the NC region could cooperate with p6 as late assembly domain in the PTAP/TSG101 sorting pathway (Dussupt et al. 2011; Bello et al. 2012). In agreement with this notion, in the pNL4.3 context, Gag expressing the first 433 amino acid (MA, CA, p1 and NC) and so lacking the p6 domain was shown to bud normally (Gan and Gould 2012).

Recently Mougel and co-workers reported that GagNC and TSG101 were in close proximity and showed the importance of the second zinc finger of NC in this proximity. Nevertheless, the low resolution of the Duolink approach (<40nm) prompt us to determine if this proximity could correspond to an interaction between GagNC and TSG101. Therefore, co-immunoprecipitation and FLIM-FRET experiments were performed on cells expressing TSG101 and a series of Gag constructs with deletion in NC and p6 regions. Results showed that both NC zinc fingers are important for the Gag-TSG101 interaction. However, deleting the NC zinc fingers did not have

an impact as drastic as deleting the entire p6 region indicating that the NC domain of Gag provides a supportive role for the interaction between p6 and TSG101. Of note, the cellular localization of the Gag-TSG101 relies on Gag trafficking and thus not restricted to the PM. Interestingly, Gag trafficking is dependent on the NC domain, and thus localization of the TSG101/Gag complex is also dependent on NC. Collectively, our results support a model where NC cooperates with p6 to recruit TSG101, thus giving an insight into the functional link between the p6 late domain motifs and NC as well as the regulatory role of NC domain in the course of recruiting components of the cellular machinery necessary for HIV-1 particle budding and release.

Materials and Methods

Plasmid DNA. The human-codon-optimized $Pr55^{Gag\text{-}TC}$ encoding plasmid was kindly provided by David E. Ott (National Cancer Institute at Frederick, Maryland) (Rudner et al. 2005). Gag ΔZF1, GagΔZF2, GagΔZF1ΔZF2, GagΔNC and GagΔp6 (Fig. 1) deletion mutants were constructed by PCR based site-directed mutagenesis using Gag-TC as substrate (El Meshri et al. 2015). pNL4-3 expressing wild type Gag and as well as zinc fingers deleted Gag were already published (Grigorov et al. 2007). HA-Tsg101 and eGFP-Tsg101 (Fig. 1) were purchased from NIH AIDS Reagent Program. The integrity of all plasmid constructs was verified by DNA sequencing.

Cell culture and plasmid DNA transfection. HeLa cells (from ATCC, ref CCL-2 Amp, HeLa; Cervical Adenocarcinoma; Human) were cultured in Dulbecco's modified eagle medium supplemented with 10% fetal calf serum (Invitrogen Corporation, Cergy Pontoise, France) and 1% of an antibiotic mixture (penicillin/streptomycin: Invitrogen Corporation Pontoise, France) at 37°C in a 5% CO2 atmosphere. HeLa cells were transfected or co-transfected using jetPEITM (Life Technologies, Saint Aubin, France) according to the supplier's recommendations. To keep a constant amount of transfected DNA, each transfection assay was supplemented with pcDNA3 (Invitrogen Corporation, Cergy Pontoise, France).

Immunoprecipitation and western blotting. HeLa cells were seeded (6 10^5 cells) and transfected with 1µg of plasmid encoding HA-TSG alone or with 1µg of plasmid encoding either Gag-TC, GagΔZF1-TC, GagΔZF2-TC, GagΔZF1ΔZF2-TC, GagΔNC-TC, GagΔp6-TC or NCp7-eGFP

(Fig. 1) using jetPEI^{TM} (Life Technologies, Saint Aubin, France) according to the supplier's recommendations. 48 hours post-transfection, cell were trypsinized and resuspended in lysis buffer (10mM Tris HCl, 150mM NaCl, 1mM EDTA, 1% NP40, 0.05% SDS) containing protease inhibitors (Complete Mini , EDTA-free Protease Inhibitor Cocktail Tablets, Roche) for 30 minutes at 4° C. After centrifugation at 14,000 rpm, the amount of protein was determined by the Bradford method and 20 µg of protein were used for input and 1 mg incubated with rabbit anti-HA (Abcam ab9110) for 2 hours at 4°C under continuous agitation. Meanwhile, 50µL protein A coated (Dynabeads) magnetic beads were washed in 1X PBS and incubated with samples for 1.5h. Beads were then washed three times with NP40 lysis buffer, denatured for 5 minutes at 95 ° C in Laemmli buffer and analysed by 12% SDS-PAGE. Membranes were incubated with mouse anti HA (Pierce, ref : 26183) or mouse anti-eGFP (Proteintech, France, ref : 66002-1-Ig) or mouse monoclonal anti Gag (Ref 6521 #24-4 ; AIDS Reagent Program, Division of AIDS, NIAID, NIH from Dr. Michael H. Malim) or mouse anti-GAPDH (Millipore,MAB374, 1 :5000) followed by anti-mouse HRP (Promega, ref W402B). Proteins were visualized by the chemiluminescent ECL system (Amersham) on a LAS 4000 apparatus.

Biarsenical labeling. HeLa cells cultured on 35-mm coverslips (µ-Dish IBIDI; Biovalley) were transfected with 1µg of plasmid encoding eGFP, or wild-type eGFP-TSG alone or together with 1.5µg of plasmid encoding for wild-type Gag-TC or its cognate mutants GagΔZF1-TC, GagΔZF2-TC, GagΔZF1ΔZF2-TC, GagΔNC-TC, GagΔp6-TC, NC-TC. Biarsenical labeling was achieved 24 h post-transfection as previously reported (Fritz et al. 2010). Briefly, a biarsenical solution was prepared by diluting 1.25µl of pure ReAsH 2 mM in 2ml of OPTI-MEM. The ReAsH solution was applied to each coverslip, incubated for 1 h at 37°C followed three washes with OPTI-MEM. Then, cells were incubated 10min. at 37°C with BAL buffer (2, 3-mercaptopropanol) and washed by OPTI-MEM. Live cells were after fixation by using 4% paraformaldehyde (PFA).

Confocal Microscopy. HeLa cells were transfected in 6-well plate containing a 18 mm cover slips with a mixture containing 0.25µg of plasmid eGFP-TSG, 0.5µg of plasmid expressing Gag (or mutated Gag) or pNL43 wild-type or mutated in Gag, as described in (Grigorov, Decimo et al. 2007), and 0.25µg of plasmid expressing Gag-mCH (or the corresponding mutated Gag-

mCherry). At 24 h. post-transfection, the cells were extensively washed, fixed with a 4% PFA/PBS solution and kept in PBS at 4°C until observation with a Leica SPE equipped with a Leica 63x 1.4NA oil immersion objective (HXC PL APO 63x/1.40 OIL CS). The eGFP images were obtained by scanning the cells with a 488 nm laser line and a 500 to 555 nm band-pass for emission. For the mCherry images, a 561 nm laser line was used with a 570 to 625 nm band-pass. The same procedure was applied for HA-TSG but using rabbit anti-HA (Abcam ab9110) followed by anti rabbit conjugated with Alexa 488 (Invitrogen Corporation, Cergy Pontoise, France, ref : A11008).

Fluorescence Lifetime Imaging Microscopy (FLIM). HeLa cells were transfected in µ-Dish IBIDI (Biovalley, France) with a mixture containing 0.25µg of plasmid eGFP-TSG and 0.75µg of plasmid expressing Gag-TC (or mutated Gag-TC) and fixed with 4% PFA 24h. post transfection. The experimental set-up for FLIM measurements has already been described (Clamme et al. 2003; Fritz et al. 2008; Richert et al. 2015). Briefly, time-correlated single-photon counting FLIM measurements were performed on a home-made two-photon excitation scanning microscope based on an Olympus IX70 inverted microscope with an Olympus 60× 1.2NA water immersion objective operating in the descanned fluorescence collection mode. Two-photon excitation at 900 nm was provided by a mode-locked titanium-saphire laser (Tsunami, Spectra Physics). Photons were collected using a set of two filters: a short pass filter with a cut-off wavelength of 680 nm (F75-680, AHF, Germany), and a band-pass filter of 520 ± 17 nm (F37-520, AHF, Germany). The fluorescence was directed to a fiber coupled APD (SPCM-AQR-14-FC, Perkin Elmer), which was connected to a time-correlated single photon counting (TCSPC) module (SPC830, Becker & Hickl, Germany).

Typically, the samples were continuously scanned for about 60 s to achieve the appropriate photon statistics in order to investigate the fluorescence decays. Data were analyzed using a commercial software package (SPCImage V2.8, Becker & Hickl, Germany).

For Fluorescence Resonance Energy Transfer (FRET) experiments with eGFP, the FRET efficiency (E) was calculated according to the equation:

$$E = 1 - \frac{\tau_{DA}}{\tau_D} = \frac{1}{1 + (R/R_0)^6} \qquad (1)$$

where τ_{DA} is the lifetime of the donor in the presence of the acceptor and τ_{D} is the lifetime of the donor in the absence of the acceptor.

Results

Contribution of NC to Gag-TSG101 complex formation and trafficking to the plasma membrane

Figure 2

Expression of Gag NC deletion mutant (GagΔNC), either in the pNL4.3 backbone or from a plasmid expressing Gag, has been shown to result in a drastic reduction in the quantity of viral particles in the supernatant (Grigorov, Decimo et al. 2007; Hogue et al. 2009; Ott et al. 2009; Dussupt, Sette et al. 2011; El Meshri et al. 2015), despite the fact that GagΔNC contains PTAP motif. Meanwhile, we have recently shown that GagΔNC can form large intracellular aggregates and oligomerize with lesser degree of compactness as compared to Gag (El Meshri, Dujardin et al. 2015). This favored the notion that deleting NC has a negative impact on the overall structure of the Gag protein and, as a consequence, potentially masking the presence of the p6 PTAP motif. To test this hypothesis, we initially followed the co-localization of wild Gag and TSG101. Therefore, 293T cells were transfected with plasmids expressing eGFP-TSG101 alone (images a-c) or with pNL4.3 (images d-f) encoding for all the viral proteins, except the ENV glycoprotein. The anti-Gag anti body being poorly efficient for detecting Gag protein at the PM, an additional plasmid was added to pNL4.3 to produce Gag-mCherry (ratio 0.9/0.1). The fluorescent protein was inserted upstream of CA (Muller et al. 2004; Hubner et al. 2007) since insertion at this location as well as its transfection together with plasmids expressing non labeled Gag proteins was shown to moderately affect the virus morphology, Gag localization and Gag budding (Muller, Daecke et al. 2004; Larson et al. 2005; Lampe et al. 2007; Jouvenet et al. 2008; Ivanchenko et al. 2009). As expected, in presence of Gag, a significant Gag-mCherry staining was monitored at the PM (image e). Since Gag-mCherry alone weakly accumulates to the PM (data not shown), this staining shows that Gag-mCherry gets embedded in Gag oligomers along the assembly process. In contrast, eGFP-TSG 101solely appears into cytosolic fluorescent dots (image a) while in the presence of Gag during the assembly process, the cytosolic fluorescence dots of eGFP-TSG101 disappeared and concentrated at the cell periphery (image d), rendering

co-localization of Gag/Gag-mCherry and eGFP-TSG101 at the PM (image f). Next, we examined the localization of eGFP-TSG101 in presence of GagΔNC (images g-i). At 24h post transfection, aggregates of GagΔNC/GagΔNC-mCherry were observed mainly in the cytoplasm (image h). Interestingly, a partial co-localization of eGFP-TSG101 was also observed with GagΔNC/GagΔNC-mCherry (image j). Taken together, these results show that upon addition of Gag, TSG101 is relocated from the cytosol to the cell PM, and that a deletion of the NC domain of Gag prevents this relocation.

Both NC zinc fingers cooperate with p6 to promote TSG101-p6 interaction

Figure 3

To further characterize the role of GagNC in TSG101 recruitment, we performed immunoprecipitation experiments on cell extracts upon expression of HA-TSG101 (Fig. 3 well 2) and wild type Gag (Fig. 3, wells 3). Similar experiments were performed with GagΔNCp7 (well 6) and Gag containing a stop codon upstream the p6 domain (well 7). In agreement with the homogeneous distribution of GADPH (Fig 3A), similar levels of HA-TSG101 were found in cells expressing either the protein alone (well 2), or in presence of Gag (wells 3) or of GagΔNCp7 (well 6) or of GagΔp6 (well 7). Cell lysates were incubated with rabbit anti-HA antibodies and the transfer membrane was probed with a mouse anti-HA anti body showing similar levels of HA-TSG101 (Fig 3B, wells 2, 3, 6, 7). As a control, in absence of anti-HA, no signal of Gag was observed (well 1').

The same membrane was re-probed with a monoclonal anti-Gag antibody and results revealed that Gag was efficiently captured by HA-TSG101 (well 3). In sharp contrast, GagΔNC was poorly precipitated by TSG101 (well 6). Interestingly, the deletion of the p6 region was found to be more drastic since only a faint reproducible signal of GagΔp6 was detected in well 7. Intensity of each signal from membranes B and m C was determined and independently normalized to the signal obtained for Gag. The ratio of IP to CoIP reported in the histogram of figure 1D shows that GagΔp6 and GagΔNC are six and two times, respectively, less efficiently iped by TSG101 as compared to wt Gag.

Next, to map the domain of NC involved in TSG101 recognition, we tested GagΔZF1 and GagΔZF2 mutants in which either the proximal or the distal NC zinc finger was deleted, (well 4

for GagΔZF1 and well 5 for GagΔZF2). To determine the role of the basic residues flanking the CCHC motifs both zinc fingers were deleted (well 8 for GagΔZF1ΔZF2). As seen on Fig 3C, GagΔZF1 (well 4) and GagΔZF2 (well 5) were equally precipitated as compared to the wild type Gag (well 3). In sharp contrast, GagΔZF1ΔZF2 was poorly precipitated by TSG101 (well 8), the efficiency of the precipitation being similar to that obtained for GagΔNC (figure 1D).
Taken together, the main interaction between Gag and TSG101 is driven by p6, but also by NC: NC contributes strongly into the recognition of TSG101 by p6.

Figure 4
Then, we examined if NC outside the context of Gag could interact with TSG101. As shown in figure 4 with the membrane blotted with anti-eGFP, HA-TSG101 was found to be able to precipitate NCp7-eGFP (well 2). Interestingly, NCp7ΔZF1 (well 3) and NCp7ΔZF2 (well 4) were also co iped while deletion of both zinc fingers in NCp7ΔZF1ΔZF2 was detrimental for the TSG-NCp7 interaction (well 5).
Next, we tested whether the NC mediated interaction between Gag and TSG101 was RNA dependent as NC has a high affinity for nucleic acids (Darlix et al. 2014). Therefore, an RNAse treatment was applied prior to the immunoprecipitation of the sample 3 containing Gag and TSG101. As shown in figure 3C, well 2', Gag was precipitated by TSG101 in the presence of RNase, thus showing that the interaction is most probably RNA independent. All together, these results showed that both zinc fingers of NCp7 are required for the interaction between NC and TSG101.

Influence of GagNC on TSG101 cellular localization

In the previous section, the effect of Gag on TSG101 localization was monitored by immunofluorescence microscopy using anti-Gag and either anti-HA-TSG101 or eGFP-TSG101 (Martin-Serrano, Zang et al. 2001; Derdowski et al. 2004; Johnson et al. 2005). In the absence of Gag, TSG101 was found in the cytoplasm and accumulating in dots. Expression of TSG101 together with Gag resulted in a total accumulation of both Gag and TSG101 at the cell periphery, in agreement with the role of TSG101 during Gag budding (Prescher, Baumgartel et al. 2015).
Figure 5

To investigate the role of GagNC in TSG localization, a plasmid expressing TSG101 was co-transfected with plasmids expressing either Gag or Gag mutants with deletions in the NC or the p6 region (Fig 1). Moreover, to monitor Gag-TSG101 interaction by means of FRET-FLIM, eGFP was used as the donor while ReAsH was the acceptor. To this end, HA-TSG101 was substituted for eGFP-TSG101 since location of eGFP at the N terminus of TGS101 does not modify its staining pattern (Fig S1). Concerning Gag, the small tetracysteine (TC) motif was added at the C-terminus of Gag to use the biarsenical-tetracysteine labeling approach (Adams et al. 2002). In this approach, TC interacts tightly with ReAsH and both the size and the location of TC has been shown to be suitable for imaging Gag trafficking in cell (Rudner, Nydegger et al. 2005; Gousset et al. 2008; Fritz, Dujardin et al. 2010).

First, these constructs were expressed and their cellular localization was assessed by confocal microscopy. Therefore, to avoid feeble detection of Gag at the PM by anti-Gag antibody, a plasmid expressing Gag-TC or Gag-TC mutants was co-transfected with plasmid expressing Gag-mCherry and Gag-mCherry counterpart. As shown in figure 5, image a, TSG101 displays a punctuate and a faint diffused staining in the cytoplasm while in presence of Gag/Gag-mCherry, TSG101 and Gag co-localize at the PM (image b). For the GagΔZF1 (image c) and GagΔZF2 (image d) mutants, we observed a comparable co-staining of Gag and TSG101 at the PM. In addition, dots containing both partners were also detected within the cytoplasm, notably for GagΔZF2. Next, we examined the localization of the GagΔZF1ΔZF2 (image e) and GagΔNC (image f) with TSG101. An increase in diffusion in the cytoplasm, accumulation in dots or in large aggregates and only a slight co-localization at the PM were observed for co-transfected TSG101 and Gag mutants. In addition, all these staining patterns turned out to be very similar to those for Gag and GagNC mutants alone (Grigorov, Decimo et al. 2007; Hogue, Hoppe et al. 2009; El Meshri, Dujardin et al. 2015), suggesting that the localization of TSG101 at the PM essentially depends on the localization of Gag at the PM with the integrity of the NC domain and especially both zinc fingers.

Next, the cells co-expressing eGFP-TSG101 and GagΔp6 were observed (image g). As shown in images g, Gag was found accumulating at the plasma membrane while TSG101 was characterized by a punctuated staining in the cytoplasm that resembles to the staining observed in cell expressing TSG101 alone (image a). Last, eGFP-TSG101 was co-expressed with NC/NC-

mCherry (image g) and NCp7 was found all over the cell with partial accumulation in the nucleolar compartment, while TSG101 was observed in form of punctuated dots. These results are in agreement with the results obtained for cells expressing NCp7 (Anton et al. 2015) (Lochmann et al. 2013) or TSG101 alone (Martin-Serrano, Zang et al. 2001; Derdowski, Ding et al. 2004; Johnson, Spidel et al. 2005).

Monitoring Gag-TSG101 interaction by FLIM

In order to image Gag-TSG101 interaction and to delineate the role of GagNC in Gag-TSG101 interaction, cells co-expressing eGFP-TSG101 and Gag-TC were treated with the membrane-permeable biarsenical dye ReAsH and analysed by confocal microscopy (figure S2), to check their co-localisation. In parallel, FRET is monitored by FLIM, using eGFP-TSG101 as the donor and Gag-TC-ReAsH as the acceptor. FRET between eGFP and ReAsH only occurs when they are less than 5.6 nm apart, a distance corresponding to intermolecular protein-protein interactions (Sun et al. 2013). Due to FRET between eGFP and ReAsH, a decrease of eGFP fluorescence lifetime (τ) is observed, which was determined by measuring the fluorescence decay at each pixel of the cell. Then FLIM images are built, by using false-color lifetime encoded pixels that directly described the spatial distribution of protein-protein interactions. We then monitored the viral determinant involved in Gag-TSG101 interaction in cells.

Figure 6 and 7

First, cells expressing eGFP-TSG101 and labeled by ReAsH were imaged to determine the intrinsic fluorescence lifetime of eGFP-TSG101. The fluorescence decay of eGFP fused to TSG101was analysed using a mono-exponential model to calculate a mean fluorescence lifetime (τ_m) of 2.26±0.07 ns. As a consequence, TSG101 staining appears as punctuated orange dots in the cytoplasm (Fig 6A, panel a). Moreover, τ_m is almost similar to that of free eGFP (2.39 ±0.08 ns, data not shown), suggesting that eGFP fluorescence was moderately modified due to its fusion to TSG101 or by the presence of the acceptor.

Next, cells expressing Gag-TC and eGFP-TSG101 were imaged by FLIM. Analysis of the fluorescence decays using a mono-exponential model gave rise to a bimodal distribution of the lifetimes with peaks centered at 1.5 ±0.1 ns and 2.3 ± 0.2 ns and a χ factor above 3. As already

described (Richert, Didier et al. 2015), to obtain a better fit fluorescence decays were analyzed with a two components model:

$$F(t) = a_1 e^{-t/\tau_1} + a_2 e^{-t/\tau_2}$$

in which the long-lived lifetime τ_2 was fixed at the lifetime of eGFP-TSG101 (2.25 ns), while the short component τ_1 and the populations (α_1 and α_2) associated with the two lifetimes were allowed to float .

Thus, it was possible to determine the short component and the associated fraction of eGFP-TSG101, in the complex. As depicted on Fig 6B, panel d, cell expressing eGFP-TSG101 and Gag-TC-ReasH were characterized by a blue color corresponding to an average τ_1 of 0.98±0.13 ns. Interestingly, this high FRET (56.3±8%, Fig7A) is homogeneously distributed all over the cell indicating that the tight interaction between the two proteins occurs in the cytoplasm, in dots (white arrows) and at the PM. The same analysis was carried out on cell expressing GagΔZF1, GagΔZF2, GagΔZF1ΔZF2 and GagΔNC (Fig 6B, panels e to h), showing the average τ_1 centered to 1.02±0.03 ns for GagΔZF1 and GagΔZF2 and to 1.18±0.04ns for GagΔZF1ΔZF2 and GagΔNC, respectively. Meanwhile, the amplitude $\alpha 1$ of the τ_1 component i.e. the fraction of eGFP-TSG101 species undergoing FRET, was found centred at 60% (Fig 7B) and was independent of the presence or the absence of any singular zinc finger. Thus, cells expressing Gag (panel i), GagΔZF1 (panel j) or GagΔZF2 (panel k) showed a comparative yellow color located at the PM, the cytoplasm and in internal dots (white arrows). Concerning, GagΔZF1ΔZF2 (panel l) and GagΔNC (panel m), amplitudes were significantly different and dropped to 31% and 41% respectively. Interestingly, the drop in distribution of the amplitude was not homogenous and was compensated by an increase at the periphery of the PM (Figure 6, panels l and m, note the evolution from bleu to orange from the cytoplasm to the PM).

Discussion

In HIV-1, there are two different sequences located in the p6 region of Gag, namely P(T/S)AP and LYPXnL, that recruit TSG101 and ALIX, respectively, and as such are essential

elements for viral particle budding (Votteler and Sundquist 2013). In addition to p6, when either GagNC is mutated or not in the vicinity of the PTAP sequence, virus budding was largely prevented indicating that GagNC has a role during the PTAP-mediated virus budding. In the present study, we showed that the removal of p6 resulted in a dramatic decrease of Gag-TSG101 interaction, in agreement with the seminal work showing the involvement of PTAP motif in the recruitment of ESCRT-I proteins (Garrus, von Schwedler et al. 2001; Martin-Serrano, Zang et al. 2001; VerPlank, Bouamr et al. 2001; Demirov et al. 2002; Pornillos, Alam et al. 2002). Nevertheless, we showed a significant level of GagΔp6 iped by TSG101 highlighting that another region of Gag is probably involved in the interaction. Our results suggest that NCp7 alone or as GagNC, is this region possibly engaged in interplay with the L domain required for virus budding and release.

This NC mediated interaction between Gag and TSG101 is dependent on the presence of at least one of the two zinc fingers, since removal of one zinc finger in GagNC or NCp7 does not alter the interaction with TSG101, as viewed by co-ip (Fig. 3 and 4) and by FLIM-FRET (Fig. 6 and 7). FLIM, a method of choice to study protein-protein interaction (Sun, Rombola et al. 2013; Richert, Didier et al. 2015) allows the monitoring of the fluorescence lifetime of eGFP-TSG101 in presence of Gag-TC-ReAsH as acceptor. Using this setup, analysis of cell expressing Gag, GagΔZF1 or GagΔZF2, using a two exponential analyses, showed that the distance between Gag and TSG101 was 54±0.1 Å. This short distance is independent from the deletion of a single zinc finger and from the site of cellular distribution of the complex in the cell (Fig. 6B, bluish color, upper raw), as shown by homogeneous distribution of τ_1 in the cytoplasm, in dots or at the PM. Interestingly, amplitudes associated to the short-lived lifetime in the cytoplasm, in dots and at the PM (fig 6B, orange color, bottom raw) is highly similar to the co-localization between Gag, GagΔZF1 or GagΔZF2 and TSG101, as observed by confocal microscopy (figure 2 and 5). All these results, suggests that Gag is the main driving force for TSG101 trafficking, but not *vice-versa*.

A slight but statistically significant increase of τ1 was observed on cells expressing GagΔZF1ΔZF2 and GagΔNC as compared with the lifetime obtained for Gag (Fig 7A). But, in comparison with the total absence of FRET for GagΔp6, this result also shows that, in the

context of Gag, the PTAP domain remains essential for interacting with TSG101. Nevertheless, the main impact of NC deletion or of the simultaneous deletion of both zinc fingers on Gag-TSG101 interaction lies in the important decrease in the population of Gag engaged in the Gag-TSG101 complex (Fig. 6B, panel l and m and Fig. 7B). This shift in population could be attributed to the decrease of Gag-TSG101 affinity thus suggesting that the NC domain of Gag strengthen the weak affinity determined for p6-TSG101 (Pornillos, Alam et al. 2002; Im et al. 2010). In accordance with this hypothesis, the NMR structure of NCp15 showed an inter-protein interaction between NCp7 and p6 with a close proximity between the central domain of NCp7 and the acidic residues of p6 (Wang et al. 2014). Since this fold back conformation interferes with the accessibility of NCp9/p6 by the protease (Wang, Naiyer et al. 2014), it may be hypothesize that PTAP motif of p6 domain is brought in a close proximity to the zinc fingers for promoting the recognition of NCp7 and p6 by TSG101. Furthermore, this dual-binding may results in compactness and stability of TSG101/Gag complex.

In addition, GagNC participates to the oligomerization of Gag and its assembly at the PM by virtue of NC interacting with the viral RNA and with membranes (Ott, Coren et al. 2009; Chukkapalli et al. 2010; Muriaux and Darlix 2010; Kerviel et al. 2013; Kempf et al. 2015). Nevertheless, these functions are independent of TSG101 recruitment, in accordance to the results obtained with G2A mutant that despite a defect in the Gag oligomerization and membrane binding co-localizes efficiently with TSG101 (Fig. S3A) and showed a FRET similar to wild type Gag (Fig. S3B). Moreover, the removal of RNA does not abrogate Gag-TSG101 interaction (Fig. 3C), which is in agreement with our results showing that basic residues surrounding zinc fingers are not directly involved in this interaction.

Interestingly, this NC-TSG101 interaction seems highly disparate as to the interaction between NC and Bro 1, occurring during the LYPXnL pathway (Popov et al. 2008; Dussupt et al. 2009). In fact, NC-Bro1 complex is sensitive to mutations in the basic domain of NC and also needs RNA that could bridge the two proteins (Bello, Dussupt et al. 2012). This brings to a hypothesis which implies that the two mechanisms, Gag/TSG101 and Gag/ALIX, maybe not redundant but concordant, in a way that the NC could recruit simultaneously both TSG101 and ALIX proteins in order to best optimize the chances of the virus to bud. Studies are currently

underway to identify a possible simultaneous recruitment of these two cellular partners by the NCp15 domain of Gag and to define the kinetics of this interaction in living cells.

In line with our results, it was recently shown by *in vitro* GST pull down assay that NC is essential for p6 in recruiting TSG101. Our results extend this result by showing that, in the context of Gag and in cell expressing NC, the GagNC directly interacts with TSG101. Moreover, the group of Mougel et al also pointed out, using the duolink approach, that the second zing finger was important for the PTAP mediated budding of the virus (Chamontin et al. 2015). Using this technique, which is also referred as Proximity Ligation Assay (Soderberg et al. 2008), they showed that the second zinc finger is important for the co-localization of Gag and TSG101 at the PM and in particles. Nevertheless, the distance between two proteins emitting PLA signal, was estimated to 30-40 nm (Soderberg et al. 2006) that hampered the assertion related to the direct interaction between the two proteins. On the contrary, using our approach of FRET we investigated more deeplyand determined that the second zinc finger was directly involved in the interaction of the two partners.

Data reported in this study shows a good correlation between experiments carried out by co-IP and by FLIM-FRET, indicating that there is a direct interaction between Gag and TSG101, that relies at least in part, on the NC region. However, one caveat between IP and FRET is when NCp7, transiently expressed in cells, was able to precipitate TSG101 while neither NC-mCherry nor NC-TC was found having FRET with eGFP-TSG101. Such a discrepancy between IP and images is probably due to the use of a surfactant that partially destroys the cell compartments. Nonetheless our results reveal that NCp7 can potentially interact with TSG101.

In summary, we have used a series of biochemical assays to underline the role of NCp7 domain of Gag for the recruitment of TSG101. These approaches have provided evidences that the complex formation of Gag-TSG101 get compacted by direct interaction of TSG101 with GagNC and by the virtue of GagNC, Gag trafficking is responsible for the docking of TSG101 to the PM.

Legends

Figure 1: Schematic representation of Gag and TSG101 fusion constructs.

MA, CA, p1, p2 and p6 are designed as black rectangles while primary sequence of NCp7 is developed highlighting ZF1 and ZF2. Deletion of each zinc finger or of both zing fingers are symbolized by a bridge linking flaking basic residues. All Gag derivatives contain either a small tetracysteine (TC) motif sequence located at the C terminus of p6 or mCherry located downstream MA. Free NCp7 was expressed either as NCp7-TC or NCp7-eGFP while NCp7 derivatives were expressed as chimera protein with eGFP at their C terminus. TSG101 is shown as black box delineating TSG101 domains and harbors either HA tag or eGFP tag to its N terminus.

Figure 2: Co-expression of eGFP-Tsg101 and pNL 4.3

293T cells were co-transfected with viral DNA, eGFP-TSG101 and Gag-mCherry expressing plasmids (in a ratio 1/1). After 24h, cells were fixed with 4% PFA, cover slips mounted in presence of DAPI and observed by confocal microscopy. Images a to c: visualization of cell expressing of eGFP-TSG101 alone. Images d to f: visualization of cell co-expressing eGFP-TSG and Gag/Gag-mCherry. Images g to i: visualization of cell expressing eGFP-TSG101 and GagΔNC/GagΔNC-mcherry.

Figure 3: Both zinc fingers of GagNC participates with p6 to recruit TSG101

Lysates of HeLa cells expressing HA-TSG101 alone or together with Gag and Gag derivatives were subjected to immunoprecipitation assay using @HA antibody and protein A magnetic dynabeads. Hela cells were not transfected (well 1) or transfected by plasmids expressing HA-TSG101 (well 2) with Gag (wells 3), or GagΔZF1 (well 4) or GagΔZF2 (well 5) or GagΔNC (well 6) or GagΔp6 (well 7) or GagΔZF1ΔZF2 (well 8). Well 1': control corresponding to beads incubated with a sample containing HA-TSG and Gag but without anti HA. Well 2': sample containing HA-TSG101 and Gag treated with RNAse prior to IP. A: total cytoplasmic extract (Input). B: immunoprecipitation using rabbit anti-HA followed by a western blot analysis using mouse anti HA. C: Blot B was re-probed with polyclonal anti-Gag to identify the presence of Gag in the immunoprecipitates. D: Ratio of Gag and Gag derivatives pulled down by eGFP-TSG101. Levels of grey corresponding to HA-TSG (membrane B) and to Gag (membrane C) were determined by Image J and normalized to the signal obtained in the supernatant containing

Gag and TSG101 (well 3). The average comes from 3 to 5 independent experiments. * unspecific detection by polyclonal anti Gag.

Figure 4: Free NCp7 needs both zinc fingers to interact alone with TSG101

Lysates of HeLa cells expressing HA-TSG101 alone or together with NCp7-eGFP or NCp7-eGFP derivatives were subjected to immunoprecipitation assay using @eGFP antibody and protein A magnetic dynabeads. Hela cells were transfected by plasmids expressing HA-TSG101 (well 1) with NCp7-eGFP (well 2), or NCp7ΔZF1-eGFP (well 3) or NCp7ΔZF2-eGFP (well 4) or NCp7ΔZF1ΔZF2 (well 5). The total cytoplasmic extract was probed by mouse anti-eGFP and mouse anti-HA (input). Immunoprecipitation was performed with rabbit anti-eGFP followed by a western blot analysis with mouse anti-HA (IP). Membrane was reblotted with mouse anti eGFP to confirm the presence of NCp7-eGFP in immunoprecipitates.

Figure 5 : Co expression of eGFP-TSG101 and Gag or Gag derivatives by confocal microscopy

Confocal microscopy of HeLa cells expressing eGFP-TSG101 (a) together with Gag/Gag-mCherry (b), or GagΔZF1/ GagΔZF1-mCherry (c), or GagΔZF2/ GagΔZF2-mCherry (d), or GagΔZF1ΔZF2/ GagΔZF1ΔZF2-mCherry (e), or GagΔNC/ GagΔNC-mcherry (f), or GagΔp6/GagΔp6-mCherry (g), or NC/NC-mCherry. For each Gag derivative, HeLa cells were transfected with 0.25µg of plasmid eGFP-TSG, 0.5µg of plasmid expressing Gag (or mutated Gag) and 0.25µg of plasmid expressing Gag-mCH (or mutated Gag-mCherry). Cells were fixed by 1.5% of PFA 24h post transfection, and analyzed by confocal microscopy. Each panel shows the major observed phenotype.

Figure 6. Impact of NC deletion on Gag-TSG101 interaction, as monitored by FLIM.

Hela cells were seeded on 35 mm coverslips and transfected with plasmids expressing eGFP-TSG101 with Gag derivatives (in a ratio 0.2 eGFP-TSG101 / 0.8 Gag). 24h post transfection, cells were washed and labeled with ReAsH. FLIM measurements carried out using a 50×50 µm scale and 128×128 pixels as settings. A: The fluorescence lifetime of eGFP-TSG101 (a) or eGFP-TSG101co-expressed with GagΔp6-TC (b), or NC-TC (c) was measured in each pixel and

analyzed by using a single exponential model. Their values were converted into a color code, ranging from blue (0.7 ns) to red (2.4 ns). B: The fluorescence lifetime of eGFP-TSG101 in cell co expressing Gag-TC (d and i), GagΔZF1-TC (e and j), GagΔZF2-TC (f and k), GagΔZF1ΔZF2-TC (g and l), or GagΔNC-TC (h and m) were measured and analyzed by using a bi-exponential model with a long-lived lifetime component τ_2 fixed to the lifetime of free eGFP-TSG101 (2.26 ns). The τ_1 (top row) and α_1 (bottom row) values were converted into a colour code ranging from blue (0.7 ns, 10%) to red (2.4 ns, 90 %) respectively.

Figure 7: Histograms presenting FRET efficiency and population of the complex between Gag or Gag derivatives with TSG101

A: Histograms representing the FRET efficiencies between TC-labeled Gag or Gag mutants and eGFP-TSG101. The FRET efficiency was calculated using the equation (1) with the average lifetime values from at least 30 cells in three independent experiments. B: Histograms representing population of TSG101 engaged in Gag-TSG101 complex. Student tests were performed to compare the FRET efficiencies and populations (*: $p<0.05$, ****: $p<10^{-3}$).

Figure S1: Gag mediated localization of either HA and eGFP-tagged Tsg101.

HeLa cells were transfected with plasmid expressing HA-TSG101or eGFP-TSG101 together with a mixture of plasmids expressing Gag and Gag-mCherry. Cells were fixed with 1.5% of PFA. Panels a and b: cells were incubated with rabbit anti HA followed by anti-Rabbit Alexa 488. Panels c and d : cells were observed by confocal microscopy without immunodetection. Note that the staining of HA-TSG101 is highly similar to the detection of eGFP-TSG101.

Figure S2: Gag-TC and Gag-TC derivatives detected by ReAsH

HeLa cells were transfected with plasmid expressing eGFP-TSG101 or together with Gag-TC or Gag-TC derivatives. Cells were incubated with ReAsH and observed by confocal microscopy with an excitation at 488nm or 561nm for eGFP and ResAsH respectively. Images correspond to the superimposition of the red and green channels.

Figure S3: Gag-TSG101 interaction is independent from Gag accumulation to the PM

A: HeLa cells were transfected with a mixture of plasmids expressing eGFP-TSG101 and GagG2A-TC/GagG2A-mCherry. 24h post transfection, cells were observed by confocal microscopy after fixation. B: HeLa cells were transfected with a mixture of plasmids expressing eGFP-TSG101 and GagG2A-TC. 24h post transfection, cells were fixed and stained with ReAsH before FLIM.

Acknowledgments:

SIDACTION, ANRS, THINPAD, INSERM, CNRS, UDS, NIH Reagents, KS for fruitful discussion, Ott et Barbara for plasmid

Figures:

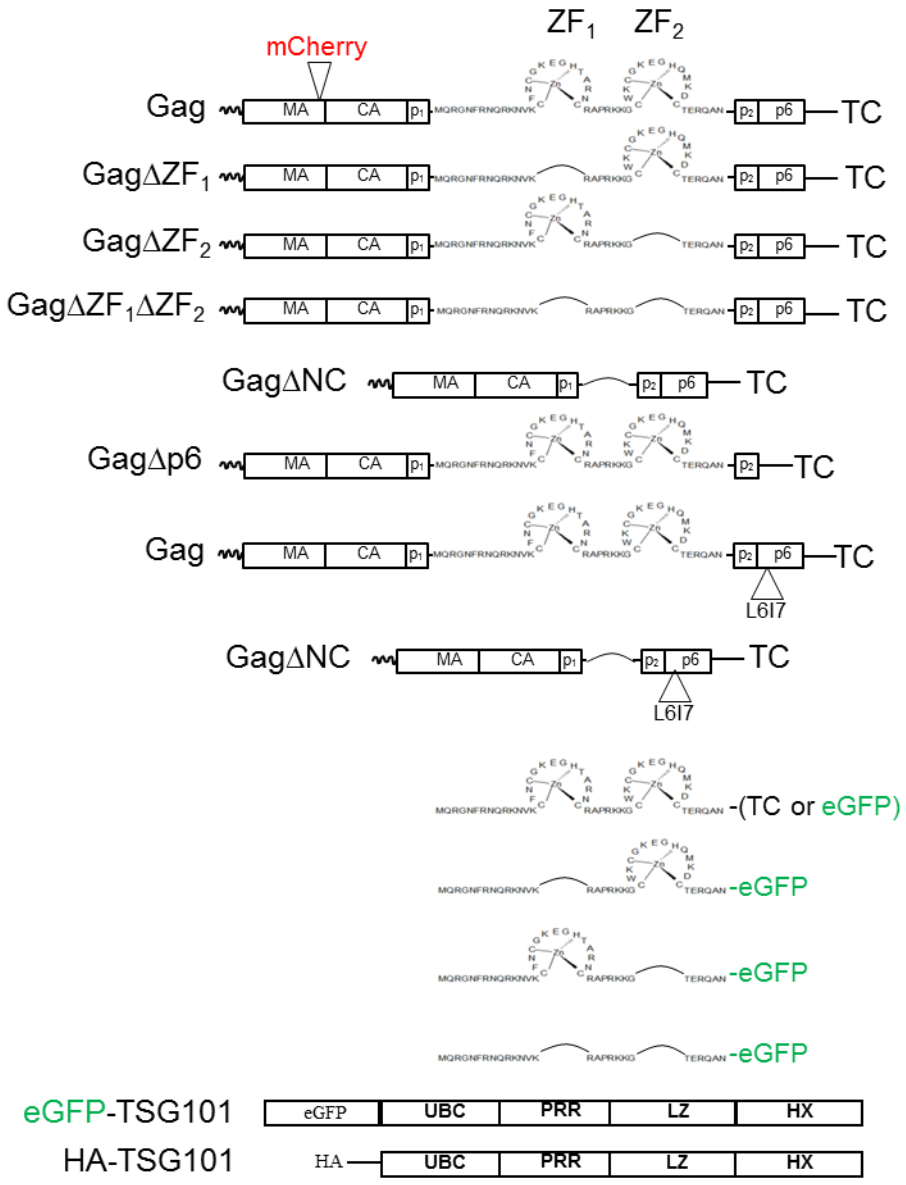

Figure 1

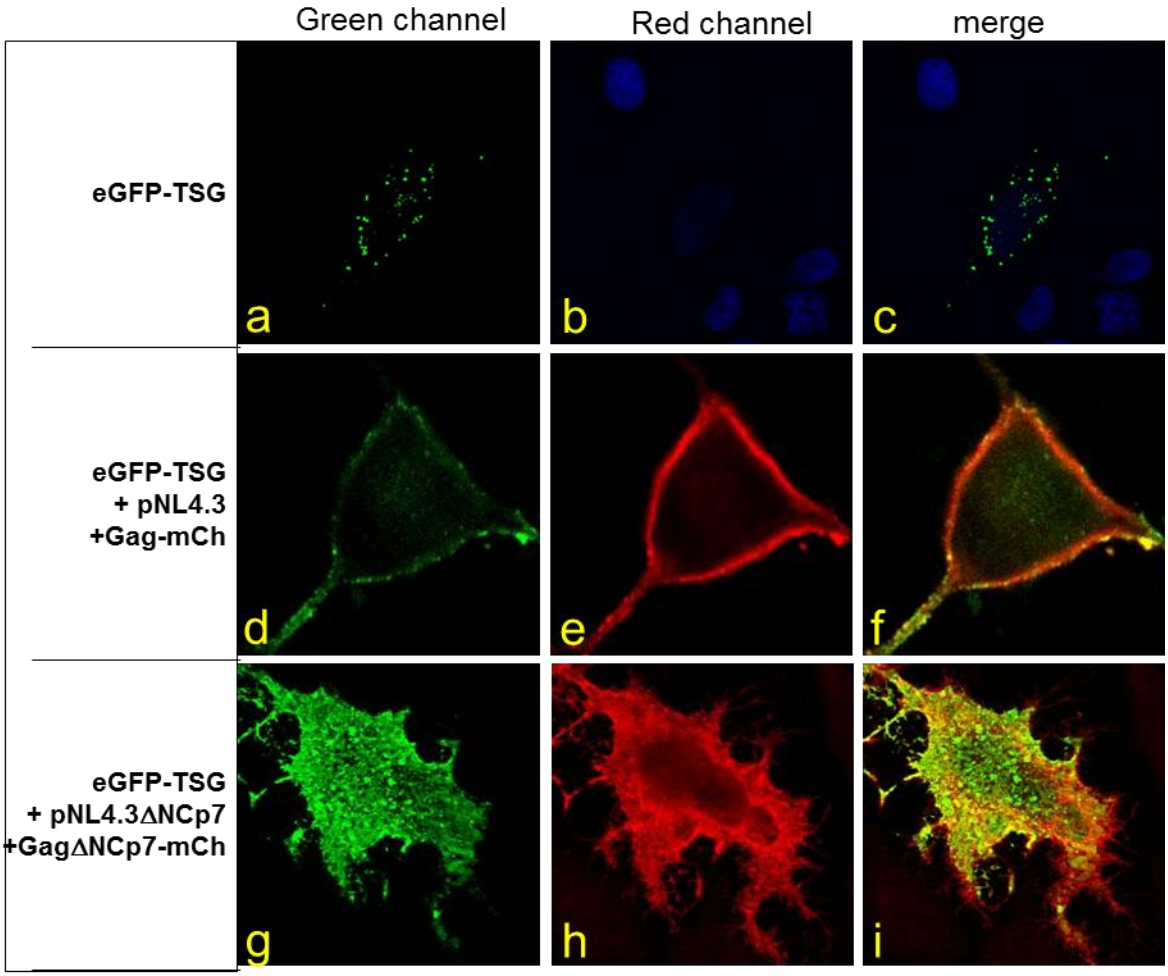
Green channel
Red channel
merge
eGFP-TSG
eGFP-TSG
+ pNL4.3
+Gag-mCh
eGFP-TSG
+ pNL4.3ΔNCp7
+GagΔNCp7-mCh
a
b
c
d
e
f
g
h
i

Figure 2

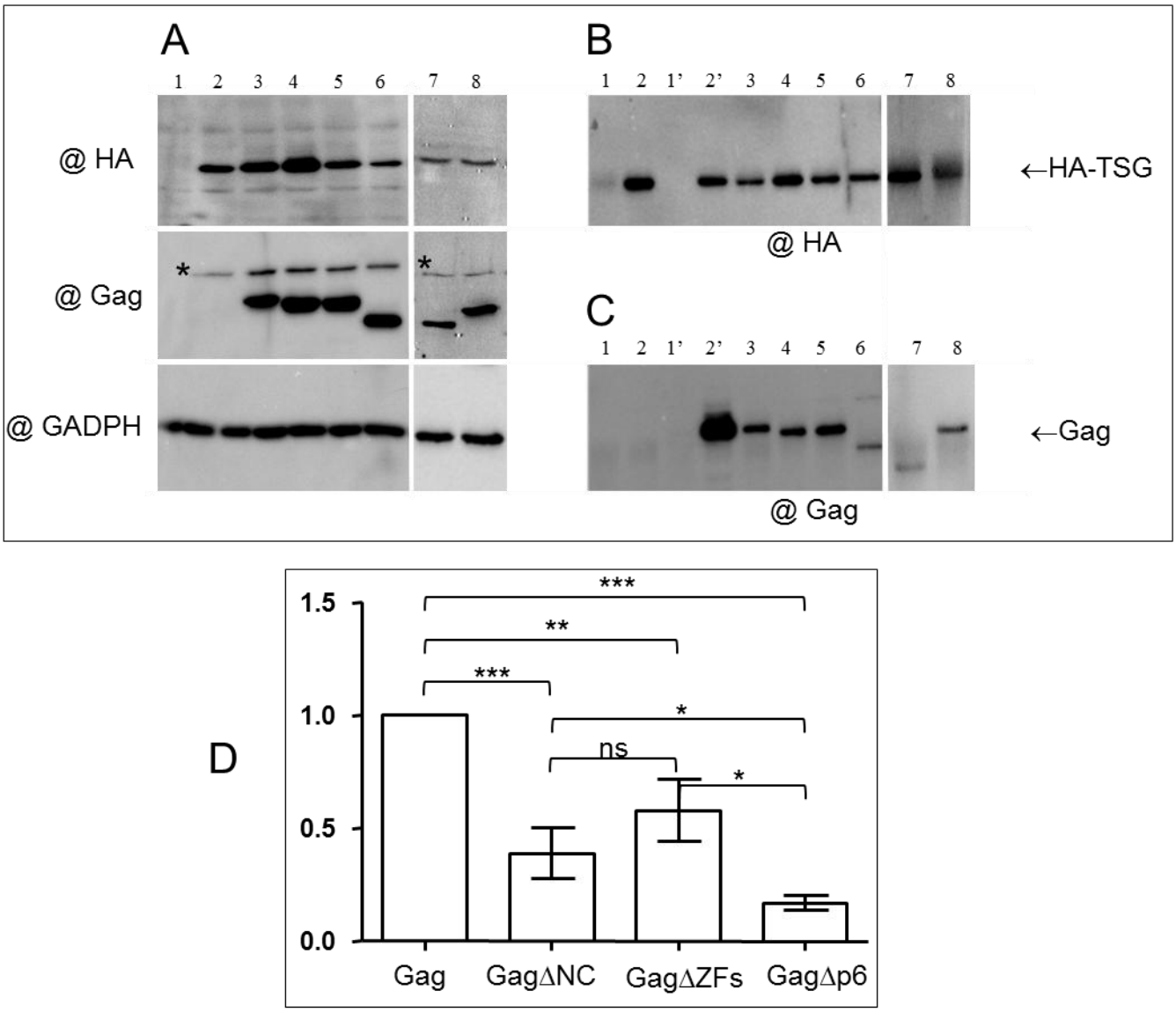
A
1 2 3 4 5 6 7 8
@ HA
@ Gag
@ GADPH
*
*
B
1 2 1' 2' 3 4 5 6 7 8
←HA-TSG
@ HA
C
1 2 1' 2' 3 4 5 6 7 8
←Gag
@ Gag
D
1.5
1.0
0.5
0.0
***
**
***
*
ns
*
Gag
GagΔNC
GagΔZFs
GagΔp6

Figure 3

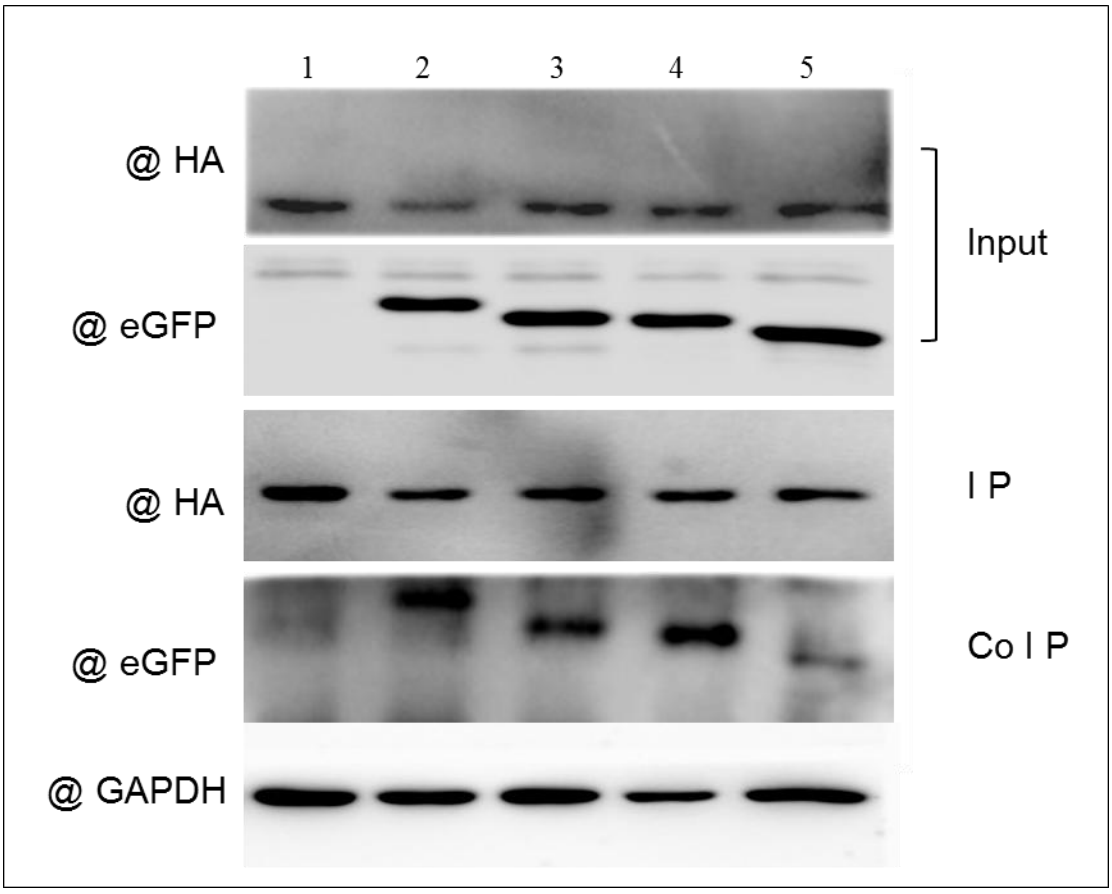

Figure 4

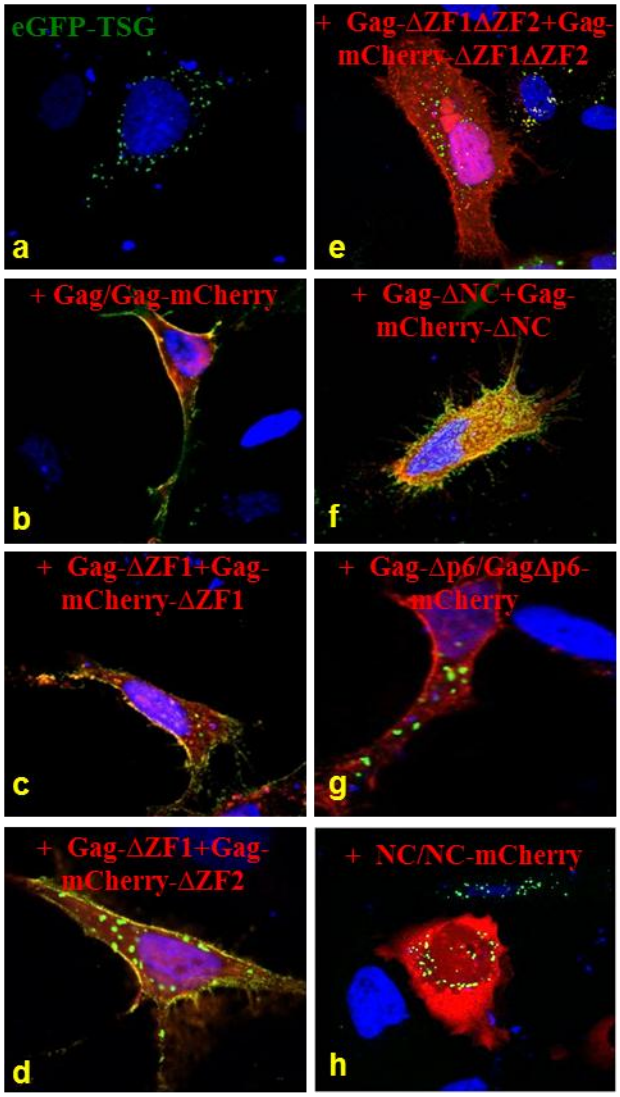
eGFP-TSG
a
+ Gag-ΔZF1ΔZF2+Gag-mCherry-ΔZF1ΔZF2
e
+ Gag/Gag-mCherry
b
+ Gag-ΔNC+Gag-mCherry-ΔNC
f
+ Gag-ΔZF1+Gag-mCherry-ΔZF1
c
+ Gag-Δp6/GagΔp6-mCherry
g
+ Gag-ΔZF1+Gag-mCherry-ΔZF2
d
+ NC/NC-mCherry
h

Figure 5

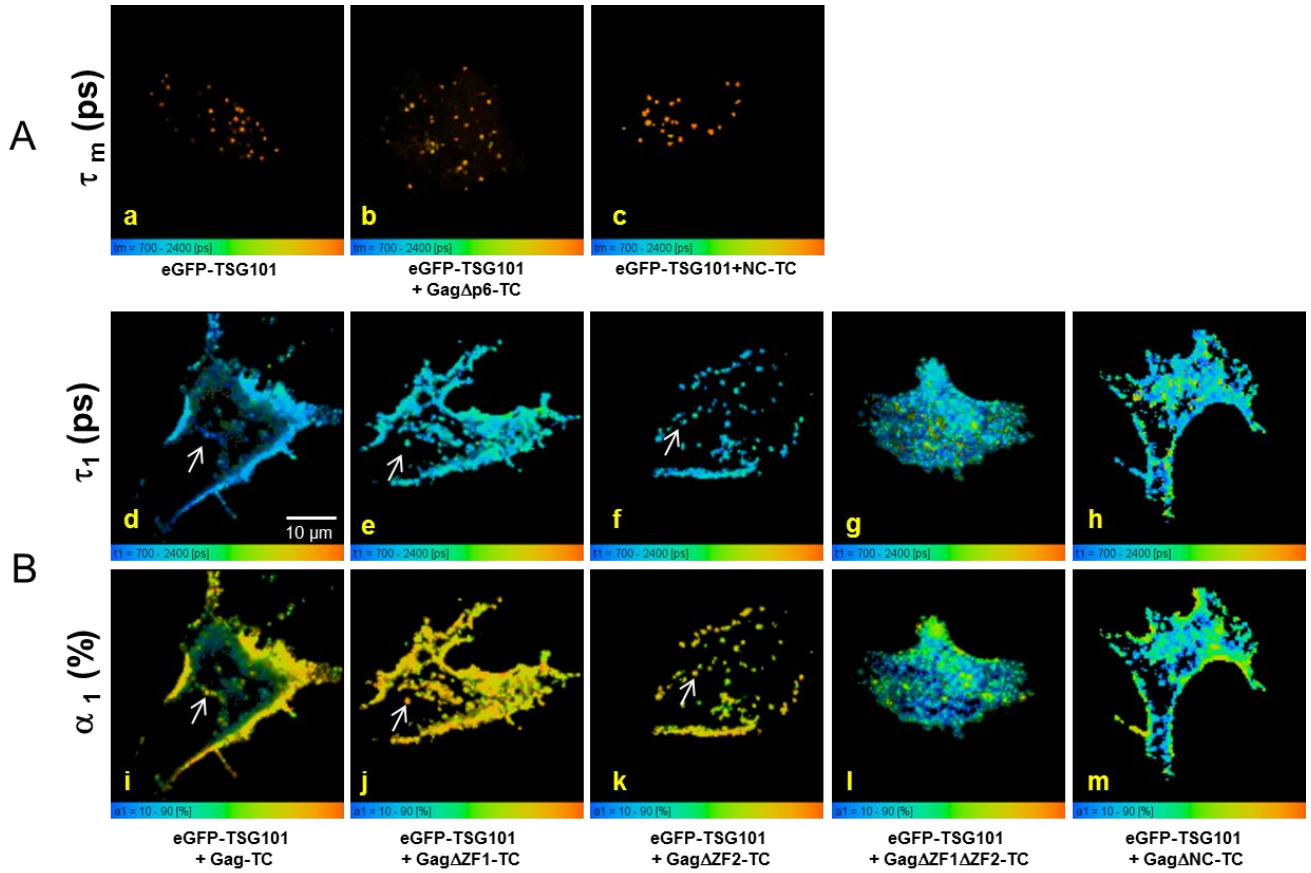
A
τ m (ps)
a
b
c
eGFP-TSG101
eGFP-TSG101
+ GagΔp6-TC
eGFP-TSG101+NC-TC
B
τ1 (ps)
d
e
f
g
h
10 µm
α 1 (%)
i
j
k
l
m
eGFP-TSG101
+ Gag-TC
eGFP-TSG101
+ GagΔZF1-TC
eGFP-TSG101
+ GagΔZF2-TC
eGFP-TSG101
+ GagΔZF1ΔZF2-TC
eGFP-TSG101
+ GagΔNC-TC

Figure 6

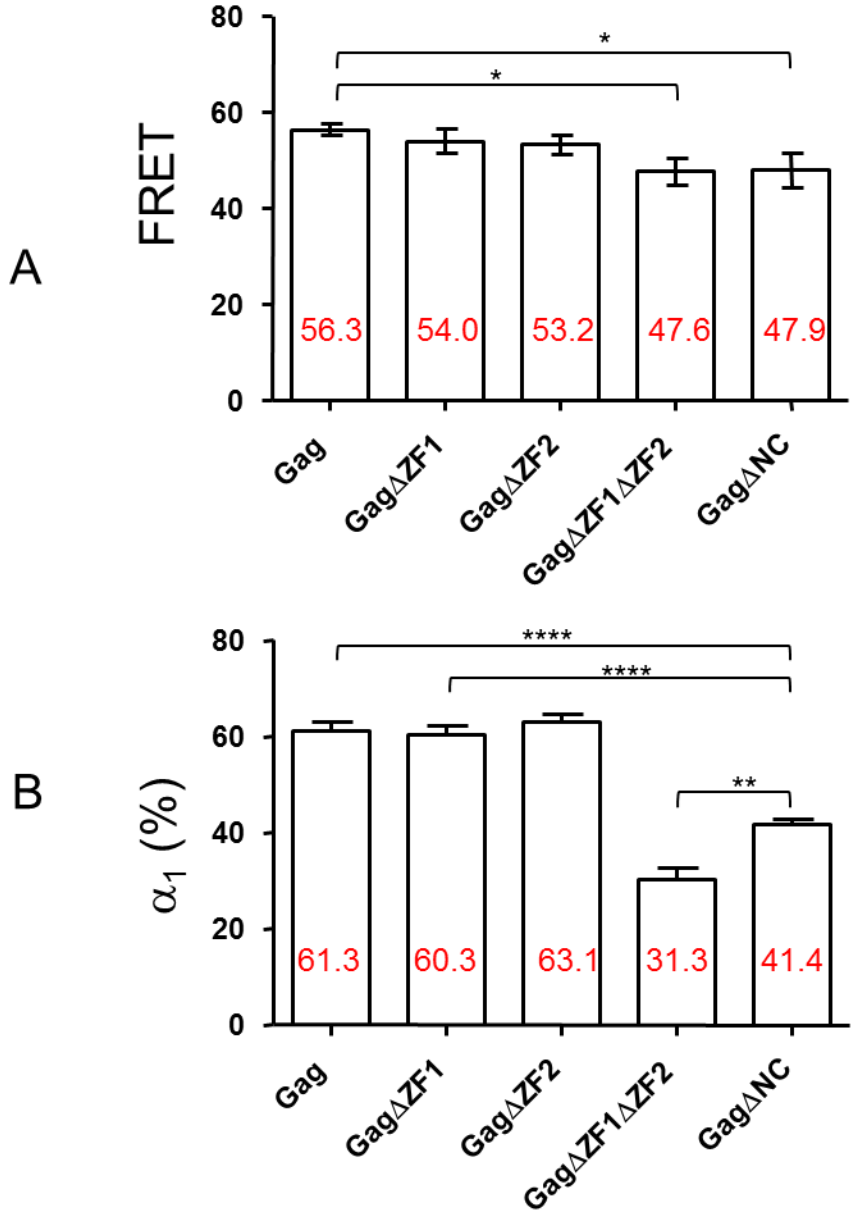

*<0.05**** <0.0001

Figure 7

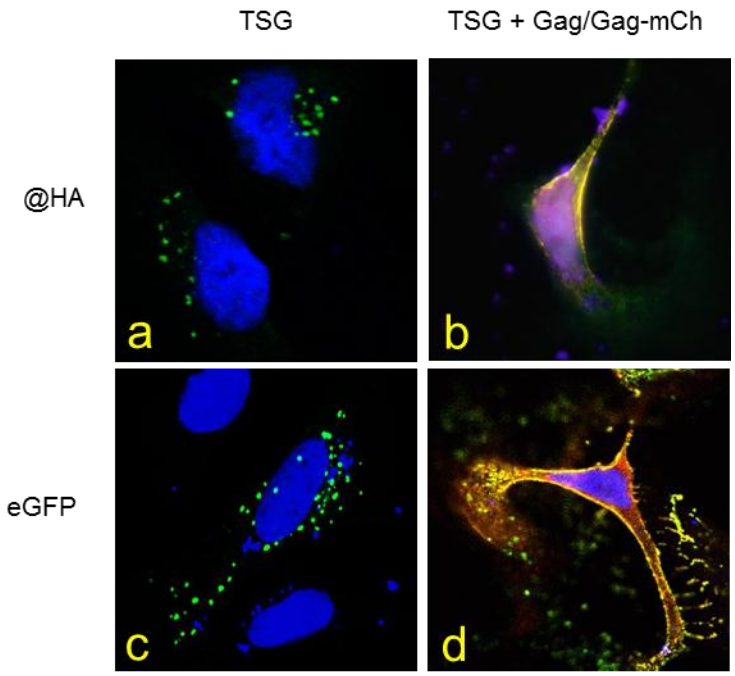

Figure S1

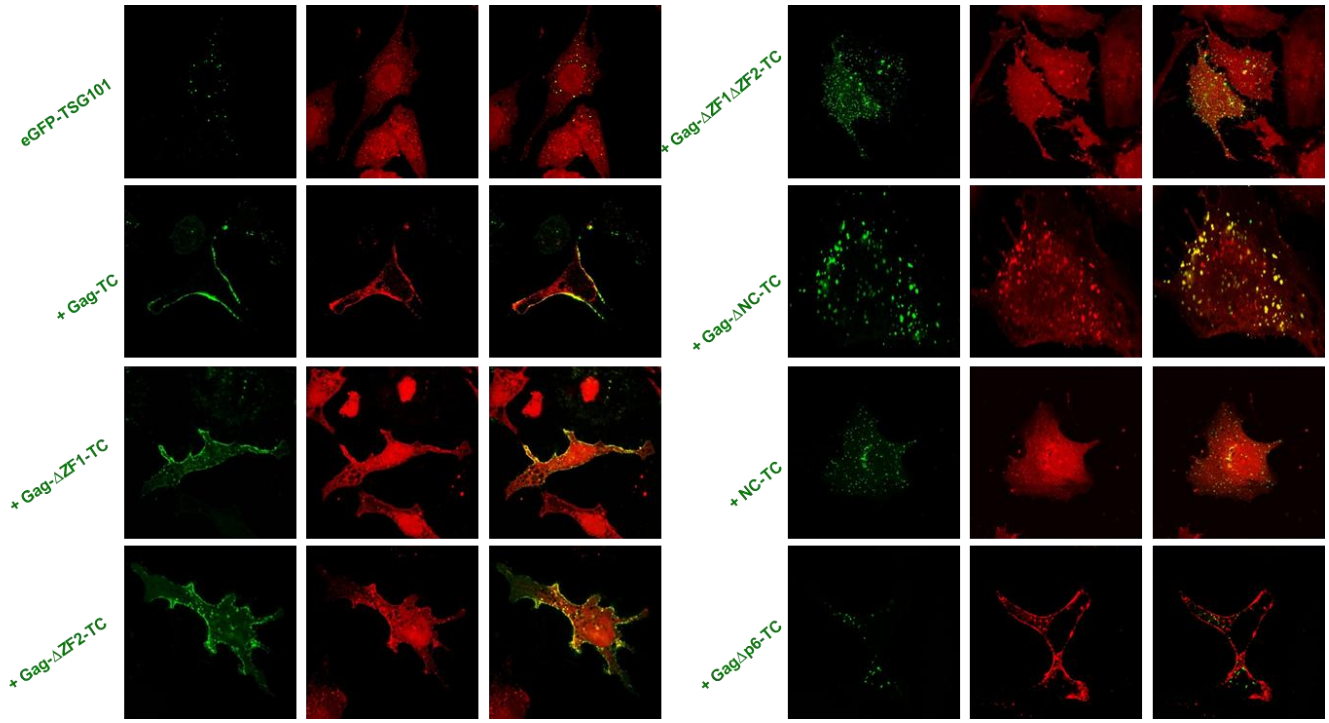

Figure S2

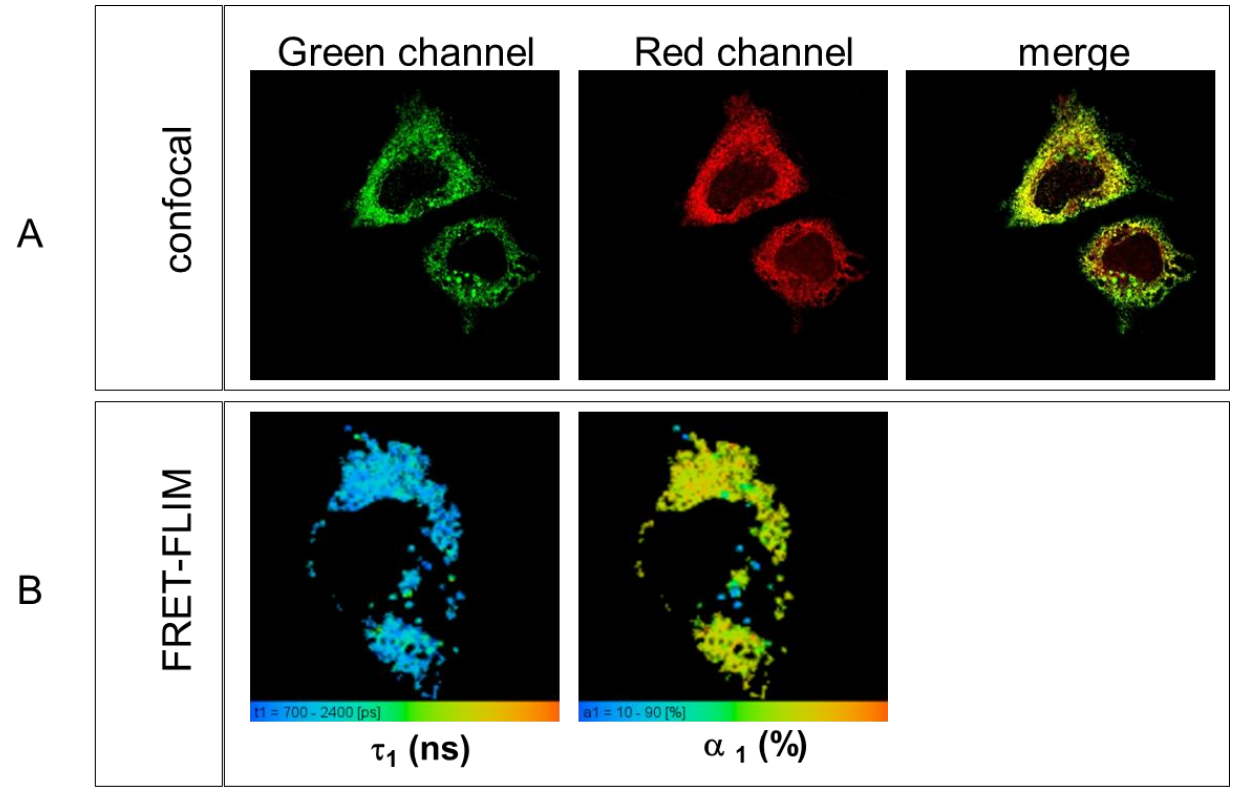
A
confocal
Green channel
Red channel
merge
B
FRET-FLIM
t1 = 700 - 2400 [ps]
a1 = 10 - 90 [%]
τ1 (ns)
α 1 (%)

Figure S3

References:

Adams, S. R., R. E. Campbell, et al. (2002). "New biarsenical ligands and tetracysteine motifs for protein labeling in vitro and in vivo: synthesis and biological applications." J Am Chem Soc **124**(21): 6063-6076.

Anton, H., N. Taha, et al. (2015). "Investigating the Cellular Distribution and Interactions of HIV-1 Nucleocapsid Protein by Quantitative Fluorescence Microscopy." PLoS One **10**(2): e0116921.

Bello, N. F., V. Dussupt, et al. (2012). "Budding of retroviruses utilizing divergent L domains requires nucleocapsid." J Virol **86**(8): 4182-4193.

Bieniasz, P. D. (2006). "Late budding domains and host proteins in enveloped virus release." Virology **344**(1): 55-63.

Bleck, M., M. S. Itano, et al. (2014). "Temporal and spatial organization of ESCRT protein recruitment during HIV-1 budding." Proc Natl Acad Sci U S A **111**(33): 12211-12216.

Chamontin, C., P. Rassam, et al. (2015). "HIV-1 nucleocapsid and ESCRT-component Tsg101 interplay prevents HIV from turning into a DNA-containing virus." Nucleic Acids Res **43**(1): 336-347.

Chukkapalli, V., S. J. Oh, et al. (2010). "Opposing mechanisms involving RNA and lipids regulate HIV-1 Gag membrane binding through the highly basic region of the matrix domain." Proc Natl Acad Sci U S A **107**(4): 1600-1605.

Cimarelli, A., S. Sandin, et al. (2000). "Basic residues in human immunodeficiency virus type 1 nucleocapsid promote virion assembly via interaction with RNA." J Virol **74**(7): 3046-3057.

Clamme, J. P., J. Azoulay, et al. (2003). "Monitoring of the formation and dissociation of polyethylenimine/DNA complexes by two photon fluorescence correlation spectroscopy." Biophys J **84**(3): 1960-1968.

Darlix, J. L., H. de Rocquigny, et al. (2014). "Retrospective on the all-in-one retroviral nucleocapsid protein." Virus Res **193**: 2-15.

Demirov, D. G., A. Ono, et al. (2002). "Overexpression of the N-terminal domain of TSG101 inhibits HIV-1 budding by blocking late domain function." Proc Natl Acad Sci U S A **99**(2): 955-960.

Demirov, D. G., J. M. Orenstein, et al. (2002). "The late domain of human immunodeficiency virus type 1 p6 promotes virus release in a cell type-dependent manner." J Virol **76**(1): 105-117.

Derdowski, A., L. Ding, et al. (2004). "A novel fluorescence resonance energy transfer assay demonstrates that the human immunodeficiency virus type 1 Pr55Gag I domain mediates Gag-Gag interactions." J Virol **78**(3): 1230-1242.

Dussupt, V., M. P. Javid, et al. (2009). "The nucleocapsid region of HIV-1 Gag cooperates with the PTAP and LYPXnL late domains to recruit the cellular machinery necessary for viral budding." PLoS Pathog **5**(3): e1000339.

Dussupt, V., P. Sette, et al. (2011). "Basic residues in the nucleocapsid domain of Gag are critical for late events of HIV-1 budding." J Virol **85**(5): 2304-2315.

El Meshri, S. E., D. Dujardin, et al. (2015). "Role of the Nucleocapsid Domain in HIV-1 Gag Oligomerization and Trafficking to the Plasma Membrane: A Fluorescence Lifetime Imaging Microscopy Investigation." J Mol Biol **427**(6 Pt B): 1480-1494.

El Meshri, S. E., D. Dujardin, et al. (2015). "Role of the nucleocapsid domain in HIV-1 Gag oligomerization and trafficking to the plasma membrane: A fluorescence lifetime imaging microscopy investigation." J Mol Biol.

Fritz, J. V., P. Didier, et al. (2008). "Direct Vpr-Vpr interaction in cells monitored by two photon fluorescence correlation spectroscopy and fluorescence lifetime imaging." Retrovirology **5**: 87.

Fritz, J. V., D. Dujardin, et al. (2010). "HIV-1 Vpr oligomerization but not that of Gag directs the interaction between Vpr and Gag." J Virol **84**(3): 1585-1596.

Gan, X. and S. J. Gould (2012). "HIV Pol inhibits HIV budding and mediates the severe budding defect of Gag-Pol." PLoS One **7**(1): e29421.

Garrus, J. E., U. K. von Schwedler, et al. (2001). "Tsg101 and the vacuolar protein sorting pathway are essential for HIV-1 budding." Cell **107**(1): 55-65.

Goila-Gaur, R., D. G. Demirov, et al. (2003). "Defects in human immunodeficiency virus budding and endosomal sorting induced by TSG101 overexpression." J Virol **77**(11): 6507-6519.

Gottlinger, H. G., T. Dorfman, et al. (1991). "Effect of mutations affecting the p6 gag protein on human immunodeficiency virus particle release." Proc Natl Acad Sci U S A **88**(8): 3195-3199.

Gousset, K., S. D. Ablan, et al. (2008). "Real-Time Visualization of HIV-1 GAG Trafficking in Infected Macrophages." PLoS Pathog **4**(3): e1000015.

Grigorov, B., D. Decimo, et al. (2007). "Intracellular HIV-1 Gag localization is impaired by mutations in the nucleocapsid zinc fingers." Retrovirology **4**: 54.

Hogue, I. B., A. Hoppe, et al. (2009). "Quantitative fluorescence resonance energy transfer microscopy analysis of the human immunodeficiency virus type 1 Gag-Gag interaction: relative contributions of the CA and NC domains and membrane binding." J Virol **83**(14): 7322-7336.

Huang, M., J. M. Orenstein, et al. (1995). "p6Gag is required for particle production from full-length human immunodeficiency virus type 1 molecular clones expressing protease." J Virol **69**(11): 6810-6818.

Hubner, W., P. Chen, et al. (2007). "Sequence of human immunodeficiency virus type 1 (HIV-1) Gag localization and oligomerization monitored with live confocal imaging of a replication-competent, fluorescently tagged HIV-1." J Virol **81**(22): 12596-12607.

Im, Y. J., L. Kuo, et al. (2010). "Crystallographic and functional analysis of the ESCRT-I /HIV-1 Gag PTAP interaction." Structure **18**(11): 1536-1547.

Ivanchenko, S., W. J. Godinez, et al. (2009). "Dynamics of HIV-1 assembly and release." PLoS Pathog **5**(11): e1000652.

Johnson, M. C., J. L. Spidel, et al. (2005). "The C-terminal half of TSG101 blocks Rous sarcoma virus budding and sequesters Gag into unique nonendosomal structures." J Virol **79**(6): 3775-3786.

Jouvenet, N., P. D. Bieniasz, et al. (2008). "Imaging the biogenesis of individual HIV-1 virions in live cells." Nature **454**(7201): 236-240.

Kempf, N., V. Postupalenko, et al. (2015). "The HIV-1 Nucleocapsid Protein Recruits Negatively Charged Lipids To Ensure Its Optimal Binding to Lipid Membranes." J Virol **89**(3): 1756-1767.

Kerviel, A., A. Thomas, et al. (2013). "Virus assembly and plasma membrane domains: which came first?" Virus Res **171**(2): 332-340.

Lampe, M., J. A. Briggs, et al. (2007). "Double-labelled HIV-1 particles for study of virus-cell interaction." Virology **360**(1): 92-104.

Larson, D. R., M. C. Johnson, et al. (2005). "Visualization of retrovirus budding with correlated light and electron microscopy." Proc Natl Acad Sci U S A **102**(43): 15453-15458.

Lochmann, T. L., D. V. Bann, et al. (2013). "NC-mediated nucleolar localization of retroviral gag proteins." Virus Res **171**(2): 304-318.

Martin-Serrano, J., A. Yarovoy, et al. (2003). "Divergent retroviral late-budding domains recruit vacuolar protein sorting factors by using alternative adaptor proteins." Proc Natl Acad Sci U S A **100**(21): 12414-12419.

Martin-Serrano, J., T. Zang, et al. (2001). "HIV-1 and Ebola virus encode small peptide motifs that recruit Tsg101 to sites of particle assembly to facilitate egress." Nat Med **7**(12): 1313-1319.

Muller, B., J. Daecke, et al. (2004). "Construction and characterization of a fluorescently labeled infectious human immunodeficiency virus type 1 derivative." J Virol **78**(19): 10803-10813.

Muriaux, D. and J. L. Darlix (2010). "Properties and functions of the nucleocapsid protein in virus assembly." RNA Biol **7**(6): 744-753.

Ott, D. E., L. V. Coren, et al. (2003). "Elimination of protease activity restores efficient virion production to a human immunodeficiency virus type 1 nucleocapsid deletion mutant." J Virol **77**(10): 5547-5556.

Ott, D. E., L. V. Coren, et al. (2005). "Redundant roles for nucleocapsid and matrix RNA-binding sequences in human immunodeficiency virus type 1 assembly." J Virol **79**(22): 13839-13847.

Ott, D. E., L. V. Coren, et al. (2009). "The nucleocapsid region of human immunodeficiency virus type 1 Gag assists in the coordination of assembly and Gag processing: role for RNA-Gag binding in the early stages of assembly." J Virol **83**(15): 7718-7727.

Popov, S., E. Popova, et al. (2008). "Human immunodeficiency virus type 1 Gag engages the Bro1 domain of ALIX/AIP1 through the nucleocapsid." J Virol **82**(3): 1389-1398.

Popova, E., S. Popov, et al. (2010). "Human immunodeficiency virus type 1 nucleocapsid p1 confers ESCRT pathway dependence." J Virol **84**(13): 6590-6597.

Pornillos, O., S. L. Alam, et al. (2002). "Structure of the Tsg101 UEV domain in complex with the PTAP motif of the HIV-1 p6 protein." Nat Struct Biol **9**(11): 812-817.

Prescher, J., V. Baumgartel, et al. (2015). "Super-resolution imaging of ESCRT-proteins at HIV-1 assembly sites." PLoS Pathog **11**(2): e1004677.

Puffer, B. A., L. J. Parent, et al. (1997). "Equine infectious anemia virus utilizes a YXXL motif within the late assembly domain of the Gag p9 protein." J Virol **71**(9): 6541-6546.

Richert, L., P. Didier, et al. (2015). "Monitoring HIV-1 Protein Oligomerization by FLIM FRET Microscopy " Advanced Time-Correlated Single Photon Counting Applications

Springer Series in Chemical Physics **111**: 277-307.

Rudner, L., S. Nydegger, et al. (2005). "Dynamic fluorescent imaging of human immunodeficiency virus type 1 gag in live cells by biarsenical labeling." J Virol **79**(7): 4055-4065.

Soderberg, O., M. Gullberg, et al. (2006). "Direct observation of individual endogenous protein complexes in situ by proximity ligation." Nat Methods **3**(12): 995-1000.

Soderberg, O., K. J. Leuchowius, et al. (2008). "Characterizing proteins and their interactions in cells and tissues using the in situ proximity ligation assay." Methods **45**(3): 227-232.

Strack, B., A. Calistri, et al. (2003). "AIP1/ALIX is a binding partner for HIV-1 p6 and EIAV p9 functioning in virus budding." Cell **114**(6): 689-699.

Strack, B., A. Calistri, et al. (2002). "Late assembly domain function can exhibit context dependence and involves ubiquitin residues implicated in endocytosis." J Virol **76**(11): 5472-5479.

Sun, Y., C. Rombola, et al. (2013). "Forster resonance energy transfer microscopy and spectroscopy for localizing protein-protein interactions in living cells." Cytometry A **83**(9): 780-793.

Sundquist, W. I. and H. G. Krausslich (2012). "HIV-1 assembly, budding, and maturation." Cold Spring Harb Perspect Med **2**(7): a006924.

VerPlank, L., F. Bouamr, et al. (2001). "Tsg101, a homologue of ubiquitin-conjugating (E2) enzymes, binds the L domain in HIV type 1 Pr55(Gag)." Proc Natl Acad Sci U S A **98**(14): 7724-7729.

von Schwedler, U. K., M. Stuchell, et al. (2003). "The protein network of HIV budding." Cell **114**(6): 701-713.

Votteler, J. and W. I. Sundquist (2013). "Virus budding and the ESCRT pathway." Cell Host Microbe **14**(3): 232-241.

Wang, W., N. Naiyer, et al. (2014). "Distinct nucleic acid interaction properties of HIV-1 nucleocapsid protein precursor NCp15 explain reduced viral infectivity." Nucleic Acids Res.

Yuan, B., S. Campbell, et al. (2000). "Infectivity of Moloney murine leukemia virus defective in late assembly events is restored by late assembly domains of other retroviruses." J Virol **74**(16): 7250-7260.

General Conclusions and Future Perspectives

Late steps of HIV-1 life cycle include assembly of structural precursors, budding of the new particle and maturation into fully infectious virions. Despite the huge number of studies devoted to the definition of molecular mechanisms regulating these steps, a number of question remains to be answered before they are clearly apprehended. Gag is 55-amino acid protein from HIV-1 virus that orchestrates the viral particles assembly and budding. It is composed of matrice (MA), capsid (CA), nucleocapsid (NCp7) and p6 domains. During the course of assembly, Gag is transported from translating ribosomes to plasma membrane, and get further involved with virion budding. In order to complete virion assembly, trafficking and ultimately budding, Gag hijacks cellular proteins of the cytoskeleton and the ESCRT (Endosomal Sorting Complex Required for Transport) like TSG101, Alix, etc.,. Till now, to understand the Gag assembly process, a panel of biochemical analyses on *in vitro* model systems and model cell lines such as HeLa cells has been used.

During this thesis the main aim was to clarify the roles of NCp7 domain of Gag (GagNC) during the assembly/budding process. In this quest, we first summarized fluorescence-based techniques notably quantitative fluorescence microscopy techniques (confocal, epifluorescence, FLIM) to decipher the mechanisms and the role of this domain of entire Gag protein in retrovirus assembly. We described the key advantage of such techniques to directly visualize and evidence Gag–Gag interactions in a cellular context. It was observed that the FLIM approach provides a much better contrast than that based on epifluorescence microscopy. We managed conditions to visualize the sub-structures, at the PM and in the cytoplasm, where Gag assembly takes place, by FLIM. The importance of the work become more in magnitude as the conditions were characterized in for live cells **(publication 1).**

Later on, we applied vigorously these quantitative fluorescent microscopy and biochemical approaches and we conclude mainly on two undermentioned aspects of budding process.

1. **Gag-Gag Oligomerisation**

To study Gag-Gag interaction, plasmids expressing Gag and mutations in Gag like GagΔNCp7, GagΔZF1, GagΔZF2 and GagΔZF1/ZF2 were transiently transfected and expression of proteins were followed by FLIM based FRET and western blot. By FRET, we were able to follow Gag-Gag interaction at the level of the plasma membrane in agreement with the role of this protein

during the formation of the viral particles. Interestingly, FRET was also observed within the cytoplasm suggesting that the polymerisation of Gag is initiated before the anchorage of Gag to the PM. When NCp7 or both Zing fingers of NCp7 were removed from the Gag precursor, the average lifetime was intermediate suggesting a profound defect in Gag-Gag assembly. Moreover, mutated Gag was only partly accumulating to the PM showing a strict correlation between Gag oligomerization and Gag accumulation at the periphery of the cell. Our results clearly indicate that Gag proteins form compact oligomers in the cytoplasm, likely as a result of both CA-CA interactions and NC-promoted binding to nucleic acids. The oligomers progressively assemble, and grow in size during trafficking from the cytoplasm toward the membrane. The NC domain favors the compactness and binding of Gag oligomers to the PM and the proper timing of viral particle assembly at the PM, likely as a result of its interaction with cell proteins involved in Gag trafficking. While the proximal zinc finger appears dispensable for oligomer compaction and membrane binding, the distal finger and the flanking basic domains appear critical for these properties. Based on these results, the full NC sequence appears important for the proper timing of Gag assembly (**Publication 2**).

Work is now in progress to describe the interaction between Gag and the RNA. Schematically, Gag interacts none specifically with cellular RNA during the assembly of the particle while a specific recognition between Gag and the viral RNA is required to encapsidate the genome. Concerning the first issue, the RNA of cell expressing Gag/Gag-eGFP will be labelled with Sytox, a chemical compound that interacts both with RNA and DNA. This chromophore was used in the lab to monitor the interaction between NCp7 and cellular RNA by FRET (Anton, Taha et al. 2015) . If a direct interaction is evidenced between Gag-eGFP and RNA-Sytox by FLIM, we will use this tool to detail Gag-RNA interaction in cellular context. First, the role of GagNC in the recognition of cellular RNA will be assessed by comparing wild type GagNC and all the constructs deleted from the zinc fingers. It can be hypothesised that GagΔZF1ZF2, containing the basic residues surrounding the zinc fingers, will interact as well as wt Gag with cellular RNA.

Meanwhile, the relationship between Gag oligomerisation and Gag-RNA interaction will be tested using Gag mutated at the level of the CA. It was shown by us and others that GagWM

could oligomerize by forming less dense structure. The level of FRET between GagWM and RNA Sytox will document the accessibility to the solvent for GagNC.

At last, the impact of the anchoring of Gag at the PM to the RNA recognition will be tested using Gag G2A construct or mutation in the HBR sequence of MA. In fact, in the actual model of Gag assembly, both MA and NC interact with the RNA and this Gag-RNA complex binds to the cytoplasmic leaflet of the PM. If the FRET varies with these constructs that would suggest that docking of Gag to the PM reorganises Gag-RNA interaction.

Concerning a specific interaction between Gag and RNA, a series of plasmids are currently under construction or obtained from the literature. Concerning the RNA, the construct contains all cis acting sequences required for the RNA to be export outside the nucleus (RRE) and encapsidated (Leader region encompassing the first 5-700 bases). In addition, this construct contains a series of stem loop interacting either with labelled MS2 or Lambda. This construct will be co-transfected with a plasmid expressing all proteins except ENV together with labelled Gag. The interaction between Gag and ψ containing RNA will be followed by FRET and/or by TIRF. Then mutations in *cis* acting and *trans* acting sequences will detail the mechanism whereby the specific GagNC is able to enrich the genomic RNA in nascent particles.

2. Gag trafficking/Gag-TSG101 interaction

After defining the vital role of NCp7 in Gag-Gag oligomerization and irreplaceable role in Gag-trafficking to the PM, we explored the interaction of Gag and, role of NCp7 domain, with other cellular proteins that may be involved during viral egress. Earlier studies with western blot technique showed that cells expressing GagΔNC resulted in decrease of viral particles production. Consistent with the role of NC region and ESCRT protein TSG101 in virus release, we investigated the interaction between TSG101 and Gag that constitute our second conclusion.

We validated the interaction between native Gag and Gag mutants like GagΔNCp7, GagΔZF1/ZF2, GagΔZF1, GagΔZF2 and GagΔp6 with TSG101, their co-localisation in cells, and the impact of Gag mutations on these assembly processes by immunopricipitation, confocal and FLIM microscopy technique. We demonstrated that the NCp7 alone or as a domain of Gag

(GagNC) was required for Gag to interact with TSG101. Our results showed a drastic decrease (4 to 6-times less as compare to wild type Gag) in binding and complete abruption of trafficking for Gag/Tsg101 complex in absence of NC domain. This indicates a reduced interaction between the two proteins when NCp7 domain is not present in the Gag precursor. Further experiments with NC mutants showed that the NCp7 mediated interaction between Gag and TSG101 necessitates at least one of the two zinc. Later on, by analyzing amplitudes associated to the short-lived lifetime in the cytoplasm, in vesicles and at the PM, it was concluded that Gag is the main driving force needed for TSG101 trafficking. As NCp7 region drives the trafficking of Gag and Gag drives the trafficking of TSG101, it is evident that NCp7 region is a must for TSG101 trafficking. Later that GagGag/TSG101 interaction is also confirmed in the context of whole virus by our collaborators in CPBS Montpellier.

Collectively, our results first support a model in which NCp7 domain cooperates with the p6 domain to interact with Tsg101, thus giving an insight into the functional link between p6 Late domain motifs and NC as well as regulatory role of NCp7 domain in the course of recruiting components of the cellular machinery necessary for HIV-1 budding. Moreover, our results also showed the RNA-independency of Gag-TSG101 interaction that seems highly contrasted to the interaction of NC and Bro 1 domain of ALIX protein during the LYPXnL pathway. This leaves to imply that the two mechanisms maybe not redundant but rather that the NC could recruit simultaneously both TSG101 and ALIX proteins in order to best optimize the chances of the virus to bud (**Publication 3**).

In the end, the regulatory effect of NCp7 domain in either TSG101 or Gag or both protein-regulated pathway during virus budding can be exploited to develop inhibitors targeting HIV-1.

Meanwhile, this information can be utilized to investigate temporal and spatial organization of Gag with respect to ESCRT proteins during HIV-1 budding, either by using *invitro* biophysical techniques or by super-resolution imaging. Another, key aspect of budding process can be explored that involve possible interactions of Gag with fission related proteins like dynamin 2, synaptojanin, endophilin, etc, by using this *invitro* approach.

REFERENCES

Abrahamyan, L. G., L. Chatel-Chaix, et al. (2010). "Novel Staufen1 ribonucleoproteins prevent formation of stress granules but favour encapsidation of HIV-1 genomic RNA." J Cell Sci **123**(Pt 3): 369-383.

Accola, M. A., A. Ohagen, et al. (2000). "Isolation of human immunodeficiency virus type 1 cores: retention of Vpr in the absence of p6(gag)." J Virol **74**(13): 6198-6202.

Accola, M. A., B. Strack, et al. (2000). "Efficient particle production by minimal Gag constructs which retain the carboxy-terminal domain of human immunodeficiency virus type 1 capsid-p2 and a late assembly domain." J Virol **74**(12): 5395-5402.

Adamson, C. S. and E. O. Freed (2007). "Human immunodeficiency virus type 1 assembly, release, and maturation." Adv Pharmacol **55**: 347-387.

Adamson, C. S. and E. O. Freed (2008). "Recent progress in antiretrovirals--lessons from resistance." Drug Discov Today **13**(9-10): 424-432.

Albertazzi, L., D. Arosio, et al. (2009). "Quantitative FRET analysis with the EGFP-mCherry fluorescent protein pair." Photochem Photobiol **85**(1): 287-297.

Alce, T. M. and W. Popik (2004). "APOBEC3G is incorporated into virus-like particles by a direct interaction with HIV-1 Gag nucleocapsid protein." J Biol Chem **279**(33): 34083-34086.

Aldovini, A. and R. A. Young (1990). "Mutations of RNA and protein sequences involved in human immunodeficiency virus type 1 packaging result in production of noninfectious virus." J Virol **64**(5): 1920-1926.

Alfadhli, A., H. McNett, et al. (2011). "HIV-1 matrix protein binding to RNA." J Mol Biol **410**(4): 653-666.

Alkalaeva, E. Z., A. V. Pisarev, et al. (2006). "In vitro reconstitution of eukaryotic translation reveals cooperativity between release factors eRF1 and eRF3." Cell **125**(6): 1125-1136.

Amarasinghe, G. K., R. N. De Guzman, et al. (2000). "NMR structure of stem-loop SL2 of the HIV-1 psi RNA packaging signal reveals a novel A-U-A base-triple platform." J Mol Biol **299**(1): 145-156.

Anton, H., N. Taha, et al. (2015). "Investigating the Cellular Distribution and Interactions of HIV-1 Nucleocapsid Protein by Quantitative Fluorescence Microscopy." PLoS One **10**(2): e0116921.

Antson, A. A., J. Otridge, et al. (1995). "The structure of trp RNA-binding attenuation protein." Nature **374**(6524): 693-700.

Auclair, J. R., K. M. Green, et al. (2007). "Mass spectrometry analysis of HIV-1 Vif reveals an increase in ordered structure upon oligomerization in regions necessary for viral infectivity." Proteins **69**(2): 270-284.

Azoulay, J., J. P. Clamme, et al. (2003). "Destabilization of the HIV-1 complementary sequence of TAR by the nucleocapsid protein through activation of conformational fluctuations." J Mol Biol **326**(3): 691-700.

Babst, M., G. Odorizzi, et al. (2000). "Mammalian tumor susceptibility gene 101 (TSG101) and the yeast homologue, Vps23p, both function in late endosomal trafficking." Traffic **1**(3): 248-258.

Bachand, F., X. J. Yao, et al. (1999). "Incorporation of Vpr into human immunodeficiency virus type 1 requires a direct interaction with the p6 domain of the p55 gag precursor." J Biol Chem **274**(13): 9083-9091.

Bacharach, E., J. Gonsky, et al. (2000). "The carboxy-terminal fragment of nucleolin interacts with the nucleocapsid domain of retroviral gag proteins and inhibits virion assembly." J Virol **74**(23): 11027-11039.

Balasubramaniam, M. and E. O. Freed (2011). "New insights into HIV assembly and trafficking." Physiology (Bethesda) **26**(4): 236-251.

Balvay, L., R. Soto Rifo, et al. (2009). "Structural and functional diversity of viral IRESes." Biochim Biophys Acta **1789**(9-10): 542-557.

Bampi, C., S. Jacquenet, et al. (2004). "The chaperoning and assistance roles of the HIV-1 nucleocapsid protein in proviral DNA synthesis and maintenance." Curr HIV Res **2**(1): 79-92.

Bardy, M., B. Gay, et al. (2001). "Interaction of human immunodeficiency virus type 1 Vif with Gag and Gag-Pol precursors: co-encapsidation and interference with viral protease-mediated Gag processing." J Gen Virol **82**(Pt 11): 2719-2733.

Barre-Sinoussi, F., J. C. Chermann, et al. (1983). "Isolation of a T-lymphotropic retrovirus from a patient at risk for acquired immune deficiency syndrome (AIDS)." Science **220**(4599): 868-871.

Basyuk, E., T. Galli, et al. (2003). "Retroviral genomic RNAs are transported to the plasma membrane by endosomal vesicles." Dev Cell **5**(1): 161-174.

Batisse, J., S. X. Guerrero, et al. (2013). "APOBEC3G impairs the multimerization of the HIV-1 Vif protein in living cells." J Virol **87**(11): 6492-6506.

Batonick, M., M. Favre, et al. (2005). "Interaction of HIV-1 Gag with the clathrin-associated adaptor AP-2." Virology **342**(2): 190-200.

Baudin, F., R. Marquet, et al. (1993). "Functional sites in the 5' region of human immunodeficiency virus type 1 RNA form defined structural domains." J Mol Biol **229**(2): 382-397.

Baumgartel, V., S. Ivanchenko, et al. (2011). "Live-cell visualization of dynamics of HIV budding site interactions with an ESCRT component." Nat Cell Biol **13**(4): 469-474.

Behnia, R. and S. Munro (2005). "Organelle identity and the signposts for membrane traffic." Nature **438**(7068): 597-604.

Beltz, H., C. Clauss, et al. (2005). "Structural determinants of HIV-1 nucleocapsid protein for cTAR DNA binding and destabilization, and correlation with inhibition of self-primed DNA synthesis." J Mol Biol **348**(5): 1113-1126.

Bender, W., Y. H. Chien, et al. (1978). "High-molecular-weight RNAs of AKR, NZB, and wild mouse viruses and avian reticuloendotheliosis virus all have similar dimer structures." J Virol **25**(3): 888-896.

Berkhout, B. (1996). "Structure and function of the human immunodeficiency virus leader RNA." Prog Nucleic Acid Res Mol Biol **54**: 1-34.

Berkowitz, R., J. Fisher, et al. (1996). "RNA packaging." Curr Top Microbiol Immunol **214**: 177-218.

Berkowitz, R. D., J. Luban, et al. (1993). "Specific binding of human immunodeficiency virus type 1 gag polyprotein and nucleocapsid protein to viral RNAs detected by RNA mobility shift assays." J Virol **67**(12): 7190-7200.

Bieniasz, P. D. (2009). "The cell biology of HIV-1 virion genesis." Cell Host Microbe **5**(6): 550-558.

Binley, J. M., T. Wrin, et al. (2004). "Comprehensive cross-clade neutralization analysis of a panel of anti-human immunodeficiency virus type 1 monoclonal antibodies." J Virol **78**(23): 13232-13252.

Bishop, N. and P. Woodman (2001). "TSG101/mammalian VPS23 and mammalian VPS28 interact directly and are recruited to VPS4-induced endosomes." J Biol Chem **276**(15): 11735-11742.

Boily, M. C., R. F. Baggaley, et al. (2009). "Heterosexual risk of HIV-1 infection per sexual act: systematic review and meta-analysis of observational studies." Lancet Infect Dis **9**(2): 118-129.

Bouamr, F., B. R. Houck-Loomis, et al. (2007). "The C-terminal portion of the Hrs protein interacts with Tsg101 and interferes with human immunodeficiency virus type 1 Gag particle production." J Virol **81**(6): 2909-2922.

Boudier, C., R. Storchak, et al. (2010). "The mechanism of HIV-1 Tat-directed nucleic acid annealing supports its role in reverse transcription." J Mol Biol **400**(3): 487-501.

Bour, S. and K. Strebel (2003). "The HIV-1 Vpu protein: a multifunctional enhancer of viral particle release." Microbes Infect **5**(11): 1029-1039.

Boutant, E., P. Didier, et al. (2010). "Fluorescent protein recruitment assay for demonstration and analysis of in vivo protein interactions in plant cells and its application to Tobacco mosaic virus movement protein." Plant J.

Bouttier, M., A. Saumet, et al. (2012). "Retroviral GAG proteins recruit AGO2 on viral RNAs without affecting RNA accumulation and translation." Nucleic Acids Res **40**(2): 775-786.

Bouyac, M., M. Courcoul, et al. (1997). "Human immunodeficiency virus type 1 Vif protein binds to the Pr55Gag precursor." J Virol **71**(12): 9358-9365.

Briggs, J. A. and H. G. Krausslich (2011). "The molecular architecture of HIV." J Mol Biol **410**(4): 491-500.

Brugger, B., B. Glass, et al. (2006). "The HIV lipidome: a raft with an unusual composition." Proc Natl Acad Sci U S A **103**(8): 2641-2646.

Bryant, M. and L. Ratner (1990). "Myristoylation-dependent replication and assembly of human immunodeficiency virus 1." Proc Natl Acad Sci U S A **87**(2): 523-527.

Buchschacher, G. L., Jr. and A. T. Panganiban (1992). "Human immunodeficiency virus vectors for inducible expression of foreign genes." J Virol **66**(5): 2731-2739.

Buonaguro, L., M. L. Tornesello, et al. (2007). "Human immunodeficiency virus type 1 subtype distribution in the worldwide epidemic: pathogenetic and therapeutic implications." J Virol **81**(19): 10209-10219.

Burniston, M. T., A. Cimarelli, et al. (1999). "Human immunodeficiency virus type 1 Gag polyprotein multimerization requires the nucleocapsid domain and RNA and is promoted by the capsid-dimer interface and the basic region of matrix protein." J Virol **73**(10): 8527-8540.

Caffrey, M. (2011). "HIV envelope: challenges and opportunities for development of entry inhibitors." Trends Microbiol **19**(4): 191-197.

Cai, M., Y. Huang, et al. (2010). "Structural basis of the association of HIV-1 matrix protein with DNA." PLoS One **5**(12): e15675.

Calmy, A., B. Hirschel, et al. (2009). "A new era of antiretroviral drug toxicity." Antivir Ther **14**(2): 165-179.

Carillo, M. A., M. Bennet, et al. (2013). "Interaction of proteins associated with the magnetosome assembly in magnetotactic bacteria as revealed by two-hybrid two-photon excitation fluorescence lifetime imaging microscopy Forster resonance energy transfer." J Phys Chem B **117**(47): 14642-14648.

Carlton, J. G. and J. Martin-Serrano (2009). "The ESCRT machinery: new functions in viral and cellular biology." Biochem Soc Trans **37**(Pt 1): 195-199.

Carr, A. (2003). "Toxicity of antiretroviral therapy and implications for drug development." Nat Rev Drug Discov **2**(8): 624-634.

Carriere, C., B. Gay, et al. (1995). "Sequence requirements for encapsidation of deletion mutants and chimeras of human immunodeficiency virus type 1 Gag precursor into retrovirus-like particles." J Virol **69**(4): 2366-2377.

Carteau, S., S. C. Batson, et al. (1997). "Human immunodeficiency virus type 1 nucleocapsid protein specifically stimulates Mg2+-dependent DNA integration in vitro." J Virol **71**(8): 6225-6229.

Cavarelli, M. and G. Scarlatti (2011). "Human immunodeficiency virus type 1 mother-to-child transmission and prevention: successes and controversies." J Intern Med **270**(6): 561-579.

Chamontin, C., P. Rassam, et al. (2015). "HIV-1 nucleocapsid and ESCRT-component Tsg101 interplay prevents HIV from turning into a DNA-containing virus." Nucleic Acids Res **43**(1): 336-347.

Chang, C. Y., Y. F. Chang, et al. (2008). "HIV-1 matrix protein repositioning in nucleocapsid region fails to confer virus-like particle assembly." Virology **378**(1): 97-104.

Charneau, P., M. Alizon, et al. (1992). "A second origin of DNA plus-strand synthesis is required for optimal human immunodeficiency virus replication." J Virol **66**(5): 2814-2820.

Chatel-Chaix, L., J. F. Clement, et al. (2004). "Identification of Staufen in the human immunodeficiency virus type 1 Gag ribonucleoprotein complex and a role in generating infectious viral particles." Mol Cell Biol **24**(7): 2637-2648.

Checkley, M. A., B. G. Luttge, et al. (2011). "HIV-1 envelope glycoprotein biosynthesis, trafficking, and incorporation." J Mol Biol **410**(4): 582-608.

Chen, J., D. Grunwald, et al. (2014). "Cytoplasmic HIV-1 RNA is mainly transported by diffusion in the presence or absence of Gag protein." Proc Natl Acad Sci U S A **111**(48): E5205-5213.

Chen, J., O. Nikolaitchik, et al. (2009). "High efficiency of HIV-1 genomic RNA packaging and heterozygote formation revealed by single virion analysis." Proc Natl Acad Sci U S A **106**(32): 13535-13540.

Cherepanov, P., G. N. Maertens, et al. (2011). "Structural insights into the retroviral DNA integration apparatus." Curr Opin Struct Biol **21**(2): 249-256.

Chin, M. P., T. D. Rhodes, et al. (2005). "Identification of a major restriction in HIV-1 intersubtype recombination." Proc Natl Acad Sci U S A **102**(25): 9002-9007.

Chojnacki, J. and B. Muller (2013). "Investigation of HIV-1 assembly and release using modern fluorescence imaging techniques." Traffic **14**(1): 15-24.

Chukkapalli, V. and A. Ono (2011). "Molecular determinants that regulate plasma membrane association of HIV-1 Gag." J Mol Biol **410**(4): 512-524.

Chung, H. Y., E. Morita, et al. (2008). "NEDD4L overexpression rescues the release and infectivity of human immunodeficiency virus type 1 constructs lacking PTAP and YPXL late domains." J Virol **82**(10): 4884-4897.

Cimarelli, A. and J. Luban (1999). "Translation elongation factor 1-alpha interacts specifically with the human immunodeficiency virus type 1 Gag polyprotein." J Virol **73**(7): 5388-5401.

Cimarelli, A. and J. Luban (2000). "Human immunodeficiency virus type 1 virion density is not determined by nucleocapsid basic residues." J Virol **74**(15): 6734-6740.

Ciuffi, A. and F. D. Bushman (2006). "Retroviral DNA integration: HIV and the role of LEDGF/p75." Trends Genet **22**(7): 388-395.

Clamme, J. P., J. Azoulay, et al. (2003). "Monitoring of the formation and dissociation of polyethylenimine/DNA complexes by two photon fluorescence correlation spectroscopy." Biophys J **84**(3): 1960-1968.

Clamme, J. P., G. Krishnamoorthy, et al. (2003). "Intracellular dynamics of the gene delivery vehicle polyethylenimine during transfection: investigation by two-photon fluorescence correlation spectroscopy." Biochim Biophys Acta **1617**(1-2): 52-61.

Clapham, P. R. and R. A. Weiss (1997). "Immunodeficiency viruses. Spoilt for choice of co-receptors." Nature **388**(6639): 230-231.

Clavel, F. and J. M. Orenstein (1990). "A mutant of human immunodeficiency virus with reduced RNA packaging and abnormal particle morphology." J Virol **64**(10): 5230-5234.

Clever, J., C. Sassetti, et al. (1995). "RNA secondary structure and binding sites for gag gene products in the 5' packaging signal of human immunodeficiency virus type 1." J Virol **69**(4): 2101-2109.

Clever, J. L., D. Miranda, Jr., et al. (2002). "RNA structure and packaging signals in the 5' leader region of the human immunodeficiency virus type 1 genome." J Virol **76**(23): 12381-12387.

Clever, J. L. and T. G. Parslow (1997). "Mutant human immunodeficiency virus type 1 genomes with defects in RNA dimerization or encapsidation." J Virol **71**(5): 3407-3414.

Clever, J. L., M. L. Wong, et al. (1996). "Requirements for kissing-loop-mediated dimerization of human immunodeficiency virus RNA." J Virol **70**(9): 5902-5908.

Coffin, J. M. (1979). "Structure, replication, and recombination of retrovirus genomes: some unifying hypotheses." J Gen Virol **42**(1): 1-26.

Coffin JM, H. S., Varmus HE (1997). Retroviruses Cold Spring Harbor Laboratory Press, Cold Spring Harbor (NY):.

Cruceanu, M., M. A. Urbaneja, et al. (2006). "Nucleic acid binding and chaperone properties of HIV-1 Gag and nucleocapsid proteins." Nucleic Acids Res **34**(2): 593-605.

D'Souza, V. and M. F. Summers (2005). "How retroviruses select their genomes." Nat Rev Microbiol **3**(8): 643-655.

Damgaard, C. K., H. Dyhr-Mikkelsen, et al. (1998). "Mapping the RNA binding sites for human immunodeficiency virus type-1 gag and NC proteins within the complete HIV-1 and -2 untranslated leader regions." Nucleic Acids Res **26**(16): 3667-3676.

Dannull, J., A. Surovoy, et al. (1994). "Specific binding of HIV-1 nucleocapsid protein to PSI RNA in vitro requires N-terminal zinc finger and flanking basic amino acid residues." EMBO J **13**(7): 1525-1533.

Darlix, J. L., H. de Rocquigny, et al. (2014). "Retrospective on the all-in-one retroviral nucleocapsid protein." Virus Res **193**: 2-15.

Darlix, J. L., C. Gabus, et al. (1990). "Cis elements and trans-acting factors involved in the RNA dimerization of the human immunodeficiency virus HIV-1." J Mol Biol **216**(3): 689-699.

Darlix, J. L., J. Godet, et al. (2011). "Flexible nature and specific functions of the HIV-1 nucleocapsid protein." J Mol Biol **410**(4): 565-581.

Darlix, J. L., M. Lapadat-Tapolsky, et al. (1995). "First glimpses at structure-function relationships of the nucleocapsid protein of retroviruses." J Mol Biol **254**(4): 523-537.

Das, A., V. Prashar, et al. (2006). "Crystal structure of HIV-1 protease in situ product complex and observation of a low-barrier hydrogen bond between catalytic aspartates." Proc Natl Acad Sci U S A **103**(49): 18464-18469.

Das, A. T., B. Klaver, et al. (1998). "The 5' and 3' TAR elements of human immunodeficiency virus exert effects at several points in the virus life cycle." J Virol **72**(11): 9217-9223.

Datta, S. A., J. E. Curtis, et al. (2007). "Conformation of the HIV-1 Gag protein in solution." J Mol Biol **365**(3): 812-824.

Datta, S. A., L. G. Temeselew, et al. (2011). "On the role of the SP1 domain in HIV-1 particle assembly: a molecular switch?" J Virol **85**(9): 4111-4121.

David L. Heymann. l.. Washington DC, U. A. P. H. A. (18th (edn) 2004). HIV Transmission via Blood to Blood Contact. In: Control of Communicable Diseases Manual. Washington DC, USA:, .

de Marco, A., B. Muller, et al. (2010). "Structural analysis of HIV-1 maturation using cryo-electron tomography." PLoS Pathog **6**(11): e1001215.

de Noronha, C. M., M. P. Sherman, et al. (2001). "Dynamic disruptions in nuclear envelope architecture and integrity induced by HIV-1 Vpr." Science **294**(5544): 1105-1108.

de Rocquigny, H., S. E. El Meshri, et al. (2014). "Role of the nucleocapsid region in HIV-1 Gag assembly as investigated by quantitative fluorescence-based microscopy." Virus Res **193**: 78-88.

De Rocquigny, H., C. Gabus, et al. (1992). "Viral RNA annealing activities of human immunodeficiency virus type 1 nucleocapsid protein require only peptide domains outside the zinc fingers." Proc Natl Acad Sci U S A **89**(14): 6472-6476.

De Rocquigny, H., C. Gabus, et al. (1992). "Viral RNA annealing activities of human immunodeficiency virus type 1 nucleocapsid protein require only peptide domains outside the zinc fingers." Proc Natl Acad Sci U S A **89**(14): 6472-6476.

de Rocquigny, H., H. Gacem, et al. (2013). "HIV-1 Gag Directed Assembly of Retroviral 1 Particles Investigated by Quantitative 2 Fluorescence Imaging." Fluorescent methods to study biological membranes **13**: 457-478.

de Rocquigny, H., P. Petitjean, et al. (1997). "The zinc fingers of HIV nucleocapsid protein NCp7 direct interactions with the viral regulatory protein Vpr." J Biol Chem **272**(49): 30753-30759.

Demirov, D. G., A. Ono, et al. (2002). "Overexpression of the N-terminal domain of TSG101 inhibits HIV-1 budding by blocking late domain function." Proc Natl Acad Sci U S A **99**(2): 955-960.

Derdowski, A., L. Ding, et al. (2004). "A novel fluorescence resonance energy transfer assay demonstrates that the human immunodeficiency virus type 1 Pr55Gag I domain mediates Gag-Gag interactions." J Virol **78**(3): 1230-1242.

Didierlaurent, L., L. Houzet, et al. (2008). "The conserved N-terminal basic residues and zinc-finger motifs of HIV-1 nucleocapsid restrict the viral cDNA synthesis during virus formation and maturation." Nucleic Acids Res **36**(14): 4745-4753.

Dong, X., H. Li, et al. (2005). "AP-3 directs the intracellular trafficking of HIV-1 Gag and plays a key role in particle assembly." Cell **120**(5): 663-674.

Dooher, J. E. and J. R. Lingappa (2004). "Conservation of a stepwise, energy-sensitive pathway involving HP68 for assembly of primate lentivirus capsids in cells." J Virol **78**(4): 1645-1656.

Dorfman, T., J. Luban, et al. (1993). "Mapping of functionally important residues of a cysteine-histidine box in the human immunodeficiency virus type 1 nucleocapsid protein." J Virol **67**(10): 6159-6169.

Dube, M., M. G. Bego, et al. (2010). "Modulation of HIV-1-host interaction: role of the Vpu accessory protein." Retrovirology **7**: 114.

Dussupt, V., M. P. Javid, et al. (2009). "The nucleocapsid region of HIV-1 Gag cooperates with the PTAP and LYPXnL late domains to recruit the cellular machinery necessary for viral budding." PLoS Pathog **5**(3): e1000339.

Dybul, M., A. S. Fauci, et al. (2002). "Guidelines for using antiretroviral agents among HIV-infected adults and adolescents. Recommendations of the Panel on Clinical Practices for Treatment of HIV." MMWR Recomm Rep **51**(RR-7): 1-55.

Dykeman, E. C., N. E. Grayson, et al. (2011). "Simple rules for efficient assembly predict the layout of a packaged viral RNA." J Mol Biol **408**(3): 399-407.

Eekels, J. J., D. Geerts, et al. (2011). "Long-term inhibition of HIV-1 replication with RNA interference against cellular co-factors." Antiviral Res **89**(1): 43-53.

Ekram W. Abd El-Wahab, Redmond P. Smyth, et al. (2014). "Specific recognition of the HIV-1 genomic RNA by the Gag precursor." nature communication.

Elia, N., R. Sougrat, et al. (2011). "Dynamics of endosomal sorting complex required for transport (ESCRT) machinery during cytokinesis and its role in abscission." Proc Natl Acad Sci U S A **108**(12): 4846-4851.

Ellis, R. J. (2001). "Macromolecular crowding: an important but neglected aspect of the intracellular environment." Curr Opin Struct Biol **11**(1): 114-119.

Engeland, C. E., H. Oberwinkler, et al. (2011). "The cellular protein lyric interacts with HIV-1 Gag." J Virol **85**(24): 13322-13332.

Fauci A.S., L. H. C. (1997). Human immunodeficiency virus (HIV) disease: AIDS and related disorders. In: Harrison's principles of internal medicine. McGraw-Hill, New York.:1791–1856.

Felber, B. K., M. Hadzopoulou-Cladaras, et al. (1989). "rev protein of human immunodeficiency virus type 1 affects the stability and transport of the viral mRNA." Proc Natl Acad Sci U S A **86**(5): 1495-1499.

Feng, Y. X., T. D. Copeland, et al. (1996). "HIV-1 nucleocapsid protein induces "maturation" of dimeric retroviral RNA in vitro." Proc Natl Acad Sci U S A **93**(15): 7577-7581.

Fisher, R. D., H. Y. Chung, et al. (2007). "Structural and biochemical studies of ALIX/AIP1 and its role in retrovirus budding." Cell **128**(5): 841-852.

Flint S.J., E. L. W., Racaniellp V. E., Skalka A. M. (2004). Principles of Virology: Moleculare Biology, Pathogensis, and control of Animal Viruses. Washington, DC;, American Societty for Microbiology Press.

Fogarty, K. H., Y. Chen, et al. (2011). "Characterization of cytoplasmic Gag-gag interactions by dual-color z-scan fluorescence fluctuation spectroscopy." Biophys J **100**(6): 1587-1595.

Franke, E. K., H. E. Yuan, et al. (1994). "Specificity and sequence requirements for interactions between various retroviral Gag proteins." J Virol **68**(8): 5300-5305.

Freed, E. O. (2002). "Viral late domains." J Virol **76**(10): 4679-4687.

Freed, E. O. (2003). "The HIV-TSG101 interface: recent advances in a budding field." Trends Microbiol **11**(2): 56-59.

Freed, E. O., J. M. Orenstein, et al. (1994). "Single amino acid changes in the human immunodeficiency virus type 1 matrix protein block virus particle production." J Virol **68**(8): 5311-5320.

Friedman-Kien, A. E. (1981). "Disseminated Kaposi's sarcoma syndrome in young homosexual men." J Am Acad Dermatol **5**(4): 468-471.

Fritz, J. V., L. Briant, et al. (2010). "HIV-1 Viral Protein R : from structure to function." Future Virol **5**: 607-625.

Fritz, J. V., P. Didier, et al. (2008). "Direct Vpr-Vpr interaction in cells monitored by two photon fluorescence correlation spectroscopy and fluorescence lifetime imaging." Retrovirology **5**: 87.

Fritz, J. V., D. Dujardin, et al. (2010). "HIV-1 Vpr oligomerization but not that of Gag directs the interaction between Vpr and Gag." J Virol **84**(3): 1585-1596.

Fujii, K., U. M. Munshi, et al. (2009). "Functional role of Alix in HIV-1 replication." Virology **391**(2): 284-292.

Gallo, R. C., P. S. Sarin, et al. (1983). "Isolation of human T-cell leukemia virus in acquired immune deficiency syndrome (AIDS)." Science **220**(4599): 865-867.

Ganser-Pornillos, B. K., M. Yeager, et al. (2008). "The structural biology of HIV assembly." Curr Opin Struct Biol **18**(2): 203-217.

Garrus, J. E., U. K. von Schwedler, et al. (2001). "Tsg101 and the vacuolar protein sorting pathway are essential for HIV-1 budding." Cell **107**(1): 55-65.

Gaudin, R., B. C. de Alencar, et al. (2013). "HIV trafficking in host cells: motors wanted!" Trends Cell Biol **23**(12): 652-662.

Gaynor, R. (1992). "Cellular transcription factors involved in the regulation of HIV-1 gene expression." AIDS **6**(4): 347-363.

Geigenmuller, U. and M. L. Linial (1996). "Specific binding of human immunodeficiency virus type 1 (HIV-1) Gag-derived proteins to a 5' HIV-1 genomic RNA sequence." J Virol **70**(1): 667-671.

Godet, J., C. Boudier, et al. (2012). "Comparative nucleic acid chaperone properties of the nucleocapsid protein NCp7 and Tat protein of HIV-1." Virus Res **169**(2): 349-360.

Godet, J., H. de Rocquigny, et al. (2006). "During the early phase of HIV-1 DNA synthesis, nucleocapsid protein directs hybridization of the TAR complementary sequences via the ends of their double-stranded stem." J Mol Biol **356**(5): 1180-1192.

Godet, J. and Y. Mely (2010). "Biophysical studies of the nucleic acid chaperone properties of the HIV-1 nucleocapsid protein." RNA Biol **7**(6): 687-699.

Goh, W. C., M. E. Rogel, et al. (1998). "HIV-1 Vpr increases viral expression by manipulation of the cell cycle: a mechanism for selection of Vpr in vivo." Nat Med **4**(1): 65-71.

Gorelick, R. J., L. E. Henderson, et al. (1988). "Point mutants of Moloney murine leukemia virus that fail to package viral RNA: evidence for specific RNA recognition by a "zinc finger-like" protein sequence." Proc Natl Acad Sci U S A **85**(22): 8420-8424.

Gorelick, R. J., S. M. Nigida, Jr., et al. (1990). "Noninfectious human immunodeficiency virus type 1 mutants deficient in genomic RNA." J Virol **64**(7): 3207-3211.

Gottlieb, M. S., R. Schroff, et al. (1981). "Pneumocystis carinii pneumonia and mucosal candidiasis in previously healthy homosexual men: evidence of a new acquired cellular immunodeficiency." N Engl J Med **305**(24): 1425-1431.

Gottlinger, H. G. (2001). "The HIV-1 assembly machine." AIDS **15 Suppl 5**: S13-20.

Gottlinger, H. G., T. Dorfman, et al. (1991). "Effect of mutations affecting the p6 gag protein on human immunodeficiency virus particle release." Proc Natl Acad Sci U S A **88**(8): 3195-3199.

Greene, W. C. (1993). "AIDS and the immune system." Sci Am **269**(3): 98-105.

Grewe, B., K. Ehrhardt, et al. (2012). "The HIV-1 Rev protein enhances encapsidation of unspliced and spliced, RRE-containing lentiviral vector RNA." PLoS One **7**(11): e48688.

Grigorov, B., F. Arcanger, et al. (2006). "Assembly of infectious HIV-1 in human epithelial and T-lymphoblastic cell lines." J Mol Biol **359**(4): 848-862.

Grigorov, B., D. Decimo, et al. (2007). "Intracellular HIV-1 Gag localization is impaired by mutations in the nucleocapsid zinc fingers." Retrovirology **4**: 54.

Guenzel, C. A., C. Herate, et al. (2014). "HIV-1 Vpr-a still "enigmatic multitasker"." Front Microbiol **5**: 127.

Guo, X., M. Kameoka, et al. (2003). "Suppression of an intrinsic strand transfer activity of HIV-1 Tat protein by its second-exon sequences." Virology **307**(1): 154-163.

Guttman, M., M. Kahn, et al. (2012). "Solution structure, conformational dynamics, and CD4-induced activation in full-length, glycosylated, monomeric HIV gp120." J Virol **86**(16): 8750-8764.

Hammarskjold, M. L., and D. Rekosh. (2011). "A Long-Awaited Structure Is Rev-ealed." Viruses **3(5), 484-492**.

Harrison, G. P. and A. M. Lever (1992). "The human immunodeficiency virus type 1 packaging signal and major splice donor region have a conserved stable secondary structure." J Virol **66**(7): 4144-4153.

Hayashi, T., T. Shioda, et al. (1992). "RNA packaging signal of human immunodeficiency virus type 1." Virology **188**(2): 590-599.

Hayashi, T., Y. Ueno, et al. (1993). "Elucidation of a conserved RNA stem-loop structure in the packaging signal of human immunodeficiency virus type 1." FEBS Lett **327**(2): 213-218.

He, J., S. Choe, et al. (1995). "Human immunodeficiency virus type 1 viral protein R (Vpr) arrests cells in the G2 phase of the cell cycle by inhibiting p34cdc2 activity." J Virol **69**(11): 6705-6711.

Henriet, S., G. Mercenne, et al. (2009). "Tumultuous relationship between the human immunodeficiency virus type 1 viral infectivity factor (Vif) and the human APOBEC-3G and APOBEC-3F restriction factors." Microbiol Mol Biol Rev **73**(2): 211-232.

Hermida-Matsumoto, L. and M. D. Resh (2000). "Localization of human immunodeficiency virus type 1 Gag and Env at the plasma membrane by confocal imaging." J Virol **74**(18): 8670-8679.

Herrington, C. S., P. J. Coates, et al. (2015). "Viruses and disease: emerging concepts for prevention, diagnosis and treatment." J Pathol **235**(2): 149-152.

Herrmann, C. H. and A. P. Rice (1995). "Lentivirus Tat proteins specifically associate with a cellular protein kinase, TAK, that hyperphosphorylates the carboxyl-terminal domain of the large subunit of RNA polymerase II: candidate for a Tat cofactor." J Virol **69**(3): 1612-1620.

Herschhorn, A. and A. Hizi (2010). "Retroviral reverse transcriptases." Cell Mol Life Sci **67**(16): 2717-2747.

Herschlag, D. (1995). "RNA chaperones and the RNA folding problem." J Biol Chem **270**(36): 20871-20874.

Hogue, I. B., A. Hoppe, et al. (2009). "Quantitative fluorescence resonance energy transfer microscopy analysis of the human immunodeficiency virus type 1 Gag-Gag interaction: relative contributions of the CA and NC domains and membrane binding." J Virol **83**(14): 7322-7336.

Hong, S. S. and P. Boulanger (1993). "Assembly-defective point mutants of the human immunodeficiency virus type 1 Gag precursor phenotypically expressed in recombinant baculovirus-infected cells." J Virol **67**(5): 2787-2798.

Houzet, L., Z. Morichaud, et al. (2008). "Nucleocapsid mutations turn HIV-1 into a DNA-containing virus." Nucleic Acids Res **36**(7): 2311-2319.

Houzet, L., J. C. Paillart, et al. (2007). "HIV controls the selective packaging of genomic, spliced viral and cellular RNAs into virions through different mechanisms." Nucleic Acids Res **35**(8): 2695-2704.

Hu, W. S. and S. H. Hughes (2012). "HIV-1 reverse transcription." Cold Spring Harb Perspect Med **2**(10).

Hu, W. S. and H. M. Temin (1990). "Retroviral recombination and reverse transcription." Science **250**(4985): 1227-1233.

Huang, H., R. Chopra, et al. (1998). "Structure of a covalently trapped catalytic complex of HIV-1 reverse transcriptase: implications for drug resistance." Science **282**(5394): 1669-1675.

Hubner, W., P. Chen, et al. (2007). "Sequence of human immunodeficiency virus type 1 (HIV-1) Gag localization and oligomerization monitored with live confocal imaging of a replication-competent, fluorescently tagged HIV-1." J Virol **81**(22): 12596-12607.

Hugues de Rocquigny*, H. G., Pascal Didier, Jean Luc Darlix and Yves Mély (2012). "HIV-1 Gag directed assembly of retroviral particles investigated by quantitative fluorescence imaging." Springer Series On Fluorescence.

Huvent, I., S. S. Hong, et al. (1998). "Interaction and co-encapsidation of human immunodeficiency virus type 1 Gag and Vif recombinant proteins." J Gen Virol **79 (Pt 5)**: 1069-1081.

Im, Y. J., L. Kuo, et al. (2010). "Crystallographic and functional analysis of the ESCRT-I /HIV-1 Gag PTAP interaction." Structure **18**(11): 1536-1547.

Isel, C., C. Ehresmann, et al. (2010). "Initiation of HIV Reverse Transcription." Viruses **2**(1): 213-243.

Ivanchenko, S., W. J. Godinez, et al. (2009). "Dynamics of HIV-1 assembly and release." PLoS Pathog **5**(11): e1000652.

Ivanyi-Nagy, R., J. P. Lavergne, et al. (2008). "RNA chaperoning and intrinsic disorder in the core proteins of Flaviviridae." Nucleic Acids Res **36**(3): 712-725.

Jaffray, A., E. Shephard, et al. (2004). "Human immunodeficiency virus type 1 subtype C Gag virus-like particle boost substantially improves the immune response to a subtype C gag DNA vaccine in mice." J Gen Virol **85**(Pt 2): 409-413.

Jones, K. A. and B. M. Peterlin (1994). "Control of RNA initiation and elongation at the HIV-1 promoter." Annu Rev Biochem **63**: 717-743.

Joshi, A., S. D. Ablan, et al. (2009). "Evidence that productive human immunodeficiency virus type 1 assembly can occur in an intracellular compartment." J Virol **83**(11): 5375-5387.

Jouvenet, N., P. D. Bieniasz, et al. (2008). "Imaging the biogenesis of individual HIV-1 virions in live cells." Nature **454**(7201): 236-240.

Jouvenet, N., S. M. Simon, et al. (2009). "Imaging the interaction of HIV-1 genomes and Gag during assembly of individual viral particles." Proc Natl Acad Sci U S A **106**(45): 19114-19119.

Jouvenet, N., S. M. Simon, et al. (2011). "Visualizing HIV-1 assembly." J Mol Biol **410**(4): 501-511.

Jowett, J. B., V. Planelles, et al. (1995). "The human immunodeficiency virus type 1 vpr gene arrests infected T cells in the G2 + M phase of the cell cycle." J Virol **69**(10): 6304-6313.

Kameoka, M., M. Morgan, et al. (2002). "The Tat protein of human immunodeficiency virus type 1 (HIV-1) can promote placement of tRNA primer onto viral RNA and suppress later DNA polymerization in HIV-1 reverse transcription." J Virol **76**(8): 3637-3645.

Kaminska, M., V. Shalak, et al. (2007). "Viral hijacking of mitochondrial lysyl-tRNA synthetase." J Virol **81**(1): 68-73.

Kanevsky, I., F. Chaminade, et al. (2005). "Specific interactions between HIV-1 nucleocapsid protein and the TAR element." J Mol Biol **348**(5): 1059-1077.

Karki, R. G., Y. Tang, et al. (2004). "Model of full-length HIV-1 integrase complexed with viral DNA as template for anti-HIV drug design." J Comput Aided Mol Des **18**(12): 739-760.

Karn, J. and C. M. Stoltzfus (2012). "Transcriptional and posttranscriptional regulation of HIV-1 gene expression." Cold Spring Harb Perspect Med **2**(2): a006916.

Katzmann, D. J., M. Babst, et al. (2001). "Ubiquitin-dependent sorting into the multivesicular body pathway requires the function of a conserved endosomal protein sorting complex, ESCRT-I." Cell **106**(2): 145-155.

Kawada, S., T. Goto, et al. (2008). "Dominant negative inhibition of human immunodeficiency virus particle production by the nonmyristoylated form of gag." J Virol **82**(9): 4384-4399.

Kempf, N., V. Postupalenko, et al. (2014). "The HIV-1 nucleocapsid protein recruits negatively charged lipids on binding to lipid membranes." J Virol.

Kieken, F., F. Paquet, et al. (2006). "A new NMR solution structure of the SL1 HIV-1Lai loop-loop dimer." Nucleic Acids Res **34**(1): 343-352.

Kim, J., S. Sitaraman, et al. (2005). "Structural basis for endosomal targeting by the Bro1 domain." Dev Cell **8**(6): 937-947.

Kim, W., Y. Tang, et al. (1998). "Binding of murine leukemia virus Gag polyproteins to KIF4, a microtubule-based motor protein." J Virol **72**(8): 6898-6901.

Klaver, B. and B. Berkhout (1994). "Comparison of 5' and 3' long terminal repeat promoter function in human immunodeficiency virus." J Virol **68**(6): 3830-3840.

Klaver, B. and B. Berkhout (1994). "Evolution of a disrupted TAR RNA hairpin structure in the HIV-1 virus." EMBO J **13**(11): 2650-2659.

Kleiman, L., C. P. Jones, et al. (2010). "Formation of the tRNALys packaging complex in HIV-1." FEBS Lett **584**(2): 359-365.

Klein, K. C., J. C. Reed, et al. (2007). "Intracellular destinies: degradation, targeting, assembly, and endocytosis of HIV Gag." AIDS Rev **9**(3): 150-161.

Kobbi, L., G. Octobre, et al. (2011). "Association of mitochondrial Lysyl-tRNA synthetase with HIV-1 GagPol involves catalytic domain of the synthetase and transframe and integrase domains of Pol." J Mol Biol **410**(5): 875-886.

Kovacs, D., M. Rakacs, et al. (2009). "Janus chaperones: assistance of both RNA- and protein-folding by ribosomal proteins." FEBS Lett **583**(1): 88-92.

Krausslich, H. G., M. Facke, et al. (1995). "The spacer peptide between human immunodeficiency virus capsid and nucleocapsid proteins is essential for ordered assembly and viral infectivity." J Virol **69**(6): 3407-3419.

Krishnamoorthy, G., G. Duportail, et al. (2002). "Structure and dynamics of condensed DNA probed by 1,1'-(4,4,8,8-tetramethyl-4,8-diazaundecamethylene)bis[4-[[3- methylbenz-1,3-oxazol-2-yl]methylidine]-1,4-dihydroquinolinium] tetraiodide fluorescence." Biochemistry **41**(51): 15277-15287.

Ku, P. I., M. Bendjennat, et al. (2014). "ALIX is recruited temporarily into HIV-1 budding sites at the end of gag assembly." PLoS One **9**(5): e96950.

Kuciak, M., C. Gabus, et al. (2008). "The HIV-1 transcriptional activator Tat has potent nucleic acid chaperoning activities in vitro." Nucleic Acids Res **36**(10): 3389-3400.

Kutluay, S. B. and P. D. Bieniasz (2010). "Analysis of the initiating events in HIV-1 particle assembly and genome packaging." PLoS Pathog **6**(11): e1001200.

Kuzembayeva, M., K. Dilley, et al. (2014). "Life of psi: how full-length HIV-1 RNAs become packaged genomes in the viral particles." Virology **454-455**: 362-370.

Laguette, N., C. Bregnard, et al. (2010). "Human immunodeficiency virus (HIV) type-1, HIV-2 and simian immunodeficiency virus Nef proteins." Mol Aspects Med **31**(5): 418-433.

Laguette, N., C. Bregnard, et al. (2014). "Premature activation of the SLX4 complex by Vpr promotes G2/M arrest and escape from innate immune sensing." Cell **156**(1-2): 134-145.

Lakowicz, J. R. (1980). "Fluorescence spectroscopic investigations of the dynamic properties of proteins, membranes and nucleic acids." J Biochem Biophys Methods **2**(1): 91-119.

Larson, D. R., M. C. Johnson, et al. (2005). "Visualization of retrovirus budding with correlated light and electron microscopy." Proc Natl Acad Sci U S A **102**(43): 15453-15458.

Laughrea, M. and L. Jette (1994). "A 19-nucleotide sequence upstream of the 5' major splice donor is part of the dimerization domain of human immunodeficiency virus 1 genomic RNA." Biochemistry **33**(45): 13464-13474.

Le Rouzic, E., A. Mousnier, et al. (2002). "Docking of HIV-1 Vpr to the nuclear envelope is mediated by the interaction with the nucleoporin hCG1." J Biol Chem **277**(47): 45091-45098.

Lee, S., A. Joshi, et al. (2007). "Structural basis for viral late-domain binding to Alix." Nat Struct Mol Biol **14**(3): 194-199.

Lee, S. K., M. Potempa, et al. (2012). "The choreography of HIV-1 proteolytic processing and virion assembly." J Biol Chem **287**(49): 40867-40874.

Lee, Y. M., B. Liu, et al. (1999). "Formation of virus assembly intermediate complexes in the cytoplasm by wild-type and assembly-defective mutant human immunodeficiency virus type 1 and their association with membranes." J Virol **73**(7): 5654-5662.

Lehmann, M., M. P. Milev, et al. (2009). "Intracellular transport of human immunodeficiency virus type 1 genomic RNA and viral production are dependent on dynein motor function and late endosome positioning." J Biol Chem **284**(21): 14572-14585.

Lever, A., H. Gottlinger, et al. (1989). "Identification of a sequence required for efficient packaging of human immunodeficiency virus type 1 RNA into virions." J Virol **63**(9): 4085-4087.

Lever, A. M. (2007). "HIV-1 RNA packaging." Adv Pharmacol **55**: 1-32.

Levin, J. G., J. Guo, et al. (2005). "Nucleic acid chaperone activity of HIV-1 nucleocapsid protein: critical role in reverse transcription and molecular mechanism." Prog Nucleic Acid Res Mol Biol **80**: 217-286.

Li, H., J. Dou, et al. (2007). "Myristoylation is required for human immunodeficiency virus type 1 Gag-Gag multimerization in mammalian cells." J Virol **81**(23): 12899-12910.

Li, L. and S. N. Cohen (1996). "Tsg101: a novel tumor susceptibility gene isolated by controlled homozygous functional knockout of allelic loci in mammalian cells." Cell **85**(3): 319-329.

Liang, C., J. Hu, et al. (2003). "A structurally disordered region at the C terminus of capsid plays essential roles in multimerization and membrane binding of the gag protein of human immunodeficiency virus type 1." J Virol **77**(3): 1772-1783.

Lindwasser, O. W. and M. D. Resh (2001). "Multimerization of human immunodeficiency virus type 1 Gag promotes its localization to barges, raft-like membrane microdomains." J Virol **75**(17): 7913-7924.

Lingappa, J. R., J. E. Dooher, et al. (2006). "Basic residues in the nucleocapsid domain of Gag are required for interaction of HIV-1 gag with ABCE1 (HP68), a cellular protein important for HIV-1 capsid assembly." J Biol Chem **281**(7): 3773-3784.

Lingappa, J. R., R. L. Hill, et al. (1997). "A multistep, ATP-dependent pathway for assembly of human immunodeficiency virus capsids in a cell-free system." J Cell Biol **136**(3): 567-581.

Liu, B., R. Dai, et al. (1999). "Interaction of the human immunodeficiency virus type 1 nucleocapsid with actin." J Virol **73**(4): 2901-2908.

Lopez-Lastra, M., C. Gabus, et al. (1997). "Characterization of an internal ribosomal entry segment within the 5' leader of avian reticuloendotheliosis virus type A RNA and development of novel MLV-REV-based retroviral vectors." Hum Gene Ther **8**(16): 1855-1865.

Lu, K., X. Heng, et al. (2011). "Structural determinants and mechanism of HIV-1 genome packaging." J Mol Biol **410**(4): 609-633.

Luban, J. and S. P. Goff (1991). "Binding of human immunodeficiency virus type 1 (HIV-1) RNA to recombinant HIV-1 gag polyprotein." J Virol **65**(6): 3203-3212.

Luban, J. and S. P. Goff (1994). "Mutational analysis of cis-acting packaging signals in human immunodeficiency virus type 1 RNA." J Virol **68**(6): 3784-3793.

Ludovic Richert, P. D., Hugues de Rocquigny and Yves Mély (2015). "Monitoring HIV-1 Protein Oligomerization by FLIM FRET Microscopy." Chemical Physics: 1/31.

Lv, W., Z. Liu, et al. (2007). "Three-dimensional structure of HIV-1 VIF constructed by comparative modeling and the function characterization analyzed by molecular dynamics simulation." Org Biomol Chem **5**(4): 617-626.

Lynch, R. M., T. Shen, et al. (2009). "Appreciating HIV type 1 diversity: subtype differences in Env." AIDS Res Hum Retroviruses **25**(3): 237-248.

Lyonnais, S., R. J. Gorelick, et al. (2013). "A protein ballet around the viral genome orchestrated by HIV-1 reverse transcriptase leads to an architectural switch: from nucleocapsid-condensed RNA to Vpr-bridged DNA." Virus Res **171**(2): 287-303.

Maldarelli, F., M. Y. Chen, et al. (1993). "Human immunodeficiency virus type 1 Vpu protein is an oligomeric type I integral membrane protein." J Virol **67**(8): 5056-5061.

Mammano, F., A. Ohagen, et al. (1994). "Role of the major homology region of human immunodeficiency virus type 1 in virion morphogenesis." J Virol **68**(8): 4927-4936.

Marcello, A., M. Zoppe, et al. (2001). "Multiple modes of transcriptional regulation by the HIV-1 Tat transactivator." IUBMB Life **51**(3): 175-181.

Martin-Serrano, J. and S. J. Neil (2011). "Host factors involved in retroviral budding and release." Nat Rev Microbiol **9**(7): 519-531.

Martin-Serrano, J., A. Yarovoy, et al. (2003). "Divergent retroviral late-budding domains recruit vacuolar protein sorting factors by using alternative adaptor proteins." Proc Natl Acad Sci U S A **100**(21): 12414-12419.

Martin-Serrano, J., T. Zang, et al. (2001). "HIV-1 and Ebola virus encode small peptide motifs that recruit Tsg101 to sites of particle assembly to facilitate egress." Nat Med **7**(12): 1313-1319.

Martin-Serrano, J., T. Zang, et al. (2003). "Role of ESCRT-I in retroviral budding." J Virol **77**(8): 4794-4804.

Mascarenhas, A. P. and K. Musier-Forsyth (2009). "The capsid protein of human immunodeficiency virus: interactions of HIV-1 capsid with host protein factors." FEBS J **276**(21): 6118-6127.

Mateu, M. G. (2009). "The capsid protein of human immunodeficiency virus: intersubunit interactions during virus assembly." FEBS J **276**(21): 6098-6109.

McBride, M. S. and A. T. Panganiban (1997). "Position dependence of functional hairpins important for human immunodeficiency virus type 1 RNA encapsidation in vivo." J Virol **71**(3): 2050-2058.

McGinty, J., D. W. Stuckey, et al. (2011). "In vivo fluorescence lifetime tomography of a FRET probe expressed in mouse." Biomed Opt Express **2**(7): 1907-1917.

McKinstry, W. J., M. Hijnen, et al. (2014). "Expression and purification of soluble recombinant full length HIV-1 Pr55(Gag) protein in Escherichia coli." Protein Expr Purif **100**: 10-18.

Michel, F., C. Crucifix, et al. (2009). "Structural basis for HIV-1 DNA integration in the human genome, role of the LEDGF/P75 cofactor." EMBO J **28**(7): 980-991.

Mirambeau, G., S. Lyonnais, et al. (2007). "HIV-1 protease and reverse transcriptase control the architecture of their nucleocapsid partner." PLoS One **2**(7): e669.

Mirambeau, G., S. Lyonnais, et al. (2010). "Features, processing states, and heterologous protein interactions in the modulation of the retroviral nucleocapsid protein function." RNA Biol **7**(6): 724-734.

Moll, M., S. K. Andersson, et al. (2010). "Inhibition of lipid antigen presentation in dendritic cells by HIV-1 Vpu interference with CD1d recycling from endosomal compartments." Blood **116**(11): 1876-1884.

Molle, D., C. Segura-Morales, et al. (2009). "Endosomal trafficking of HIV-1 gag and genomic RNAs regulates viral egress." J Biol Chem **284**(29): 19727-19743.

Moore, M. D., W. Fu, et al. (2007). "Dimer initiation signal of human immunodeficiency virus type 1: its role in partner selection during RNA copackaging and its effects on recombination." J Virol **81**(8): 4002-4011.

Morellet, N., S. Bouaziz, et al. (2003). "NMR structure of the HIV-1 regulatory protein VPR." J Mol Biol **327**(1): 215-227.

Morellet, N., H. Demene, et al. (1998). "Structure of the complex between the HIV-1 nucleocapsid protein NCp7 and the single-stranded pentanucleotide d(ACGCC)." J Mol Biol **283**(2): 419-434.

Morellet, N., S. Druillennec, et al. (2005). "Helical structure determined by NMR of the HIV-1 (345-392)Gag sequence, surrounding p2: implications for particle assembly and RNA packaging." Protein Sci **14**(2): 375-386.

Morellet, N., N. Jullian, et al. (1992). "Determination of the structure of the nucleocapsid protein NCp7 from the human immunodeficiency virus type 1 by 1H NMR." EMBO J **11**(8): 3059-3065.

Morellet, N., B. P. Roques, et al. (2009). "Structure-function relationship of Vpr: biological implications." Curr HIV Res **7**(2): 184-210.

Morikawa, Y., S. Hinata, et al. (1996). "Complete inhibition of human immunodeficiency virus Gag myristoylation is necessary for inhibition of particle budding." J Biol Chem **271**(5): 2868-2873.

Morikawa, Y., D. J. Hockley, et al. (2000). "Roles of matrix, p2, and N-terminal myristoylation in human immunodeficiency virus type 1 Gag assembly." J Virol **74**(1): 16-23.

Morita, E. and W. I. Sundquist (2004). "Retrovirus budding." Annu Rev Cell Dev Biol **20**: 395-425.

Mouland, A. J., J. Mercier, et al. (2000). "The double-stranded RNA-binding protein Staufen is incorporated in human immunodeficiency virus type 1: evidence for a role in genomic RNA encapsidation." J Virol **74**(12): 5441-5451.

Muller, B., J. Daecke, et al. (2004). "Construction and characterization of a fluorescently labeled infectious human immunodeficiency virus type 1 derivative." J Virol **78**(19): 10803-10813.

Muriaux, D. and J. L. Darlix (2010). "Properties and functions of the nucleocapsid protein in virus assembly." RNA Biol **7**(6): 744-753.

Muriaux, D., H. De Rocquigny, et al. (1996). "NCp7 activates HIV-1Lai RNA dimerization by converting a transient loop-loop complex into a stable dimer." J Biol Chem **271**(52): 33686-33692.

Muriaux, D., P. M. Girard, et al. (1995). "Dimerization of HIV-1Lai RNA at low ionic strength. An autocomplementary sequence in the 5' leader region is evidenced by an antisense oligonucleotide." J Biol Chem **270**(14): 8209-8216.

Neil, S. J., S. W. Eastman, et al. (2006). "HIV-1 Vpu promotes release and prevents endocytosis of nascent retrovirus particles from the plasma membrane." PLoS Pathog **2**(5): e39.

Neil, S. J., T. Zang, et al. (2008). "Tetherin inhibits retrovirus release and is antagonized by HIV-1 Vpu." Nature **451**(7177): 425-430.

Nikolaitchik, O. A., K. A. Dilley, et al. (2013). "Dimeric RNA recognition regulates HIV-1 genome packaging." PLoS Pathog **9**(3): e1003249.

Nitahara-Kasahara, Y., M. Kamata, et al. (2007). "Novel nuclear import of Vpr promoted by importin alpha is crucial for human immunodeficiency virus type 1 replication in macrophages." J Virol **81**(10): 5284-5293.

Nydegger, S., M. Foti, et al. (2003). "HIV-1 egress is gated through late endosomal membranes." Traffic **4**(12): 902-910.

O'Carroll, I. P., F. Soheilian, et al. (2013). "Elements in HIV-1 Gag contributing to virus particle assembly." Virus Res **171**(2): 341-345.

O'Reilly, M. M., M. T. McNally, et al. (1995). "Two strong 5' splice sites and competing, suboptimal 3' splice sites involved in alternative splicing of human immunodeficiency virus type 1 RNA." Virology **213**(2): 373-385.

Ono, A. (2009). "HIV-1 Assembly at the Plasma Membrane: Gag Trafficking and Localization." Future Virol **4**(3): 241-257.

Ono, A., S. D. Ablan, et al. (2004). "Phosphatidylinositol (4,5) bisphosphate regulates HIV-1 Gag targeting to the plasma membrane." Proc Natl Acad Sci U S A **101**(41): 14889-14894.

Ono, A., D. Demirov, et al. (2000). "Relationship between human immunodeficiency virus type 1 Gag multimerization and membrane binding." J Virol **74**(11): 5142-5150.

Ono, A. and E. O. Freed (2004). "Cell-type-dependent targeting of human immunodeficiency virus type 1 assembly to the plasma membrane and the multivesicular body." J Virol **78**(3): 1552-1563.

Ono, A., J. M. Orenstein, et al. (2000). "Role of the Gag matrix domain in targeting human immunodeficiency virus type 1 assembly." J Virol **74**(6): 2855-2866.

Ott, D. E. (2008). "Cellular proteins detected in HIV-1." Rev Med Virol **18**(3): 159-175.

Ott, D. E., L. V. Coren, et al. (2005). "Redundant roles for nucleocapsid and matrix RNA-binding sequences in human immunodeficiency virus type 1 assembly." J Virol **79**(22): 13839-13847.

Ott, D. E., L. V. Coren, et al. (1996). "Cytoskeletal proteins inside human immunodeficiency virus type 1 virions." J Virol **70**(11): 7734-7743.

Ott, D. E., L. V. Coren, et al. (2009). "The nucleocapsid region of human immunodeficiency virus type 1 Gag assists in the coordination of assembly and Gag processing: role for RNA-Gag binding in the early stages of assembly." J Virol **83**(15): 7718-7727.

Padilla-Parra, S., N. Auduge, et al. (2009). "Quantitative comparison of different fluorescent protein couples for fast FRET-FLIM acquisition." Biophys J **97**(8): 2368-2376.

Paillart, J. C., M. Dettenhofer, et al. (2004). "First snapshots of the HIV-1 RNA structure in infected cells and in virions." J Biol Chem **279**(46): 48397-48403.

Paillart, J. C., R. Marquet, et al. (1994). "Mutational analysis of the bipartite dimer linkage structure of human immunodeficiency virus type 1 genomic RNA." J Biol Chem **269**(44): 27486-27493.

Paillart, J. C., R. Marquet, et al. (1996). "Dimerization of retroviral genomic RNAs: structural and functional implications." Biochimie **78**(7): 639-653.

Paillart, J. C., M. Shehu-Xhilaga, et al. (2004). "Dimerization of retroviral RNA genomes: an inseparable pair." Nat Rev Microbiol **2**(6): 461-472.

Paillart, J. C., E. Westhof, et al. (1997). "Non-canonical interactions in a kissing loop complex: the dimerization initiation site of HIV-1 genomic RNA." J Mol Biol **270**(1): 36-49.

Pantaleo, G., C. Graziosi, et al. (1993). "New concepts in the immunopathogenesis of human immunodeficiency virus infection." N Engl J Med **328**(5): 327-335.

Parent, L. J. and N. Gudleski (2011). "Beyond plasma membrane targeting: role of the MA domain of Gag in retroviral genome encapsidation." J Mol Biol **410**(4): 553-564.

Perlman, M. and M. D. Resh (2006). "Identification of an intracellular trafficking and assembly pathway for HIV-1 gag." Traffic **7**(6): 731-745.

Pestova, T. V., I. B. Lomakin, et al. (2000). "The joining of ribosomal subunits in eukaryotes requires eIF5B." Nature **403**(6767): 332-335.

Pettit, S. C., M. D. Moody, et al. (1994). "The p2 domain of human immunodeficiency virus type 1 Gag regulates sequential proteolytic processing and is required to produce fully infectious virions." J Virol **68**(12): 8017-8027.

Piller, S. C., G. D. Ewart, et al. (1999). "The amino-terminal region of Vpr from human immunodeficiency virus type 1 forms ion channels and kills neurons." J Virol **73**(5): 4230-4238.

Pisarev, A. V., C. U. Hellen, et al. (2007). "Recycling of eukaryotic posttermination ribosomal complexes." Cell **131**(2): 286-299.

Plantier, J. C., M. Leoz, et al. (2009). "A new human immunodeficiency virus derived from gorillas." Nat Med **15**(8): 871-872.

Poole, E., P. Strappe, et al. (2005). "HIV-1 Gag-RNA interaction occurs at a perinuclear/centrosomal site; analysis by confocal microscopy and FRET." Traffic **6**(9): 741-755.

Poon, D. T., J. Wu, et al. (1996). "Charged amino acid residues of human immunodeficiency virus type 1 nucleocapsid p7 protein involved in RNA packaging and infectivity." J Virol **70**(10): 6607-6616.

Popov, S., E. Popova, et al. (2008). "Human immunodeficiency virus type 1 Gag engages the Bro1 domain of ALIX/AIP1 through the nucleocapsid." J Virol **82**(3): 1389-1398.

Pornillos, O., S. L. Alam, et al. (2002). "Structure of the Tsg101 UEV domain in complex with the PTAP motif of the HIV-1 p6 protein." Nat Struct Biol **9**(11): 812-817.

Pornillos, O., S. L. Alam, et al. (2002). "Structure and functional interactions of the Tsg101 UEV domain." EMBO J **21**(10): 2397-2406.

Ptak, R. G., W. Fu, et al. (2008). "Cataloguing the HIV type 1 human protein interaction network." AIDS Res Hum Retroviruses **24**(12): 1497-1502.

Pugliese, A., V. Vidotto, et al. (2005). "A review of HIV-1 Tat protein biological effects." Cell Biochem Funct **23**(4): 223-227.

Purohit, P., S. Dupont, et al. (2001). "Sequence-specific interaction between HIV-1 matrix protein and viral genomic RNA revealed by in vitro genetic selection." RNA **7**(4): 576-584.

Ramalanjaona, N., H. de Rocquigny, et al. (2007). "Investigating the mechanism of the nucleocapsid protein chaperoning of the second strand transfer during HIV-1 DNA synthesis." J Mol Biol **374**(4): 1041-1053.

Rana, T. M. and K. T. Jeang (1999). "Biochemical and functional interactions between HIV-1 Tat protein and TAR RNA." Arch Biochem Biophys **365**(2): 175-185.

Refaeli, Y., D. N. Levy, et al. (1995). "The glucocorticoid receptor type II complex is a target of the HIV-1 vpr gene product." Proc Natl Acad Sci U S A **92**(8): 3621-3625.

Reicin, A. S., S. Paik, et al. (1995). "Linker insertion mutations in the human immunodeficiency virus type 1 gag gene: effects on virion particle assembly, release, and infectivity." J Virol **69**(2): 642-650.

Rein, A. (2010). "Nucleic acid chaperone activity of retroviral Gag proteins." RNA Biol **7**(6): 700-705.

Rein, A., S. A. Datta, et al. (2011). "Diverse interactions of retroviral Gag proteins with RNAs." Trends Biochem Sci **36**(7): 373-380.

Ren X, P. S., Bonifacino JS, Hurley JH. (2014). "How HIV-1 Nef hijacks the AP-2 clathrin adaptor to downregulate CD4." eLife: 3:e01754.

Rey, O., J. Canon, et al. (1996). "HIV-1 Gag protein associates with F-actin present in microfilaments." Virology **220**(2): 530-534.

Rhodes, T., H. Wargo, et al. (2003). "High rates of human immunodeficiency virus type 1 recombination: near-random segregation of markers one kilobase apart in one round of viral replication." J Virol **77**(20): 11193-11200.

Rogel, M. E., L. I. Wu, et al. (1995). "The human immunodeficiency virus type 1 vpr gene prevents cell proliferation during chronic infection." J Virol **69**(2): 882-888.

Roitt, I. M. (1989). "Basic concepts and new aspects of vaccine development." Parasitology **98 Suppl**: S7-12.

Rudner, L., S. Nydegger, et al. (2005). "Dynamic fluorescent imaging of human immunodeficiency virus type 1 gag in live cells by biarsenical labeling." J Virol **79**(7): 4055-4065.

Ruthardt, N., D. C. Lamb, et al. (2011). "Single-particle tracking as a quantitative microscopy-based approach to unravel cell entry mechanisms of viruses and pharmaceutical nanoparticles." Mol Ther **19**(7): 1199-1211.

Saad, J. S., J. Miller, et al. (2006). "Structural basis for targeting HIV-1 Gag proteins to the plasma membrane for virus assembly." Proc Natl Acad Sci U S A **103**(30): 11364-11369.

Sakalian, M., S. D. Parker, et al. (1996). "Synthesis and assembly of retrovirus Gag precursors into immature capsids in vitro." J Virol **70**(6): 3706-3715.

Salter, J. D., G. A. Morales, et al. (2014). "Structural insights for HIV-1 therapeutic strategies targeting Vif." Trends Biochem Sci **39**(9): 373-380.

Sawaya, B. E., K. Khalili, et al. (1998). "Cooperative actions of HIV-1 Vpr and p53 modulate viral gene transcription." J Biol Chem **273**(32): 20052-20057.

Schmalzbauer, E., B. Strack, et al. (1996). "Mutations of basic amino acids of NCp7 of human immunodeficiency virus type 1 affect RNA binding in vitro." J Virol **70**(2): 771-777.

Services, U. S. D. o. H. a. H. (2011). Panel on Antiretroviral Guidelines for Adults and Adolescents.Guidelines for the use of antiretroviral agents in HIV-1-infected adults and adolescents.

Sette, P., V. Dussupt, et al. (2012). "Identification of the HIV-1 NC binding interface in Alix Bro1 reveals a role for RNA." J Virol **86**(21): 11608-11615.

Shah, A. H., B. Sowrirajan, et al. (2010). "Degranulation of natural killer cells following interaction with HIV-1-infected cells is hindered by downmodulation of NTB-A by Vpu." Cell Host Microbe **8**(5): 397-409.

Singh, A. R., R. L. Hill, et al. (2001). "Effect of mutations in Gag on assembly of immature human immunodeficiency virus type 1 capsids in a cell-free system." Virology **279**(1): 257-270.

Skripkin, E., J. C. Paillart, et al. (1994). "Identification of the primary site of the human immunodeficiency virus type 1 RNA dimerization in vitro." Proc Natl Acad Sci U S A **91**(11): 4945-4949.

Smith, D. K., L. A. Grohskopf, et al. (2005). "Antiretroviral postexposure prophylaxis after sexual, injection-drug use, or other nonoccupational exposure to HIV in the United States: recommendations from the U.S. Department of Health and Human Services." MMWR Recomm Rep **54**(RR-2): 1-20.

Spearman, P. and L. Ratner (1996). "Human immunodeficiency virus type 1 capsid formation in reticulocyte lysates." J Virol **70**(11): 8187-8194.

Steeg, C. M. and V. M. Vogt (1990). "RNA-binding properties of the matrix protein (p19gag) of avian sarcoma and leukemia viruses." J Virol **64**(2): 847-855.

Strack, B., A. Calistri, et al. (2000). "A role for ubiquitin ligase recruitment in retrovirus release." Proc Natl Acad Sci U S A **97**(24): 13063-13068.

Strack, B., A. Calistri, et al. (2003). "AIP1/ALIX is a binding partner for HIV-1 p6 and EIAV p9 functioning in virus budding." Cell **114**(6): 689-699.

Strambio-de-Castillia, C. and E. Hunter (1992). "Mutational analysis of the major homology region of Mason-Pfizer monkey virus by use of saturation mutagenesis." J Virol **66**(12): 7021-7032.

Strauss., J. H. S. E. G. (2002). Viruses and Human Disease. San Diego., S. F., New York., Boston., London., Sydney., Tokyo;.

Suhasini, M. and T. R. Reddy (2009). "Cellular proteins and HIV-1 Rev function." Curr HIV Res **7**(1): 91-100.

Sundquist, W. I. and H. G. Krausslich (2012). "HIV-1 assembly, budding, and maturation." Cold Spring Harb Perspect Med **2**(7): a006924.

Swanson, C. M. and M. H. Malim (2006). "Retrovirus RNA trafficking: from chromatin to invasive genomes." Traffic **7**(11): 1440-1450.

Syed, F. and M. A. McCrae (2009). "Interactions in vivo between the Vif protein of HIV-1 and the precursor (Pr55(GAG)) of the virion nucleocapsid proteins." Arch Virol **154**(11): 1797-1805.

Tahirov, T. H., N. D. Babayeva, et al. (2010). "Crystal structure of HIV-1 Tat complexed with human P-TEFb." Nature **465**(7299): 747-751.

Tang, C., E. Loeliger, et al. (2004). "Entropic switch regulates myristate exposure in the HIV-1 matrix protein." Proc Natl Acad Sci U S A **101**(2): 517-522.

Temin, H. M. (1991). "Sex and recombination in retroviruses." Trends Genet **7**(3): 71-74.

Temin, H. M. (1995). "Genetics of retroviruses." Ann N Y Acad Sci **758**: 161-165.

Thomson, M. M., L. Perez-Alvarez, et al. (2002). "Molecular epidemiology of HIV-1 genetic forms and its significance for vaccine development and therapy." Lancet Infect Dis **2**(8): 461-471.

Tramier, M., M. Zahid, et al. (2006). "Sensitivity of CFP/YFP and GFP/mCherry pairs to donor photobleaching on FRET determination by fluorescence lifetime imaging microscopy in living cells." Microsc Res Tech **69**(11): 933-939.

Turner, B. G. and M. F. Summers (1999). "Structural biology of HIV." J Mol Biol **285**(1): 1-32.

Usami, Y., S. Popov, et al. (2008). "Efficient and specific rescue of human immunodeficiency virus type 1 budding defects by a Nedd4-like ubiquitin ligase." J Virol **82**(10): 4898-4907.

Usami, Y., S. Popov, et al. (2009). "The ESCRT pathway and HIV-1 budding." Biochem Soc Trans **37**(Pt 1): 181-184.

Van Damme, N., D. Goff, et al. (2008). "The interferon-induced protein BST-2 restricts HIV-1 release and is downregulated from the cell surface by the viral Vpu protein." Cell Host Microbe **3**(4): 245-252.

Verli, H., A. Calazans, et al. (2007). "Molecular dynamics analysis of HIV-1 matrix protein: clarifying differences between crystallographic and solution structures." J Mol Graph Model **26**(1): 62-68.

VerPlank, L., F. Bouamr, et al. (2001). "Tsg101, a homologue of ubiquitin-conjugating (E2) enzymes, binds the L domain in HIV type 1 Pr55(Gag)." Proc Natl Acad Sci U S A **98**(14): 7724-7729.

von Schwedler, U. K., K. M. Stray, et al. (2003). "Functional surfaces of the human immunodeficiency virus type 1 capsid protein." J Virol **77**(9): 5439-5450.

von Schwedler, U. K., M. Stuchell, et al. (2003). "The protein network of HIV budding." Cell **114**(6): 701-713.

Wachsmuth, M., W. Waldeck, et al. (2000). "Anomalous diffusion of fluorescent probes inside living cell nuclei investigated by spatially-resolved fluorescence correlation spectroscopy." J Mol Biol **298**(4): 677-689.

Walker, L. M., M. Huber, et al. (2011). "Broad neutralization coverage of HIV by multiple highly potent antibodies." Nature **477**(7365): 466-470.

Walker, L. M., S. K. Phogat, et al. (2009). "Broad and potent neutralizing antibodies from an African donor reveal a new HIV-1 vaccine target." Science **326**(5950): 285-289.

Wang, F., C. B. Marshall, et al. (2013). "Transcriptional/epigenetic regulator CBP/p300 in tumorigenesis: structural and functional versatility in target recognition." Cell Mol Life Sci **70**(21): 3989-4008.

Wang, L., S. Mukherjee, et al. (1995). "Interaction of virion protein Vpr of human immunodeficiency virus type 1 with cellular transcription factor Sp1 and trans-activation of viral long terminal repeat." J Biol Chem **270**(43): 25564-25569.

Wang, W., N. Naiyer, et al. (2014). "Distinct nucleic acid interaction properties of HIV-1 nucleocapsid protein precursor NCp15 explain reduced viral infectivity." Nucleic Acids Res **42**(11): 7145-7159.

Watts, J. M., K. K. Dang, et al. (2009). "Architecture and secondary structure of an entire HIV-1 RNA genome." Nature **460**(7256): 711-716.

Weiss, E. R. and H. Gottlinger (2011). "The role of cellular factors in promoting HIV budding." J Mol Biol **410**(4): 525-533.

Weiss, E. R., E. Popova, et al. (2010). "Rescue of HIV-1 release by targeting widely divergent NEDD4-type ubiquitin ligases and isolated catalytic HECT domains to Gag." PLoS Pathog **6**(9): e1001107.

Weldon, R. A., Jr., W. B. Parker, et al. (1998). "Type D retrovirus capsid assembly and release are active events requiring ATP." J Virol **72**(4): 3098-3106.

Welsch, S., O. T. Keppler, et al. (2007). "HIV-1 buds predominantly at the plasma membrane of primary human macrophages." PLoS Pathog **3**(3): e36.

WHO (2014). "HIV Epidemic Updates.".

Wilk, T., B. Gowen, et al. (1999). "Actin associates with the nucleocapsid domain of the human immunodeficiency virus Gag polyprotein." J Virol **73**(3): 1931-1940.

Wilkinson, K. A., R. J. Gorelick, et al. (2008). "High-throughput SHAPE analysis reveals structures in HIV-1 genomic RNA strongly conserved across distinct biological states." PLoS Biol **6**(4): e96.

Willey, R. L., F. Maldarelli, et al. (1992). "Human immunodeficiency virus type 1 Vpu protein induces rapid degradation of CD4." J Virol **66**(12): 7193-7200.

Williams, M. C., I. Rouzina, et al. (2001). "Mechanism for nucleic acid chaperone activity of HIV-1 nucleocapsid protein revealed by single molecule stretching." Proc Natl Acad Sci U S A **98**(11): 6121-6126.

Wills, J. W. and R. C. Craven (1991). "Form, function, and use of retroviral gag proteins." AIDS **5**(6): 639-654.

Wu, T., S. A. Datta, et al. (2010). "Fundamental differences between the nucleic acid chaperone activities of HIV-1 nucleocapsid protein and Gag or Gag-derived proteins: biological implications." Virology **405**(2): 556-567.

Wu, X., Z. Y. Yang, et al. (2010). "Rational design of envelope identifies broadly neutralizing human monoclonal antibodies to HIV-1." Science **329**(5993): 856-861.

Xie, W., L. Li, et al. (1998). "Cell cycle-dependent subcellular localization of the TSG101 protein and mitotic and nuclear abnormalities associated with TSG101 deficiency." Proc Natl Acad Sci U S A **95**(4): 1595-1600.

Yang, B., L. Gao, et al. (2003). "Potent suppression of viral infectivity by the peptides that inhibit multimerization of human immunodeficiency virus type 1 (HIV-1) Vif proteins." J Biol Chem **278**(8): 6596-6602.

Yang, S., Y. Sun, et al. (2001). "The multimerization of human immunodeficiency virus type I Vif protein: a requirement for Vif function in the viral life cycle." J Biol Chem **276**(7): 4889-4893.

Yeager, M. (2011). "Design of in vitro symmetric complexes and analysis by hybrid methods reveal mechanisms of HIV capsid assembly." J Mol Biol **410**(4): 534-552.

Yedavalli, V. S. and K. T. Jeang (2010). "Trimethylguanosine capping selectively promotes expression of Rev-dependent HIV-1 RNAs." Proc Natl Acad Sci U S A **107**(33): 14787-14792.

Yuan, X., X. Yu, et al. (1993). "Mutations in the N-terminal region of human immunodeficiency virus type 1 matrix protein block intracellular transport of the Gag precursor." J Virol **67**(11): 6387-6394.

Zhai, Q., R. D. Fisher, et al. (2008). "Structural and functional studies of ALIX interactions with YPX(n)L late domains of HIV-1 and EIAV." Nat Struct Mol Biol **15**(1): 43-49.

Zhang, Y., H. Qian, et al. (1998). "Analysis of the assembly function of the human immunodeficiency virus type 1 gag protein nucleocapsid domain." J Virol **72**(3): 1782-1789.

Zhong, Q., Y. Chen, et al. (1998). "Perturbation of TSG101 protein affects cell cycle progression." Cancer Res **58**(13): 2699-2702.

Zhou, W., L. J. Parent, et al. (1994). "Identification of a membrane-binding domain within the amino-terminal region of human immunodeficiency virus type 1 Gag protein which interacts with acidic phospholipids." J Virol **68**(4): 2556-2569.

Zhu, P., E. Chertova, et al. (2003). "Electron tomography analysis of envelope glycoprotein trimers on HIV and simian immunodeficiency virus virions." Proc Natl Acad Sci U S A **100**(26): 15812-15817.

Zimmerman, C., K. C. Klein, et al. (2002). "Identification of a host protein essential for assembly of immature HIV-1 capsids." Nature **415**(6867): 88-92.

Summary in French

Etude du trafic intracellulaire de la protéine Gag du VIH et rôle de son domaine NCp7.

PhD Student: EL MESHRI Salah Edin

PhD Director: DE ROCQUIGNY Hugues (hderocquigny@unistra.fr)

UMR 7213 - Laboratoire de biophotonique et pharmacologie

Préambule :

Les étapes tardives du cycle de réplication du VIH correspondent à l'assemblage des protéines structurales Gag, le bourgeonnement de la particule et sa maturation. Beaucoup de travaux ont été menés sur ces différents aspects. Cependant, le rôle joué par les différents partenaires à savoir les protéines virales et cellulaires et les acides nucléiques restent à préciser d'un point de vue mécanistique et dans le cadre d'une recherche de molécules douées d'activités anti virale.

I - Introduction :

I-1- Le VIH et le SIDA

Le virus de l'immunodéficience humaine (VIH) qui est responsable du SIDA est un lentivirus enveloppé qui appartient à la famille des retroviridae. Depuis sa découverte en 1983 on estime que 30-35 million de personnes de part le monde sont décédées et qu'environ autant de personnes sont de nos jours infectées. En France, le nombre de personne concerné est d'environ 150 000 pour un nombre de décès annuel de 6000 cas. Sa transmission s'effectue essentiellement par les fluides biologiques lors de rapports sexuels non protégés, lors de l'allaitement ou de transfusion sanguine.

L'infection se passe en plusieurs étapes (Figure 1). Schématiquement, 15 à 30 jours suivant la contamination, le virus se réplique activement. Cette phase se traduit dans 75% des cas par quelques symptômes comme fièvre, ganglions, éruptions cutanées. Les cellules infectées par le VIH correspondent aux lymphocytes T_{CD4+} *helper (ou auxilaire),* en particulier les cellules T_{CD4+} mémoires ainsi que les cellules dendritiques, les macrophages… qui sont impliquées dans l'initiation de la réponse T auxiliaire et de l'amplification des diverses fonctions du système immunitaire. La cytotoxicité du virus (détournement de la machinerie cellulaire à son profit) ou de certaines de ces protéines conduit a une déplétion rapide du système immunitaire. La primo-

infection est suivie d'une phase asymptomatique ; il s'agit de la séroconversion. Dans cette phase de latence, il n'y a pas de symptômes, le système immunitaire est efficace, il y a un équilibre entre la multiplication et la réaction immunitaire qui se maintient un certain temps. La charge virale augmente progressivement tandis que le nombre de lymphocytes T_{CD4+} diminue lentement. Puis, la phase symptomatique qui se

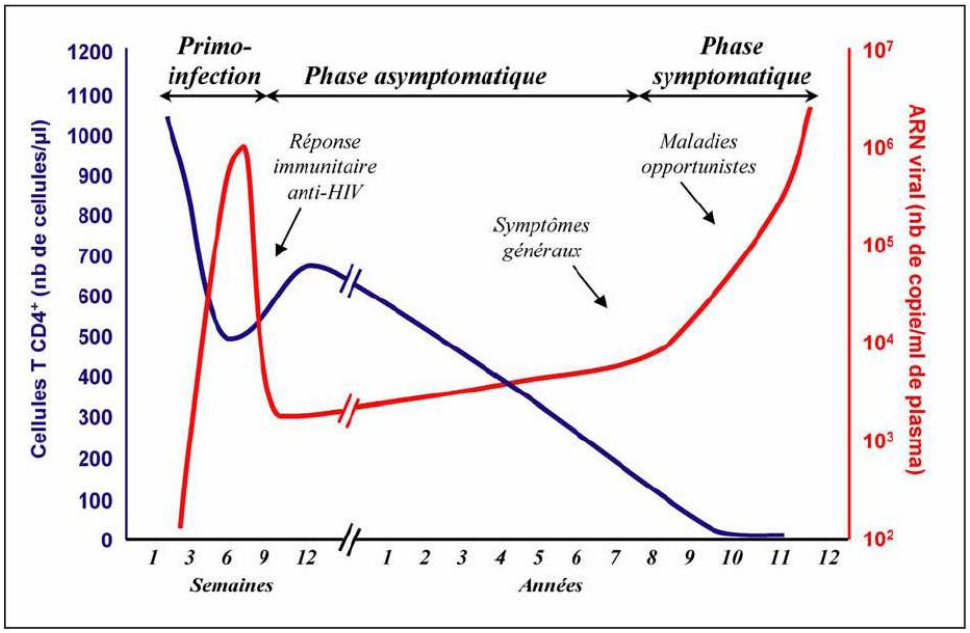

Figure 1 : Evolution clinique de l'infection par le VIH-1.

Les trois phases de l'infection par le VIH-1 sont représentées par l'évolution de la charge virale plasmatique (quantité de virus dans le plasma, en rouge) et du nombre de lymphocytes T CD4+ circulants (en bleu) au cours du temps.

manifeste de 1 à 10 ans après la contamination. On voit apparaître de graves symptômes tels que l'amaigrissement rapide, fièvres longues et intenses, diarrhées persistantes, ganglions importants, infections pulmonaires inhabituelles. A ce stade le déficit immunitaire est sévère, la mort survient par des maladies opportunistes et non par le virus du SIDA lui-même. On observe un brusque infléchissement de la pente de déplétion des cellules $_{CD4+}$ 6 à 18 mois avant le survenu du stade SIDA et un déclin rapide jusqu'à la disparition complète des lymphocytes T_{CD4+} au stade SIDA.

La plupart des patients infectés par le VIH, dans les pays occidentaux, reçoivent un traitement de type HAART (highly active antiretroviral therapy), soit une association de trois médicaments provenant d'au moins deux classes d'antirétroviraux. Ce traitement vise à obtenir une suppression maximale et durable du VIH, d'une charge virale indécelable. est de restaurer un nombre de lymphocytes T_{CD4+}. Plusieurs classes d'antirétroviraux existent à savoir des anti RT (eux-mêmes divisés en deux familles de type nucléosidique ou non nucléosidique), des anti protéases et plus récemment des anti fusions (qui ne sont plus préscrits), des anti CCR5 et des anti intégrase.

I-2- Structure du virus :

Le VIH-l forment des particules sphériques d'un diamètre de 80 à 120 nm et sont produits par bourgeonnement à la surface des cellules infectées. Ces particules sont formées d'une enveloppe externe et d'une nucléocapside dense et excentrée en forme de trapèze ou de barreau à l'intérieur de la particule virale. L'enveloppe est constituée d'une bicouche lipidique d'origine cellulaire et de deux glycoprotéines virales formant les spicules: la gp120 et la gp41. Elle est tapissée d'une matrice (MA) sur sa face intérieure. Le cœur du virus est formé par la protéine de CA entourant la nucléocapside (NCp7) qui renferme le génome viral constitué de deux molécules d'ARN de haut poids moléculaire ainsi que les enzymes nécessaires à sa réplication: la transcriptase inverse, l'endonucléase ou intégrase et la protéase.

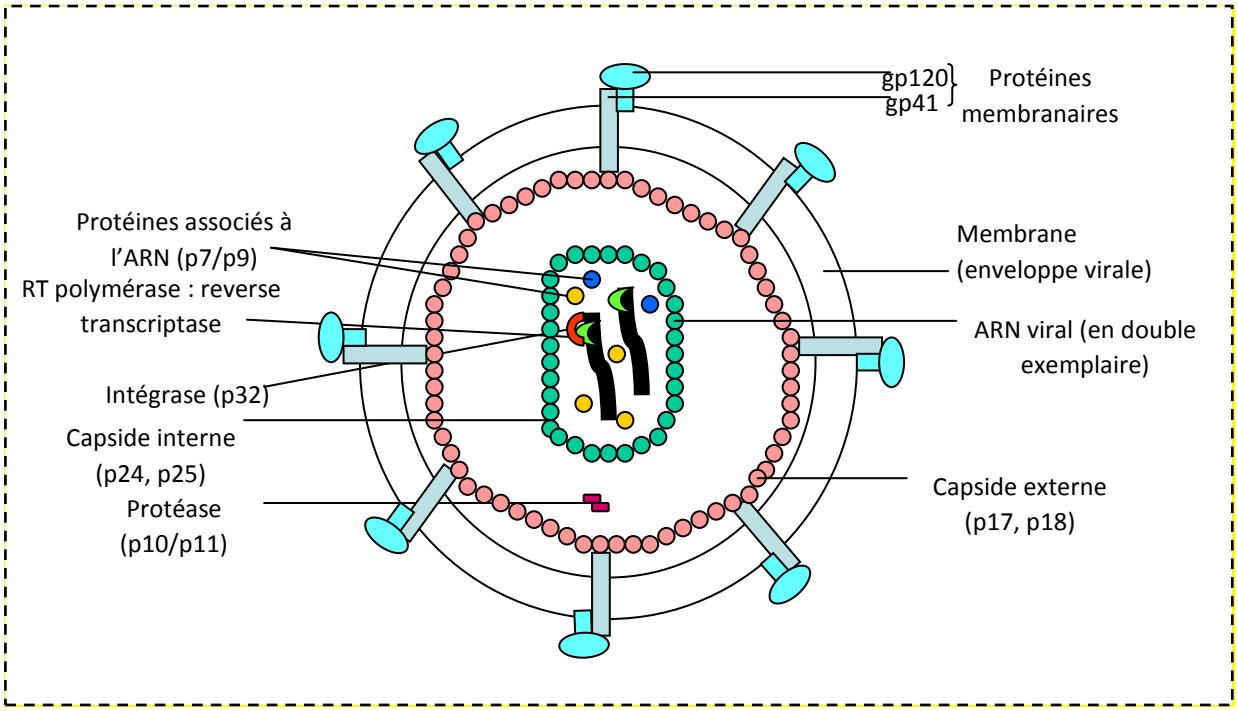

Figure 2 : Structure du virus HIV-1

Le génome du VIH-1 est constitué de deux brins d'ARN non épissés identiques, d'environ 9.2 kb, maintenus ensemble par des interactions non covalentes. Le site majeur d'interaction des ARN, nommé « Dimer Linkage Structure » (DLS), a été visualisé par microscopie électronique au niveau des extrémités 5' (1,2). Ces molécules d'ARN sont issues d'une transcription par l'ARN polymérase II cellulaire et sont donc toutes deux coiffées à leur extrémité 5' et polyadénylées à leur extrémité 3'. Le génome viral comporte 3 régions codantes principales, correspondant aux séquences des polyprotéines Gag, GagPol et Env. Elles codent respectivement pour les protéines de structure, les enzymes virales et les protéines d'enveloppe. Le génome code également six autres protéines dites protéines auxiliaires ou régulatrices : Nef, Rev, Vif, Vpr, Vpu et Tat

Au cours de ma thèse, je me suis focalisé essentiellement sur la protéine Gag. Elle est composée de différents domaines, matrice (MA), capside (CA), nucléocapside (NCp7) et de p6.

• La matrice (MA) est une protéine de 132 acides aminés et présente un poids moléculaire de 17 kDa. Cette protéine possède plusieurs signaux de ciblage (signal d'adressage à la membrane, signal de localisation nucléaire, signal d'export nucléaire) régulés par des

modifications structurales et biochimiques telles que la myristoylation, la multimérisation, ou la phosphorylation.

• La capside CA se subdivise en un domaine N-terminal (résidus 1 à 145) et un domaine C-terminal (résidus 146 à 231). Le domaine CTD est composée de 4 hélices alpha et une petite partie C-terminale de 12 acides aminés, très flexible n'adoptant pas de structure particulière. C'est ce domaine CTD qui assure l'essentiel de l'interaction Gag-Gag (3) requises lors de l'assemblage.

• La protéine virale de nucléocapside NCp7 se compose sous sa forme mature de 55 acides aminés et présente un poids moléculaire de 7 kDa. C'est une petite protéine basique, caractérisée par deux motifs en doigts de zinc très conservés, CX2CX4HX4C, aussi appelés CCHC, connectés par une séquence basique. Ces doigts de zinc sont aussi appelés motifs dactyles et ils lient le zinc avec une très forte affinité (Ka = $10^{-14}M^{-1}$) (4).

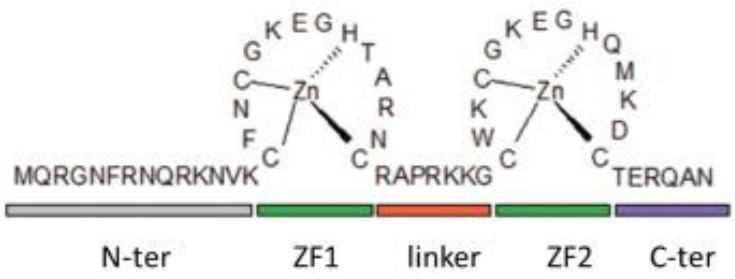

Figure 3 : Structure primaire de la protéine de nucléocapside NCp7

Cette liaison impose un repliement de chaque motif CCHC autour de l'ion et une proximité spatiale grâce à la conformation du pont basique ^{29}RAPRKKG situé entre les deux motifs. Cette organisation conduit à la formation d'un plateau hydrophobe à la surface de la NCp7 du fait du rapprochement des résidus Val13, Phe16, Thr24, Ala25, Trp37 et Met46 (5,6). Si on mute une des histidines par une cystéine, cela entraîne une déformation de la structure des deux doigts de zinc qui se traduit par la production de virus non infectieux (7-10,11 ,12). La NC possède de nombreuses fonctions au cours du cycle viral. Une activité de chaperonne des acides

nucléiques qui est essentielle lors de la transcription inverse, en induisant l'hybridation de l'ARNt^{Lys3} à l'ARN viral, en augmentant la vitesse de la réverse transcriptase et en activant fortement le saut des brins (13,14). Cette activité consiste à promouvoir le réarrangement des acides nucléiques vers leur conformation la plus stable en favorisant les duplex (15). Cette activité se décompose en trois étapes : interaction avec les acides nucléiques cibles, déstabilisation des brins et hybridation des brins complémentaires. La NCp7 permet aussi la protection de l'ARNg viral contre la dégradation par les nucléases et augmente également l'efficacité d'intégration de l'ADN viral dans la cellule hôte en permettant la formation d'un complexe IN-NCp7-ADN plus stable (16,17). Enfin, NCp7 a un rôle très important dans l'encapsidation de l'ARN génomique. Elle présente une forte affinité pour les tige-boucles SL1, SL3 et SL4 (18,19). Elle est le médiateur de la reconnaissance de l'ARN viral parmi l'ensemble des acides nucléiques cellulaires. Les tige-boucles SL1, SL2, SL3 et SL4 ont chacune une affinité différente pour la NCp7 de telle manière que le site reconnu par la protéine est réparti sur les quatre tige-boucles (20) même si plus récemment il a été montré que la boucle SL1 contenait probablement un site de haute affinité (21). Les doigts de zinc sont nécessaires à l'encapsidation (22,23) mais n'ont pas la même importance. En général, toute mutation entraînant la déstructuration des doigts aura pour effet de diminuer l'encapsidation de l'ARN génomique au profit d'autres ARN notamment les ARN ribosomiques (23) (24). Mais le doigt à l'extrémité N-terminale joue un rôle plus important que l'autre doigt puisqu'il reconnaît l'ARN viral (25). Une mutation de ce doigt a pour effet de faire baisser considérablement l'affinité de la NCp7 pour la séquence SL3 (11).

• Enfin, la protéine p6 qui se situe à l'extrémité C-terminale du précurseur polyprotéique Gag. Cette protéine mature se compose de 52 acides aminés et a un poids moléculaire de 5 kDa et est surtout impliquée dans le bourgeonnement des particules virales (26). Elle possède deux domaines appelés domaines tardifs ou 'late motif' qui interagissent avec plusieurs protéines de la famille des ESCRT. Ces protéines cellulaires sont impliquées dans la fission des membranes permettant 1- de fusionner des vésicules dans les MVB (multivesicular bodies) et 2- de séparer les cellules filles lors de la cytokinèse (revue dans (27)). Le premier motif tardif est une séquence riche en proline PTAP qui permet l'interaction avec le domaine UEV TSG101 du complexe ESCRT-1 (28-30). Le deuxième motif tardif qui semble moins important chez VIH-1 mais au contraire primordial chez d'autres rétrovirus est localisé dans la partie C terminal de p6. C'est la

séquence YPXL qui recrute la protéine Alix et qui est en fait un co-facteur des protéines ESCRT (31,32). De manière intéressante cette protéine ALIX, notamment son domaine Bro est aussi reconnu par la NCp7 lors du bourgeonnement de la particule (33-35). Ces deux types d'interactions entre Gag et TSG101 ou ALIX permettent surtout à VIH-1 de détourner les protéines cellulaires de la famille des ESCRT à son profit. En effet, cette interaction permet le recrutement des domaines ESCRT-3 (notamment le domaine CHMP4) et de VPS-4. La protéine CHMP4 est une protéine héliocoïdale qui, en étant recrutée, va polymériser de manière spirale en créant un point de bourgeonnement (36). Cette polymérisation va aussi permettre l'interaction avec la protéine VPS4, qui est une hydrolase dépendante ATP et qui en hydrolysant les protéines du domaine ESCRT-3 libère le virus de la cellule infectée (37). L'ensemble de ce processus impliquant la protéine p6 est très dynamique et de nombreuses études notamment utilisant des outils modernes de microscopie de fluorescence ont montré que le recrutement des protéines ESCRT nécessitait environ 10 minutes (38,39) suivi d'environ 2 minutes pour libérer la particule sous l'action de la VPS4 (38 ,40).

I-3- Rôle de Gag dans l'assemblage et le bourgeonnement viral:

La polyprotéine Gag du VIH-1, est l'élément central pilotant la formation des particules virales (41). De nombreux travaux montrent que cet assemblage résulte d'une polymérisation de Gag impliquant deux plateformes. L'une est lipidique avec l'ancrage du myristate en N terminal du domaine MA de Gag dans une membrane cellulaire et l'interaction de ses acides aminés basiques avec les charges négatives des phosphatidylinositol 4,5-biphosphate de la membrane plasmique (MP) (42). L'autre plateforme est nucléique avec une interaction entre la (NCp7) de Gag et l'ARN génomique. Par ailleurs, les domaines de Gag indispensables à sa polymérisation sont localisés au niveau de la capside (région MHR (*Major Homology Region)* (43)) et dans le domaine N terminal de la NC (44-47).

Plus récemment, il a été montré que dans la phase tardive du cycle la NCp7, au sein du précurseur Gag (appelée ci-dessous GagNC), possédait aussi un rôle essentiel dans l'assemblage (pour revue (48)). En effet, les parties basiques de la protéine sont indispensables pour la formation des polymères Gag-Gag et permettent également la reconnaissance 'non spécifique' d'un ARN (24 ,33,45-47,49). De leur côté, les motifs dactyles seraient plus impliqués dans le

trafic intracellulaire de Gag (50) et dans la reconnaissance des partenaires cellulaires lors du bourgeonnement (33,34). Enfin, des mutations de la NCp7 donnent lieu à une RT tardive suggérant que la NCp7 via son rôle dans les interactions Gag-Gag puisse contrôler de manière temporelle le déclenchement de la reverse transcription (51,52).

Les études sur l'assemblage de Gag puis son trafic et sa localisation à la MP aboutissant au bourgeonnement ont soulevé de nombreuses questions. Ainsi, le degré d'oligomérisation de Gag dans le cytoplasme et le mécanisme d'assemblage au niveau de la MP restent mal connus (33,53). Par ailleurs, l'assemblage a lieu principalement à la MP dans des cellules HeLa, Cos, 293T et T alors que dans les cellules de type macrophage et dendritique, il a lieu principalement au niveau de compartiments intracellulaires type LE (*Late Endosomes*)/MVB (*Multi-Vesicular Body*) (54). Cette localisation intracellulaire pourrait provenir soit d'un trafic par la voie endosomale de Gag soit de la MP après endocytose avant d'être dirigé vers une dégradation (55,56 ,57 ,58 ,59). Outre les différents types cellulaires et une éventuelle différence de détectabilité des différentes populations de Gag par immunofluorescence ou pas fusion à la GFP (60), le facteur temps pourrait être à l'origine de ces différences de voies. En effet, beaucoup d'expériences sont réalisées à un temps fixe post-transfection alors que des études en temps réel ont montré un parallèle entre la diminution de Gag dans des vésicules et l'augmentation de celle-ci à la MP (57,61). Enfin, parallèlement à cet assemblage, la partie C terminale de Gag correspondant à la NCp15 (NC+p6) recrute des facteurs cellulaires (Tsg 101, ALIX) permettant la fermeture des membranes et le relarguage des particules (62) (Figure 28).

Les avancées techniques récentes dans le domaine de la microscopie à fluorescence ont permis de suivre la protéine Gag dans les cellules vivantes. La protéine fluorescente XFP (X= eGFP, mCherry, C, Y) a été placée soit en position C terminale soit en aval de la matrice. Dans ce dernier cas les propriétés d'assemblage et la fonctionnalité de la protéine sont proches de la protéine sauvage (63). Ces études détectent des interactions Gag-Gag principalement au niveau de la MP (49 ,64,65). Par ailleurs, un tag tetra-cystéine (TC) a été placé aux mêmes positions ; la taille de cette séquence de 12 résidus étant compatible avec le suivi des particules dans les cellules (66). Cette séquence interagit de manière irréversible avec FlAsH ou ReAsH pour une émission de fluorescence respectivement dans le vert ou dans le rouge (67). Avec cette approche, le groupe de Freed montre que, dans les macrophages, les vésicules intracellulaires de Gag

seraient plus particulièrement utilisées pour infecter une cellule saine par contact cellule-cellule (68). De plus, avec une approche similaire il a été confirmé, dans les cellules HeLa, que Gag utilisait la voie MVB/LE pour s'assembler (69). De façon tout à fait complémentaire, des études biochimiques de fractionnement sub-cellulaires de lymphocytes-T chroniquement infectés et d'immunofluorescence de cellules HT montrent également un possible assemblage de Gag intracellulaire (56,57). Tous ces résultats soulignent l'importance des modèles cellulaires utilisés pour étudier le trafic et l'assemblage de Gag.

Enfin, des données récentes, utilisant une approche de microscopie TIRF (*Total Reflection Internal Fluorescence*) ont permis de suivre l'apparition/disparition de la particule virale au niveau de la membrane plasmique. Ces données, obtenues sur cellules HeLa, montrent qu'une première population de particules virales apparait/disparait avec des temps très courts (5-10 sec.) et leur co-localisation avec le marqueur d'endosomes CD63 suggère leur internalisation par endocytose (39). Une deuxième population est décrite avec une cinétique d'apparition de Gag de l'ordre de dix minutes suivie d'une période plus longue d'environ 25 minutes pouvant correspondre soit à un assemblage au niveau de la MP à partir d'une fraction cytosolique de Gag soit à une ré-internalisation de Gag dans le cytoplasme (38,39). Ainsi, cette étape de localisation de Gag à la membrane et de bourgeonnement pourrait être influencée par un équilibre entre le relargage extracellulaire de Gag sous forme de particule virale et son internalisation dans la cellule par endocytose.

II-Projet de thèse :

Le but de ma thèse a été de décrire le rôle de la NCp7 dans l'assemblage et le bourgeonnement de Gag dans la cellule en utilisant notamment la microscopie quantitative fluorescente. Au cours de mes études, j'ai construit mes expériences autour de deux objectifs :

• Le premier objectif de la thèse est d'analyser l'influence du doigt de zinc NC (ZF) sur la localisation intracellulaire et l'assemblage du VIH-1. Par conséquent, nous avons utilisé des dérivés de Gag fluorescents tels que Gag-eGFP et Gag-mCherry, où le fluorophore est inséré à côté du domaine de MA. Puis la formation du complexe Gag-Gag a été caractérisée par FRET en suivant le temps de vie de fluorescence de l'eGFP par microscopie à deux photons. Des analyses détaillées des images FRET ont révélé une distribution homogène de complexe Gag-Gag dans

les cellules avec une concentration progressive des oligomères Gag en dessous de la membrane plasmique (PM) favorisant un modèle dans lequel l'oligomérisation de Gag dans le cytoplasme précède l'assemblage du virus de la PM. Dans ce modèle, l'absence du domaine NC de Gag donne naissance à de gros agrégats qui sont dispersés dans le cytoplasme, à une diminution de la condensation de Gag et à un retard pour les complexes Gag-Gag à atteindre le PM. Ainsi NC est impliquée directement par l'interaction protéine-protéine ou indirectement par sa vertu d'interagir avec l'ARN à la formation et au trafique de Gag dans la cellule.

• Au cours de ces premiers travaux, nous avons relevé une forte diminution de VLP au niveau de la PM qui, est en accord avec des données de la littérature, indiquait un défaut dans Gag, dans le surnageant de cellule exprimant GagΔNC. Tenant compte de l'importance de TSG101 dans bourgeonnement Gag, notre deuxième objectif de la thèse était de déterminer le rôle de la NC dans la voie de TSG101. Pour cela, les cellules ont été transfectées avec HA-TSG101 avec des plasmides exprimant Gag ou des protéines Gag mutées au niveau des motifs à doigts de zinc ou l'ensemble du domaine NC. En utilisant une série d'expériences comprenant une immunoprécipitation, microscopie à fluorescence confocale et FLIM-FRET, nous avons trouvé que NC seule ou dans le cadre de Gag, interagit directement avec TSG101 et peut participer avec p6 dans le recrutement de ESCRT-I du bourgeonnement du VIH-1.

III-Résultats:

III-1- Suivi du complexe Gag-Gag en milieu cellulaire:

Nous avons cloné les protéines Gag-eGFP, Gag-mCherry ainsi que de nombreux mutants des motifs CCHC (doigts de zinc ou motifs dactyles) du domaine NC de Gag. L'interaction Gag-Gag est suivie par FLIM à différents temps post transfection. Cette technique d'imagerie permet d'enregistrer le déclin de fluorescence de l'eGFP à chaque pixel de l'image (publication 1). Le traitement de ce déclin avec un modèle à deux composantes permet de calculer le temps de vie de fluorescence et la portion des protéines impliquées dans cette interaction. Une interaction protéine-protéine va induire du FRET qui va se traduire par une diminution du temps de vie de l'eGFP ($\tau_{contrôle}$ = 2.4ns). La figure ci-dessous montre un exemple d'images de FLIM 12h et 24h post transfection du couple Gag-eGFP/Gag-mCherry. Les images du haut correspondent à la

répartition des temps de vie (Fig 1, image a : τ_m=1.4ns et image b τ_m=1.2ns) donnant un FRET d'environ 50% ce qui traduit un complexe Gag-Gag très compact. Les images du bas (c et d) décrivent les pourcentages de population de Gag qui forment des oligomères.

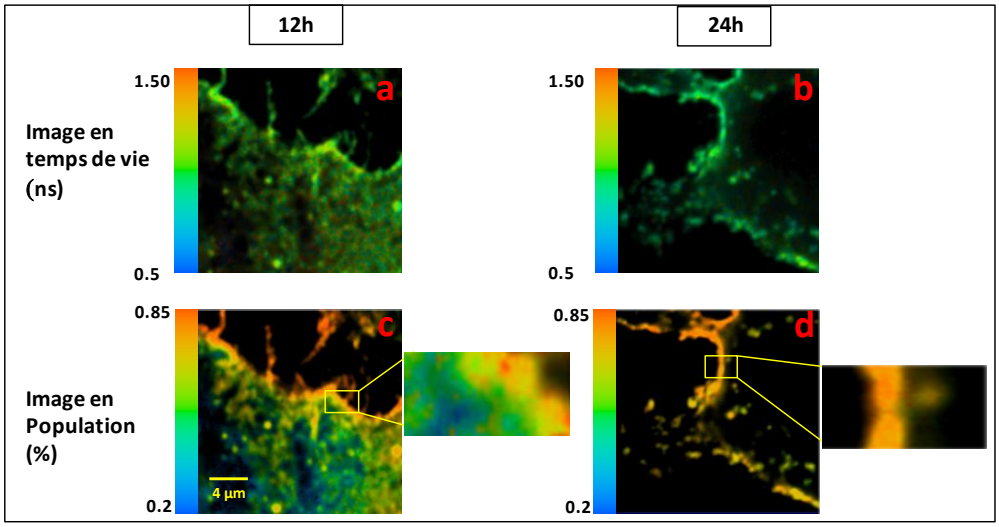

Figure 4 : Assemblage de Gag à la membrane :

Interaction Gag-Gag par FLIM. Images a et b : répartition du temps de vie sur des cellules exprimant Gag-eGFP/Gag-mCherry 12 h (image a) et 24h (image b) post transfection. Images c et d : répartition de la population de Gag impliquée dans l'interaction. L'échelle des couleurs est arbitraire, la couleur orange signifiant des valeurs supérieurs et la bleu des valeurs inférieurs. On notera qu'à 12h, le complexe Gag-Gag formé dans le cytoplasme s'accumule progressivement du cytoplasme (insert couleurs froides) à la membrane plasmique (insert couleurs chaudes).

Les principaux résultats, décrits dans une publication acceptée (Salah El Meshri et al, 2015, publication 2), sont : 1- le temps de vie est significativement plus élevé à 12h qu'à 24h (Figure 4, image b possède un vert plus sombre que l'image a), ce qui s'interprète par le fait que le complexe Gag-Gag devient plus compact avec le temps. Par contre, ce temps de vie varie très peu dans l'espace (vert uniformément réparti dans les cellules des images a et b) montrant que le complexe Gag-Gag s'organise bien avant d'arriver à la membrane sans subir de profonde modification structurale en s'accrochant à la PM. 2- à 12h on constate une accumulation progressive à la PM de la population de Gag engagée dans l'interaction (gradient de couleur image c et insert) alors qu'à 24h toutes les protéines interagissant sont massées à la PM (image b).

Puis nous avons construit toute une série de protéines en délétant chaque motif dactyle de la NCp7 de Gag, les deux en même temps ou l'intégralité de la protéine. L'interaction Gag-Gag de tous ces mutants a été suivie par FRET à 12 et 24h. La figure 5 ci-dessous montre que 1- la délétion de GagNC (ronds noirs) ou simultanée des deux motifs dactyles (courbe bleue) diminue la compaction de Gag et la quantité de protéine impliquée dans l'interaction ; 2- La délétion d'un seul motif dactyle ralenti considérablement la formation du complexe Gag-Gag sans effet majeur sur la compaction du complexe Gag-Gag ; 3- la délétion GagNC montre un défaut très important d'accumulation de Gag à la membrane en accord avec le rôle du domaine NCp7 dans l'interaction de Gag avec les membranes (70).

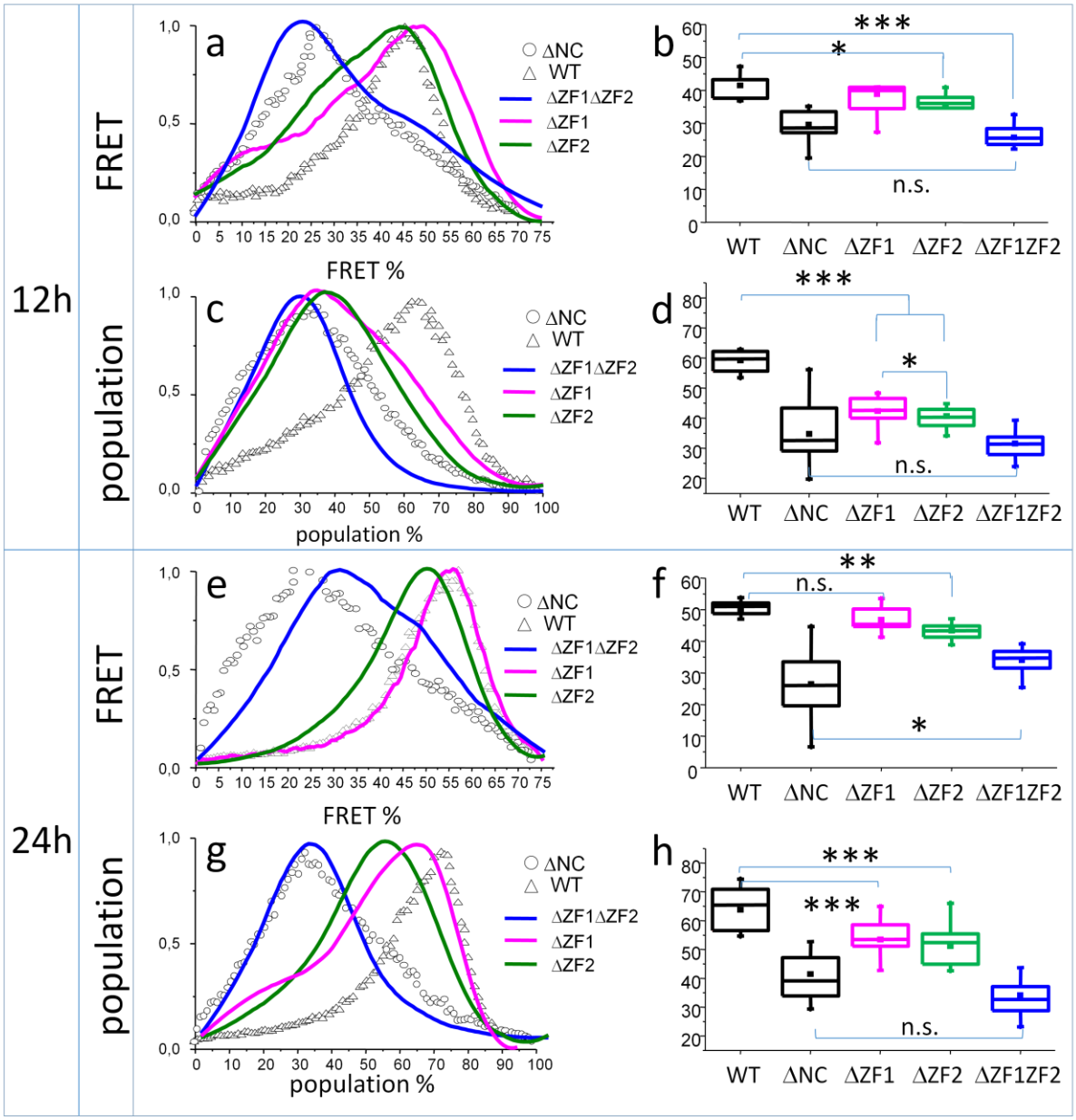

Figure 5 : Rôle de la NC dans l'assemblage de Gag

Distribution du FRET et de la population de Gag engagée dans l'interaction à 12h (a et c) et à 24h (e et g). Les moyennes de ces distributions sont représentées sous forme de 'boites à moustaches'. Triangle noir et rond noir correspondent à Gag et GagΔNC alors que les couleurs magenta, vert et bleue correspondent aux mutants GagΔZF1, GagΔZF2 et GagΔZF1ΔZF2.

En conclusion, la polymérisation de Gag est initiée dans le cytoplasme, bien avant de s'accumuler au niveau de la membrane plasmique. Dans nos études nous montrons que le domaine NC de Gag est important lors des étapes d'assemblage et de trafique de Gag dans la cellule. Les défauts observés avec la protéine GagΔNC sont probablement dus à un défaut de reconnaissance de l'ARN, interaction essentiellement médiée par le domaine NC et indispensable à la polymérisation de Gag dans le cytoplasme. Une étude est maintenant en cours pour suivre cette interaction entre les ARN cellulaires et la protéine Gag en utilisant une technique développée au laboratoire (71).

III-2- Rôle potentiel de la NC dans l'interaction Gag-TSG101

Les travaux ci dessus ont aussi confirmé (non montré) que l'expression de GagΔNC se traduisait par une nette diminution de la production des particules virales (50 ,72 ,73). Cependant, cette construction possède les deux domaines tardifs PTAP and $LYPX_nL$ de la p6 qui interagissent avec la protéine TSG permettant l'export des particules virales. Nous avons donc pris comme hypothèse que le domaine GagNC pouvait aussi être impliqué dans le bourgeonnement du virus. Dans un premier temps nous avons effectué des expériences de co précipitation entre la protéine TSG101 et différentes constructions de Gag (figure 6). Nous montrons ainsi que la protéine GagΔp6 est peu efficacement précipitée par TSG101 (comparer figure 6C, puits 3 avec Gag et puits 7 pour GagΔp6) en accord avec les données de la littérature montrant l'importance du domaine PTAP de p6 dans le recrutement de la TSG101 (28,30,74 ,75). Cependant, le signal restant dans le puits 7 sous entend qu'une autre partie de Gag puisse être importante dans cette interaction. A la lumière du défaut de bourgeonnement observé avec les mutants de Gag, nous avons poursuivi ces expériences avec les constructions de Gag délétées de la NC ou simultanément des deux motifs dactyles.

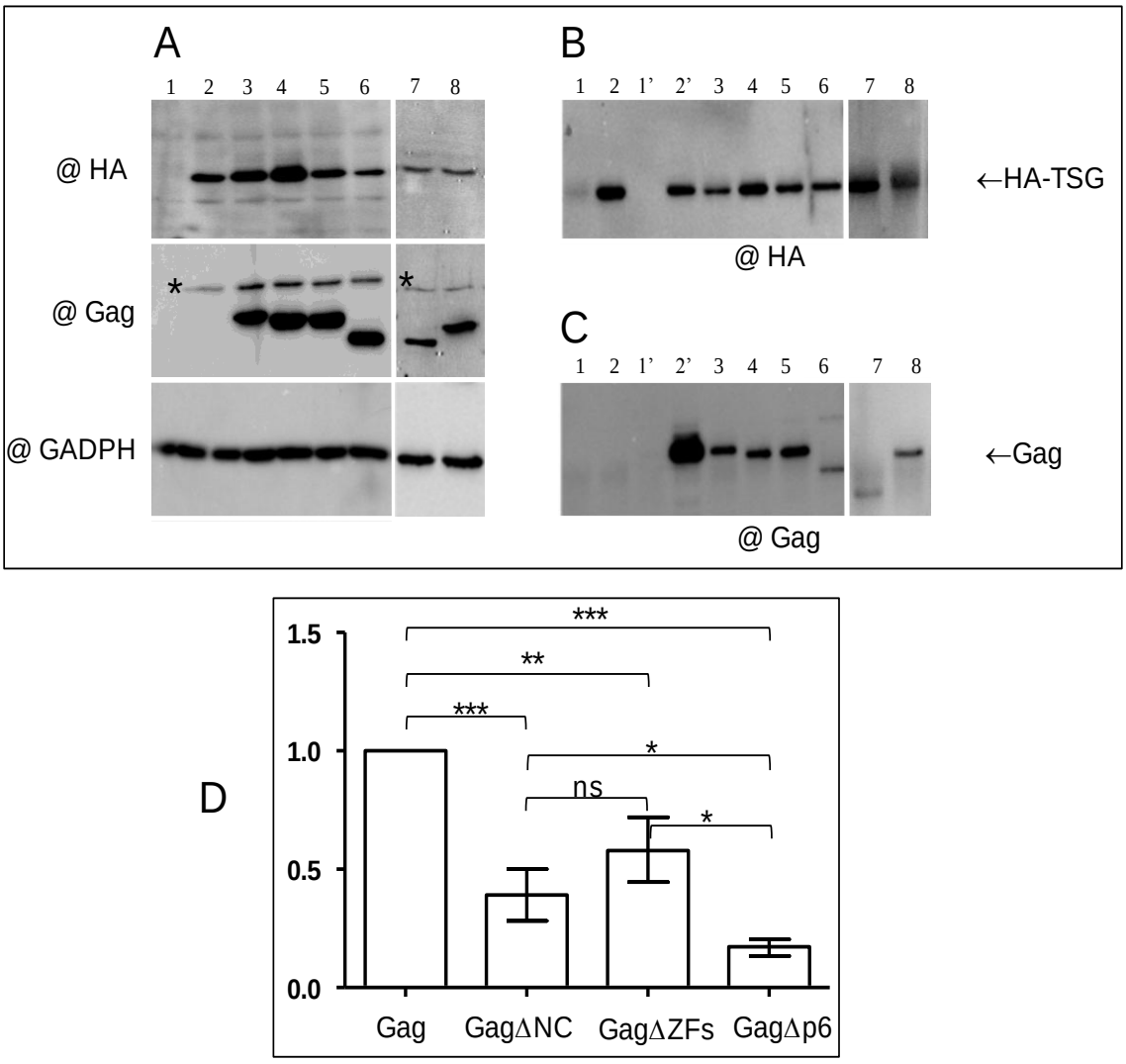

Figure 6 : Le domaine NC de Gag peut avec le domaine p6 participer à l'interaction Gag-TSG101.

A : analyse par western blot de l'input montrant que la TSG101 (anti-HA) et Gag (anti-Gag) et les mutants de Gag sont sensiblement exprimés de manière égale dans les différents échantillons les différentes constructions par rapport à la GADPH. B : l'anti-corps anti-HA précipite de manière similaire la protéine HA-TSG101. C : la membrane B est aussi révélée par l'anti Gag et montre que les différentes constructions de Gag ne sont pas toutes précipitées par la protéine TSG101. D : Histogramme montrant le niveau de précipitation de Gag par TSG101 en fonction des différentes constructions de Gag.

Les résultats précédents (Figure 6) sont en faveur du fait que la NC puisse de manière directe ou indirecte interagir avec la protéine TSG101 ou à minima permettre à la p6 une interaction supérieur. Pour répondre à cette question, nous avons poursuivi nos expériences de co-précipitation sur des cellules co exprimant TSG101 et NCp7-eGFP (figure 7).

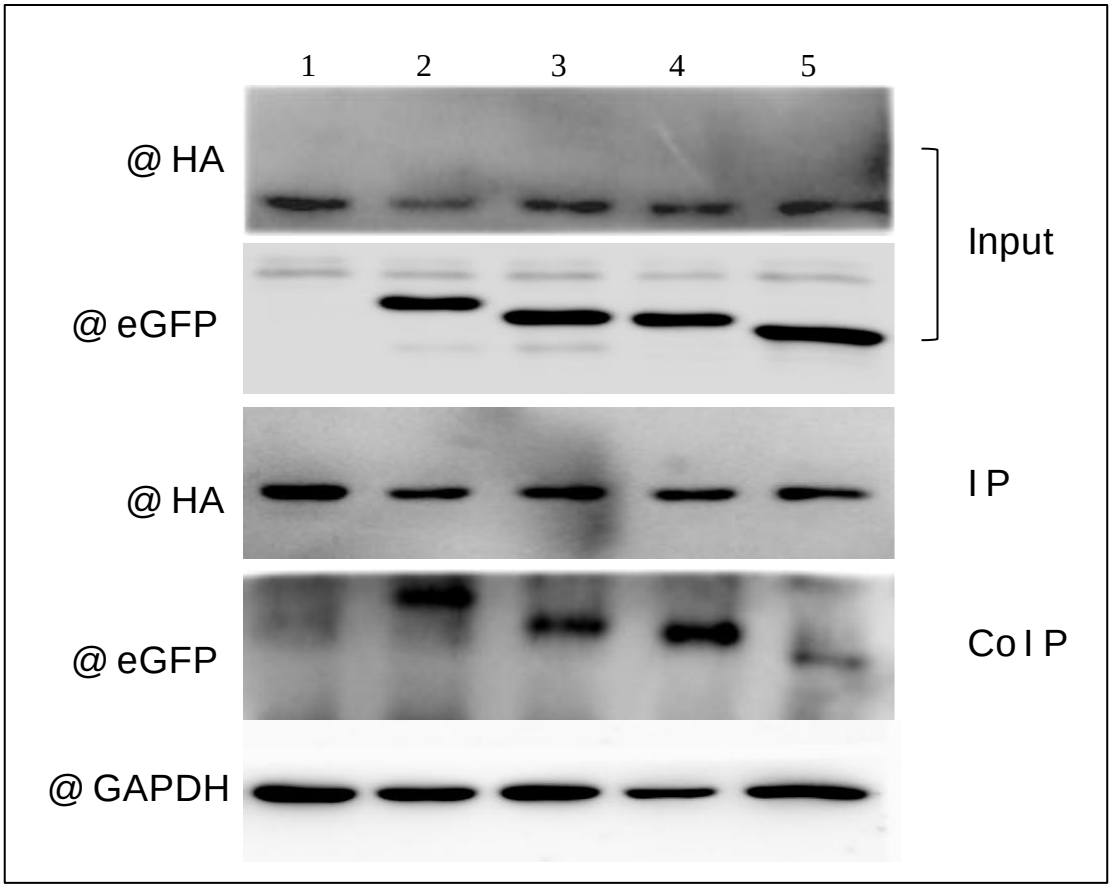

Figure 7 : Précipitation de TSG101 par la NCp7-eGFP

Cellules exprimant que HA-TSG101, puits 1, en présence de NCp7-eGFP, puits 2, ou de NCp7ΔZF1-eGFP, puits 3, ou de NCp7ΔZF2-eGFP puitst 4 ou NCp7ΔZF1ΔZF2-eGFP, puits 5.

Ces expériences montrent plusieurs points intéressants à savoir 1- la NCp7 seule est immunoprécipitée par TSG101 (puits 2) ; 2- aucune différence n'est observée lorsque chaque motif dactyle est enlevé ; 3-Inversement, le fait d'enlever simultanément les deux motifs dactyles se traduit par une nette diminution de la quantité de NC précipitée par HA-TSG101.

Cette diminution de l'interaction GagNC-TSG a été confirmée par FLIM. En suivant le même approche que précédemment nous avons suivi le FRET entre la protéine eGFP-TSG101 et Gag-TC-ReAsH. L'analyse des images nous a permis d'obtenir les paramètres regroupés dans la figure 8. Dans ces conditions, la protéine Gag interagit avec TSG101 avec une efficacité de FRET d'~56%. En accord avec les expériences de coi p, la délétion de chaque motif dactyle a

peu d'importance sur l'efficacité de FRET alors qu'un effet sensible sur celui-ci a été observé dans le cas de la déletion de la NC ou simultanée des deux motifs dactyles.

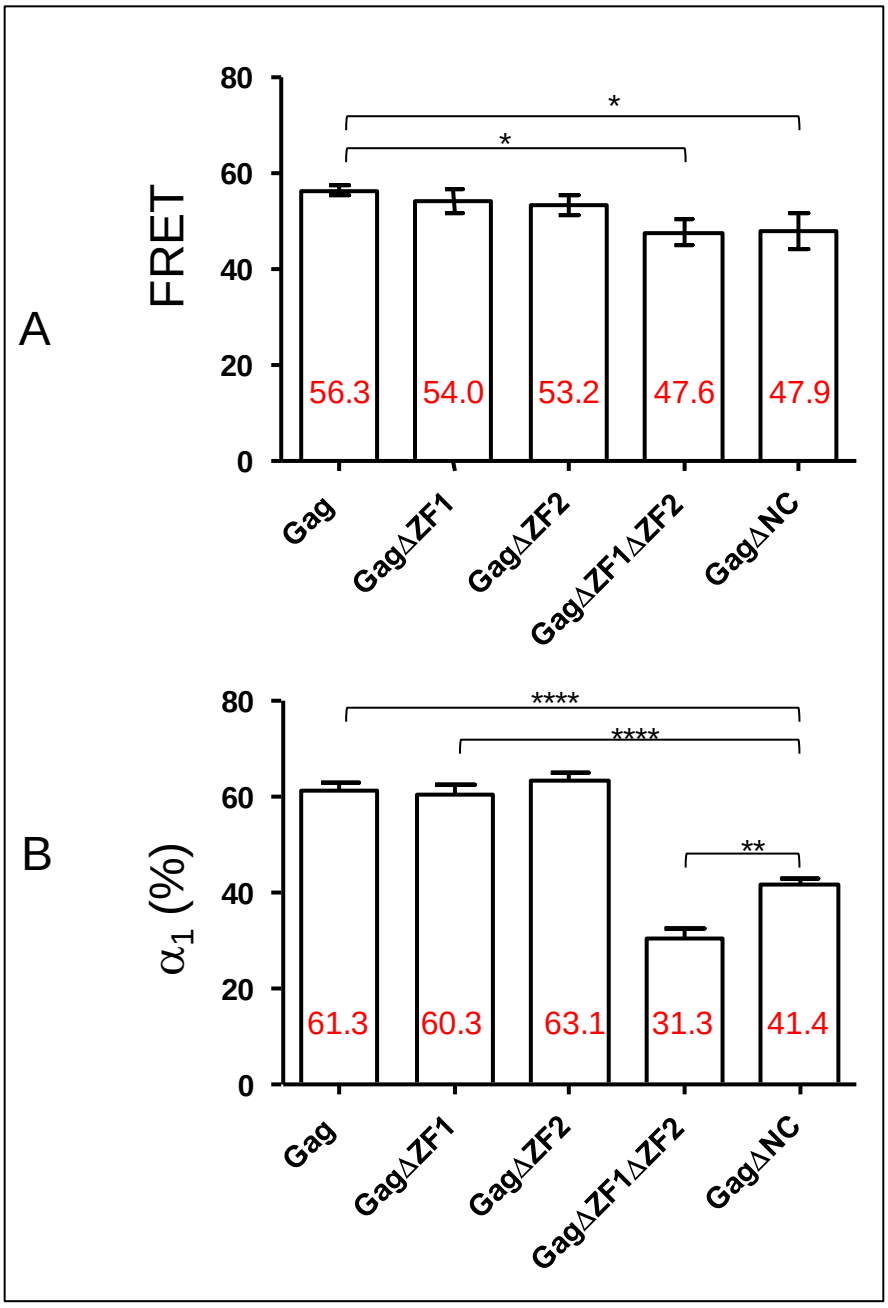

Figure 8 : Pourcentage de FRET et de la population d'eGFP-TSG101 interagissant avec Gag vue par FLIM.
Les cellules sont transfectées avec les différentes constructions et analysées par FLIM en utilisant une loi bi-exponentielle permettant de calculer le temps de vie (converti en FRET en utilisant le temps de vie du contrôle eGFP seul, histogramme A) et la population associée à ce FRET (histogramme B).

L'effet le plus important concerne le paramètre de l'amplitude du FRET. Dans les trois premiers cas, environ 60% de la population de TSG est impliquée dans le complexe Gag-TSG alors que dans les deux derniers cas, une nette diminution est observée.

L'ensemble de ces résultats nous permettent de proposer que l'absence de bourgeonnement des particules virales GagΔNCp7 pourrait être du à une absence de recrutement de la protéine TSG101. Mais cette absence de recrutement ne serait pas forcement due à une interaction directe GagNC et TSG mais peut être à un défaut structural de l'oligomères de Gag comme le montre nos expériences publiés dans JMB (76). Un manuscrit est en cours de rédaction sur ce sujet.

Ce sujet de thèse a donné lieu à une revue [1], une publication [2] et un manuscrit qui sera prochainement soumis [3].

[1]- de Rocquigny, H., **El Meshri**, S. E., Richert, L., Didier, P., Darlix, J. L., and Mely, Y. (2014) Role of the nucleocapsid region in HIV-1 Gag assembly as investigated by quantitative fluorescence-based microscopy, ***Virus Res*** 193, 78-88

[2]- **El Meshri, S. E**., Dujardin, D., Godet, J., Richert, L., Boudier, C., Darlix, J. L., Didier, P., Mely, Y., and de Rocquigny, H. (2015) Role of the Nucleocapsid Domain in HIV-1 Gag Oligomerization and Trafficking to the Plasma Membrane: A Fluorescence Lifetime Imaging Microscopy Investigation, ***J Mol Biol*** 427, 1480-1494

[3]- Salah Edin **El Meshri**, E.Boutant, Audrey Thomas, Vivet Boudout, Hala El Mekdad, Ludovic Richert, Yves Mély, Delphine Muriaux and Hugues de Rocquigny Influence of the nucleocapsid region of the HIV-1 Gag polyprotein precursor on the recruitment and trafficking of the Tumor susceptibility gene 101.

Références

(1) Bender, W., and Davidson, N. (1976) Mapping of poly(A) sequences in the electron microscope reveals unusual structure of type C oncornavirus RNA molecules, *Cell* 7, 595-607

(2) Coffin, J. M. (1979) Structure, replication, and recombination of retrovirus genomes: some unifying hypotheses, *J Gen Virol* 42, 1-26

(3) Gamble, T. R., Yoo, S., Vajdos, F. F., von Schwedler, U. K., Worthylake, D. K., Wang, H., McCutcheon, J. P., Sundquist, W. I., and Hill, C. P. (1997) Structure of the carboxyl-terminal dimerization domain of the HIV-1 capsid protein, *Science* 278, 849-853

(4) Mely, Y., Jullian, N., Morellet, N., De Rocquigny, H., Dong, C. Z., Piemont, E., Roques, B. P., and Gerard, D. (1994) Spatial proximity of the HIV-1 nucleocapsid protein zinc fingers investigated by time-resolved fluorescence and fluorescence resonance energy transfer, *Biochemistry* 33, 12085-12091

(5) Morellet, N., Jullian, N., De Rocquigny, H., Maigret, B., Darlix, J. L., and Roques, B. P. (1992) Determination of the structure of the nucleocapsid protein NCp7 from the human immunodeficiency virus type 1 by 1H NMR, *The EMBO journal* 11, 3059-3065

(6) Summers, M. F., Henderson, L. E., Chance, M. R., Bess, J. W., Jr., South, T. L., Blake, P. R., Sagi, I., Perez-Alvarado, G., Sowder, R. C., 3rd, Hare, D. R., and et al. (1992) Nucleocapsid zinc fingers detected in retroviruses: EXAFS studies of intact viruses and the solution-state structure of the nucleocapsid protein from HIV-1, *Protein Sci* 1, 563-574

(7) Demene, H., Dong, C. Z., Ottmann, M., Rouyez, M. C., Jullian, N., Morellet, N., Mely, Y., Darlix, J. L., Fournie-Zaluski, M. C., Saragosti, S., and et al. (1994) 1H NMR structure and biological studies of the His23-->Cys mutant nucleocapsid protein of HIV-1 indicate that the conformation of the first zinc finger is critical for virus infectivity, *Biochemistry* 33, 11707-11716

(8) Demene, H., Jullian, N., Morellet, N., de Rocquigny, H., Cornille, F., Maigret, B., and Roques, B. P. (1994) Three-dimensional 1H NMR structure of the nucleocapsid protein NCp10 of Moloney murine leukemia virus, *J Biomol NMR* 4, 153-170

(9) Gorelick, R. J., Fu, W., Gagliardi, T. D., Bosche, W. J., Rein, A., Henderson, L. E., and Arthur, L. O. (1999) Characterization of the block in replication of nucleocapsid protein zinc finger mutants from moloney murine leukemia virus, *J Virol* 73, 8185-8195

(10) Gorelick, R. J., Gagliardi, T. D., Bosche, W. J., Wiltrout, T. A., Coren, L. V., Chabot, D. J., Lifson, J. D., Henderson, L. E., and Arthur, L. O. (1999) Strict conservation of the retroviral nucleocapsid protein zinc finger is strongly influenced by its role in viral infection processes: characterization of HIV-1 particles containing mutant nucleocapsid zinc-coordinating sequences, *Virology* 256, 92-104

(11) Tanchou, V., Decimo, D., Pechoux, C., Lener, D., Rogemond, V., Berthoux, L., Ottmann, M., and Darlix, J. L. (1998) Role of the N-terminal zinc finger of human immunodeficiency virus type 1 nucleocapsid protein in virus structure and replication, *J Virol* 72, 4442-4447

(12) Dorfman, T., Luban, J., Goff, S. P., Haseltine, W. A., and Gottlinger, H. G. (1993) Mapping of functionally important residues of a cysteine-histidine box in the human immunodeficiency virus type 1 nucleocapsid protein, *J Virol* 67, 6159-6169

(13) Godet, J., de Rocquigny, H., Raja, C., Glasser, N., Ficheux, D., Darlix, J. L., and Mely, Y. (2006) During the early phase of HIV-1 DNA synthesis, nucleocapsid protein directs hybridization of the TAR complementary sequences via the ends of their double-stranded stem, *J Mol Biol* 356, 1180-1192

(14) Ramalanjaona, N., de Rocquigny, H., Millet, A., Ficheux, D., Darlix, J. L., and Mely, Y. (2007) Investigating the mechanism of the nucleocapsid protein chaperoning of the second strand transfer during HIV-1 DNA synthesis, *J Mol Biol* 374, 1041-1053

(15) Darlix, J. L., Garrido, J. L., Morellet, N., Mely, Y., and de Rocquigny, H. (2007) Properties, functions, and drug targeting of the multifunctional nucleocapsid protein of the human immunodeficiency virus, *Advances in pharmacology (San Diego, Calif* 55, 299-346

(16) Krishnamoorthy, G., Duportail, G., and Mely, Y. (2002) Structure and dynamics of condensed DNA probed by 1,1'-(4,4,8,8-tetramethyl-4,8-diazaundecamethylene)bis[4-[[3- methylbenz-1,3-oxazol-2-yl]methylidine]-1,4-dihydroquinolinium] tetraiodide fluorescence, *Biochemistry* 41, 15277-15287

(17) Lapadat-Tapolsky, M., De Rocquigny, H., Van Gent, D., Roques, B., Plasterk, R., and Darlix, J. L. (1993) Interactions between HIV-1 nucleocapsid protein and viral DNA may have important functions in the viral life cycle, *Nucleic Acids Res* 21, 831-839

(18) Berkowitz, R. D., Hammarskjold, M. L., Helga-Maria, C., Rekosh, D., and Goff, S. P. (1995) 5' regions of HIV-1 RNAs are not sufficient for encapsidation: implications for the HIV-1 packaging signal, *Virology* 212, 718-723

(19) Clever, J., Sassetti, C., and Parslow, T. G. (1995) RNA secondary structure and binding sites for gag gene products in the 5' packaging signal of human immunodeficiency virus type 1, *J Virol* 69, 2101-2109

(20) Lochrie, M. A., Waugh, S., Pratt, D. G., Jr., Clever, J., Parslow, T. G., and Polisky, B. (1997) In vitro selection of RNAs that bind to the human immunodeficiency virus type-1 gag polyprotein, *Nucleic Acids Res* 25, 2902-2910

(21) Abd El-Wahab, E. W., Smyth, R. P., Mailler, E., Bernacchi, S., Vivet-Boudou, V., Hijnen, M., Jossinet, F., Mak, J., Paillart, J. C., and Marquet, R. (2014) Specific recognition of the HIV-1 genomic RNA by the Gag precursor, *Nature communications* 5, 4304

(22) Aldovini, A., and Young, R. A. (1990) Mutations of RNA and protein sequences involved in human immunodeficiency virus type 1 packaging result in production of noninfectious virus, *J Virol* 64, 1920-1926

(23) Gorelick, R. J., Nigida, S. M., Jr., Bess, J. W., Jr., Arthur, L. O., Henderson, L. E., and Rein, A. (1990) Noninfectious human immunodeficiency virus type 1 mutants deficient in genomic RNA, *J Virol* 64, 3207-3211

(24) Muriaux, D., Mirro, J., Harvin, D., and Rein, A. (2001) RNA is a structural element in retrovirus particles, *Proc Natl Acad Sci U S A* 98, 5246-5251

(25) Poon, D. T. K., Wu, J., and Aldovini, A. (1996) Charged amino acid residues of human immunodeficiency virus type 1 nucleocapsid p7 protein involved in RNA packaging and infectivity, *Journal of virology* 70, 6607-6616

(26) Gottlinger, H. G., Dorfman, T., Sodroski, J. G., and Haseltine, W. A. (1991) Effect of mutations affecting the p6 gag protein on human immunodeficiency virus particle release, *Proc Natl Acad Sci U S A* 88, 3195-3199

(27) Im, Y. J., Kuo, L., Ren, X., Burgos, P. V., Zhao, X. Z., Liu, F., Burke, T. R., Jr., Bonifacino, J. S., Freed, E. O., and Hurley, J. H. (2010) Crystallographic and functional analysis of the ESCRT-I /HIV-1 Gag PTAP interaction, *Structure* 18, 1536-1547

(28) Garrus, J. E., von Schwedler, U. K., Pornillos, O. W., Morham, S. G., Zavitz, K. H., Wang, H. E., Wettstein, D. A., Stray, K. M., Cote, M., Rich, R. L., Myszka, D. G., and Sundquist, W. I. (2001) Tsg101 and the vacuolar protein sorting pathway are essential for HIV-1 budding, *Cell* 107, 55-65

(29) Herbert, S., Soares, H., Zimmer, C., and Henriques, R. (2012) Single-molecule localization super-resolution microscopy: deeper and faster, *Microscopy and microanalysis : the official journal of Microscopy Society of America, Microbeam Analysis Society, Microscopical Society of Canada* 18, 1419-1429

(30) VerPlank, L., Bouamr, F., LaGrassa, T. J., Agresta, B., Kikonyogo, A., Leis, J., and Carter, C. A. (2001) Tsg101, a homologue of ubiquitin-conjugating (E2) enzymes, binds the L domain in HIV type 1 Pr55(Gag), *Proc Natl Acad Sci U S A* 98, 7724-7729

(31) Strack, B., Calistri, A., Craig, S., Popova, E., and Gottlinger, H. G. (2003) AIP1/ALIX is a binding partner for HIV-1 p6 and EIAV p9 functioning in virus budding, *Cell* 114, 689-699

(32) Usami, Y., Popov, S., and Gottlinger, H. G. (2007) Potent rescue of human immunodeficiency virus type 1 late domain mutants by ALIX/AIP1 depends on its CHMP4 binding site, *J Virol* 81, 6614-6622

(33) Dussupt, V., Javid, M. P., Abou-Jaoude, G., Jadwin, J. A., de La Cruz, J., Nagashima, K., and Bouamr, F. (2009) The nucleocapsid region of HIV-1 Gag cooperates with the PTAP

and LYPXnL late domains to recruit the cellular machinery necessary for viral budding, *PLoS pathogens* 5, e1000339

(34) Popov, S., Popova, E., Inoue, M., and Gottlinger, H. G. (2008) Human immunodeficiency virus type 1 Gag engages the Bro1 domain of ALIX/AIP1 through the nucleocapsid, *J Virol* 82, 1389-1398

(35) Popov, S., Popova, E., Inoue, M., and Gottlinger, H. G. (2009) Divergent Bro1 domains share the capacity to bind human immunodeficiency virus type 1 nucleocapsid and to enhance virus-like particle production, *J Virol* 83, 7185-7193

(36) Morita, E., and Sundquist, W. I. (2004) Retrovirus budding, *Annu Rev Cell Dev Biol* 20, 395-425

(37) Im, Y. J., and Hurley, J. H. (2008) Integrated structural model and membrane targeting mechanism of the human ESCRT-II complex, *Dev Cell* 14, 902-913

(38) Ivanchenko, S., Godinez, W. J., Lampe, M., Krausslich, H. G., Eils, R., Rohr, K., Brauchle, C., Muller, B., and Lamb, D. C. (2009) Dynamics of HIV-1 assembly and release, *PLoS pathogens* 5, e1000652

(39) Jouvenet, N., Bieniasz, P. D., and Simon, S. M. (2008) Imaging the biogenesis of individual HIV-1 virions in live cells, *Nature* 454, 236-240

(40) Jouvenet, N., Simon, S. M., and Bieniasz, P. D. (2011) Visualizing HIV-1 assembly, *J Mol Biol* 410, 501-511

(41) Adamson, C. S., and Freed, E. O. (2007) Human immunodeficiency virus type 1 assembly, release, and maturation, *Advances in pharmacology (San Diego, Calif* 55, 347-387

(42) Waheed, A. A., and Freed, E. O. (2009) Lipids and membrane microdomains in HIV-1 replication, *Virus Res* 143, 162-176

(43) Wills, J. W., and Craven, R. C. (1991) Form, function, and use of retroviral gag proteins, *AIDS (London, England)* 5, 639-654

(44) Berthoux, L., Pechoux, C., Ottmann, M., Morel, G., and Darlix, J. L. (1997) Mutations in the N-terminal domain of human immunodeficiency virus type 1 nucleocapsid protein affect virion core structure and proviral DNA synthesis, *J Virol* 71, 6973-6981

(45) Cimarelli, A., and Luban, J. (2000) Human immunodeficiency virus type 1 virion density is not determined by nucleocapsid basic residues, *J Virol* 74, 6734-6740

(46) Cimarelli, A., Sandin, S., Hoglund, S., and Luban, J. (2000) Basic residues in human immunodeficiency virus type 1 nucleocapsid promote virion assembly via interaction with RNA, *J Virol* 74, 3046-3057

(47) Sandefur, S., Smith, R. M., Varthakavi, V., and Spearman, P. (2000) Mapping and characterization of the N-terminal I domain of human immunodeficiency virus type 1 Pr55(Gag), *J Virol* 74, 7238-7249

(48) de Rocquigny, H., El Meshri, S. E., Richert, L., Didier, P., Darlix, J. L., and Mely, Y. (2014) Role of the nucleocapsid region in HIV-1 Gag assembly as investigated by quantitative fluorescence-based microscopy, *Virus Res* 193, 78-88

(49) Derdowski, A., Ding, L., and Spearman, P. (2004) A novel fluorescence resonance energy transfer assay demonstrates that the human immunodeficiency virus type 1 Pr55Gag I domain mediates Gag-Gag interactions, *J Virol* 78, 1230-1242

(50) Grigorov, B., Decimo, D., Smagulova, F., Pechoux, C., Mougel, M., Muriaux, D., and Darlix, J. L. (2007) Intracellular HIV-1 Gag localization is impaired by mutations in the nucleocapsid zinc fingers, *Retrovirology* 4, 54

(51) Didierlaurent, L., Houzet, L., Morichaud, Z., Darlix, J. L., and Mougel, M. (2008) The conserved N-terminal basic residues and zinc-finger motifs of HIV-1 nucleocapsid restrict the viral cDNA synthesis during virus formation and maturation, *Nucleic Acids Res* 36, 4745-4753

(52) Houzet, L., Morichaud, Z., Didierlaurent, L., Muriaux, D., Darlix, J. L., and Mougel, M. (2008) Nucleocapsid mutations turn HIV-1 into a DNA-containing virus, *Nucleic Acids Res* 36, 2311-2319

(53) Gomez, C. Y., and Hope, T. J. (2006) Mobility of human immunodeficiency virus type 1 Pr55Gag in living cells, *J Virol* 80, 8796-8806

(54) Bieniasz, P. D. (2009) The cell biology of HIV-1 virion genesis, *Cell host & microbe* 5, 550-558

(55) Jouvenet, N., Neil, S. J., Bess, C., Johnson, M. C., Virgen, C. A., Simon, S. M., and Bieniasz, P. D. (2006) Plasma membrane is the site of productive HIV-1 particle assembly, *PLoS biology* 4, e435

(56) Grigorov, B., Arcanger, F., Roingeard, P., Darlix, J. L., and Muriaux, D. (2006) Assembly of infectious HIV-1 in human epithelial and T-lymphoblastic cell lines, *J Mol Biol* 359, 848-862

(57) Molle, D., Segura-Morales, C., Camus, G., Berlioz-Torrent, C., Kjems, J., Basyuk, E., and Bertrand, E. (2009) Endosomal trafficking of HIV-1 gag and genomic RNAs regulates viral egress, *J Biol Chem* 284, 19727-19743

(58) Finzi, A., Orthwein, A., Mercier, J., and Cohen, E. A. (2007) Productive human immunodeficiency virus type 1 assembly takes place at the plasma membrane, *J Virol* 81, 7476-7490

(59) Welsch, S., Keppler, O. T., Habermann, A., Allespach, I., Krijnse-Locker, J., and Krausslich, H. G. (2007) HIV-1 buds predominantly at the plasma membrane of primary human macrophages, *PLoS pathogens* 3, e36

(60) Ono, A., Waheed, A. A., Joshi, A., and Freed, E. O. (2005) Association of human immunodeficiency virus type 1 gag with membrane does not require highly basic sequences in the nucleocapsid: use of a novel Gag multimerization assay, *J Virol* 79, 14131-14140

(61) Sherer, N. M., Lehmann, M. J., Jimenez-Soto, L. F., Ingmundson, A., Horner, S. M., Cicchetti, G., Allen, P. G., Pypaert, M., Cunningham, J. M., and Mothes, W. (2003) Visualization of retroviral replication in living cells reveals budding into multivesicular bodies, *Traffic (Copenhagen, Denmark)* 4, 785-801

(62) Carlton, J. G., Agromayor, M., and Martin-Serrano, J. (2008) Differential requirements for Alix and ESCRT-III in cytokinesis and HIV-1 release, *Proc Natl Acad Sci U S A* 105, 10541-10546

(63) Muller, B., Daecke, J., Fackler, O. T., Dittmar, M. T., Zentgraf, H., and Krausslich, H. G. (2004) Construction and characterization of a fluorescently labeled infectious human immunodeficiency virus type 1 derivative, *J Virol* 78, 10803-10813

(64) Larson, D. R., Johnson, M. C., Webb, W. W., and Vogt, V. M. (2005) Visualization of retrovirus budding with correlated light and electron microscopy, *Proc Natl Acad Sci U S A* 102, 15453-15458

(65) Hubner, W., Chen, P., Del Portillo, A., Liu, Y., Gordon, R. E., and Chen, B. K. (2007) Sequence of human immunodeficiency virus type 1 (HIV-1) Gag localization and oligomerization monitored with live confocal imaging of a replication-competent, fluorescently tagged HIV-1, *J Virol* 81, 12596-12607

(66) Rudner, L., Nydegger, S., Coren, L. V., Nagashima, K., Thali, M., and Ott, D. E. (2005) Dynamic fluorescent imaging of human immunodeficiency virus type 1 gag in live cells by biarsenical labeling, *J Virol* 79, 4055-4065

(67) Martin, B. R., Giepmans, B. N., Adams, S. R., and Tsien, R. Y. (2005) Mammalian cell-based optimization of the biarsenical-binding tetracysteine motif for improved fluorescence and affinity, *Nat Biotechnol* 23, 1308-1314

(68) Gousset, K., Ablan, S. D., Coren, L. V., Ono, A., Soheilian, F., Nagashima, K., Ott, D. E., and Freed, E. O. (2008) Real-Time Visualization of HIV-1 GAG Trafficking in Infected Macrophages, *PLoS pathogens* 4, e1000015

(69) Perlman, M., and Resh, M. D. (2006) Identification of an intracellular trafficking and assembly pathway for HIV-1 gag, *Traffic (Copenhagen, Denmark)* 7, 731-745

(70) Kempf, N., Postupalenko, V., Bora, S., Didier, P., Arntz, Y., de Rocquigny, H., and Mely, Y. (2015) The HIV-1 Nucleocapsid Protein Recruits Negatively Charged Lipids To Ensure Its Optimal Binding to Lipid Membranes, *J Virol* 89, 1756-1767

(71) Anton, H., Taha, N., Boutant, E., Richert, L., Khatter, H., Klaholz, B., Ronde, P., Real, E., de Rocquigny, H., and Mely, Y. (2015) Investigating the Cellular Distribution and Interactions of HIV-1 Nucleocapsid Protein by Quantitative Fluorescence Microscopy, *PloS one* 10, e0116921

(72) Hogue, I. B., Hoppe, A., and Ono, A. (2009) Quantitative fluorescence resonance energy transfer microscopy analysis of the human immunodeficiency virus type 1 Gag-Gag interaction: relative contributions of the CA and NC domains and membrane binding, *J Virol* 83, 7322-7336

(73) Ono, A., and Freed, E. O. (2001) Plasma membrane rafts play a critical role in HIV-1 assembly and release, *Proc Natl Acad Sci U S A* 98, 13925-13930

(74) Ono, A., and Freed, E. O. (2004) Cell-type-dependent targeting of human immunodeficiency virus type 1 assembly to the plasma membrane and the multivesicular body, *J Virol* 78, 1552-1563

(75) Pornillos, O., Alam, S. L., Davis, D. R., and Sundquist, W. I. (2002) Structure of the Tsg101 UEV domain in complex with the PTAP motif of the HIV-1 p6 protein, *Nat Struct Biol* 9, 812-817

(76) El Meshri, S. E., Dujardin, D., Godet, J., Richert, L., Boudier, C., Darlix, J. L., Didier, P., Mely, Y., and de Rocquigny, H. (2015) Role of the Nucleocapsid Domain in HIV-1 Gag Oligomerization and Trafficking to the Plasma Membrane: A Fluorescence Lifetime Imaging Microscopy Investigation, *J Mol Biol* 427, 1480-1494